ISTANBUL TECHNICAL UNIVERSITY ★ GRADUATE SCHOOL

STRATEGIES FOR SEISMIC RISK MITIGATION BY CONSIDERING ECONOMIC CRITERIA ON A REGIONAL BASIS

Ph.D. THESIS

Hasan Hüseyin AYDOĞDU

Department of Earthquake Engineering

Earthquake Engineering Programme

FEBRUARY 2024

ISTANBUL TECHNICAL UNIVERSITY ★ GRADUATE SCHOOL

STRATEGIES FOR SEISMIC RISK MITIGATION BY CONSIDERING ECONOMIC CRITERIA ON A REGIONAL BASIS

Ph.D. THESIS

Hasan Hüseyin AYDOĞDU
(802162205)

Department of Earthquake Engineering

Earthquake Engineering Programme

Thesis Advisor: Prof. Dr. Alper İLKİ

FEBRUARY 2024

ISTANBUL TEKNİK ÜNİVERSİTESİ ★ LİSANSÜSTÜ EĞİTİM ENSTİTÜSÜ

BÖLGE BAZINDA EKONOMİK KRİTERLER GÖZ ÖNÜNDE TUTULARAK DEPREM RİSKLERİNİN AZALTILMASINA YÖNELİK STRATEJİLER

DOKTORA TEZİ

Hasan Hüseyin AYDOĞDU
(802162205)

Deprem Mühendisliği Anabilim Dalı

Deprem Mühendisliği Programı

Tez Danışmanı: Prof. Dr. Alper İLKİ

ŞUBAT 2024

Hasan Hüseyin AYDOĞDU, a Ph.D. student of İTÜ Graduate School student ID 802162205, successfully defended the thesis/dissertation entitled "STRATEGIES FOR SEISMIC RISK MITIGATION BY CONSIDERING ECONOMIC CRITERIA ON A REGIONAL BASIS", which he prepared after fulfilling the requirements specified in the associated legislations, before the jury whose signatures are below.

Thesis Advisor :	**Prof. Dr. Alper İLKİ** İstanbul Technical University	.....
Jury Members :	**Prof. Dr. Oğuz Cem ÇELİK** İstanbul Technical University	.....
	Prof. Dr. Özgür AVŞAR Eskişehir Technical University	.....
	Prof. Dr. Ufuk YAZGAN İstanbul Technical University	.....
	Prof. Dr. Kutay ORAKÇAL Boğaziçi University	.....

Date of Submission : 27 December 2023
Date of Defense : 21 February 2024

To my dear family,

FOREWORD

The 1999 earthquakes were not only a milestone of seismic awareness in our country, but also increased our curiosity about earthquakes because they happened in the childhood era of our generation. As children who were in secondary school, we became so interested in earthquakes that we were trying to calculate how many years were left until the next earthquake, by looking at earthquake zonation maps and catalogs published by newspapers. This curiosity continued while I was choosing a profession, and when I was deciding on the department of the university that I would proceed, I chose civil engineering in order to focus on earthquake engineering. For almost 10 years, I have been studying earthquake engineering to unleash the answers to questions in my mind, and have been enjoying every moment of my research. As long as I continue my studies in this area, I will have great pleasure in seeking out the truth beneath the unknown phenomena of our field of work.

Firstly, I would like to thank and express my deepest gratitude to my supervisor Dr. Alper İLKİ for his comments, recommendations, guidance, and precious support during my whole Ph.D. study. During my Ph.D. studies Dr. İLKİ and his team provided invaluable opportunities to broaden my horizon in terms of structural and earthquake engineering.

I am also thankful to Dr. Oğuz Cem ÇELİK, Dr. Özgür AVŞAR, and Dr. Cem DEMİR for their invaluable contributions to the preparation of this thesis. I would like to deeply appreciate and thank Dr. Tayfun KAHRAMAN and Sibel ÖZKAN for their support as well.

I also wish to express my gratefulness to Dr. Mehmet Nuray AYDINOĞLU, Dr. Zekai CELEP, Dr. Ufuk YAZGAN, Dr. Kutay ORAKÇAL, Nusret SUNA, Dr. Recep İYİSAN, and Dr. Mustafa ERDİK for their help and recommendations in the conducted pilot study. The valuable contributions of Dr. Nahit KUMBASAR, Dr. Mustafa CÖMERT, Mucip TAPAN, and Denizhan ULUĞTEKİN during the development of the initial version of PERA method are highly acknowledged.

I acknowledge the technical support provided by Istanbul Metropolitan Municipality for supplying the structural parameters of the buildings in Istanbul (permission date 08.01.2021, BK ID=8 and permission date 15.12.2021, ID= 1621140). As the deputy manager of the directorate that implements the building investigation service, I was responsible to create the academic background and technical outlines of this procedure. Thus, I studied my Ph.D. on this topic with provided permission given by İŞAT directorate. During these studies, my colleagues at Istanbul Metropolitan Municipality were also worked to develop these studies and evaluate the buildings in Istanbul.

I also want to acknowledge the support of Middle East Technical University SERU Database for supplying the plans of the damaged buildings.

For their invaluable contributions to my academic life and my earthquake engineering perspective, I would like to give my thanks to Dr. Barış ERKUŞ, Dr. İhsan Engin BAL, and Dr. Yücel GÜNEY.

For being a wonderful teammate during all our site visits to the disaster area of the 2023 Kahramanmaras Earthquakes and his great friendship during our PhD adventure, I sincerely thank Dr. Kurtuluş ATASEVER.

I am also thankful to Selahaddin GÜMÜŞ, my elementary school teacher, who taught me the virtue of fairness and idealism as a child, the late Colonel Adnan MÜEZZİNOĞLU, my Math teacher, who taught the logic of Math in the military school, my Commander Colonel Emin ARIKAN, Cimbom Old Boys, players of The Wall Spor Kulübü, cyclists of Reservoir Dogs, my colleagues at İŞAT.

I would like to thank my family members for their support in my graduate studies.

My beloved one and dear wife, Atife Elif TÜRK AYDOĞDU, deserves the most special spot in this chapter. I am always amazed at how she has been understanding, supportive, and patient during my graduate studies. During the hard times in the proficiency phase and my thesis, I found the strength to overcome every obstacle thanks to her. I dedicate my thesis to her for all the happiness she gave me.

Finally, I want to thank the founder of the modern Turkish Republic, Mustafa Kemal ATATÜRK, for demonstrating the importance of progress in the direction of civilization and science.

December 2023

Hasan Hüseyin AYDOĞDU
(M.Sc. In Earthquake Engineering)

TABLE OF CONTENTS

Page

ABBREVIATIONS

AFAD	**:** Disaster and Emergency Management Presidency
AS2008	**:** Abrahamson and Silva (2008)
C	**:** Collapse
CD	**:** Controlled damage
CP	**:** Collapse prevention
EDC	**:** Earthquake Design Classes
GIS	**:** Geographic Information Systems
GMPE	**:** Ground motion prediction equations
IDA	**:** Incremental dynamic analysis
IEMP	**:** Istanbul Earthquake Master Plan
IMM	**:** Istanbul Metropolitan Municipality
PGA	**:** Peak Ground Acceleration
PRC	**:** Performance Reduction Coefficient
RBTE-2019	**:** Provisions for the Seismic Risk Evaluation of Existing Buildings 2019
RC	**:** Reinforced Concrete
RVS	**:** Rapid Visual Screening
SSR	**:** Seismic Safety Ratio
TBEC-2018	**:** Turkish Building Earthquake Code 2018
TSDC-1975	**:** Turkish Seismic Design Code 1975
TSDC-1998	**:** Turkish Seismic Design Code 1998
TSDC-2008	**:** Turkish Seismic Design Code 2007

SYMBOLS

A_c	: Cross-sectional area of the columns and shear walls
A_{sh}	: Cross-sectional area of transverse reinforcement
f_{cm}	: Compressive strength of concrete
f_i	: Non-destructive test result of the column
H_w	: Shear wall height
l_w	: Shear wall length
N_k	: Axial load acting on each column and shear wall
Nr	: Column axial load capacity
m_{limit}	: Demand/capacity ratio limit for the element
M_w	: Moment magnitude
n	: The number of columns and shear walls
s	: Stirrup spacing
S_{DS}	: Short period design spectral acceleration coefficients
T_1	: Vibration period of first mode
V_e	: Flexural shear demand
V_r	: Shear strength
V_{s30}	: Average shear-wave velocity in the top 30 m layer of the soil
V_{risky}	: The sum of the shear forces carried by critical story columns and shear walls that are classified as risky
V_{story}	: Story shear force
w	: Crack width
$(\delta/h)_{limit}$	: Allowed drift limit for the element
ξ	: Damping ratio

LIST OF TABLES

Page

LIST OF FIGURES

Page

STRATEGIES FOR SEISMIC RISK MITIGATION BY CONSIDERING ECONOMIC CRITERIA ON A REGIONAL BASIS

SUMMARY

Exposure, hazard and vulnerability are the components of seismic risk, and knowledge on the vulnerability of the existing buildings is vital to properly assess their risks in seismically active regions. Unfortunately, it is not easy to assess the vulnerability of individual buildings realistically in large building stocks, particularly for regions where the buildings do not comply with the current and/or previous code regulations. The first step for ensuring seismic resilience is the identification of risky buildings, which is a difficult challenge for metropolises like Istanbul since the building stock consists of over a million buildings. Applying code-based detailed assessments to so many buildings is not practical in terms of time and cost. Moreover, the current code-based detailed assessment methodologies provide discrete predictions for existing buildings as either risky or non-risky. However, a ranking system based on a reliable and realistic risk classification to prioritize the buildings is needed. To cope with this problem, a simplified and economical, yet reliable and realistic rapid seismic assessment method need to be applied to hundreds of thousands of buildings to pave the way for planning interventions in a rational and prioritized way. Thus, this huge problem can be reduced to a manageable scale.

In this thesis, for assessing the reliability, applicability and cost-effectiveness of available rapid seismic safety assessment procedures for individual reinforced concrete buildings in huge building stocks, five second stage and three rapid visual screening methods are examined in a comparative manner. For this purpose, these eight methods are used to assess the seismic risks of actual service buildings of Istanbul Metropolitan Municipality, which had been previously evaluated by the third-level detailed code-based seismic performance assessment procedures. Furthermore, comprehensive site works have been conducted to compute the average time required for collecting data on each parameter necessary to use the investigated rapid assessment methods.

Then, based on the findings of this study, the reliability of the most accurate and yet cost/time-efficient rapid assessment method, PERA2019, is evaluated by comparing the risk classes of the buildings determined by the implementation of the rapid assessment methodology with actual earthquake-induced damages. Also, another reliability assessment is made by comparing the risk classess of actual buildings with the results of a more detailed assessment procedure (Incremental Dynamic Analysis). Consequently, the safety margin of the classification approach was measured in light of the findings. The validation studies showed that all heavily damaged or collapsed buildings are found high or very high risky according to the methodology.

Based on the outputs of evaluation of rapid seismic safety assessment methods on a substandard reinforced concrete building stock in Istanbul, which is prepared as Chapter 2 of this thesis, as a pilot project, nearly 23,000 reinforced concrete buildings from 37 different districts of Istanbul have already been investigated by Istanbul Metropolitan Municipality through the PERA2019 rapid assessment methodology by considering the Design Level and Scenario-Based Earthquake cases. In this thesis, the structural characteristics of the building stock of Istanbul obtained through the site investigations conducted during this study are outlined. Furthermore, a discussion is

presented on the estimated seismic performances of the examined existing residential buildings based on the analyses conducted for the Design Level and Scenario-Based Earthquake cases through the presented algorithm. Finally, an estimation study on the seismic risk of the building stock in Istanbul is made based on the generated probability of exceedance curves from the data provided from the site works. Then, two different risk mitigation strategies are proposed, and a cost-benefit analysis is made to evaluate the efficiency of the risk mitigation strategies proposed. The findings of this thesis show that the highest post-earthquake costs are observed in the absence of any pre-earthquake intervention. The maximum reduction in the cost is not reached in the case of intervening all buildings. The optimum amount of building must be intervened to reach the maximum cost reduction varies with respect to considered intervention strategy.

With the original studies carried out within the scope of this dissertation, a method was proposed to determine the seismic risk levels of building stock in metropolises that are waiting for their next major earthquake in the near future in a rapid way without compromising consistency; a solution to fill the gap in current regulations was studied. Then, an incremental risk ranking and classification approach for sub-standard buildings, which is not defined in 2019 Provisions for the Seismic Risk Evaluation of Existing Buildings and 2018 Turkey Building Earthquake Code, was proposed; the reliability of the approach was evaluated. Risk distribution and preliminary cost/benefit estimates based on the data of approximately 23,000 buildings examined through the outputs of this thesis showed that risk reduction studies to be carried out in accordance with the recommended prioritization approach reflect the most efficient strategy.

BÖLGE BAZINDA EKONOMİK KRİTERLER GÖZ ÖNÜNDE TUTULARAK DEPREM RİSKLERİNİN AZALTILMASINA YÖNELİK STRATEJİLER

ÖZET

Türkiye'de 1960'lı yıllara kadar %30'un altında olan kentsel nüfus oranı, bu dönemden itibaren yaşanan göçlerle başlamış, bu artış 70'li yıllarla birlikte doruğa ulaşmıştır. Kentlerde bu süreçte artan barınma talebine karşılık verecek miktarda konut bulunmaması hızlı ve kontrolsüz bir yapılaşmayı beraberinde getirmiş, birçok konut türü bina mühendislik hizmeti almadan ve yapıldıkları dönemde yürürlükte olan deprem ve tasarım yönetmeliklerine uyulmadan üretilmiştir. Dahası, yönetmeliklere göre tasarlanan binalar çoğu zaman tasarım projelerine ve dikkate alınan malzeme standartlarına uyulmadan, kötü işçilikle üretilmiştir. Aktif bir deprem kuşağında yer alan ülkemizde geçmişten beri yerleşim birimleri depremler sebebiyle önemli kayıplar yaşamış olsa da 1999 yılında Marmara Bölgesi'nde gerçekleşen Kocaeli ve Düzce depremlerinin ağır sonuçlarıyla karşılaşılana kadar ülkede deprem farkındalığı yeterince oluşmamış, 2001 yılında Yapı Denetim Kanunu yürürlüğe girene kadar bir denetim mekanizması işlememiştir. Bu dönem sonrasında ise denetim mekanizmasının kurulması, 1999 depremlerinin sağladığı bilinçlenme, malzeme teknolojisindeki gelişmeler, deprem mühendisliği alanındaki bilgi birikiminin ilerlemesi gibi sebeplerle inşa edilen binaların deprem güvenliklerinde gözle görülür bir artış gerçekleşmiştir. Ancak İstanbul'da mevcut bulunan binaların %68'i 2000 yılı öncesinde inşa edilmiştir. Bu binaların büyük bir çoğunluğu; 1972 Deprem Bölgeleri Haritasında ikinci derece deprem bölgesine ait taleple tasarlandığı ve bahsedilen eksikliklere sahip olduklarından, günümüzde yürürlükte olan 2018 Türkiye Bina Deprem Yönetmeliği veya 2019 Riskli Bina Tespit Esaslarına göre incelenmeleri sonucunda Riskli ya da Göçme Bölgesinde çıkmaları olasıdır. Ancak bilinmektedir ki günümüzde yeterli deprem güvenliğini sağlayamadığı düşünülse de eski yönetmeliklere uygun yapılan binalar, geçmiş depremlerde can güvenliğini sağlamayı başarabilmiştir. Bunun yanında, İstanbul gibi büyük kentlerde bulunan yüz binlerce 2000 yılı öncesi inşa edilmiş binayı mevcut yönetmeliklere göre detaylı mühendislik incelemesine tabi tutmak zaman ve ekonomi kriterlerine göre verimli gözükmemektedir. Gelecekte İstanbul'u etkilemesi olası bir depremde can ve mal kayıplarının en aza indirilmesi ve risk azaltma çalışmalarında kaynakların en verimli şekilde değerlendirilebilmesi için söz konusu görece yüksek riskli bina stokunun yapısal olarak hızlı, mekanik ve tutarlılığı yüksek bir yöntemle incelenmesi ve incelenen binaların sınıflandırılarak bir triyaj sistemine tabi tutulması gerekmektedir. İstanbul Deprem Master Planı (2003) bu doğrultuda kademeli bir değerlendirme yaklaşımı tanımlamış; bahse konu bina stokunun tamamına yakını hakkında alınacak kararın, binaların içerisinden taşıyıcı sistem bilgilerinin toplandığı ve mekanik hesaplamalar yapılan ikinci kademe değerlendirme aşamasında alınması gerektiği, kritik öneme sahip olan ya da performans olarak gri bölgede kalan binalarda ancak daha ayrıntılı bir inceleme çalışması yapılmasının uygun olacağı belirtilmiştir. Bu ihtiyaçlar doğrultusunda İstanbul genelinde gerçekleştirilecek yaygın bina inceleme çalışmalarında kullanılmak

üzere, 5 adet ikinci kademe, 3 adet ise birinci kademe sokak taraması yöntemi pilot bir çalışmayla incelenmiştir. Seçilen yöntemlerin tutarlılığı, ayrıntılı olarak yürürlükteki deprem yönetmeliklerine göre incelenmiş binaların sonuçlarıyla karşılaştırılarak tespit edilmiş, bu çalışmalar tezin 2. bölümünde derlenmiştir. Yapılan çalışmalar sonucunda hız, tutarlılık ve ekonomiklik bakımından en verimli yöntem olarak, yönetmelik tabanlı değerlendirme yaklaşımına sahip olan PERA2019 yöntemi seçilmiştir. Yapılan analizler sonucunda 615,000 1-10 katlı betonarme binanın 2'şer mühendisten oluşan 100 ekiple seçilen yönteme göre incelenmesinin 4.4 yıl süreceği ve bu çalışmanın Türkiye Bina Deprem Yönetmeliğine göre bu binaların incelenmesi maliyetinin %3'üne mal olacağı görülmüştür. Çalışmanın aynı ekip miktarıyla Türkiye Bina Deprem Yönetmeliğine uygun bir şekilde tamamlanabilmesi için yaklaşık 147 yıllık bir zaman zarfı gerekmektedir.

Tezin 3. bölümünde PERA2019 yöntemi, yöntemin artımsal yaklaşımı ve önerilen 5 risk sınıflı derecelendirme sisteminin güvenilirliği deprem hasarlı binalar ve artımsal dinamik analiz sonuçlarıyla karşılaştırılarak belirlenmiştir. Çalışmalar göstermiştir ki yöntem ağır hasarlı ve yıkık binaların tamamını yüksek veya çok yüksek riskli olarak değerlendirmeyi başarmış, hasarsız ve hafif hasarlı binalardaki riski ise genel olarak daha düşük seviyede göstermiştir. Ayrıca artımsal dinamik analizler göstermiştir ki yöntemin bulduğu deprem güvenliği oranı değerleri ve risk sınıfları büyük çoğunlukla ayrıntılı yöntemin sonuçlarıyla uyumlu bulunmuştur. Bunun yanında, bu bölümde incelenen binalar içerisinde 1975 yönetmeliğine göre tasarlanmış olanların, projelerine uygun olarak inşa edilmiş olmaları halinde mevcut durumlarına oranla ortalama 2 kattan fazla deprem güvenliği sağlamış olacağı sonucuna varılmıştır.

Bu bilgiler ışığında PERA2019 yöntemi ve belirlenen risk sınıflandırma yaklaşımı İstanbul'un 37 ilçesinde yaklaşık 25000 binaya uygulanmıştır. Uygulanan binalar üzerinden yapılan çıkarımlar 4. bölümde özetlenmiş, saha çalışmaları sonucunda ise binaların tamamına yakınının günümüz yönetmeliklerinin deprem taleplerini karşılayamadığı görülmüştür. Bu bölümde yapılan çalışmalarla, mevcut binaların sınıflandırılması ve risklerinin azaltılmasında, yeni bina tasarımı için talep edilen deprem seviyesi olan Tasarım Depreminin kullanılmasından ziyade, 7.5 büyüklüğündeki Senaryo Depreminin parametrelerinin kullanılması, yaklaşan depreme hazırlık çalışmalarında çok daha etkili bir yaklaşım olarak ön plana çıkmış; Tasarım Depremine göre incelemelerde binaların yaklaşık %80'inin yüksek veya çok yüksek riskli olması nedeniyle problemin çözümsüz bir noktaya geldiği anlaşılmıştır. Ayrıca yapım yıllarına göre binaların durumları incelendiğinde, 1999-2000 yıllarına kadar bina stokunun deprem güvenliği ve yapısal parametrelerinde gözle görülür bir iyileşme tespit edilememiştir.

Gerçekleştirilen çalışmalarda yapılan çıkarımlar, incelenen binaların kapsamıyla sınırlı olacağından, bina stokunun geneli hakkında bir görüş elde ederek, risk azaltma stratejilerinin gerçeğe daha yakın şekilde üretilebilmesi adına risk dağılımı ve ekonomik kayıp tahmini çalışmaları, saha çalışmalarından elde edilen veriler ışığında gerçekleştirilmiştir. İlçelerden gelen verilerle her ilçeye has kırılganlık eğrileri, farklı kat sayısına sahip binalar için üretilmiştir. Bu eğriler yardımıyla yaklaşık 580,000 bina üzerinde risk tahmini yapılmıştır. Çalışma sonucunda gelen risk dağılımları, saha çalışmalarıyla paralel olmakla birlikte, Senaryo Depremine göre stokun %19'u çok yüksek riskli, %22'si ise yüksek riskli çıkarken; Tasarım Depremine göre çok yüksek riskli binaların oranı %40, yüksek riskli binaların oranı ise %31 olarak tespit edilmiştir.

Tezin son bölümünde fayda/maliyet analizleri tamamlanmıştır. Analizler ışığında yalnızca yıkıp yapma yönteminin maddi olarak kayıp azaltmada yeterince etkili olmadığı belirlenmiştir. Çalışmalar göstermiştir ki optimum sayıdaki binaya kadar binaların riskini azaltmak, deprem öncesi müdahale ve deprem sonrası zarar maliyetlerinin toplamını azaltırken, bu miktardan fazla binaya müdahale ediyor olmak (yıkıp yeniden yapma veya güçlendirme) toplam maliyeti artırmaktadır. Bu husus, yüksek ve çok yüksek riskli bulunan binaların risk azaltma çalışmalarında ilk müdahale edilmesi gerekenler olarak ele alınması, orta ve düşük riskli olarak tespit edilmiş binaların ise çok sonra müdahale edilecek binalar olarak öncelik dışı nitelendirilmesi gerektiğini göstermektedir. Ayrıca, yeniden yapım ile güçlendirme seçeneği arasında maliyet/fayda analizi açısından ciddi getiri farkı tespit edilmiştir. Hem risk azaltma çalışmalarının aciliyeti, hem de problemin boyutları düşünüldüğünde; yüksek veya çok yüksek riskli olup güçlendirilmesi verimli çıkan bütün binaların güçlendirilip, verimli bir şekilde güçlendirilemeyen binaların yeniden yapıldığı hibrit bir stratejide, mevcut durumda 7.5 büyüklüğündeki Senaryo Depreminin gerçekleşmesiyle oluşacak zarara kıyasla %72 seviyesine kadar maliyet azalışı sağlanabilmektedir. Aynı miktarda binanın yeniden yapıldığı senaryo ise ancak %49'luk bir maliyet azalışı yaratacaktır ve bu müdahale stratejisinin uygulama süresinin hibrit stratejiye göre çok daha uzun olacağı tespit edilmiştir.

Bu doktora tezi kapsamında yapılan çalışmalar ile yakın gelecekte büyük bir depreme maruz kalma tehlikesi altında bulunan şehirlerde konut stokunun riskinin, tutarlılıktan taviz vermeden en hızlı bir şekilde tespiti için bir yöntemin önerilmesi yapılmış; yasal mevzuattaki bu eksiklik için bir çözüm önerisi yapılmıştır. Ardından günümüzde 2019 Riskli Bina Tespit Esasları ve 2018 Türkiye Bina Deprem Yönetmeliğinin barındırmadığı, mevzuatın şartlarını sağlamayan mevcut binaların risk seviyelerine göre önceliklendirilmesi önerilmiş, önerilen artımsal sıralama ve sınıflandırma yöntemlerinin güvenilirliği incelenmiştir. Üretilen çıktılar üzerinden incelemesi yapılan yaklaşık 23,000 binanın verisinden yola çıkarak gerçekleştirilen risk dağılımı ve fayda/maliyet tahminleri ise önerilen önceliklendirme yaklaşımına uyularak yapılacak risk azaltma çalışmalarının en verimli stratejiyi yansıttığını göstermektedir. 6 Şubat 2023 depremleri sonrasında görülmüştür ki bu tezin önerdiği şekilde deprem öncesinde yapılacak müdahaleler, afet kayıplarının önlenmesi açısından kritik öneme sahiptir.

1. INTRODUCTION

1.1 Purpose and Outlines of Thesis

Seismic risk mitigation is a great challenge in earthquake-prone regions of the world. To reduce seismic losses in future earthquakes, a widespread structural assessment campaign should take place to identify buildings with insufficient seismic performance. According to "Istanbul Metropolitan Municipality, Project for Updating Probable Earthquake Loss Estimates for Istanbul Province", which was prepared by Istanbul Metropolitan Municipality (IMM) and Bogaziçi University in 2019 (Cakti et al, 2019), the building inventory of Istanbul consists of 1,163,000 buildings, which include residential, industrial, commercial and public ones. Aerial photographs, base maps, orthophotos, and satellite images show that nearly 70% of the buildings in Istanbul were constructed before the 1999 Marmara earthquakes. Seismic evaluation of the building stock is the primary step of the seismic risk mitigation works in Istanbul, which is one of the biggest metropolises and is prone to a potential severe earthquake in the near future. Cakti et al. (2019) state that nearly 194,000 buildings (16% of all buildings) in Istanbul will experience intermediate or heavy damage under an Mw=7.5 scenario earthquake, which has a return period of about 250 to 300 years and is defined on a 120 km long fault segment (named as Model A in Earthquake Master Plan for Istanbul, 2003 - EMPI, 2003) from west of the 1999 Kocaeli Earthquake fault to Silivri district. This estimation was made through fragility analyses on the city scale, and the buildings were classified according to their structural systems, number of stories, and year of construction. To reduce the potential losses during future earthquakes, seismic performances of the existing substandard buildings must be improved and this should be done through a realistic prioritization since the resources are limited. However, the building stock of Istanbul has a wide range of unknowns to be unleashed. Those unknowns stem from an era that starts with the massive population growth in the mid-1970s, a time when a huge need for accommodation emerged and the residential building inventory could not meet that demand. Consequently, a rapid construction process started in the city, since the

capacity of producing residential buildings in the country was insufficient when compared to the new building demand. Indeed, this situation led to a lack of control over construction. Most of the buildings were built without having proper engineering service and control during their design and construction phases. Furthermore, in many cases, the ones that had a structural design project were not constructed as compliant with their projects. After 1999, seismic awareness in Turkey started to increase due to two major earthquakes striking the eastern part of the Marmara region (Ilki and Kumbasar, 2000; Ozmen, 2000; Ozdemir et al, 2002). As a result, the structural characteristics of most of the old buildings constructed prior to the 2000s in Istanbul do not comply with the provisions of current and past regulations.

In general, it can be indicated that as the seismic evaluation method gets more detailed and complicated (as in the case of code-level methods), the accuracy of the method increases. However, approximately 800,000 buildings in Istanbul were constructed before the year 2000, and performing code-level thorough investigations for such a high number of buildings is not efficient or feasible both in terms of time and cost. To overcome this problem, simplified and economical, yet reliable and realistic seismic assessment methods need to be applied, so that this vast problem at hand can be reduced to a manageable scale. Besides the code-based detailed seismic evaluation methods, there are many rapid seismic evaluation methods available for existing buildings. EMPI (2003) proposes three stages for the evaluation of the seismic safety of buildings. In the first stage of the procedure, which is called rapid visual screening (RVS) in this paper, buildings are ranked according to simple parameters, which are collected through a street survey, that takes approximately 20 minutes per building. This phase of the assessment procedure yields a rough seismic performance ranking for building stock, and the regional concentration of seismically vulnerable buildings is determined. The RVS methods are mostly based on empirical approaches. The second stage evaluation requires more detailed mechanical parameters to be collected in one to two hours per building. The calculation steps of these methods are developed based on mechanical computations. EMPI (2003) asserts that the decisions of almost all low-rise buildings should be made with this level of knowledge.

The third stage assessment is for public and service buildings or complex structures, which shouldn't be evaluated by simplified methods according to EMPI (2003). The works to be carried out for this comprehensive seismic assessment stage is detailed by

the current seismic assessment codes and guidelines. The data collection process at this stage is significantly longer than rapid assessment methods. Various insitu works for collecting data on the material qualities (i.e. concrete core or steel bar samples to be extracted from the structural members), destructive and non-destructive inspections for reinforcement details and building geometry are collected depending on the seismic evaluation document that is considered. Generally, a finite element model is established to conduct the structural analysis and the obtained internal forces and deformations (such as drift ratios, rotations or material strains) are compared with the thresholds provided by the code for target performance levels. All three levels of knowledge have their own benefits. It is generally assumed that the RVS is the quickest and most cost-friendly evaluation approach, while detailed assessment is the most accurate and expensive one in terms of time and cost. Second stage preliminary assessments are at the optimum point between cost and accuracy.

In Chapter 2 of this thesis, five second stage and three RVS methods are applied on service buildings of Istanbul Metropolitan Municipality, which were previously evaluated by detailed code-level assessments. To demonstrate which available rapid building-scale seismic safety assessment method better fits the existing building stock in Istanbul in terms of yielding realistic results and applicability, actual site investigations are conducted on a large number of existing buildings, which are selected to reflect the characteristics of the building stock in Istanbul including many sub-standard ones built before the 2000s. The required time to collect the necessary data for each assessment method is determined based on the outputs of the performed site work, which constitutes another original aspect of the presented thesis. Then, the results of the considered methods are compared with code-based analyses to evaluate the accuracy of the methods and choose the methods that can be applied to nearly 23,000 sub-standard reinforced concrete buildings in Istanbul by IMM. Such a comparative study is believed to be crucial to avoid significant loss of time and budget through the use of less realistic and inefficient rapid seismic safety evaluation approaches. Additionally, a feasibility study is also conducted for the potential application of the investigated methods to nearly 600,000 pre-2000 RC buildings in Istanbul in terms of the required time and budget. Recently, the urgency of rapid seismic assessment of the existing building stock has been better understood after the destruction caused by the 2023 Kahramanmaraş-Hatay Earthquakes in Turkey, and

rapid assessment works have been initiated in many cities. Also in Istanbul, it is reported that demand from the citizens to IMM for rapid assessment studies has nearly reached to 150,000 buildings. Furthermore; this chapter of the thesis is very timely because many city administrations in seismic areas of the world tend to utilize rapid methods for such evaluations (Url-1, Url-2, Url-3). So that the intervention strategies for loss mitigation can be shaped and developed for buildings with high seismic risks.

As aforementioned, these relatively old, sub-standard and deteriorated buildings must be assessed urgently in terms of their potential seismic performance in order to take necessary measures in a rationally prioritized approach to minimize losses against future earthquakes. On the other hand, conducting a widespread code-based detailed evaluation for such a high number of buildings is inefficient both in terms of cost and time, if not impossible. To reduce this huge problem to a manageable scale, a simplified and economical, yet reliable and realistic rapid seismic assessment method is needed for planning intervention strategies in a rational and prioritized way.

Current regulations on seismic assessment in Turkey such as Provisions for the Seismic Risk Evaluation of Existing Buildings under Urban Renewal Law (2019) (RBTE-2019) and Turkish Building Earthquake Code (2018) (TBEC-2018) classify the existing buildings either as risky or un-risky or satisfying a target performance level (such as life safety-controlled damage) or not. As aforementioned, a structural engineering investigation according to the code classification of the buildings of Istanbul will probably show the fact that almost every ordinary building constructed before the year 2000 is to be labeled as risky (or they will not satisfy the life safety/controlled damage performance target). Considering hundreds of thousands of such buildings, obviously, this is not a sustainable approach, and the vastness of the problem puts back the efforts to make Istanbul more resilient. A rapid, reliable, and realistic seismic performance ranking procedure for building stock is a key issue to prioritize buildings, which is missing in current official seismic design codes in most countries. A considerable way to fill this gap is sorting the building inventory by their approximately calculated seismic capacity to demand ratios so that the primary targets for mitigation works can be determined in an effective way. Actually, in some earthquake-prone countries, important steps have recently been taken toward such categorization. A risk-based framework for managing earthquake-prone buildings has been published in New Zealand (NZSEE, 2017), and the validation of the SLaMa

procedure available in this framework was made by Gentile et al. (2019). The procedure classifies buildings into six risk classes in terms of the New Building Standard% (NBS%). D and E Class buildings, with an NBS% less than 1/3, have to be intervened to reach at least 2/3 NBS level. The allowed time window to mitigate the seismic risk of the building changes with the seismicity of the region and the building's importance. In Italy, the Sismabonus framework which enables tax deductions after seismic strengthening interventions on buildings has been introduced (Di Ludovico et al, 2016; Polese et al, 2018; Cosenza et al, 2018). This mechanism defines the seismic risk class of a building as the minimum class defined by the building safety index at the ultimate limit state IS-V and the one related to expected annual loss EAL (Polese et al, 2018). The building safety index IS-V divides buildings into 7 different classes A+ to F.

As the probability of a catastrophic earthquake that could hit Istanbul is very high in the near future (Parsons et al, 2000), it is gravely important to identify the most vulnerable existing buildings and prioritize them according to their seismic risks to minimize losses. Thus, the aim of the rapid seismic methodology that is assessed in this thesis is to find those buildings with a cost and time-effective yet sufficiently accurate approach. IMM has started a rapid and cost/time-efficient seismic assessment campaign in Istanbul through PERA2019 methodology. In Chapter 3 of this thesis, the reliability of the rapid seismic safety assessment methodology used in Istanbul (PERA2019) and its risk prioritization approach are evaluated through a database of actual structural seismic damages of actual buildings established based on damage survey reports prepared after earthquakes that affected different regions of Turkey (Afyon, 2002; Bingöl, 2003; Aegean Sea, 2020). The validation study showed that all heavily damaged or collapsed buildings are found high or very high risky according to the methodology. The seismic performance of the buildings that were constructed before 2000 during the 2023 Kahramanmaraş earthquakes was investigated thoroughly in the disaster area by the author of this thesis several times. Most of the buildings that caused life losses were not built according to their codes and did not meet the minimum requirements of their era's seismic design codes. The lessons that were learned from the 2023 Kahramanmaraş earthquakes dictate that there is an urgency of implementing seismic performance assessment on the country scale in Turkey. Computing the seismic safety of the buildings and classifying them through an economical and time-

effective yet sufficiently accurate rapid performance based analysis approach can respond to the urgency of the risk mitigation studies, so interventions can start from the buildings containing the highest seismic risk. The proposed approach takes the deficiencies that the building stock has and the probable effects of these weaknesses into consideration.

In Chapter 4 of this thesis, seismic performances of nearly 23,000 sub-standard buildings, which were investigated by IMM, are evaluated through PERA2019 methodology and ranked by their seismic risk level from low risk to very high risk. The PERA2019 methodology shares the common approach of defining the seismic safety index of the building as the ratio of the building's seismic capacity to demand (i.e. code-based demand for a new building or demand from a scenario earthquake) as also done for NBS% of NZSEE (2017) and IS-V of Sismabonus frameworks. The method is comprised of simplified data collection from the building, determination of seismic demand in means of peak ground acceleration (PGA) and spectral acceleration, and a series of linear analyses for calculating the PGA capacity of the building corresponding to the critical story mechanism case. The PERA2019 approach steps forward among similar methods with its ease in application to low- and mid-rise reinforced concrete buildings not only for simplified data collection (an investigation team can inspect, assess and report three to five buildings per day) but also for easy-to-follow linear analysis algorithm already familiar to many engineers. The structural characteristics of the building stock of Istanbul obtained through the site investigations conducted during this study are outlined. The detailed structural information is gathered, processed and presented from actual 23,000 pre-2000 buildings through an extensive site study campaign. These buildings are in Istanbul, which is one of the most critical cities in the world in terms of seismic risk. This is a very significant number for the application of a second-stage seismic assessment methodology. No such application in this scale exists in the summarized literature. Few previous screening studies are conducted through RVS (street survey) approaches and mostly on small scales as mentioned above. The main target of this chapter of the thesis is to identify those with the highest risk of causing loss of life out of 800,000 pre-2000 buildings, which are known to have a certain level of risk, and to intervene them as quickly as possible. As aforementioned, randomly intervening this amount of buildings without implementing rapid yet reliable structural assessment procedures is

not practical. Furthermore, a discussion is presented on the estimated seismic performances of the examined existing residential buildings based on the analyses conducted for the Design Level and Scenario-Based Earthquake cases through the presented algorithm. This chapter of the thesis demonstrates that it would not be reasonable to prioritize this amount of buildings according to the design level earthquake, and this approach will require long years to complete the risk mitigation study in Istanbul, in which the probability of a catastrophic earthquake could hit is very high in the near future (Parsons et al, 2000).

In Chapter 5, 12 existing buildings reflecting a wide range of SSR values were selected and modeled, which is to be submitted as another academic study. Also, 10 of them were modeled as in their original projects, which were prepared according to TSDC-1975. Then, incremental dynamic analysis (IDA) and PERA2019 methodologies were conducted for each building, and the results were compared to each other for validation of the proposed risk classification and performance-based incremental rapid assessment procedure. In the final step, seismic safety and the risk classes of the buildings for as-built and as-designed cases are determined to evaluate the seismic safety provided by TSDC-1975.

In Chapter 6, the outputs and findings of the site works are extrapolated to the building stock in Istanbul based on the probability of exceedance curves obtained from 37 districts of the city to exhibit the extents of the seismic risk mitigation needs. The probability of exceedance of the spectral acceleration demands for actual buildings is determined for different typologies. Afterward, an estimation study is performed to predict the risk class distribution for all structures of the city on the district and neighborhood scale. This study highlights the high priority regions for performing widespread performance-based analysis work and foresight for further steps of the mitigation efforts, such as the approximate number of buildings to be intervened. Then, cost-benefit analysis of pre-earthquake studies and post-earthquake costs are made to determine the optimum intervention strategy. The seismic preparedness studies to be made before earthquakes prevent the enormous economical losses that will occur after the earthquake. In this section, the outputs of the studies carried out within the scope of this thesis and the efficiency of seismic risk mitigation strategies in terms of risk and cost reduction are determined based on the example of the building stock in

Istanbul. In the final step, a comment is made on the most efficient intervention strategies.

2. EVALUATION OF RAPID SEISMIC SAFETY ASSESSMENT METHODS ON A SUBSTANDARD REINFORCED CONCRETE BUILDING STOCK IN ISTANBUL[1]

2.1 General Outlines

Exposure, hazard and vulnerability are the components of seismic risk, and knowledge on the vulnerability of the existing buildings is vital to properly assess their risks in seismically active regions. Unfortunately, it is not easy to assess the vulnerability of individual buildings realistically in large building stocks, particularly for regions where the buildings do not comply with the current and previous code regulations. In this study, for assessing the accuracy, applicability and cost-effectiveness of available rapid seismic safety assessment procedures for individual reinforced concrete buildings in huge building stocks, five second stage and three rapid visual screening methods are examined in a comparative manner. For this purpose, these eight methods are used to assess the seismic risks of actual service buildings of Istanbul Metropolitan Municipality, which had been previously evaluated by the third-level detailed code-based seismic performance assessment procedures. Furthermore, comprehensive site works have been conducted to compute the average time required for collecting data on each parameter necessary to use the investigated rapid assessment methods. Finally, the most cost and time-effective, and highly accurate rapid assessment method among the examined ones is selected to be applied to a vast amount of structures in Istanbul to prioritize them in terms of their seismic risks and plan the large volume mitigation interventions through a realistic and efficient approach.

[1] This chapter is based on the following publication: Aydogdu, H. H., Demir, C., Kahraman, T., and Ilki, A. (2023) Evaluation of Rapid Seismic Safety Assessment Methods on a Substandard Reinforced Concrete Building Stock in Istanbul, Structures, Volume 56, 2023, 104962, ISSN 2352-0124, https://doi.org/10.1016/j.istruc.2023.104962.

2.2 Summary of the Literature

Seismic risk mitigation is a great challenge in earthquake-prone regions of the world. To reduce seismic losses in future earthquakes, a widespread structural assessment campaign should take place to identify buildings with insufficient seismic performance. According to “Istanbul Metropolitan Municipality, Project for Updating Probable Earthquake Loss Estimates for Istanbul Province”, which was prepared by Istanbul Metropolitan Municipality (IMM) and Bogaziçi University in 2019 (Cakti et al, 2019), the building inventory of Istanbul consists of 1,163,000 buildings, which include residential, industrial, commercial and public ones. Aerial photographs, base maps, orthophotos, and satellite images show that nearly 70% of the buildings in Istanbul were constructed before the 1999 Marmara earthquakes. Seismic evaluation of the building stock is the primary step of the seismic risk mitigation works in Istanbul, which is one of the biggest metropolises and is prone to a potential severe earthquake in the near future. Cakti et al. (2019) state that nearly 194,000 buildings (16% of all buildings) in Istanbul will experience intermediate or heavy damage under an Mw=7.5 scenario earthquake, which has a return period of about 250 to 300 years and is defined on a 120 km long fault segment (named as Model A in Earthquake Master Plan for Istanbul, 2003 - EMPI, 2003) from west of the 1999 Kocaeli Earthquake fault to Silivri district. This estimation was made through fragility analyses on the city scale, and the buildings were classified according to their structural systems, number of stories, and year of construction. To reduce the potential losses during future earthquakes, seismic performances of the existing substandard buildings must be improved and this should be done through a realistic prioritization since the resources are limited. However, the building stock of Istanbul has a wide range of unknowns to be unleashed. Those unknowns stem from an era that starts with the massive population growth in the mid-1970s, a time when a huge need for accommodation emerged and the residential building inventory could not meet that demand. Consequently, a rapid construction process started in the city, since the capacity of producing residential buildings in the country was insufficient when compared to the new building demand. Indeed, this situation led to a lack of control over construction. Most of the buildings were built without having proper engineering service and control during their design and construction phases. Furthermore, in many cases, the ones that had a structural design project were not constructed as compliant

with their projects. After 1999, seismic awareness in Turkey started to increase due to two major earthquakes striking the eastern part of the Marmara region (Ilki and Kumbasar, 2000; Ozmen, 2000; Ozdemir et al, 2002). As a result, the structural characteristics of most of the old buildings constructed prior to the 2000s in Istanbul do not comply with the provisions of current and past regulations.

Dolce (2012) described the Italian National Seismic Prevention Program in three main steps: improvement of knowledge, reduction of the vulnerability and mitigation of the effects, which are also valid for other seismic-prone countries. The very first stage of this process starts with the seismic evaluation of the buildings. Plenty of researchers and institutions have been putting a lot of efforts into applying widespread seismic assessment works to identify seismically vulnerable structures. In the United States, in 1996 the Guidelines for Seismic Evaluation and Retrofit of Concrete Buildings (ATC-40) was prepared to assess and mitigate seismic risk. In 2001, the Standard for Seismic Evaluation of Existing Reinforced Concrete Buildings (JBDPA, 2001) was published by the Japan Building Disaster Prevention Association. The New Zealand Society for Earthquake Engineering published Assessment and Improvement of the Structural Performance of Buildings in Earthquakes (2006) in 2006 to minimize earthquake losses, which was then revised in 2017 (NZSEE, 2017). The Greek Organization for Seismic Planning and Protection updated the Greek Seismic Design Code (GSDC, 2000) in 2000, later was modified in parallel with Eurocode-8 (CEN, 2004) in 2012. The Italian Guideline for the Seismic Risk Classification of Constructions was approved in 2017, and tax reduction incentives were granted with the Sismabonus program (Cosenza et al, 2018). In 2003, the Istanbul Metropolitan Municipality published a comprehensive inter-disciplinary document titled Earthquake Master Plan for Istanbul (EMPI, 2003), which evaluated various seismic evaluation methods for different levels of knowledge. With the coming into force of the Turkish Earthquake Code 2007 (TSDC-2007), seismic evaluation of the existing buildings was introduced as a new chapter for the first time in Turkey. This code was followed by Provisions for the Seismic Risk Evaluation of Existing RC Buildings under Urban Renewal Law (2013) that was further updated in 2019 (Provisions for the Seismic Risk Evaluation of Existing RC Buildings under Urban Renewal Law, 2019) and the most recent version of the Turkish Seismic Design Code (Turkish Building Earthquake Code, 2018).

In general, it can be indicated that as the seismic evaluation method gets more detailed and complicated (as in the case of code-level methods), the accuracy of the method increases. However, approximately 800,000 buildings in Istanbul were constructed before the year 2000, and performing code-level thorough investigations for such a high number of buildings is not efficient or feasible both in terms of time and cost. To overcome this problem, simplified and economical, yet reliable and realistic seismic assessment methods need to be applied, so that this vast problem at hand can be reduced to a manageable scale. Besides the code-based detailed seismic evaluation methods, there are many rapid seismic evaluation methods available for existing buildings. EMPI (2003) proposes three stages for the evaluation of the seismic safety of buildings. In the first stage of the procedure, which is called rapid visual screening (RVS) in this paper, buildings are ranked according to simple parameters, which are collected through a street survey, that takes approximately 20 minutes per building. This phase of the assessment procedure yields a rough seismic performance ranking for building stock, and the regional concentration of seismically vulnerable buildings is determined. The RVS methods are mostly based on empirical approaches and the FEMA-154 (2015), METU Method (Sucuoglu et al, 2007), the method proposed by Canadian National Research Council (NRCC, 1993) and BOUN-YTU (EMPI, 2003) are among the well-known examples of the first stage assessments. In addition to these, in literature, there exists a variety of methods and implementation examples in various parts of the world. Achs and Adam (2012) introduced a pilot project aiming at the rapid assessment of masonry buildings in Vienna. A rapid visual screening method is proposed by Perrone et al. (2015) to determine a Safety Index for hospital buildings and validated the method on two hospital buildings damaged during the 2009 L'Aquila Earthquake. Shah et al. (2016) introduced a case study conducted in two districts of Jeddah, Saudi Arabia. A first-order loss assessment was performed in North Macedonia by Mircevska et al. (2019). Recently, in Italy, Dolce et al. (2020) developed a methodology for consensus-based national seismic risk assessment, and Brando et al. (2021) calibrated a 14 parameters-based empirical method to perform a rapid seismic vulnerability assessment of minor historical centers, and Del Gaudio et al. (2021) conducted a seismic loss prediction study for infilled reinforced concrete (RC) buildings via a simplified analytical method. Kassem et al. (2021) implemented

a Rapid Visual Screening (RVS) procedure in two towns in Malaysia. Del Gaudio et al. (2019) developed fragility and vulnerability curves based on damage data of the last 50 years for different types of RC buildings in Italy. Calvi et al. (2006) summarized the developments in and the most significant contributions to seismic vulnerability assessment methodologies and specified the main advantages and disadvantages of different procedures. Ruggieri et al. (2020) proposed a RVS methodology to assess the seismic risk of RC school buildings.

The second stage evaluation requires more detailed mechanical parameters to be collected in one to two hours per building. The calculation steps of these methods are developed based on mechanical computations. EMPI (2003) asserts that the decisions of almost all low-rise buildings should be made with this level of knowledge. PERA Method (Ilki et al, 2014), the method proposed by New Zealand Society for Earthquake Engineering (2006), Japanese Seismic Index Method (JBDPA, 2001), Hassan & Sozen Method (Hassan and Sozen, 1997), P25 Method (Bal et al, 2007), Yakut Method (Yakut, 2004), Ruggieri et al. (2022a) and Ruggieri et al. (2022b) are among the methods that can be used for second stage evaluation. The third stage assessment is for public and service buildings or complex structures, which shouldn't be evaluated by simplified methods according to EMPI (2003). The works to be carried out for this comprehensive seismic assessment stage is detailed by the current seismic assessment codes and guidelines. The data collection process at this stage is significantly longer than rapid assessment methods. Various insitu works for collecting data on the material qualities (i.e. concrete core or steel bar samples to be extracted from the structural members), destructive and non-destructive inspections for reinforcement details and building geometry are collected depending on the seismic evaluation document that is considered. Generally, a finite element model is established to conduct the structural analysis and the obtained internal forces and deformations (such as drift ratios, rotations or material strains) are compared with the thresholds provided by the code for target performance levels. The considered detailed assessment methods in the seismic provisions in Turkey are discussed comprehensively below.

All three levels of knowledge have their own benefits. It is generally assumed that the RVS is the quickest and most cost-friendly evaluation approach, while detailed assessment is the most accurate and expensive one in terms of time and cost. Second

stage preliminary assessments are at the optimum point between cost and accuracy. Despite these general assumptions, there is limited data on the comparative evaluation of different rapid assessment methods that exist in the literature. Most of the previous efforts focused on the comparison of RVS procedures with each other, such as Harirchian and Lahmer (2020a), Harirchian and Lahmer (2020b) and Bhalkikar and Ramancharla (2021). Recently Doğan et al. (2021) performed two RVS and four second stage assessment methods on 30 buildings to compare their results. Selman (2019) implemented in-detail research on P25 (Bal et al, 2007) and Yakut (Yakut, 2004) Methods and proposed adopting an approach with a visual inspection of structural members to these procedures.

In this study, five second stage and three RVS methods are applied on service buildings of Istanbul Metropolitan Municipality, which were previously evaluated by detailed code-level assessments. To demonstrate which available rapid building-scale seismic safety assessment method better fits the existing building stock in Istanbul in terms of yielding realistic results and applicability, actual site investigations are conducted on a large number of existing buildings, which are selected to reflect the characteristics of the building stock in Istanbul including many sub-standard ones built before the 2000s. The required time to collect the necessary data for each assessment method is determined based on the outputs of the performed site work, which constitutes another original aspect of the presented study. Then, the results of the considered methods are compared with code-based analyses to evaluate the accuracy of the methods and choose the methods that can be applied to nearly 23,000 sub-standard reinforced concrete buildings in Istanbul by IMM. Such a comparative study is believed to be crucial to avoid significant loss of time and budget through the use of less realistic and inefficient rapid seismic safety evaluation approaches. Additionally, a feasibility study is also conducted for the potential application of the investigated methods to nearly 600,000 pre-2000 RC buildings in Istanbul in terms of the required time and budget. Recently, the urgency of rapid seismic assessment of the existing building stock has been better understood after the destruction caused by the 2023 Kahramanmaraş-Hatay Earthquakes in Turkey, and rapid assessment works have been initiated in many cities. Also in Istanbul, it is reported that demand from the citizens to Istanbul Metropolitan Municipality for rapid assessment studies has nearly reached to 150,000 buildings. Furthermore; this study is very timely because many city administrations in seismic

areas of the world tend to utilize rapid methods for such evaluations. So that the intervention strategies for loss mitigation can be shaped and developed for buildings with high seismic risks.

2.3 Seismic Assessment Methods

FEMA-154 (2015), METU (Sucuoglu et al, 2007) and BOUN-YTU (EMPI, 2003) RVS methods and PERA2019 (Ilki et al, 2021), Hassan & Sozen (Hassan and Sozen, 1997), P25 (Bal et al, 2005), DURTES (Temur, 2006), and AURAP (Kaplan et al, 2018) second stage assessment methods were selected and applied to a group of existing buildings. Most of the methods have been prepared according to the damage statistics in previous earthquakes. The authors of each method calibrated their parameters according to their experiences, so some of the vulnerability parameters have a weighted effect on the final score of the methods. As a result of this fact, the scores of the buildings may vary for different procedures.

The overall list of the required parameters for each of the RVS and second stage assessment methods and the average time required to collect each parameter, which is determined through site work, are listed in Table 2.1. Hassan & Sozen method is clearly the simplest second stage method among the others with only four parameters needed, while PERA2019, DURTES and AURAP methods require more than 20 parameters for performing.

The severity of available irregularities in plan and elevation defines the penalty score (i.e. the percentage of the short columns and the clear heights of the columns should be considered comprehensively) for P25 method. AURAP considers the frame discontinuity thoroughly. Consideration of the lateral load bearing capacity of the infill walls is the main difference between DURTES over AURAP, where AURAP ignores the infill walls for the sake of practicality. PERA2019 is the only method that requires the longitudinal reinforcement ratio to compute the column moment-axial load interaction curve. Also, the consideration of column locations (i.e. corner, side or middle) to distribute the gravity loads accordingly and the arrangement of ties of columns to determine the ductility of the members are among the unique aspects of the PERA2019 method.

Table 2.1 : Required parameters to perform the procedures evaluated in this study.

	Second Stage Assessment Methods					RVS Methods			
	PERA2019	AURAP	DURTES	P25	HASSAN & SÖZEN	METU	BOUN-YTU	FEMA-154	Time to Collect(min)
Number of Stories	√	√	√	√	√	√	√	√	3
Colum/Shear Wall Cross Sections	√	√	√	√	√	X	X	X	15
Column Clear Heights	√	X	X	√	X	X	X	X	1
Column Locations	√	X	X	X	X	X	X	X	10
Story Heights	√	√	√	√	X	X	√	X	5
Plan Area	√	√	√	√	√	X	X	X	10
Compressive Strength of Concrete	√	√	√	√	X	X	X	X	10
Reinforcement Class	√	√	√	X	X	X	X	X	5
Longitudinal Reinforcement Ratio	√	X	X	X	X	X	X	X	2
Transverse Reinforcement Spacing and Diameter	√	√	√	√	X	X	X	X	1
Column Transverse Reinforcement Details	√	X	X	X	X	X	X	X	1
Corrosion	√	X	X	√	X	X	X	X	1
Confinement Zones	√	√	√	X	X	X	X	X	1
Irregularities	√	√	√	√	X	√	√	√	5
Seismicity*	√	√	√	√	X	√	√	√	0
Soil Class*	√	√	√	√	X	√	√	√	0
Year of Construction	√	√	√	X	X	X	X	√	1
Type of Slab	√	√	√	X	X	X	X	X	1
Type of Foundation	X	√	√	√	X	X	X	X	1
Infill Wall Dimensions	X	X	√	√	√	X	X	X	20
Dilatation	X	√	√	X	X	X	X	X	5
Overhangs and Area	√	√	X	√	X	√	X	X	5
Retrofitted Structure	X	X	√	X	X	X	X	√	2
Different Story Levels of Adjacent Buildings	√	√	√	√	X	√	√	√	1
Corner Column Problem	X	√	X	X	X	X	X	X	5
Function of Building	√	√	√	X	X	X	X	X	2
Max. Span Length	X	√	√	X	X	X	X	X	3
Existence of Blueprints	X	√	√	X	X	X	X	X	5
Basements	X	√	√	X	X	X	X	X	2
Continuous Frames	X	√	√	X	X	X	X	X	10
Elevation Difference in the Same Floor	X	X	X	√	X	X	X	X	2
Liquefaction*	X	X	X	√	X	X	X	√	0
Short Colum	√	√	√	√	X	√	√	X	5
Visual Quality	X	X	X	X	X	√	√	X	1
Total Number of Parameters	22	24	24	18	4	8	8	8	
Average Total Required Time (min)	85	101	113	85	48	20	20	12	141

* These data are automatically assigned from the GIS database.

The actual site data collection work conducted by the staff of the Istanbul Metropolitan Municipality provided the average required durations for the collection of site data for all methods (Table 2.1). Accordingly, the most time-consuming method is clearly DURTES, while the most time-efficient second stage method is Hassan & Sozen. P25 and PERA2019 require similar durations to collect the data. However, some further secondary information is needed for P25 (i.e. depth of the foundation, heavy façade elements, mezzanine floor existence, etc.), which increases the data collection duration when compared to PERA2019.

2.3.1 Rapid visual screening methods

Since the RVS methods do not consider main structural parameters (i.e. material strength, reinforcement details, cross-section dimensions of structural elements, etc.),

their accuracies are expected to be low on the building scale. However, due to their practicality, the RVS methods are generally preferred for defining the seismic risk distribution on a regional scale, since the collected irregularity and vulnerability data are statistically vital indicators of the seismic deficiency on a regional scale. The RVS methods employed in the scope of this study on a group of existing buildings are briefly introduced below.

2.3.1.1 FEMA-154 RVS method

FEMA-154 (2015) (Rapid Visual Screening of Buildings for Potential Seismic Hazards, 2002) is among the most popular RVS methods. The procedure has initial scores for different types of structural systems. The base score is reduced with the vulnerability modifiers, such as vertical and plan irregularities. Then, the building is evaluated according to the corresponding seismicity level of the site. Retrofitting history, whether the building is pre-code or not, soil class of the site, and the number of stories of the building, are also considered. Any additional data about other hazards such as pounding potential, deterioration of the structural system, geologic hazards, and falling risk of exterior elements are taken into consideration. The seismic risk of the building increases as the final score decreases. The method defines a minimum score for various types of structural systems. For example, the minimum score is 0.5 for reinforced concrete buildings.

2.3.1.2 METU RVS method

This RVS method was introduced by Sucuoglu et al. (2007) for mid-rise buildings. The parameters, which are required by the method, were selected through their suitability for the street survey. The procedure defines an initial performance score according to local seismicity and the number of stories. After that, the penalty scores of each vulnerability parameter are added to the base score. The method was calibrated with data from 454 buildings that experienced the 1999 Duzce Earthquake. The penalty scores of the vulnerability parameters, such as the number of stories, irregularities, short columns, apparent building quality, local soil conditions, the topography of the site, etc., were defined by considering the data from that validation study.

2.3.1.3 BOUN-YTU RVS method

This method aims to estimate the seismic demand in terms of roof displacement. The method was developed by Bogazici University and Yildiz Technical University for the EMPI (2003). The required parameters to perform the method are similar to the METU method. The first mode natural vibration period of the RC building, which is used to calculate the spectral displacement demand, is assumed as 15% of the number of stories. Base drift capacities for life safety and collapse prevention criteria are assumed as 0.8% and 1.4%, respectively. These base drift capacities are multiplied with capacity reduction factors, which are penalty multipliers related to structural irregularities. The score of the building is defined as the ratio of drift capacity to drift demand.

2.3.2 Second stage evaluation methods

Second stage assessment procedures are more detailed than RVS and typically require more comprehensive data to be gathered from the buildings. Thus, these methods can also provide building-scale risk information. According to EMPI (2003), the risk ranking of almost all low-rise buildings should be made with this level of knowledge to save time and precious public resources. In this study, five different methods are studied diligently to determine their accuracies compared to detailed code-level assessment methods.

2.3.2.1 PERA2019 method

The PERA method was first introduced by Ilki et al. (2014) for evaluating the seismic performance of RC frame buildings economically and reliably. The application of the method is limited up to 10-story buildings to ensure that the first mode vibrations are mostly dominant in the dynamic behavior of the structure. The methodology has been developed extensively over the past years in several aspects. In 2019, PERA was adapted to be applicable to RC buildings with shear walls, and the compatibility of the methodology with recently published seismic assessment documents was ensured (Ilki et al, 2021a; Demir et al, 2022; Cömert et al, 2022). Cross-section dimensions of the vertical RC members, concrete quality, and reinforcement details at the critical story and local soil class are needed to perform the simplified structural analysis.

The seismic safety rating defined for the PERA method is based on determining a global structural capacity/seismic demand ratio, and is named as Seismic Safety Ratio (SSR, equation. 2.1). The capacity of the building is calculated iteratively through simplified linear structural analyses and evaluation phases, as defined by Ilki et al. (2021a). The iterations are performed over the PGA value of the demand spectrum starting from scaled-down ordinate values which are increased gradually at each step (i.e. with increments of 0.01g). The reference limits to determine if the building satisfies the performance target are in parallel with the Provisions for the Seismic Risk Evaluation of Existing Buildings (2019). When the evaluation mechanism is considered, in means of the structural analysis carried out, this method is closer to the code-level detailed assessment level than other second stage methods included in this study. The method proposes five risk classes; A (SSR≥100, low risk), B(100>SSR≥75, low risk), C(75>SSR≥50, medium risk), D(50>SSR≥25, high risk), and E(25>SSR, very high risk) to classify the buildings.

$$\text{Seismic Safety Ratio (SSR, \%)} = 100 \times \frac{PGA_{Capacity}}{PGA_{Demand}} \tag{2.1}$$

2.3.2.2 P25 method

The P25 method (Bal et al, 2007), is an improved version of the previously introduced P5 method (Tezcan et al, 2003). The authors of P25 applied the P5 method to 23 buildings, which experienced different damage levels in previous earthquakes, and the method was calibrated according to the results of this study. The method was then further used for 311 damaged or new buildings, and the calibration was completed regarding the results obtained.

Seven different P scores are assigned to the buildings by the P25 method, such as the basic structural score, short column score, soft/weak story score, overhangs and frame discontinuity score, pounding score, liquefaction potential score, and soil failure score. Also, the α coefficient is defined with respect to the live load reduction factor, building importance factor and seismicity zone, while the β coefficient is dependent on the weighted average of the P scores. The final P score is determined according to equation (2.2). Note that, P_{min} is the minimum one of all P scores.

$$\mathrm{P} = \alpha\beta P_{min} \tag{2.2}$$

The seismic risk of the building decreases as the P score increases. The authors of the method suggest that the buildings with a P score greater than 35 have a low risk, while

the P < 25 group has a high risk. P scores between 25 and 35 are in the grey area, and buildings that fall into this area should be investigated in detail.

2.3.2.3 DURTES method

The DURTES method (Temur, 2006), requires material quality and cross-sections of the vertical RC members as well as infill walls at the critical story to calculate the Structural Safety Factor (SSF) of the building. SSF is basically the elastic base shear capacity to demand ratio. The Relative Score (RS) of the building is evaluated through the multiplication of nearly 100 vulnerability parameters. The buildings are classified according to their seismic risk according to their SSF and DURTES scores where the DURTES score is obtained by multiplication of SSF and RS.

According to DURTES method, buildings with SSF ≥ 1.0 have a minimum risk level. Buildings with SSF<1.0 are classified regarding their DURTES scores (i.e. DURTES score ≥ 75 is specified as a low risk grade, 50 ≤ DURTES score < 75 is medium risk grade, 25 ≤ DURTES score < 50 is high risk grade, and DURTES score < 25 is very high risk grade).

2.3.2.4 AURAP method

The DURTES method has been modified by Kaplan et al. (2018) to develop the AURAP method. The main aim of the AURAP procedure is to assess the seismic risk of the existing buildings with fewer parameters. In parallel with DURTES, AURAP also needs dimensions of the vertical RC members and material properties. However, infill walls are not considered in order to increase the practicality of the method. The structural safety factor (SSF) is obtained by the ratio of elastic base shear capacity to base shear force demand. Relative Building Score (RBS) is evaluated by the multiplication of penalty coefficients (P_i) of each potential vulnerability parameter (equation 2.3). The final assessment score (FAS) is determined by equation (2.4).

$$\mathrm{RBS} = 100 \prod_1^N P_i \tag{2.3}$$

$$\mathrm{FAS} = \mathrm{SSF}.\,\mathrm{RBS} \tag{2.4}$$

The AURAP methodology proposes that buildings with FAS ≥ 150 are considered as low risk, while structures with FAS < 50 are considered as high risk, and buildings with FAS between 50 and 150 are classified as medium risk.

2.3.2.5 Hassan and Sozen method

Hassan and Sozen (1997) method is the simplest second stage assessment method among the ones evaluated in this study. Cross-section dimensions of the columns, shear walls and infill walls are needed to perform the evaluation, as well as floor areas and the number of stories. Percentages of the column and wall areas to the total floor area are the final defining parameters (column index and wall index) of the method. The effective cross-section area of vertical members is computed with 10% of the infill wall areas, 50% of the column areas and 100% of the shear wall areas. Hassan & Sozen procedure simply calculates the effective cross-section area/total floor area ratio of the columns and shear walls as PI index and has only one risk threshold (PI<20%). Seismicity, material strength and reinforcement properties do not participate in this procedure. Forty-six buildings that experienced the 1992 Erzincan Earthquake were studied to investigate the accuracy of the method. The results indicated that buildings become more vulnerable as the sum of the column and the wall indices decreases.

2.3.3 Detailed assessment methods

These are the methods that are described by the current provisions in Turkey, and their results on the buildings investigated in this study are used as reference values for the comparison of the RVS and second stage assessment methods.

2.3.3.1 Provisions for the seismic risk evaluation of existing buildings (RBTE-2019)

The first version of the Provisions for the Seismic Risk Evaluation of Existing Buildings was published in 2013 by the Ministry of Environment and Urbanization of Turkey to minimize the efforts of the detailed assessment of the existing buildings and accelerate the urban renewal processes. Then these provisions were revised in 2019 (Provisions for the Seismic Risk Evaluation of Existing RC Buildings under Urban Renewal Law, PSREEB-2019). The method is similar to the linear assessment approaches of seismic codes such as TSDC-2007, but the level of knowledge is limited only to the critical story and a limited amount of material tests is required. In parallel with the obvious aim of the provisions, a single performance limit is defined to distinguish risky buildings from non-risky ones.

During the implementation of PSREEB (2019) linear assessment methodology, the demand/capacity and drift ratios of the columns and shear walls are compared with the corresponding limit values defined in the provision. If a vertical structural member exceeds the defined limit values, it is sorted as a risky member. The shear forces that are resisted by the risky members are summed at each story for x and y directions in the plan. Then these summed shear forces are divided by the story shear forces and compared with the limit value obtained by considering the average vertical member axial load ratio of the story. If the average axial load ratio at the critical story is less than 10%, the risky elements are allowed to carry 35% of the story shear force, while none of the columns and shear walls are allowed to exceed their performance limits if the mean axial load ratio is greater than 65%. The average axial load ratio is computed by equation (2.5), where N_i is the axial load acting on vertical structural members, A_i is the cross-sectional area of vertical member, f_{cm} is the compressive strength of concrete and n is the total number of columns and shear walls. Interpolation should be used in order to calculate the allowed story shear limit for buildings where the mean axial load ratio is between 10% and 65% (Table 2.2).

$$\text{Average axial load} = \frac{\sum_{i=1}^{n} \frac{N_i}{A_c f_{cm}}}{n} \tag{2.5}$$

Table 2.2 : The total allowed shear force ratio of columns and shear walls exceeding their risk limits.

Average axial load on the columns and shear walls at the critical story	$(\frac{Vrisky}{Vstory})_{allowed}$
≥ 65%	0
10% ≥	35%

V_{risky}: The total shear force that is carried by risky elements
V_{story}: Story shear force at critical story

2.3.3.2 Turkish building earthquake code

Procedures for seismic evaluation of the existing buildings were first introduced in the 2007 version of the Turkish Earthquake Code (TSDC-2007). A new deformation-based linear approach was introduced by the current version of the Turkish Building Earthquake Code (TBEC-2018), while TSDC-2007 allowed a force-based linear procedure. For assessing the global performance of the building, three member damage limits are defined for columns, shear walls and beams (Figure 2.1): limited damage (LD), controlled damage (CD) and collapse prevention (CP). Similar steps are followed to determine the global performance of an existing building according to both seismic codes. The overall performance of the building is evaluated for the considered

performance target (i.e. Controlled Damage for ground motion with 475 year return period) by considering the conditions provided below:

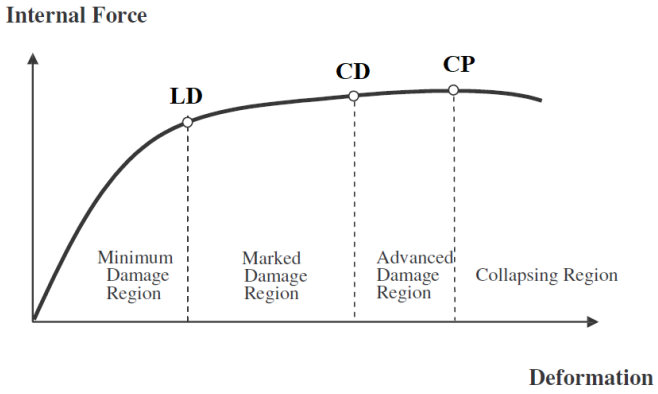

Figure 2.1 : Member damage limits according to TBEC-2018.

Continued operation: None of the structural members should exceed the limited damage member limit state.

Limited damage: For each earthquake direction at each story, at most 20% of the beams can experience marked damage, and the rest of the elements must remain at the minimum damage region.

Controlled damage: No more than 35% of the primary beams can exceed the advanced damage zone. Also, the total shear force of the vertical elements in the advanced damage zone should not exceed 20% of the total shear force of the story. All other elements should be in the minimum or marked damage zone. However, the total shear forces of the vertical elements that go beyond the limited damage limit at both upper and lower sections, for any story cannot be greater than 30% of the total shear force of the corresponding story. The buildings that can satisfy these criteria meet the controlled damage performance level.

Collapse prevention: At most 20% of the primary beams can exceed the collapse prevention limit. All other elements should be in the minimum, marked or advanced damage zone. However, the total shear forces of the vertical elements pass the controlled damage limit at both upper and lower sections, for any story cannot be greater than 30% of the total shear force of the corresponding story.

Collapse: The buildings that cannot satisfy the collapse prevention performance level are at the collapse level.

2.4 Evaluated Buildings

Within the scope of this comparative study, 72 buildings, which are the service, office or housing buildings of the Istanbul Metropolitan Municipality, were examined. The buildings with different functions were selected to reflect different types of buildings in the inventory. The buildings represent the typical reinforced concrete design and construction practice of the times that they were built. The structural systems of the buildings consist of either reinforced concrete frame or dual frame-wall systems. The comprehensive information about the structural features of the buildings investigated in this study is given in Table A.1, and typical structural plan layouts presented in Figure 2.2. The buildings investigated in this study consist of RC plates with beams or one-way joist floor systems.

Information on the main characteristics of the investigated buildings, such as construction year, number of stories, reinforcement type (S220 for plain bars with a characteristic yield strength of 220 MPa and S420 for deformed bars with 420 MPa characteristic yield strength), stirrup spacing in the column confinement zones, and compressive strength of concrete, are provided in Figure 2.3. The buildings have been selected to reflect the current situation of the building stock of Istanbul. Most of the buildings were built before the year 2000, and the number of stories varies between one and eight, whilst the most frequent type is 4-story buildings. The average transverse reinforcement spacing at the confinement zone of the columns is approximately 20 cm, and the spacing values vary between 7 and 35 cm. The average concrete compressive strength for investigated buildings, obtained through concrete core compression tests, is 14.6 MPa. The considered material parameters were obtained during the site work and used in the application phase of the second stage (except for Hassan & Sozen method) and detailed assessment methods to perform mechanical computations. To provide objective evaluation between methods, determined structural parameters were directly used in the implementation phase of each rapid assessment method independent of their data collection methodologies. Since RVS methods are street surveys and do not require any mechanical computation, material parameters and reinforcement details are not required by these procedures. The required structural parameters for each method are given in Table 2.1.

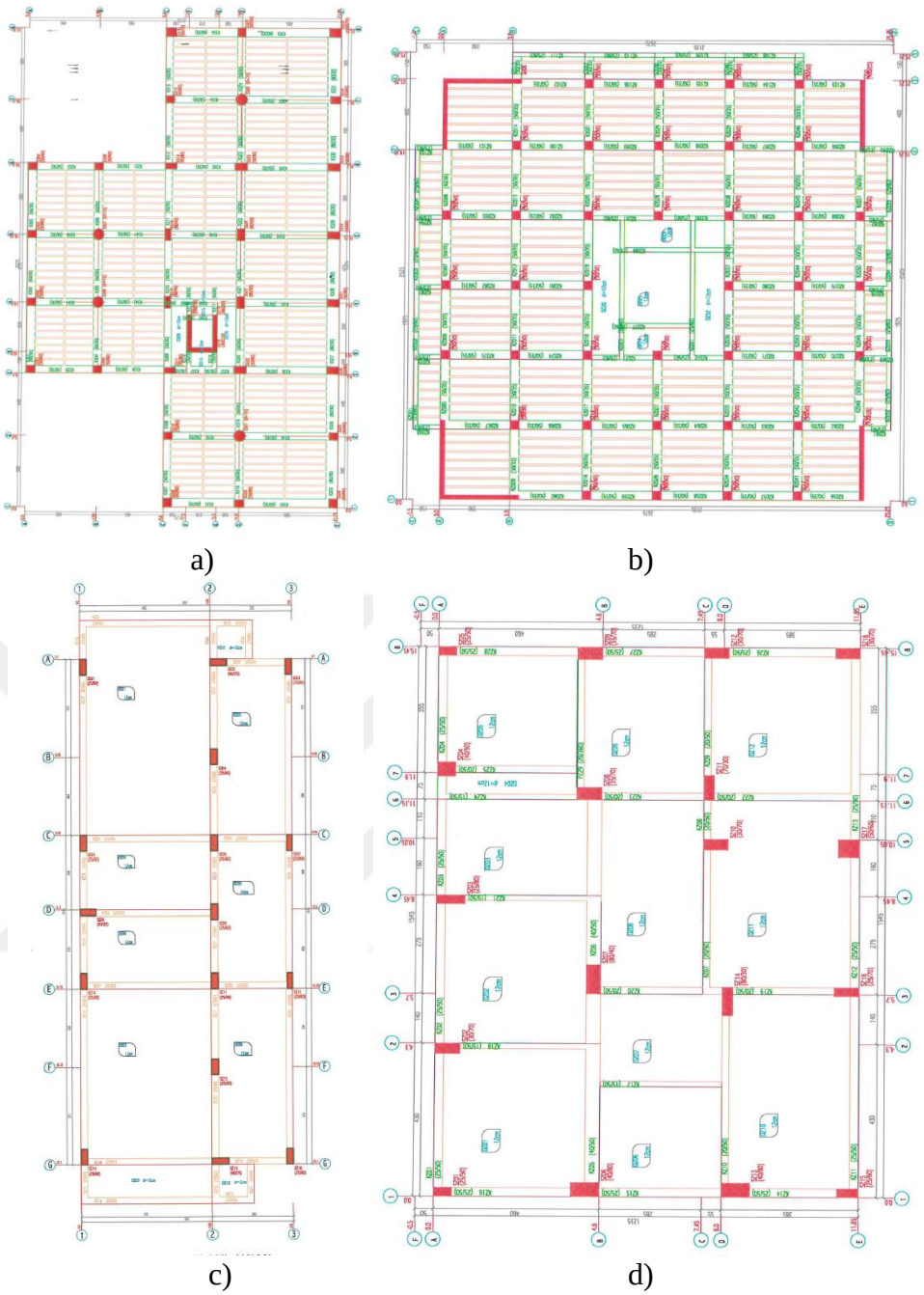

Figure 2.2 : Column/Beam layout plan of the sample buildings a) ID=78 (public), b) ID=107 (public), c) ID=13 (residential/office), d) ID=4 (residential/office).

Detailed assessment reports of the buildings were prepared considering the TBEC-2018, TSDC-2007 or PSREEB-2019 detailed assessment approaches. TBEC-2018 was applied to 22 buildings, while 38 of them were investigated through TSDC-2007, and the rest of the buildings were assessed according to PSREEB-2019. To stay consistent, corresponding seismicity and spectrum coefficients of respective codes were preferred while performing all of the rapid evaluation procedures. Views of three-dimensional (3D) finite element models of two public service and two

residential/office buildings are shown in Figure 2.4. The investigated buildings potentially had different types of irregularities. Accordingly, 33% had torsional, 15% had vertical element discontinuity, 38% had soft/weak story, 13% had slab discontinuity, 11% had plan shape irregularities and 11% of the buildings had pounding potential with the adjacent buildings. Information on the available irregularities of the buildings is given in Table A.1.

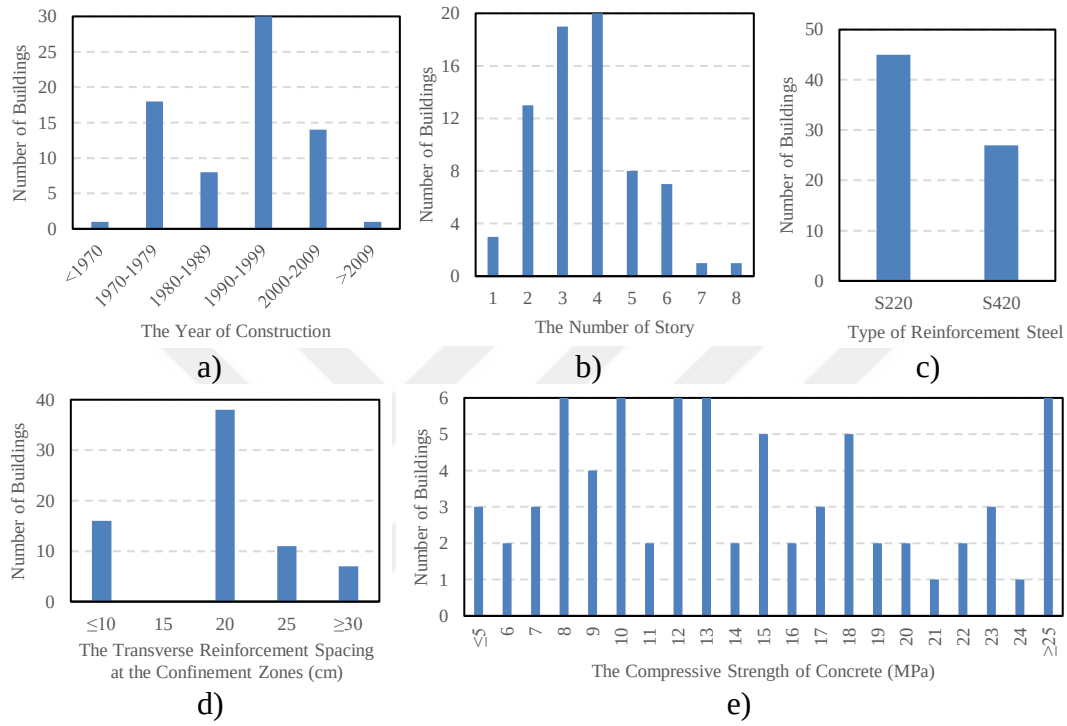

Figure 2.3 : The distribution of the structural characteristics of the buildings. a) the year of construction of the buildings, b) the number of stories, c) reinforcement steel class, d) the transverse spacing at confinement zones, e) the compressive strength of concrete.

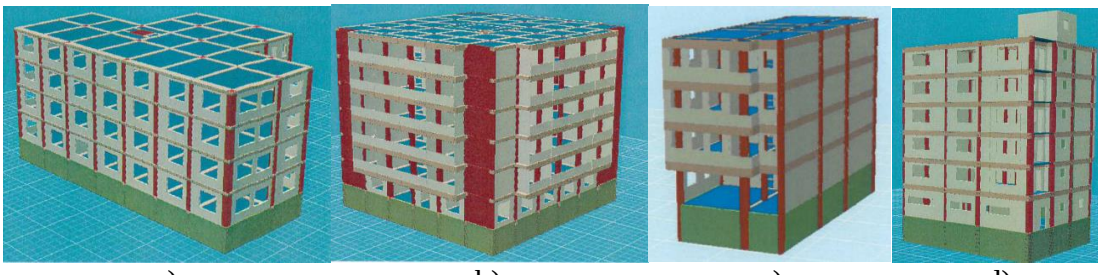

Figure 2.4 : 3D models of sample buildings a) ID=78 (public), b) ID=107 (public), c) ID=13 (residential/office), d) ID=4 (residential/office).

2.5 Results and Discussion

In order to assess the performances of RVS and second stage methodologies covered in this study, the seismic performance predictions of PSREEB-2019, TSDC-2007 and TBEC-2018 were accepted as the benchmark results and they were compared with the results of investigated rapid seismic safety assessment methods. To ensure the compatibility of the performance limits of PSREEB-2019 and both earthquake codes (TSDC-2007 and TBEC-2018), the buildings that were found risky according to PSREEB-2019 were assumed to be in the collapse limit state. For the sake of consistency in the comparisons, linear assessment methodologies of the codes were used for all buildings. The nonlinear behavior was accounted indirectly by considering the internal force demand/capacity ratios and chord rotations of the structural members which are respectively compared with the limits defined by PSREEB-2019, TBEC-2018 and TSDC-2007 for different member damage states. Member damage limits, required for evaluating if a building performance target is met, were defined by considering the ductility levels of the members that depend on the shear demand/capacity ratio, axial load/axial capacity ratio and transverse reinforcement characteristics. The detailed code-level seismic performance assessment results for buildings evaluated in this study are given in Table 2.3, together with their RVS and the second stage assessment scores. The numerical computations conducted for each method will be included in the following sections of this Ph.D. thesis. Accordingly, among 72 considered building cases, 54 buildings reached the collapse performance level, 5 buildings the collapse prevention performance level, and 13 buildings satisfied the controlled damage performance requirements. Note that RVS methods were applied to only two to six-story buildings in order to stay within the limits of the methods.

For all considered RVS and second stage methods, as the score assigned to the building increases, the building seismic safety level also increases. However, each assessment method implies different scoring ranges. To compare the results of each procedure, the mean scores, standard deviations and coefficient of variations for distinct seismic performance levels were determined (Table 2.4).

Table 2.3 : Seismic performance scores of buildings for methods considered in this study.

Building ID	Detailed Assessment Score	Second Stage Assessment					RVS		
		PERA2019	AURAP	DURTES	P25	Hassan & Sozen	METU	BOUN-YTU	FEMA154
1	C	7	35	46	16	22%	72	17	0.6
2	C	34	324	422	40	95%	-	-	-
3	C	27	81	100	21	31%	-	-	-
4	C	12	13	47	14	16%	-	-	-
5	C	23	44	60	13	27%	87	13	0.6
6	C	9	36	52	9	20%	-8	7	1.1
7	C	12	39	58	10	35%	-23	8	1.1
8	C	28	54	68	36	29%	77	20	1.1
9	C	29	12	51	25	13%	162	14	1.3
10	C	51	20	101	41	31%	-	-	-
12	CP	62	105	140	35	30%	77	12	0.5
13	C	27	36	57	21	32%	-3	13	1.1
14	CD	90	174	195	18	52%	172	21	2.0
15	C	39	64	82	25	39%	107	21	1.9
16	C	12	48	63	9	24%	12	9	0.6
19	C	34	62	82	11	39%	47	15	1.1
22	C	36	89	118	13	37%	47	16	1.1
25	C	31	66	97	12	37%	27	13	1.1
28	C	9	39	51	6	22%	12	9	0.6
31	C	32	52	76	8	31%	27	13	1.1
34	C	21	53	77	7	26%	17	11	0.2
37	C	18	81	118	6	31%	17	11	0.2
40	C	32	39	54	17	39%	57	15	1.1
43	C	0	13	18	8	10%	37	11	1.1
49	C	35	64	81	16	19%	87	11	1.5
50	C	0	19	30	9	14%	-	-	-
51	C	18	29	37	21	26%	62	19	0.6
52	C	12	19	24	14	24%	22	10	0.6
53	C	7	19	24	10	15%	22	10	0.6
54	C	25	32	40	16	18%	52	12	1.1
55	C	32	23	85	32	48%	62	16	0.6
56	C	40	53	69	30	39%	107	12	1.5
57	CD	109	36	147	64	40%	152	13	1.2
61	CD	47	29	111	39	21%	182	18	1.3
62	CD	52	191	203	42	27%	57	11	0.9
63	C	42	67	98	20	28%	72	14	1.9
64	C	21	16	50	31	22%	162	12	1.7
68	CD	49	35	135	43	21%	182	18	1.3
69	C	19	41	51	18	12%	57	9	1.1
70	C	18	8	41	17	17%	7	12	1.1
71	C	17	32	41	17	14%	32	11	1.1
72	CD	87	72	70	39	21%	142	11	2.0
73	C	22	37	46	16	23%	37	13	1.1
74	CD	131	69	177	52	34%	162	16	2.0
75	C	53	52	202	19	32%	217	20	1.3
77	CD	54	58	224	65	32%	217	20	1.3
78	C	26	149	158	31	28%	102	11	1.2
81	CP	52	146	155	32	39%	102	11	1.2
84	C	32	116	122	44	55%	167	17	1.3
87	CD	63	142	142	45	29%	162	14	1.3
90	C	23	10	52	27	42%	52	23	0.5
91	C	17	41	57	15	18%	22	11	1.1
92	CP	40	81	115	25	36%	67	21	1.1
95	CP	79	186	183	29	26%	67	13	1.5
98	CD	131	251	272	22	41%	47	12	1.5
101	CD	84	196	213	22	47%	132	12	2.0
104	CD	120	194	211	22	41%	47	12	1.5
107	C	37	30	39	21	65%	42	12	1.3
108	CP	54	88	89	40	22%	162	17	1.3
109	CD	63	117	126	26	26%	27	9	0.9
110	C	14	23	32	18	19%	-53	10	1.1

Table 2.3 (continued): Seismic performance scores of buildings for methods considered in this study.

Building ID	Detailed Assessment Score	Second Stage Assessment					RVS		
		PERA2019	AURAP	DURTES	P25	Hassan & Sozen	METU	BOUN-YTU	FEMA154
111	C	4	2	13	10	28%	-48	6	1.1
112	C	35	33	50	15	14%	-33	13	1.1
113	C	7	4	22	8	24%	-43	7	1.1
114	C	42	11	81	8	63%	-58	7	1.1
115	C	21	9	48	8	18%	-58	7	1.1
116	C	20	23	30	15	18%	7	11	1.1
117	C	13	4	25	15	34%	27	11	1.1
118	C	9	4	27	8	24%	-58	7	1.1
119	C	8	3	16	7	13%	-48	7	1.1
120	C	9	3	18	12	44%	27	9	1.1
121	C	25	10	39	18	14%	2	10	1.1

C: Collapse, CP: Collapse Prevention, CD: Controlled Damage

Table 2.4 : The mean, standard deviation and coefficient of variation values for scores of rapid assessment methods, corresponding to each seismic performance state obtained through detailed assessments.

		Detailed Assessment Results of the Buildings		
Method		C	CP	CD
PERA	Mean Score	22.7	57.2	83.0
	Standard Dev.	12.4	13.1	30.0
	Coef. of Variation	0.5	0.2	0.4
P25	Mean Score	17.3	32.0	38.4
	Standard Dev.	9.3	5.2	15.0
	Coef. of Variation	0.5	0.2	0.4
DURTES	Mean Score	67.5	136.4	171.1
	Standard Dev.	60.6	32.2	53.0
	Coef. of Variation	0.9	0.2	0.3
HASSAN &SOZEN	Mean Score	0.29	0.31	0.33
	Standard Dev.	0.15	0.06	0.10
	Coef. of Variation	0.53	0.20	0.30
AURAP	Mean Score	42.30	121.31	120.31
	Standard Dev.	48.43	39.57	72.54
	Coef. of Variation	1.14	0.33	0.60
BOUN-YTU (Street Survey)	Mean Score	12.2	14.6	14.3
	Standard Dev.	4.0	3.9	3.6
	Coef. of Variation	0.3	0.3	0.3
METU (Street Survey)	Mean Score	37.10	95.00	129.31
	Standard Dev.	60.72	35.86	60.21
	Coef. of Variation	1.64	0.38	0.47
FEMA (Street Survey)	Mean Score	1.05	1.12	1.48
	Standard Dev.	0.35	0.34	0.39
	Coef. of Variation	0.33	0.30	0.26

The most critical challenge for rapid assessment methods is separating the buildings that possess poor seismic performance from the others. According to mean score values provided in Table 2.4, PERA2019, P25 and DURTES second stage methods represent a good distinction with respect to code-level performance predictions, and the mean scores corresponding to Collapse, Collapse Prevention and Controlled

Damage performance levels tend to increase as expected. However, this tendency is weak for Hassan & Sozen method where mean scores are quite close to each other. The trend is interrupted for AURAP method since the Controlled Damage mean score is almost the same as the Collapse Prevention score. Additionally, DURTES and AURAP methods have high coefficient of variation values around 1.0 for the buildings in the collapse limit state. Among the investigated RVS procedures, in BOUN-YTU the trend for mean scores was not coherent with the code-level performance predictions and whereas the METU method exhibited a high variation for buildings in collapse state (coefficient of variation 1.6). FEMA-154 methodology demonstrated better performance in grading the vulnerability of buildings with increasing mean scores from collapse to controlled damage states.

Histograms prepared from the results of each method, compared to performance criteria determined through detailed assessments are demonstrated in Figure 2.5. The histograms reflect the frequencies of the rapid assessment scores relative to each performance level determined through detailed assessment. Additionally, the score distributions and seismic risk classification limits of each method are illustrated in Figure 2.6, together with the detailed assessment results, which are the reference results to investigate the accuracy of the rapid assessment methods. In the general sense, it can be inferred from these figures that second stage assessments are much more successful than the RVS methods in distinguishing buildings with adequate earthquake resistance from inadequate ones.

According to Figure 2.5a and 2.6a, the D and E Class limits (high and very high risk buildings, respectively) of PERA2019 method are able to catch 96% of the buildings in the collapse region. High and very high risk classes of DURTES cover 43% of the buildings in the collapse region (Figure 2.5e and 2.6e). However, with a coefficient of variation of 0.9 as reported in Table 2.4, 33% of the buildings with collapse state are found to be in low or minimum risk regions by DURTES which may lead to unsafe predictions for such weak buildings. In the case of Hassan & Sozen method, almost 66% of the buildings in the collapse state have index values greater than 20%, which is the risk limit of the method (Figure 2.5b and 2.6b). According to AURAP method results, 70% of the buildings in the collapse state are effectively identified as high risk

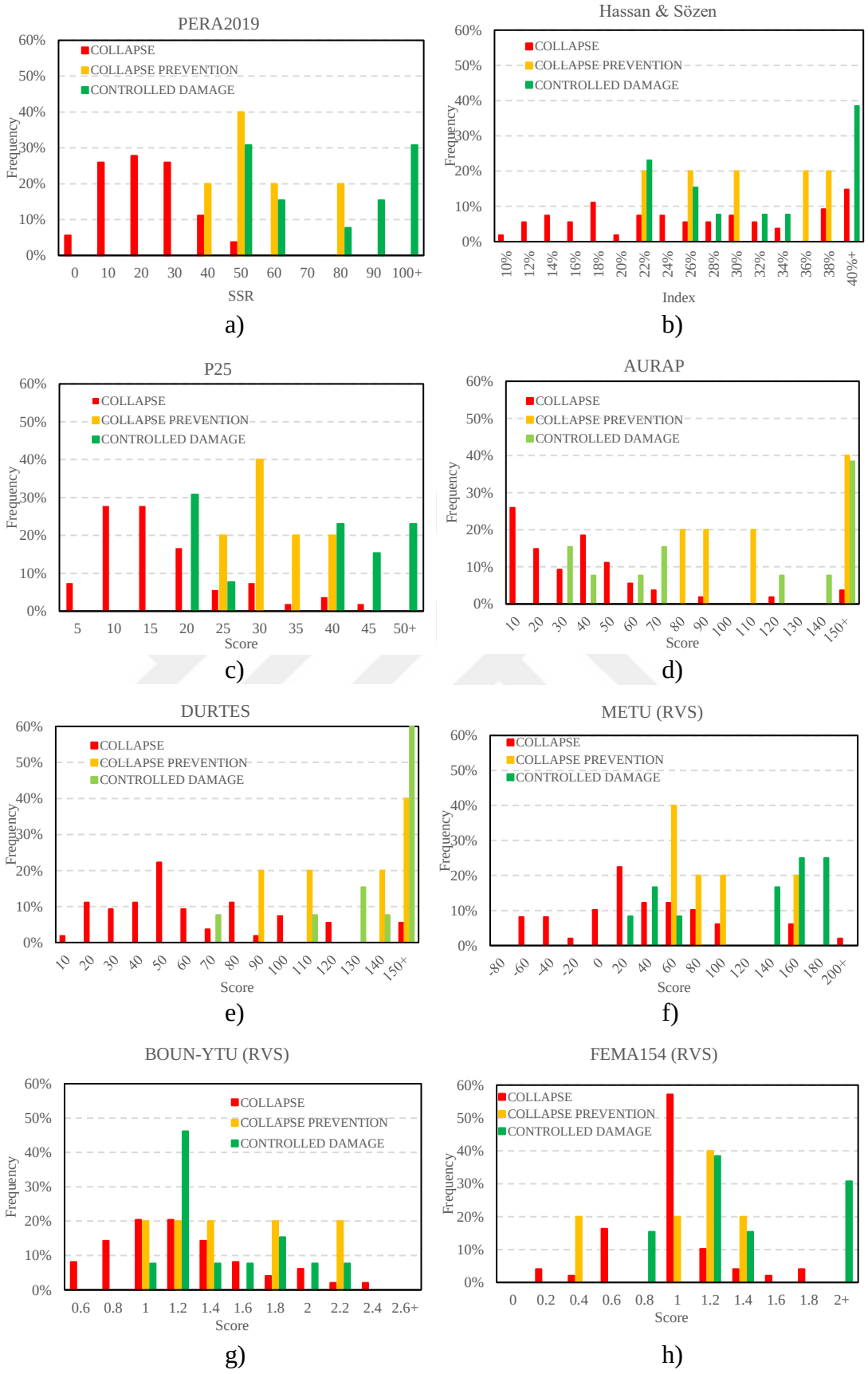

Figure 2.5 : Detailed assessment results and histograms of results according to a) PERA2019, b) Hassan & Sozen, c) P25, d) AURAP, e) DURTES, f) METU (RVS), g) BOUN-YTU (RVS) h) FEMA154 (RVS) methods.

Figure 2.6 : Comparison of detailed assessment results and final scores of buildings according to a) PERA2019, b) Hassan & Sozen, c) P25, d) AURAP, e) DURTES, f) METU (RVS), g) BOUN-YTU (RVS) h) FEMA154 (RVS) methods.

buildings (below the high risk limit score value of 50) (Figure 2.5d and 2.6d). The building with ID number 2, which is a single-story building and in the collapse region

according to the seismic design code, has a score of more than 300 according to DURTES and AURAP methods. The P25 method can successfully capture 82% of the buildings in the collapse region as seen in Figure 2.5c and 2.6c. However, 6% of collapse state buildings are above the grey zone limit, thus, classified as low risk.

PERA2019 second stage evaluation method appears to perform better at distinguishing good seismic performance buildings from poor ones. The method does not label any buildings with CP or CD state as E class risk which points to a very high level of seismic risk and determines 83% of these buildings either as A, B or C Class. PERA2019 also conservatively classifies 15% of the buildings in CD state as high risk buildings. DURTES exhibits good performance in identifying the buildings with relatively better seismic performances (buildings in CD and CP states, Figure 2.5e and 2.6e) and the procedure does not classify any buildings with CP or CD states as high or very high risk. Similar to DURTES method, the Hassan & Sozen method also successfully identifies the buildings with CD and CP states, but fails to classify the collapse state buildings due to their high scatter. AURAP method results show that 23% of the buildings in the CD state are conservatively determined as high risk buildings and buildings that satisfied the CD and CP performance targets were scattered among all risk regions. According to the P25 method results, 39% of the CD and 60% of the CP buildings are either in the grey or collapse zones. Liquefaction is a very dominant parameter in the algorithm of P25, as well as the bearing capacity of the soil. Buildings 98, 101 and 104 were found to be in the controlled damage performance range according to the code-based analysis. However, P25 found them in the collapse area of the methodology, due to the liquefaction probability of the buildings' site. Based on this information, P25 is found to be more conservative in terms of soil conditions.

As seen in Figure 2.5f-2.5h and 2.6f-2.6h, the scatter for scores of all investigated RVS methods with respect to code-level performance states are found to be significantly high, particularly for the collapse state buildings. Even the FEMA-154 method that was found to be providing reasonable results at the building stock level, failed to provide accurate performance predictions at the individual building level. Thus, it can be inferred that the assessment of seismic risks of such substandard individual buildings by employment of RVS procedures, which mainly depend on the visual physical features of buildings, may lead to significant errors. Thus, the employment of

RVS methods on such sub-standard building stocks should normally be limited to determining the regional risk and high-priority areas. The effect of the number of stories on the general seismic performance based on the evaluation of nearly 23,000 buildings was analyzed elsewhere (Aydogdu et al, 2023b). The outputs provided from the mentioned study show that the seismic safety of buildings with the same number of stories built in the same period can be at different levels. However, even though the determined standard deviation is high, seismic safety ratios exhibit a logarithmically decreasing trend as the number of stories increases.

The success of RVS methods on ranking of seismic risk is also considerable subject of evaluation. As the code-based background of PERA2019 yields congruent results with respect to outputs of detailed assessment methods, incremental approach of SSR is adopted as reference results for assessment of ranking success of RVS procedures, and comparison of RVS results with SSR values are prepared (Figure 2.7). Linear regression lines demonstrated that RVS methods are inclined to yield higher scores as SSR value increases. However, the consistency rates of the RVS procedures are quite low. METU and FEMA154 methods have 26% and 30% R^2 values, while this value is 8% for BOUN-YTU method.

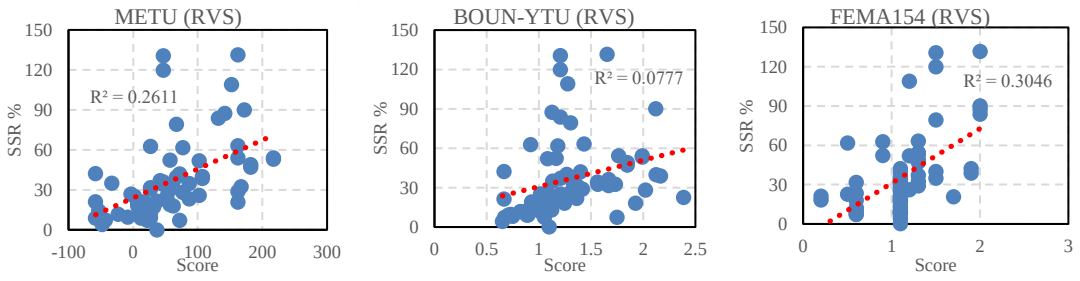

a) b) c)

Figure 2.7 : Comparison SSR values of PERA2019 with RVS results: a) METU, b) BOUN-YTU, c) FEMA154 methods.

The number of low- and mid-rise reinforced concrete buildings (including up to 10 story residential, industrial, commercial and public buildings) constructed before the year 2000 in the Istanbul metropolitan area are estimated to be approximately 620,000. The required duration (days and years) and estimated costs to evaluate all these buildings by using second stage methodologies are predicted and presented in Table 2.5. It is clear that the prioritization of the buildings using second-stage assessment methods is vital in terms of both time and financial aspects, since code-level evaluation

of the whole building stock would cost almost 30 times more money than conducting a second stage assessment procedure (Estimated based on the data from Table 2.5).

Table 2.5 : Total required days and estimated costs to analyze all reinforced concrete buildings that were constructed before 2000 for second stage evaluation methods. An eight-hour daily working period, 250 workdays in a year, and a workforce of 100 teams are assumed.

	PERA2019	AURAP	DURTES	P25	HASSAN & SOZEN
Average Required Time (min/building)	85	101	113	85	48
Total Required Workdays to Complete the Study	1090	1296	1449	1090	616
Total Years Required	4.4	5.2	5.8	4.4	2.5
Estimated Cost (million €)*	41.0	48.8	54.6	41.0	23.2
Ratio to Complete Code-Based Analysis Cost*	3.0%	3.6%	4.0%	3.0%	1.7%

* Costs are calculated based on the average cost of inspection of an average building. The information is provided by the IMM in November 2021.

Hassan & Sozen method is determined to be the most time- and cost-effective second stage method. However, the technical accuracy of this method is not sufficient to evaluate the seismic performance of the building stock. AURAP and DURTES are the most time-consuming two methods, as the average required time to complete the assessment of 620,000 buildings is more than 5 years for both. PERA2019 and P25 methods require the same onsite workload to complete the assessment procedure, yet P25 method needs secondary data to be defined in the office as foundation depth and groundwater table.

Results of this study reveal that even if each approach will have its own set of merits the PERA2019 method comes forward among the procedures investigated in the scope of this work, not only for its ability in realistic and sufficiently conservative seismic risk classification (being compatible with code-based performance criteria, PERA2019 catches 96% of the buildings in collapse state with respect to code-level assessment, which is the highest ratio compared to other methods) but also for its cost- and time-wise feasibility. In light of this information, it has been revealed that the building stock of Istanbul needs to be prioritized starting from the buildings with the lowest SSR value of the PERA2019 methodology. Thus, IMM has selected PERA2019 method for its application to 23,000 existing buildings in Istanbul. The findings of this study can be found elsewhere (Ilki et al, 2021; Aydogdu et al, 2023b).

2.6 Discussion on the Reliability of Rapid Assessment Methods

This study was conducted as a preliminary stage of a widespread structural safety assessment campaign to be carried out in Istanbul by IMM. The predictions of the selected RVS and the second stage evaluation methods are compared with the code-based detailed seismic assessment results for 72 service buildings of IMM in the scope of this study. Thereafter, the most accurate and efficient rapid seismic safety assessment method in terms of time and cost has been applied to nearly 23,000 reinforced concrete buildings that were built before the year 2000 as the continuation of this study. Consequently, the objective of this study was to decide on a quick, yet reliable rapid safety seismic safety assessment procedure to determine the buildings with poor seismic performance in huge building stocks and rank them with respect to their seismic risks.

RVS procedures demonstrated a fair anticipation of the general vulnerability of the buildings investigated in the scope of this article. However, the individual building-based risk determination capability of these methods is found insufficient. The main reason for this is the large differences in seismic performances of existing buildings which look similar from the outside. This is due to non-standard construction practices of buildings that have been constructed before 2000s without a proper inspection. This study clearly demonstrated that it may lead to remarkable mistakes if seismic risks of such substandard individual buildings are estimated based on RVS procedures without collecting and processing further and more detailed information from the buildings. In light of these facts, the use of RVS procedures on substandard and non-code-complying building stocks like the ones in Istanbul should be limited to the assessment of risks in a regional scale.

As expected, it is observed that the second stage assessment methods generally showed a better agreement with code-based detailed seismic performance assessment results when compared to RVS methods. Based on the extensive comparisons outlined above, the PERA2019 method is determined as the most convenient procedure due to its consistency with the code-based detailed assessment procedure, and its efficiency in terms of time and cost for application in a huge city like Istanbul, where hundreds of thousands of existing substandard buildings are to be examined. The buildings determined to be in D and E risk classes according to PERA2019 method (two highest

risk classes among five in this method) cover 96% of the buildings determined to be in “collapse” state according to the code-based detailed seismic performance assessment results for the buildings that are examined in the scope of this research. Likewise, most of the buildings determined to be satisfying the performance limits of “controlled damage” or “collapse prevention” according to the code-based detailed seismic performance assessment results were in the risk classes of C, B and A, which correspond to moderate and low risk in PERA2019 method.

The examination of the costs and the time needed to conduct a structural investigation on hundreds of thousands of buildings demonstrated that conducting the second stage assessment methods to the whole building stock of Istanbul constructed before the year 2000 costs 1.7~4.0% of that of the detailed seismic performance assessment through TBEC-2018. As a final comparison, the application of PERA2019 procedure to 615,700 existing reinforced concrete buildings in Istanbul that were built before the year 2000 by an estimated workforce of 100 technical teams composed of an engineer and a technician will take approximately 4-5 years, whereas the detailed assessment of seismic performances of these buildings according to the TBEC-2018 would take 150 years. Consequently, it is clear that only a widespread application of the second stage assessment procedures may realistically address the need for classifying all buildings in terms of seismic risk in big cities like Istanbul due to limited financial resources available to be allocated for this purpose and time constraints.

3. CASE STUDY FOR A PERFORMANCE BASED RAPID SEISMIC ASSESSMENT METHODOLOGY (PERA2019) BASED ON ACTUAL EARTHQUAKE DAMAGES[2]

3.1 Outlines of the Chapter

Most of the buildings in Turkey constructed before 1999 Kocaeli and Duzce Earthquakes do not have sufficient seismic resistance due to construction errors and do not satisfy the recent Turkish Building Earthquake Code (2018) or its preceding versions. In Istanbul, the building stock consists of 1,166,300 buildings. Clearly, seismic safety assessment of this amount of buildings is not practically possible by code-based detailed assessment approaches, which generally assess the seismic performance of buildings in terms of pass or fail, rather than rank and classify/prioritize these buildings considering their seismic safety. Moreover, the probability of a catastrophic earthquake that could hit Istanbul is high. Therefore, to minimize casualties and economic losses, it is important to determine the most vulnerable existing buildings effectively in terms of cost and duration. Accordingly, Istanbul Metropolitan Municipality has started to evaluate the seismic safety of existing reinforced concrete buildings using the PERA2019 method considering the actual structural data collected on site. The buildings are then divided into 5 seismic risk classes from low-risk to very high-risk according to the computed seismic safety ratio. In this study, the reliability of the PERA2019 is evaluated by considering the predicted risk classes of another large group of actual buildings that have been subjected to actual earthquakes and experienced earthquake-induced damages in different extents. The comparative evaluation of actual seismic damages and predictions of PERA2019 showed clearly that the methodology has a sound ability to estimate the structural seismic performance of the investigated buildings.

[2] This chapter is based on the following publication:Case Study for a Performance Based Rapıd Seısmıc Assessment Methodology (PERA2019) Based on Actual Earthquake Damages, Bulletin of Earthquake Engineering, accepted on 05.12.2023.

3.2 Summary of the Literature

Turkey has suffered from devastating earthquakes in the past. The experience of previous earthquakes shows that the buildings in seismically active regions in Turkey are extremely prone to heavy damage or collapse (Bibbee et al, 2000; Holzer et al, 2000; Scawthorn and Johnson, 2000; Ozmen, 2000; Erdik, 2001; Bruneau, 2001; Celep et al, 2011; Tapan et al, 2013). After the heavy losses of the 1999 Marmara Earthquakes, a common seismic awareness has arisen in Turkey, and the year 2000 has been accepted as a milestone (Ilki and Kumbasar, 2000; Ozdemir et al, 2002). Although there has always been an up-to-date seismic design code in force in Turkey since 1940's, most of the existing buildings built before the year 2000 have been constructed improperly without complying with the seismic code regulations and original design projects, with poor quality materials and workmanship, and incorrect structural details. Deterioration of these poorly constructed buildings over time, mostly because of damages due to corrosion of reinforcing bars, further magnifies the problem (Inci et al, 2013).

These relatively old, sub-standard and deteriorated buildings must be assessed urgently in terms of their potential seismic performance in order to take necessary measures in a rationally prioritized approach to minimize losses against future earthquakes. On the other hand, conducting a widespread code-based detailed evaluation for such a high number of buildings is inefficient both in terms of cost and time, if not impossible. To reduce this huge problem to a manageable scale, a simplified and economical, yet reliable and realistic rapid seismic assessment method is needed for planning intervention strategies in a rational and prioritized way. However, current seismic regulations such as Provisions for the Seismic Risk Evaluation of Existing RC Buildings under Urban Renewal Law (2019) and Turkish Building Earthquake Code (2018) do not involve a building-based ranking/prioritization system, but they rather lead decisions as pass or fail (i.e. risky or not, providing life safety or not). A usual structural engineering investigation of the existing buildings in Istanbul according to the current seismic regulations will probably end up with the fact that almost every ordinary building constructed before the year 2000 is risky (or they will not satisfy life safety-controlled damage performance target). Therefore, making use of a reliable and rapid seismic performance ranking procedure for individual buildings is a key issue for prioritizing buildings with respect to their seismic risks. Sorting the buildings by

their seismic capacity to demand ratios is a reasonable way to fill this gap. Actually, in some countries that are in active seismic regions, important steps have recently been taken towards such a categorization. In New Zealand, SLaMA, a new risk-based methodology for intervening earthquake-prone buildings has been published (NZSEE, 2017). The procedure divides buildings into six risk classes in terms of the New Building Standard% (NBS%). D and E Class buildings with a NBS% less than 1/3, have to be intervened to reach at least 2/3 NBS level. The allowed time window to mitigate the seismic risk of the building changes with the seismicity of the region and the importance/function of the building. Gentile et al. (2019) performed a validation study to investigate the accuracy of the SLaMA procedure via comparison with pushover analysis on 40 RC frames. As the probability of a catastrophic earthquake that could hit Istanbul is very high in the near future (Parsons et al, 2000), it is gravely important to identify the most vulnerable existing buildings and prioritize them according to their seismic risks to minimize losses. The evaluation and prioritization of earthquake-prone buildings according to their seismic performance were studied by various researchers. Sextos et al. (2007) proposed a combined pre and post-earthquake assessment approach with a GIS-integrated system. The pre-earthquake assessment method is based on street survey applications. Marasco et al. (2021) introduced a simplified procedure with a surrogated model for large-scale building stocks, and the authors performed a validation study through nonlinear finite element models.

According to Cakti et al. (2019), the building stock in Istanbul consists of 1,116,300 buildings, and 194,000 of them will be subjected to moderate, heavy or very heavy damage after a Mw=7.5 scenario earthquake. The code-based detailed evaluation of over 1 million buildings cannot respond to the urgency of risk mitigation studies in Istanbul. Thus, the aim of the rapid seismic methodology that is assessed in this study is to find those buildings with a cost and time-effective yet sufficiently accurate approach. Istanbul Metropolitan Municipality has started a rapid and cost/time-efficient seismic assessment campaign in Istanbul. In the scope of this study, nearly 23,000 sub-standard reinforced concrete buildings were investigated through PERA2019 method (Ilki et al, 2021a) and ranked them by their seismic risk level from low risk to very high risk (Aydogdu et al. 2022b). Detailed performance-based assessment efforts are saved for high and very-high risky buildings to reduce the scale of risk mitigation studies and increase the feasibility of the process. Currently, the

Municipality has also started a campaign aiming to retrofit thousands of buildings starting from very high risky ones determined through the PERA2019 methodology.The good agreement of the used rapid assessment methodology with the detailed seismic safety assessment results obtained based on the Provisions for the Seismic Risk Evaluation of Existing RC Buildings under Urban Renewal Law (2019) and Turkish Building Earthquake Code (2018) through three-dimensional structural analyses was already presented by Aydogdu et al. (2023a) before. In the same study, the reliability of 5 second stage assessment and 3 street survey methods were compared too, and the results showed that the PERA2019 method yielded the most compliant outputs with the code-based detailed assessment assessments, which is the consequence of the code-compliant algorithm of PERA2019.

The seismic performance of the buildings that were constructed before 2000 during the 2023 Kahramanmaraş earthquakes was investigated thoroughly in the disaster area by the authors several times. Most of the buildings that caused life losses were not built according to their codes and did not meet the minimum requirements of their era's seismic design codes. The lessons that were learned from the 2023 Kahramanmaraş earthquakes dictate that there is an urgency of implementing seismic performance assessment on the country scale in Turkey. Computing the seismic safety of the buildings and classifying them through an economical and time-effective yet sufficiently accurate rapid performance based analysis approach can respond to the urgency of the risk mitigation studies, so interventions can start from the buildings containing the highest seismic risk. The proposed approach takes the deficiencies that the building stock has and the probable effects of these weaknesses into consideration. Moreover, the PERA2019 methodology has demonstrated its success on buildings that were subjected to different earthquakes, as well as code-based assessment comparisons. In this study, the reliability of the rapid seismic safety assessment methodology used in Istanbul (PERA2019) is evaluated through a database of actual structural seismic damages of actual buildings established based on damage survey reports prepared after earthquakes that affected different regions of Turkey (Afyon, 2002; Bingöl, 2003; Aegean Sea, 2020).

3.3 PERA2019: General Information on the Methodology

The PERA method was initially introduced by Ilki et al. (2014) to determine the seismic performance of reinforced concrete (RC) frame buildings rapidly and reliably based on the criteria provided by Turkish Seismic Design Code (2007). The method was modified in 2019 to assure conformity with the up-to-date seismic provisions (Provisions for the Seismic Risk Evaluation of Existing RC Buildings under Urban Renewal Law 2019). The use of the modified version of the methodology is not limited to frames, but can also be applied for RC buildings with shear walls. The overall flow and background of the method have recently been summarized by Ilki et al. (2021a) and Aydogdu et al. (2023b). The method is developed for buildings up to 10-story high, for which the first mode of vibration is generally dominant. In the first step, the critical story is identified based on engineering judgment; typically the ground story. The number of stories, plan dimensions of the stories, story heights, cross-section dimensions of the critical story columns and shear walls, locations of the columns and shear walls in the building plan, slab type and common beam cross-section dimensions, compressive strength of concrete, reinforcement type (plain/deformed) and details in terms of spacing of transverse reinforcement and the ratio of longitudinal reinforcement, irregularities in plan and elevation, reinforcement diameter loss due to corrosion and seismic demand parameters determined considering ground conditions are required to perform the analysis. The data required for the implementation of the PERA2019 methodology is summarized in Table 3.1. A typical team consisting of a civil engineer and a technician or an architect can evaluate and finalize data collection for an ordinary building in 1.5 hours on average.

The seismic capacity is determined by an incremental approach repeating the simplified structural analyses and assessment procedures at each increment of seismic demand beginning from very small seismic actions until the seismic capacity of the building is reached (Figure 3.1a). The incremental analysis begins with the first step, which is corresponding to 1% of the acceleration demand spectrum. If the building is not determined critical (this process is explained below), the spectral acceleration values of the spectrum are increased by 1% (such as 2%, 3%...) until the step that the building is determined critical which is the iteration step i+1. Then, step i is determined as the last step for which the building is not critical, and the PGA value of the spectrum applied at iteration i is defined as the PGA capacity of the building. Seismic Safety

Ratio (SSR), determined through this incremental procedure is the ratio of PGA capacity to PGA demand (equation 3.1). For example, the SSR value of 50% means that the PGA capacity of the considered building is 50% of the PGA demand. If the building satisfies the PGA demand, the SSR value of that building is equal to or greater than 100%.

Table 3.1 : The data required for the PERA2019 methodology.

Collected Data		Remarks
Building address, ID number and geo-location		Building ID, address and coordinates (latitude and longitude values) are noted
Building geometry	Number of stories	Stories below and above the ground level
	Plan dimensions of the stories	To be measured, cantilevers included
	Story heights	To be measured
	Critical story	To be identified based on the engineering judgment, typically the ground story unless the basement stories are not bounded by rigid RC walls
	Clear heights of the columns and shear walls at the critical story	Particularly important for short columns
	Cross-section dimensions of the critical story columns and shear walls	To be measured in situ
	Locations of the columns and shear walls in the building plan	Interior, Edge or Corner; Locations are used to proportionally distribute the column axial loads
	Slab type and common beam cross-section dimensions	Most common slab type (slabs with beams, ribbed slab, flat slab), common beam cross-section width and height
Concrete compressive strength		To be obtained either by destructive (concrete coring) or non-destructive (i.e. Schmidt Hammer) methods
Column and shear wall reinforcement details		Longitudinal reinforcement type and ratios, transverse reinforcement type, spacing and diameter, to be determined by concrete cover removal on a few members and by using a rebar locator
Potential structural irregularities and weaknesses (Torsional irregularity, projections in plan, floor discontinuities, soft/weak story, discontinuity of vertical structural members, adjacent buildings with different slab levels)		Based on site observations engineering judgment is employed
Reinforcement diameter loss due to corrosion		Is corrosion widespread at the critical story? Longitudinal and transverse bar diameter loss percentage
Seismicity	Local soil class	To be decided based on microzonation studies, V_s30 shear wave velocity maps, existing geotechnical investigation studies
	Spectral parameters (i.e. short period and 1-second spectral acceleration coefficients S_{DS} and S_{D1})	To be obtained from the seismic hazard map or scenario earthquake studies

$$\text{Seismic Safety Ratio (SSR, \%)} = 100 \times \frac{PGA_{Capacity}}{PGA_{Demand}} \qquad (3.1)$$

The capacity values of the elements are calculated according to TS500 (2000). The distribution of base shear to columns in RC frame buildings is done in proportion to the rigidity of the columns. The structural calculation steps are explained thoroughly elsewhere (Ilki et al, 2014). RC frame buildings with shear walls are evaluated according to the proposed principles by Macleod (1972); equivalent frame and shear wall systems are evaluated separately and shear forces are distributed to these two different systems. Then, element forces are appointed proportionately to the rigidity of elements from each system's total shear force. Moment forces of column and shear walls are calculated according to equation (3.2) and equation (3.3), and the schematic

demonstration of the approach is given in Figure 3.1b and Figure 3.2c, respectively. M_c is the column moment, V_c is the column shear force, h_i is story height, M_w is the shear wall moment, H is the height of the shear wall up to top story as cantilever, V_w is the shear force of the shear wall.

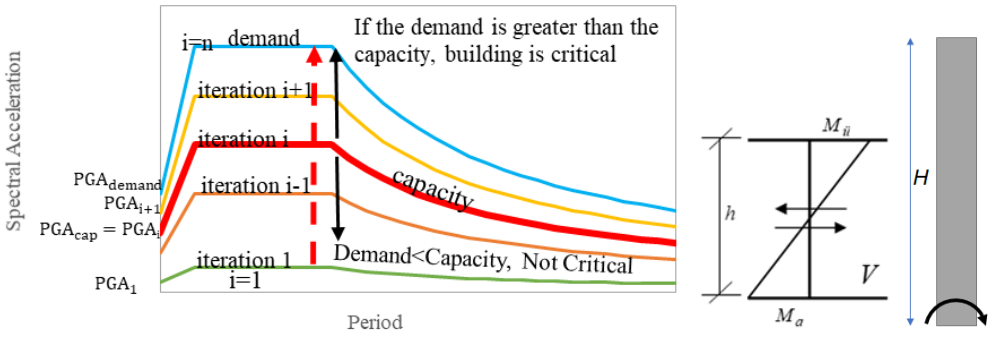

a) b) c)

Figure 3.1 : a) Typical elastic acceleration spectra scaled at various levels for iterations, b) calulation of column moments, c) calculation of shear wall moments.

$$M_c=0.6\ h_i\ V_c \tag{3.2}$$

$$M_w=0.67\ H\ V_w \tag{3.3}$$

In the computation phase of the method, the reference limits for deciding if the building satisfies the performance target are in parallel with the Provisions for the Seismic Risk Evaluation of Existing Buildings-2019 (RBTE-2019). A validation study for the previous version of this seismic document, Provisions for the Seismic Risk Evaluation of Existing Buildings-2013 (RBTE-2013), was presented by Binici et al. (2013). The ratio of the sum of the shear forces that are carried by risky columns and shear walls (V_{risky}) to the total base shear force (V_{story}) must be calculated to determine whether the building can sustain the seismic demands considered. To determine if a vertical element is risky, these members are classified into member categories based on their confinement conditions and flexural shear loading ratios as given in Table 3.2. Afterwards, the columns and shear walls, which exceed either the demand/capacity or interstory drift ratio limits defined in Table 3.3 according to their member categories, are classified as risky members. It should be noted that the interstory drift ratio is the lateral displacement divided by the height of the considered column. The demand/capacity or interstory drift ratio limit approaches adapted from RBTE-2019 (2019) are similar to the acceptance criteria for reinforced concrete columns and shear walls defined by ASCE 41-17 (2017).

Table 3.2 : Categorization of columns and shear walls.

Columns			Shear Walls		
V_e/V_r	s≤100 mm, 135° hooks, $A_{sh}\geq 0.06sb_k$ (f_{cm}/f_{ywm})*	All other cases		$V_e/V_r\leq 1.0$	$1.0\leq V_e/V_r$
$V_e/V_r \leq 0.7$	A	B	$2.0\leq H_w/l_w$	A	B
$0.7< V_e/V_r \leq 1.1$	B	B	$H_w/l_w>2.0$	B	B
$1.1< V_e/V_r$	B	C			

s: stirrup spacing, Ash: cross-sectional area of transverse reinforcement, H_w: wall height, l_w: wall length
V_e: flexural shear demand, V_r: shear strength.

Table 3.3 : Demand/capacity and interstory drift ratio limits for reinforced concrete columns and shear walls.

A Class Columns			B Class Columns				C Class Columns	
$N_K/(A_cf_{cm})$	m_{limit}	$Drift(\%)_{limit}$	$N_K/(A_cf_{cm})$	$A_{sh}/(sb_k)$	m_{limit}	$Drift(\%)_{limit}$	m_{limit}	$Drift(\%)_{limit}$
≤0.1	5	0.035	≤0.1	≤0.0005	2	0.01	1	0.005
				≥0.006	5	0.03		
≥0.6	2.5	0.0125	≥0.6	≤0.0005	1	0.005		
				≥0.006	2.5	0.0075		

A Class Shear Walls					B Class Shear Walls		
$N_K/(A_cf_{cm})$	$V_e/(b_wdf_{ctm})$	Boundary Region	m_{limit}	$Drift(\%)_{limit}$	$V_e/(b_wdf_{ctm})$	m_{limit}	$Drift(\%)_{limit}$
<0.1	≤0.9	Exists	6	0.03	≤0.9	4	0.02
		N/A	4	0.015			
	≥1.3	Exists	3.5	0.015			
		N/A	2	0.0075			
>0.25	≤0.9	Exists	3.5	0.02	≥1.3	2	0.01
		N/A	2	0.01			
	≥1.3	Exists	2	0.01			
		N/A	1.5	0.005			

N_k: the axial load of the element, A_c: cross-sectional area of the element, m_{limit}: demand/capacity ratio limit for the element.
$Drift(\%)_{limit}$: allowed drift limit for the element, b_w: width of the element, f_{ctm}: the tensile strength of concrete, d: depth of the section

Figure 3.2 illustrates the computation of the global performance of the structural system. If the average axial load ratio is less than 10% at the critical story, the total shear force of the risky columns and shear walls (V_{unsafe}) are allowed up to 35% of the story shear force (V_{story}), while none of the columns and shear walls is allowed to exceed their demand/capacity ratio limits for the buildings that have average axial load ratio greater than 65%. For the cases where the average axial stress is between 10% and 65% at the critical story, interpolation should be made in order to calculate the allowed story shear limit. The normalised average axial load ratio is computed by equation (3.4).

In the equation, S_{av} is the normalised average axial load ratio, $N_{k,i}$ is the axial load acting on vertical structural members (i.e. column or shear wall) at the critical story, A_i is the cross-sectional area of vertical member, f_{cm} is the compressive strength of the existing concrete and n is the total number of columns and shear walls. The axial loads on the columns and shear walls are calculated considering the tributary area of these vertical members with an assumption of 10 kN/m^2 and 13 kN/m^2 unit gravity loads for residential and public buildings, respectively. The assumed gravity loads are

determined by taking into account dead loads and reduced live loads. The contribution of longitudinal reinforcement on axial load capacity of vertical elements is not considered. It should be noted that the definition of N_k is slightly different with respect to the definition of N_k in RBTE-2019.

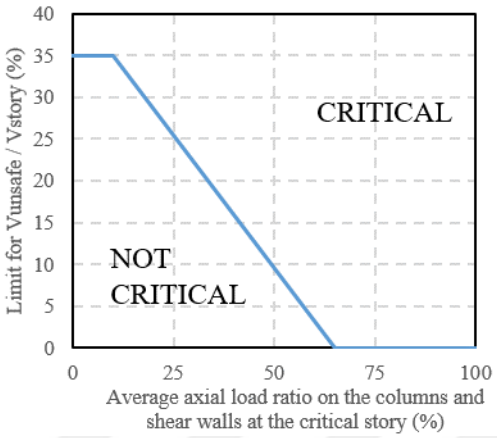

Figure 3.2 : The total allowed shear force ratio of columns exceeding their demand/capacity ratio limits. The ratio is dependent on the average axial load ratio at the critical story (V_{unsafe}: The total shear force that is carried by risky elements, V_{story}: The total shear force of the story).

$$S_{av} = \frac{\sum_{i=1}^{n} \frac{N_{k,i}}{A_i f_{cm}}}{n} \tag{3.4}$$

Finally, the buildings in the examined region can be prioritized concerning their seismic risk levels depending on their SSR values. Building risk classes defined by Ilki et al. (2021a) are given in Table 3.4. As the SSR value is lower, the seismic risk of the building is higher. A similar classification approach in the SLaMa procedure (NZSEE 2017) divides buildings into six risk classes in terms of the New Building Standard% (NBS%). The buildings with an NBS% less than 1/3 have to be intervened to reach at least 2/3 NBS level according to SLaMa. A similar classification approach to New Zealand is in force In Italy. In addition, the expected annual economic loss is also a key parameter that is taken into consideration in Italy. Further information on this classification approach can be found in Polese et al. (2018).

A brief summary of the general flow of PERA2019 to compute SSR value is given in Figure 3.3. In this figure, the Performance Reduction Coefficient (PRC) corresponds to the cumulative multiplication of 0.9 for each structural irregularity and weakness. A more comprehensive summary of the PERA2019 methodology was explained by Ilki et al. (2021a).

Table 3.4 : Building risk classes and risk levels corresponding to various SSR intervals for the global structural system.

SSR (%)	Building Risk Class	Risk Level
≥100	A	Low Risk
75-<100	B	Low Risk
50-<75	C	Medium Risk
25-<50	D	High Risk
<25	E	Very High Risk

In addition to the validation study of the initial version of the PERA method (limited to frame structures), which was based on detailed analyses of 672 buildings by Ilki et al. (2014) as well as real earthquake damages of 21 buildings after the 1995 Dinar, 1999 Kocaeli, 2002 Afyon, and 2011 Van earthquakes, the reliability of the PERA2019 method (applicable for the frame and frame-shear wall buildings) has studied through a numerical study focusing on 73 existing reinforced concrete buildings by Aydogdu et al. (2023a). In that study, a good agreement was demonstrated between the SSR values of the buildings and detailed code-based (TSDC-2007; TBEC-2018; RBTE-2019) structural seismic assessment results. The results of the numerical study presented by Aydogdu et al. (2023a) have demonstrated that contents of D and E risk classes of buildings as determined by the PERA2019 method capture 95% of the buildings that were found to be in collapse limit state according to detailed code-based assessment procedure (TSDC-2007; TBEC-2018; RBTE-2019). Most of the buildings in collapse prevention or controlled damage performance according to the code-based assessment procedure were found to be in C, B or A risk classes according to predictions of the PERA2019 method (Figure 2.5a and Figure 2.6a). Further details on the PERA2019 method can be found elsewhere (Ilki et al. 2021a).

3.4 Case Study

One of the effective ways to examine the reliability of a seismic evaluation method is to compare the results of the method with actual earthquake-induced damages. Within the scope of this comparative study, SSR values and risk classes of 42 buildings, which were subjected to earthquake excitations in real life, are computed to examine the reliability of the methodology. Then, the damage states of the buildings are compared with the assigned risk classes through the PERA2019 method.

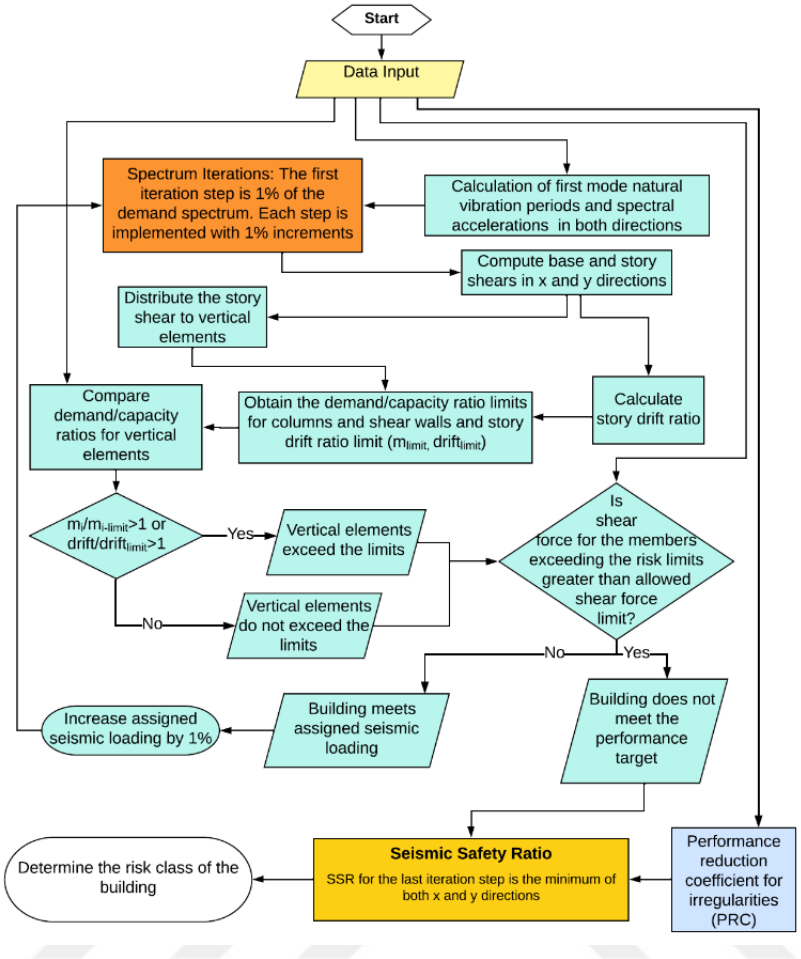

Figure 3.3 : A brief flowchart of the algorithm for the PERA2019 method (Aydogdu et al. 2022b). The information about input data is given in the first paragraph of this section.

3.4.1 Buildings

The structural characteristics and damages of 18 buildings that experienced Afyon (2002) and 22 buildings that experienced Bingöl (2003) earthquakes were taken from the SERU database (METU, 2003). Besides these 40 buildings with different extents of seismic damage, two buildings, which experienced the Aegean Sea Earthquake (2020) and were also investigated in this chapter. Also, 7 buildings added to this study after 2023 Kahramanmaraş earthquake to enrich the outputs. The structural information of the buildings experienced Aegean Sea and Kahramanmaras earthquakes was collected from the site directly, while the others are gathered from the SERU database of Middle East Technical University (METU, 2003). The buildings in Afyon are located in 6 different districts, while the ones in Bingöl are divided into 4 regions according to their location and soil parameters. In addition, 2 buildings in Izmir are located near Karşıyaka and Izmir stations. Nurdagi district of Gaziantep is the

location of 4 buildings experienced Kahramanmaras Earthquake, while 2 buildings are located in Iskenderun-Hatay and 1 building located in Kahramanmaras city center. Figure 3.4 demonstrates the distribution of the number of stories, compressive strength of the existing concrete, reinforcement type and axial load ratio acting on vertical structural members of the buildings. The average compressive strength of concrete is 10 MPa and the frequency of smooth S220 type rebar is nearly 90%. These distributions reflect the overall characteristics of the Turkish building stock, which have been presented by Aydogdu et al. (2023b) for Istanbul, comprehensively. The number of buildings that were built before the publication of TSDC-1998 is 32, while 13 of the evaluated buildings were built after 1998, but before the publication of the two most recent seismic design codes in Turkey, which have been published in 2007 and 2018, respectively.

Minimum requirements in various Turkish Seismic Design Codes for high-seismicity regions are given in Table 3.5, which demonstrates that seismic design codes in Turkey have involved most of the crucial structural details since 1975. Apparently, 98% of the evaluated buildings fail to comply with the minimum compressive strength of concrete requirements of all seismic design codes given in Table 3.5, and 67% of them have at least 1 vertical structural member that cannot satisfy the maximum axial stress limit of TBEC-2018. The damage photos given in subsequent parts of this study demonstrate that most of the examined buildings do not comply with the confinement provisions of the up-to-date seismic design codes. This observation is also supported by Aydogdu et al. (2023b) and others (i.e. Tapan et al, 2013 and Gurbuz et al, 2022) stating that the columns of almost all pre-2000 building stock in Turkey have transverse reinforcement spacing between 200 to 300 mm at the confinement zones. It can be inferred that these buildings, like many buildings constructed in the same period, are far from meeting the design and construction regulations of their era. This case may stem from the lack of control mechanism, seismic awareness and economic resources as narrated by Aydinoglu (2007), Ilki and Celep (2012), Makra et al. (2021), Gurbuz et al. (2022), Aydogdu et al. (2023b).

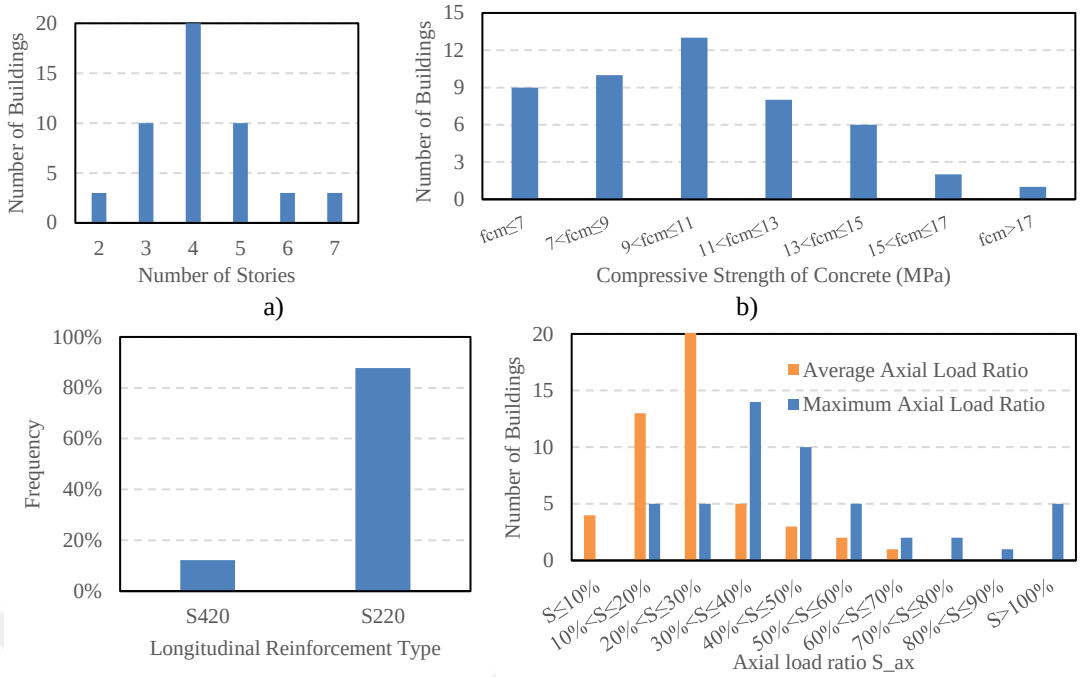

Figure 3.4 : Distribution of the structural parameters of the buildings: a) number of stories, b) equivalent cylindrical compressive strength of concrete (fcm, from concrete hammer), c) reinforcement steel class, where S420 is deformed and S220 is plain reinforcement bars, d) average and maximum axial load ratio acting on vertical structural members.

Table 3.5 : Minimum requirements in various Turkish Seismic Design Codes.

	Seismic Design Code			
	1975	1998	2007	2018
Min. Longitudinal Reinforcement for Columns	1%	1%	1%	1%
Confinement Zone Max. Stirrup Spacing (cm)	10	10	10	10
135° Hook Ends	Yes	Yes	Yes	Yes
Min. Compressive Strength of the Concrete (MPa)	18	20	20	25
Compulsory Deformed Longitudinal Reinforcement	No	No	Yes	Yes
Max. N_d/A_cf_{ck} allowed	0.6*	0.5	0.5	0.4
Shear Wall End Zones	Yes	Yes	Yes	Yes

*from TS500 - Requirements for design and construction of reinforced concrete structures.

The most recent three seismic zoning maps in Turkey are given in Figure 3.5a-3.5c. According to the 1972 Seismic Zoning Map (Turkish Ministry of Public Works and Settlement), Bingöl and Afyon are in the second degree seismic zone, and Izmir is in the first degree seismic zone. By the 1996 Seismic Zoning Map (Turkish Ministry of Public Works and Settlement), the city center of Bingöl became a first degree seismic zone, and the rest of the cities stayed in the same seismic zone assigned by the previous map. In 2018, the zonation map concept was abandoned and a new coordinate-based earthquake hazard map was published (Turkish Ministry of Interior Affairs Disaster and Emergency Management Presidency, 2018). Change in the base shear coefficient

for a representative building (5-story building with V_{s30}=300 m/s soil condition) in Bingol, Afyon and Izmir districts according to various seismic design codes in Turkey is given in Figure 3.5d. The base shear is the maximum shear force demand estimated, which is correlated with the effective seismic weight of the building, seismicity, soil parameters, the importance of the building and ductility of the system. The graph states that base shear demands for the representative buildings increased remarkably according to updated seismic design provisions in 1998, whereas the base shear demand slightly decreased for Afyon and Izmir in 2018. The evolution of the seismic design codes and seismic hazard maps in Turkey are summarized in the timeline given in Figure B.1 as well as the devastating earthquakes that happened in Turkey.

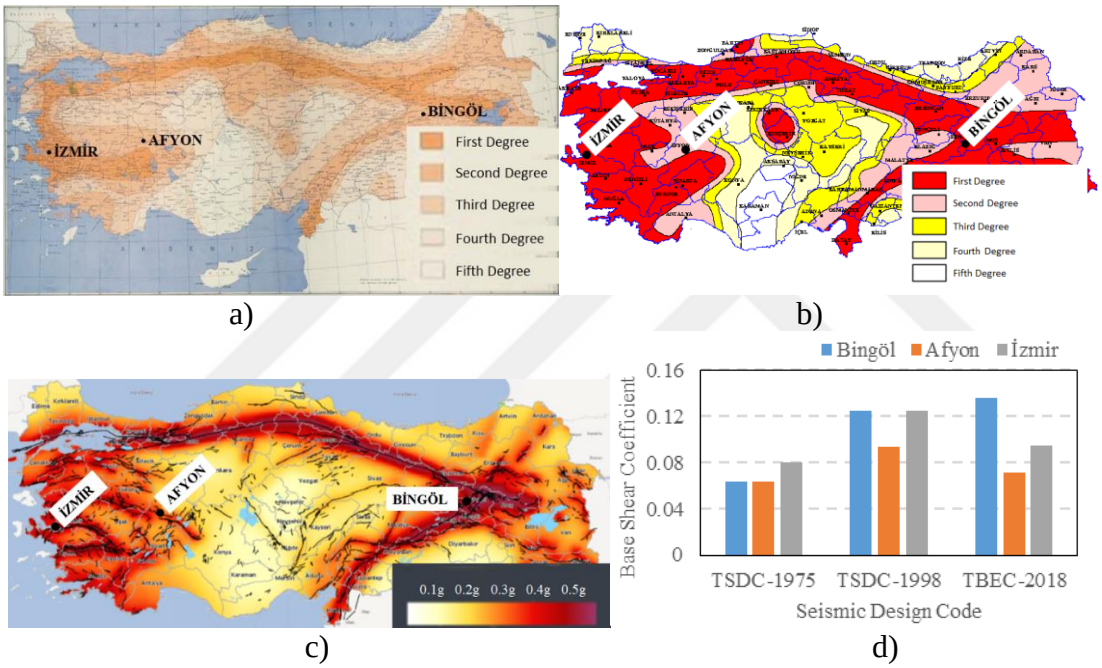

Figure 3.5 : a) 1972 Turkish Seismic Zoning Map (Turkish Ministry of Public Works and Settlement), b) 1996 Turkish Seismic Zoning Map (Turkish Ministry of Public Works and Settlement), c) Earthquake Hazard Map of Turkey (Turkish Ministry of Interior Affairs Disaster and Emergency Management Presidency 2018), d) Change in the base shear coefficient for a representative building in Bingol, Afyon and Izmir districts according to various seismic design codes in Turkey.

The building set consists of 35 reinforced concrete frame system buildings, while 7 of the buildings have dual reinforced concrete frame and wall structural systems. Dimensions of vertical structural members and structural system layouts of 8 representative buildings are given in Figure 3.6. The rest of the layouts and structural information can be found in the SERU database (METU, 2003). Also, exterior photos of 4 representative buildings from Kahramanmaras earthquake is given in Figure 3.7.

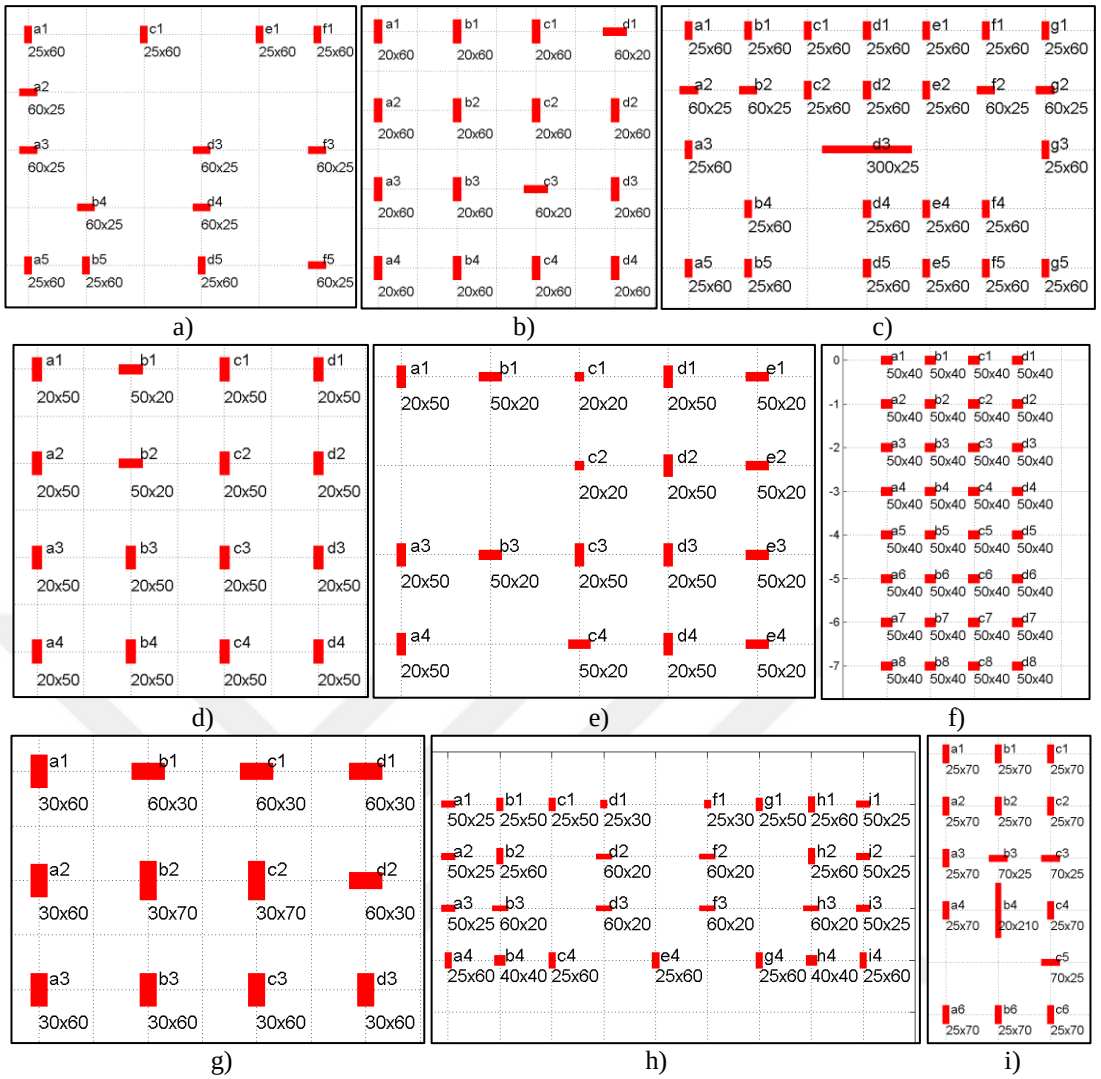

Figure 3.6 : Column layouts of representative buildings, a) BNG-11-4-4, b) BNG-6-4-3, c) BNG-6-4-7, d) AFY-Ç-06, e) AFY-ÇO-05, f) AFY-Y-01, g) AFY-Ç-07, h) AFY-ÇO-02, i) Karşıyaka01(units of column dimensions are cm). Building IDs are used as they are defined in the SERU database (METU 2003).

a) b) c) d)

Figure 3.7 : Exterior photos of buildings from Kahramanmaras Earthquake: a)nurdagi4, b)iskenderun1, c)iskenderun2, d)nurdagi2.

The compressive strength of the existing concrete is assigned based on the concrete hammer test results. A conversion equation of concrete hammer (equation 3.5), which is derived from the chart (Figure 3.8a) provided by the manufacturer (Proceq, 2002), is used to compute the equivalent of cubic (15x15x15 cm) compressive strength of concrete. The influence of the carbonation and the age of the concrete are also taken into consideration; a reduction factor depending on the age of the concrete, which is also provided by the producer of the test hammer, is used (Figure 3.8b). The cylindrical equivalent of the cubic compressive strength is determined through equation (3.6). To calculate the in-situ compressive strength of the concrete for the structures, equation (3.7) is used as suggested by Turkish Building Earthquake Code (2018).

$$f_i = (0.0108 * n^2 + 0.9021 * n - 12.87) * A * 0.8 \quad (3.5)$$

$$f_{c,i} = \propto * f_{cc,i} \quad (3.6)$$

$$f_{cm} = max(0.85 \sum_{i=1}^{z} \frac{f_i}{z}; \sum_{i=1}^{z} \frac{f_i}{z} - std.dev(f_{i=1}^{z})) \quad (3.7)$$

Note that n is the rebound number of the concrete test hammer, A is the age factor, $f_{cc,i}$ is the equivalent of cubic (15x15x15 cm) compressive strength of concrete, $\propto$ is the shape conversion factor to 15x15x15 cm cubic strength to 10x10 cylindrical strength, $f_{c,i}$ is the cylindrical compressive strength of concrete, the z is the number of points that the non-destructive tests were performed, and f_{cm} is the estimated in-situ cylindrical compressive strength of the building.

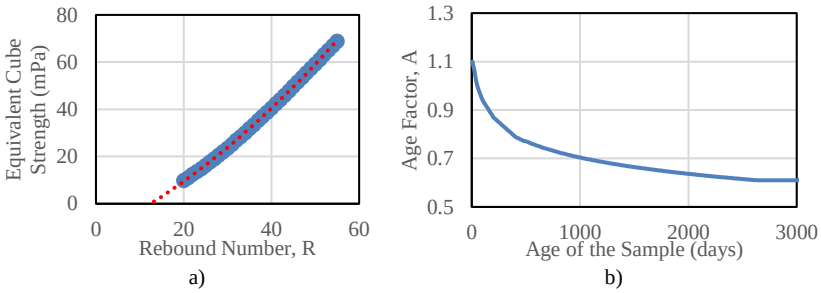

Figure 3.8 : a) The conversion factor for rebound number of the concrete hammer to equivalent cube strength, b) age factor for concrete.

The type of reinforcement bars for each building is reported in the SERU database (METU, 2003). However, the information on the longitudinal reinforcement ratio for columns and shear walls, transverse reinforcement diameter and spacing, which are key parameters to perform PERA2019, are not specified in the database. To overcome

this obstacle, reinforcement information and spacing values are determined from damage photos, when the reinforcements are visible. Otherwise, these parameters are selected based on assumptions made (Table 3.6) considering the common practice of construction along the range of construction years of the investigated buildings (Ilki and Celep, 2012; Ilki et al, 2014; Yakut et al, 2021; Gurbuz et al, 2022; Aydogdu et al, 2022b) together with the minimum requirements of seismic design code valid at that time.

Table 3.6 : The assumptions made in absence of data.

Parameter	Requirements of TSDC-1975	Requirements of TSDC-1998	Year of Construction	Assumption
Longitudinal Reinforcement Ratio	Min. 1.00%	Min. 1.00%	Before 1975 After 1975	0.75% 1.00%
Transverse Reinforcement Spacing at Confinement Zone	Max. 10 cm	Max. 10 cm	Before 2000 After 2000	25 cm 20 cm
Stirrup diameter	8 mm	8 mm		8 mm
Average Beam Cross-Section	20/30 cm	20/30 cm		25/60 cm

3.4.2 Earthquake events

General information on the earthquakes that the investigated buildings were subjected to is given in Table 3.7, and the acceleration-time histories of each earthquake are given in the following sections. The arias intensity is a significant indicator of the strength of a seismic event and demonstrates the time interval in which the energy of the ground motion is distributed. This parameter reflects the significant duration of an earthquake: the difference between the times when arias intensity is 5% and 95% is the significant duration according to Bommer and Martinez-Pereira (1999). Figure 3.9 demonstrates the arias intensities of the Afyon, Bingöl and Aegean Sea earthquakes, and the significant durations of these earthquakes are 12.1s, 4.6s and 20.6s respectively.

Table 3.7 : General information of considered earthquakes.

Date	Epicenter	Depth (km)	M_w	Station (Code)	V_{s30} (m/s)	PGA (cm/s^2)	PGV (cm/s)	PGD (cm)	dip (º)
03.02.2002	Sultandağı - Afyon	22.1	6.5	Afyon (0301)	226	113	13	3	69
01.05.2003	Bingöl	10	6.3	Bingöl (1201)	529	501	37	16	82
30.10.2020	Aegean Sea - Izmir	14.9	6.6	Kuşadası (0905)	369	179	23	5	43

* The codes of the stations that recorded the PGA value are given in parentheses. The locations of these stations can be seen in figures 3.11, 3.14 and 3.17.

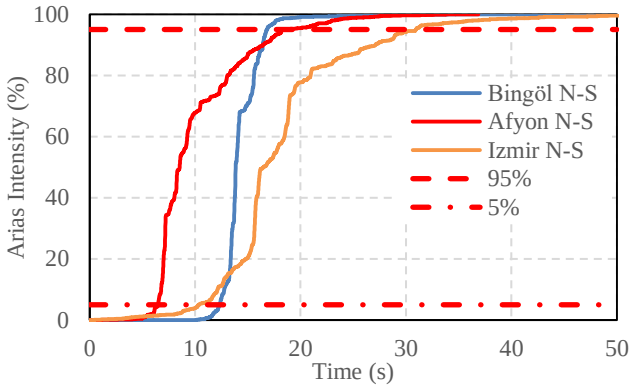

Figure 3.9 : Arias intensity curves computed for N-S records of all investigated earthquakes.

For the buildings in Bingöl and Izmir, the orientation of the buildings was recorded on the plans. Therefore, the horizontal components of the strong ground motions were processed and adapted to be applied along their main orthogonal directions to accurately represent the seismic actions that these buildings were subjected to. The direction of the plan and response in both directions can be extremely critical during an earthquake for irregular structures, the effect of which was studied in detail by Cimellaro et al. (2014). On the other hand, the orientations of buildings in the plans were not noted for the buildings examined in Afyon. Therefore, in absence of information on the plan orientation of the buildings, the geometric mean spectrum of the strong ground motion couple is assigned as seismic demand in both X and Y directions of the buildings in Afyon. Since the buildings in Izmir are very close to strong ground motion recorders in Karşıyaka and Bostanlı districts, acceleration records of these stations were directly used in the analyses. The spectral acceleration value at the first mode period of the building is defined as the seismic demand of the building.

In the case of the Afyon and Bingol earthquakes, there was only one strong ground motion record for each. Therefore, ground motion prediction equations (GMPE) were used to reduce the uncertainties for the investigation of buildings in Afyon and Bingol. For this purpose, Abrahamson and Silva (2008) ground motion prediction equations (GMPE) were used in order to obtain the acceleration spectrum that the buildings were subjected to for the location of each building. The GMPE was developed to estimate the acceleration spectrum and logarithmic standard deviation values for any specific earthquake. The model is applicable to magnitudes between 5 and 8.5 and distances between 0-200, according to developers of the GMPE. In order to reduce the

uncertainties of the ground motions for each seismic event, residuals must be calculated for every location of ground motion recorders in that event to visualize the spatial distribution of the residuals. However, there is a single record for Afyon and Bingol events. Therefore, the spatial distribution of residuals couldn't be produced. To overcome this problem, Bal and Smyrou (2016) proposed an assumption of identical intra-event variability and equal residuals for two locations for the same event. The same approach was used in this study. Several parameters are required for computing the GMPE functions. M_w is the moment magnitude of the event, R_{rup} is the closest distance to the surface rupture, R_x is the horizontal distance to the rupture, W is the rupture width of the fault, R_{jb} is the Joyner-Boore distance, δ is the dip angle, V_{s30} is the average shear-wave velocity of the top 30 m of the soil, Z_{tor} is the depth to the top of rupture and calculated in accordance with the empirical equation introduced by Mai et al. (2005), Z_{HYP} is the hypocentral depth, $Z_{1.0}$ is the depth to a shear-wave velocity of 1.0 km/s at the site. The authors of the used GMPE also recommend scaling for hanging wall sites, the effect of which is evaluated by Beyen (2018). After implementation of the GMPE, median acceleration spectrum (μ) and logarithmic standard deviation of spectral acceleration estimation (σ) parameters are yielded as outputs. TBEC-2018 proposes a scaling procedure between 0.2 and 1.5 times the fundamental period of the structure. Scaling dependent to the first mode period of a structure will yield different scaling factors for two buildings in the same location. However, a location can have only one residual value for a seismic event. Thus, the spectral match is performed over the range of 0.3s and 2.0s periods, which covers %99 of the periods of approximately 23,000 investigated reinforced concrete buildings according to Aydogdu et al. (2023b).

3.4.2.1 Afyon earthquake

According to the Disaster and Emergency Management Presidency, the city center and districts of Afyon province were shaken on 3 February 2002 by a M_w=6.5 earthquake with a 22.1 km focal depth which was also felt strongly in surrounding cities (Url-4). The acceleration records taken from the Afyon city center are given in Figure 3.10. The event occurred on a normal fault zone. The closest ground motion record was taken in the city center of Afyon. The investigated buildings for this earthquake were located in 6 different spots: Afyon city center, Çay, Çobanlar, Sultandağı, Bolvadin and Yeşilçiftlik neighborhoods (Figure 3.11).

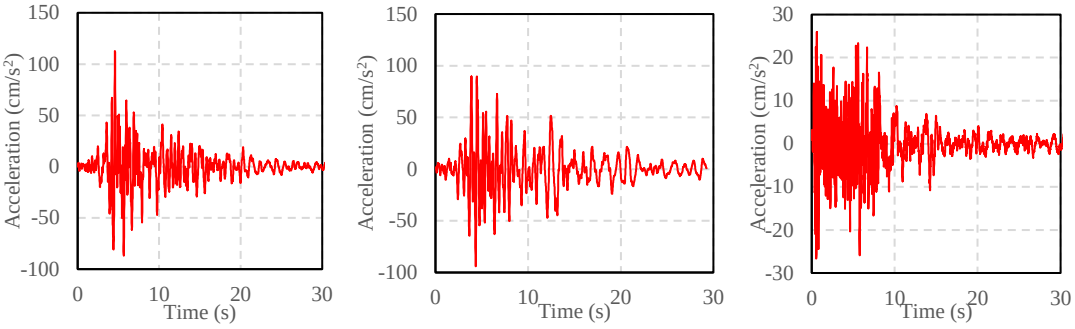

Figure 3.10 : Acceleration-time histories for the Afyon earthquake: a) N-S record, b) E-W record, c) Vertical record (TADAS database, AFAD, 2020).

According to the geology map, the buildings investigated within the scope of this study are on similar geological formation. Akşehir and Eber Lakes and Aksu Stream are located circumference of the field of study, where the soil consists of alluvial sediments. These locations are also represented with similar V_{s30} values according to the global V_{s30} map (Url-5). Thus, the V_{s30} value (226 m/s) of the ground motion recorder in Afyon, which is provided by TADAS database (AFAD, 2020), is assigned to all other locations. The parameters needed to perform the computation for Abrahamson and Silva (2008) equations to obtain acceleration spectra for each district are given in Table 3.8. W, Z_{tor} and $Z_{1.0}$ values are 12 km, 14.9 km and 625 m for all locations, respectively.

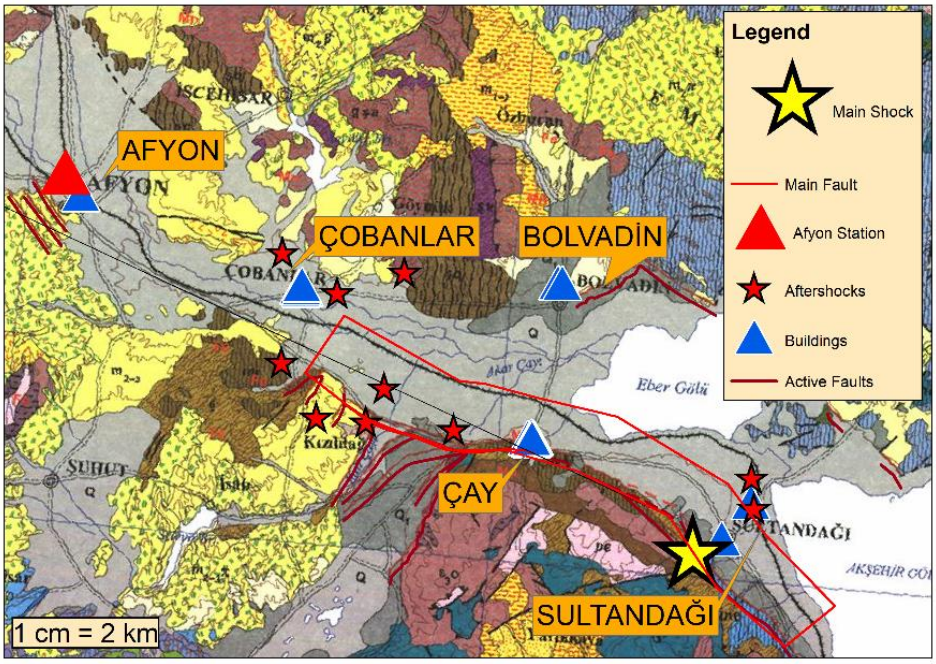

Figure 3.11 : Geology map of Afyon province (taken from the General Directorate of Mineral Exploration and Research). The main event, aftershocks, fault zone and the buildings are shown on the map.

Table 3.8 : The parameters needed to calculate the GMPE.

Location	R_{rup} (km)	R_{jb} (km)	R_x (km)
Afyon (Station)	40.8	31.4	4.8
Sultandağı	14.9	0.0	3.1
Çay	14.9	0.0	1.2
Bolvadin	28.3	10.8	15.1
Çobanlar	17.1	8.5	5.7
Yeşilçiftlik	15.5	4.1	7.4

Acceleration spectra of east-west and north-south components of the Afyon record and GMPE results are given in Figure 3.12a. Here, AS indicates results of GMPE defined by Abrahamson and Silva (2008). Spectral matching is performed to equalize the areas under the period range between 0.3 s and 2.0 s, which is the expected period range of the structures examined in this paper. For the east-west component of the earthquake, a spectral match is reached with the $\mu+0.18\sigma$ spectrum of the GMPE, while for the north-south component, the overlap is with the $\mu+0.13\sigma$ spectrum. As aforementioned, the geometric mean spectra of GMPE results are assigned as seismic demand in both X and Y directions of the buildings in Afyon in absence of plan orientations of these buildings. The geometric mean spectrum of the GMPE result couple for these values is given in Figure 3.12b. The logarithmic standard deviation difference between the observed and predicted spectral value is determined as the residual (ε). Since there is no other available strong ground motion record for this event, the calculated residual for the location of the strong ground motion recorder is appointed for every location for this seismic event, and the demand spectra for all districts are computed accordingly (Figure 3.12c).

3.4.2.2 Bingol earthquake

On 1 May 2003, a Mw=6.4 earthquake struck Bingöl province which occurred on a strike-slip fault (Url-6). The earthquake was felt strongly in surrounding towns. The epicenter of the event is about 14 km northwest of Bingöl. The strong ground motion records obtained from the city center are the only available data for this earthquake (Figure 3.13). The main fault, and locations of examined buildings, aftershocks and the seismic station are demonstrated on the geology map of the province (Figure 3.14). The spatial distribution of the aftershocks with M>4 is in the north-northwest direction for Bingöl city. Also, having a 2.23 km R_{jb} value according to the Disaster and Emergency Management Presidency of Turkey, it is accepted that the ruptured segment of the fault extends into the Bingöl city center. The peak spectral acceleration

of this earthquake is 2.4g at 0.16s period for the N-S component of the record. Such a great seismic demand is expected to create widespread destruction in the city. However, as aforementioned, the significant duration of the earthquake is relatively short compared to the other earthquakes.

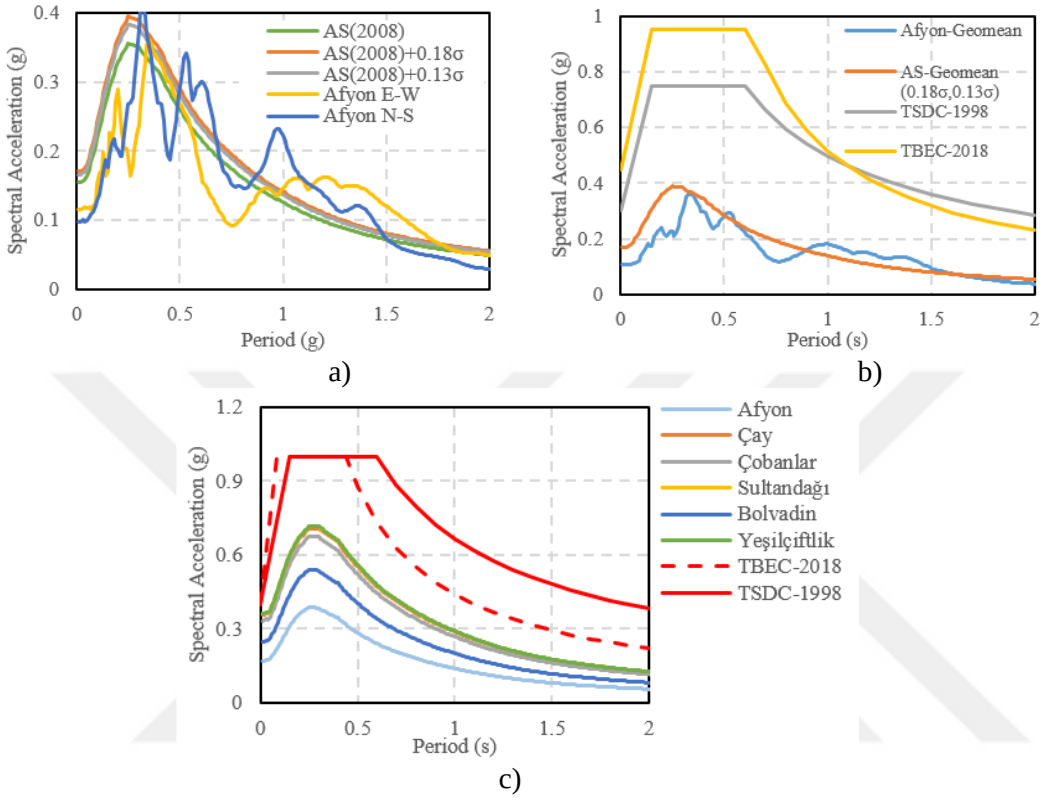

Figure 3.12 : a) Acceleration spectra of east-west and north-south components of Afyon record with matched spectra of GMPE, b) geometric mean spectrum of Afyon record and the design spectrum of the central district of the city according to TSDC-1998 and TBEC-2018, c) GMPE results for 6 different locations and the design spectrum of Çay district according to TSDC-1998 and TBEC-2018.

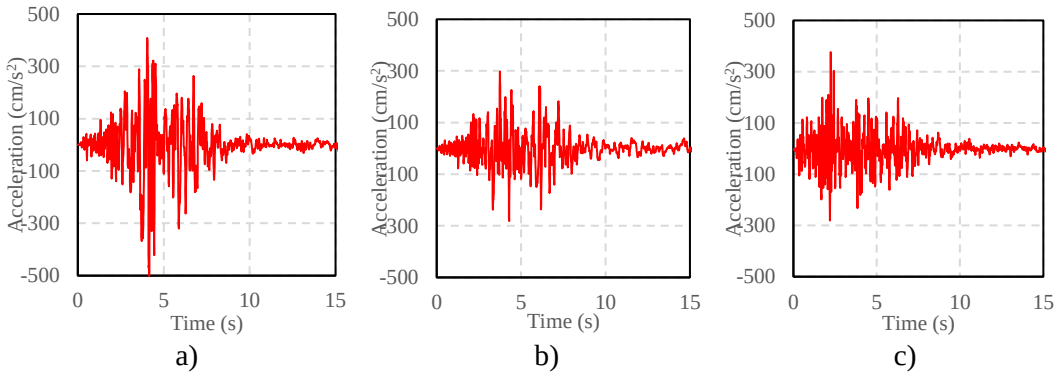

Figure 3.13 : Acceleration-time histories for the Bingöl earthquake: a) N-S record, b) E-W record, c) Vertical record (TADAS database, AFAD, 2020).

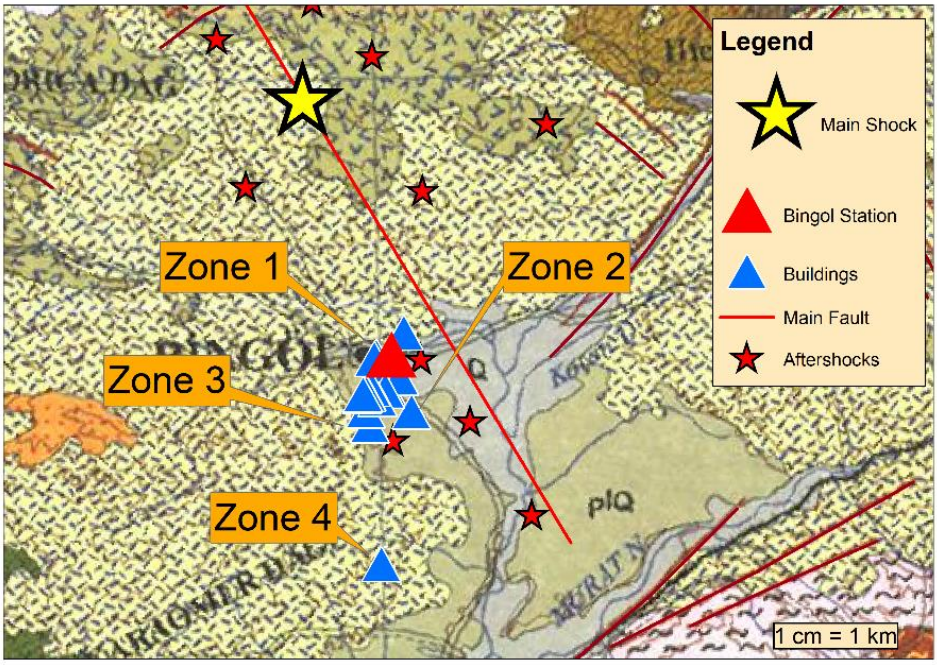

Figure 3.14 : Geology map of Bingöl province (taken from the General Directorate of Mineral Exploration and Research). The main event, aftershocks, fault line and the buildings are shown on the map.

According to the local soil parameters of the seismic station, the recorder is established on relatively hard soil (V_{s30} = 529 m/s). However, the rest of the city is estimated to be on relatively loose soil, based on the Bingöl Earthquake Evaluation Report of the General Directorate of Mineral Exploration and Research (2003) which states that the soil characteristics change from rock formations to fine-grained sediments when going from east to west or towards the plain. Likewise, the global V_{s30} map of USGS (Url-5) suggests 256 m/s shear wave velocity for the plain of Bingöl. As shown below, the locations of the investigated buildings in Bingöl are grouped into four zones, based on the ground conditions. Correspondingly, the GMPE calculations are made to determine the acceleration spectra for these four zones:

- First Zone: Stiff soil and close to the strong ground motion recorder (3 buildings).
- Second Zone: Loose soil in the eastern part of the city (3 buildings).
- Third Zone: Loose soil in the western part of the city (15 buildings).
- Fourth Zone: Loose soil 9 km southwest of the city (1 building).

The parameters needed for the calculation of GMPEs for these locations are given in Table 3.9. W and Z_{tor} values are 8.7 km and 4.8 km for all locations, respectively.

Table 3.9 : The parameters needed to calculate the GMPE.

Zone	R_{rup} (km)	R_{jb} (km)	R_x (km)	$Z_{1.0}$ (m)	V_{s30} (m/s)
1 (Recorder)	5.8	2.2	2.2	171	529
2	5.4	2.5	2.5	545	250
3	6.2	4.0	4.0	545	250
4	9.8	8.6	7.0	545	250

Acceleration spectra determined by the GMPE approach presented above and computed based on east-west and north-south components of the Bingöl record are given in Figure 3.15a. Acceleration spectra of the record and GMPE results between 0.3 s and 2.0 s are matched. For the east-west component of the earthquake, a spectral match is reached with the μ-0.18σ spectrum of the GMPE, while for the north-south component, the overlap is obtained with the μ+0.55σ spectrum. The matched spectra with north-south and east-west components for each zone are given in Figure 3.15b and Figure 3.15c, respectively. Similar to Afyon Earthquake; the calculated residual of the acceleration record is appointed to every other location.

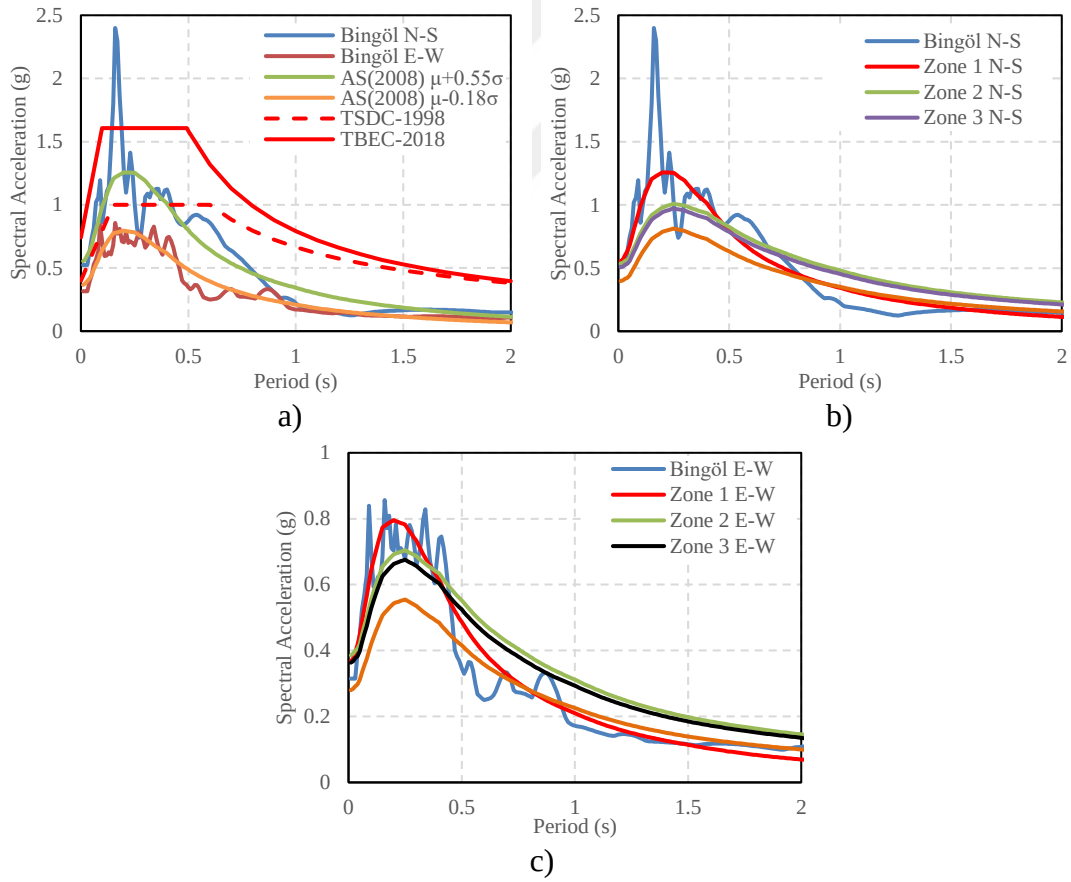

Figure 3.15 : a) Acceleration spectra of east-west and north-south components of the record with matched spectra of GMPE and the design spectrum of the site according to TSDC-1998 and TBEC-2018, b) GMPE results for north-south direction for each location with μ +0.55 ε, c) GMPE results for east-west direction for each location with μ -0.18 ε.

3.4.2.3 Aegean Sea earthquake

An earthquake with M_w=6.6 occurred in the Aegean Sea on 30 October 2020. Even though the distance is nearly 80 km far from the epicenter, which is northeast of Samos Island, Izmir city center was affected by the earthquake seriously. The acceleration records taken from the Izmir city center (Karşıyaka district) are given in Figure 3.16. The main shock occurred on a normal fault (TADAS database, AFAD, 2020). Two buildings that experienced this earthquake are evaluated within the scope of this study. The buildings are located in the vicinity of the recorders in Karşıyaka and Bayraklı districts (Figure 3.17a). Thus, acceleration spectra of corresponding records are assigned as demand spectrum directly. The record couples are rotated based on the orientation of the building (Figure 3.17b).

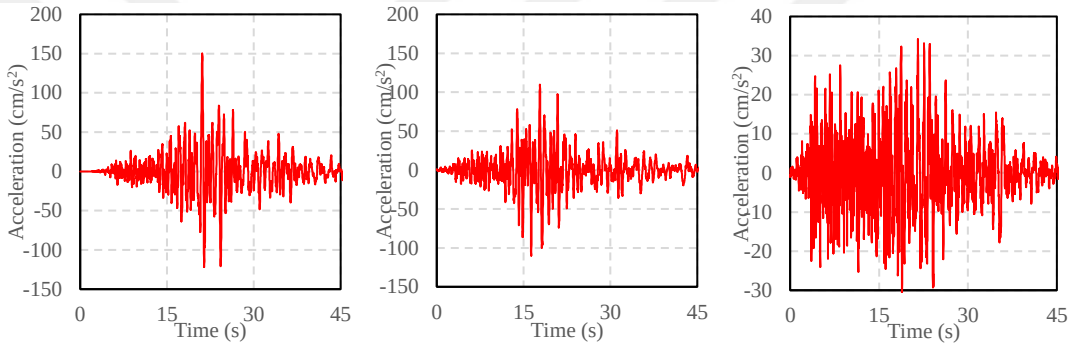

Figure 3.16 : Acceleration-time histories for the Aegean Sea earthquake: a) N-S record, b) E-W record, c) Vertical record (TADAS database, AFAD, 2020). Vs30 parameter of the site, of which the recorder is located, is 131 m/s.

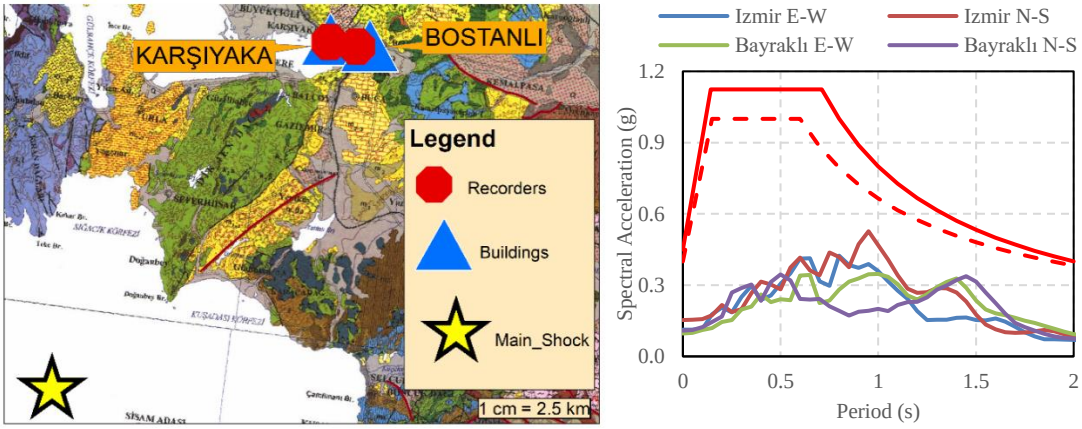

Figure 3.17 : a) Geology map (taken from the General Directorate of Mineral Exploration and Research) and the locations of the buildings and strong ground motion stations (records), b) Acceleration spectra of the records and the design spectrum of the site according to TSDC-1998 and TBEC-2018.

3.4.2.4 Kahramanmaras earthquake

On 6_{th} February 2023, a series of seismic sequence started on the East Anatolian Fault Zone (EAF) line including M_w=7.8 and M_w=7.5 earthquakes, and they are followed by 4 aftershocks (Table 3.10) with magnitudes between 6.0 and 6.9.

Table 3.10 : The list of the earthquakes in the sequence (USGS).

Date & Time	Latitude	Longitude	Depth (km)	Magnitude
6.02.2023 01:17	37.2256	37.0143	10	7.8
6.02.2023 10:24	38.0106	37.1962	7	7.5
6.02.2023 01:28	37.1893	36.8929	10	6.7
20.02.2023 17:04	36.1616	36.0251	16	6.3
6.02.2023 12:02	38.0582	36.5114	9	6
6.02.2023 10:26	38.0315	38.0984	10	6

To conduct GMPE procedures, Vs30 properties of the disaster area are appointed from USGS global Vs30 map. There were more than 60 strong ground motion recorders within the 50 km buffer zone of the ruptured fault line during the seismic event. However, acceleration-time histories of 14 stations (Station IDs: 4630, 4629, 4632, 4626, 2709, 2707, 7901, 0208, 4631, 213, 3112, 0201, 0210, 0214) were cut off in the early stages of the earthquake, so these records were excluded in this study.PGA values of the used stations, ruptured fault line, and the spatial distribution of residual values for the disaster area is given in Figure 3.18.

3.5 Results and discussion

3.5.1 Structural Damages

In the literature, there are post-earthquake damage assessment methods at different levels of detail. Since the number of damage photos of the examined buildings is limited, the rapid damage inspection approach, which is the quickest among the other methods, introduced by damage assessment trainings of the Turkish Ministry of Environment, Urbanization and Climate Change is used to assign the damage levels to the examined buildings. The general flowchart of the damage assessment procedure is given in Figure 3.19. Damage information of the buildings with an insufficient number of photos is taken directly from the SERU database. The damage classification of reinforced concrete members is made based on the damage limits given in Table 3.11 (Ilki et al, 2020; Akkar et al, 2021; Ilki et al, 2021b).

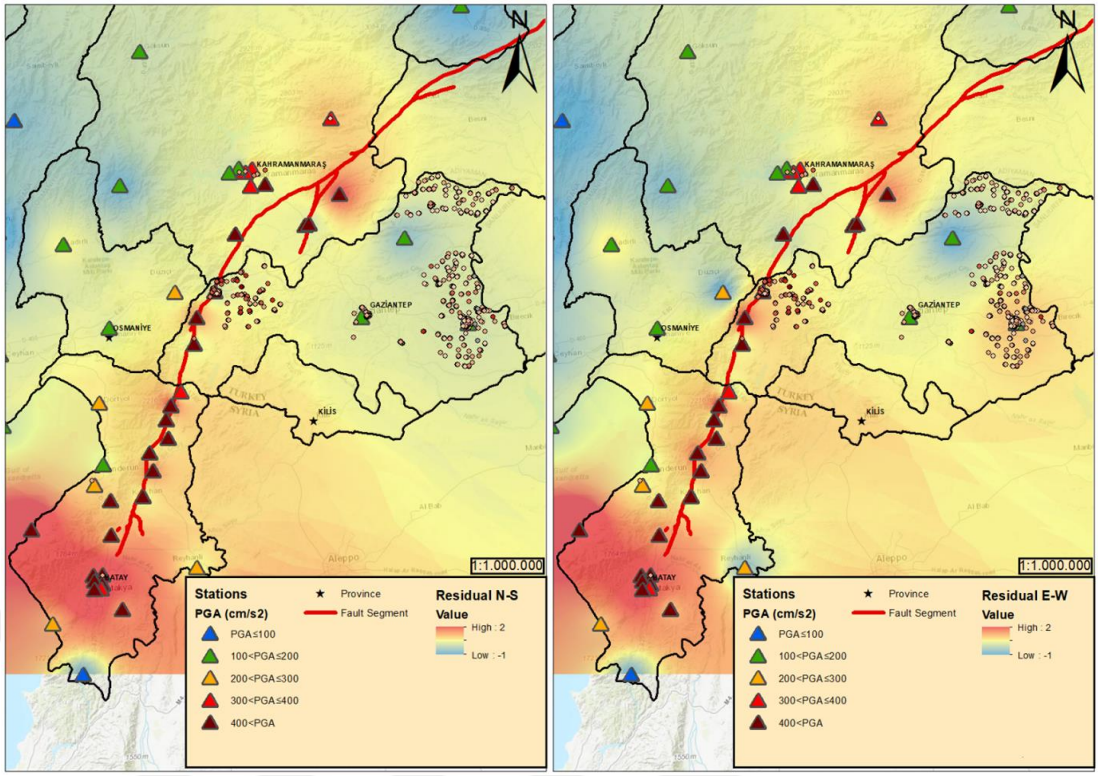

a) b)

Figure 3.18 : Calculated residual values for a) north-south and b) east-west components of the earthquake.

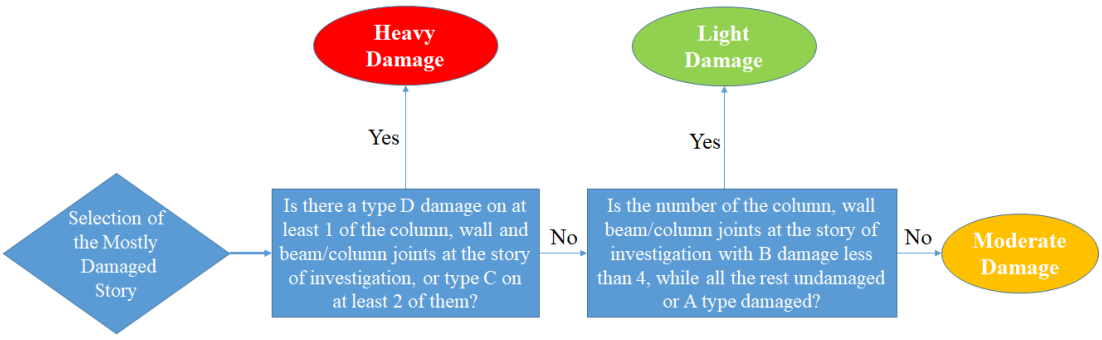

Figure 3.19 : Decision tree algorithm for damage assessment.

Table 3.11 : Element damage type classification.

Damage Type	Crack Width	Compression Damage
0	-	-
A	w≤0.5 mm	-
B	0.5<w≤3.0 mm	Crushing of Concrete Cover
C	-	Spalling of Concrete Cover
D	-	Reinforcement Buckling - Crushing of Concrete Core

A lightly damaged building is given in Figure 3.20. The building contains a column with a Type A shear crack and is identified as slightly damaged since it does not have any higher damage type elements. A building that experienced Afyon Earthquake

(2002), which was under construction during the earthquake, is shown in Figure 3.21a. The building contains a Type B flexural crack (Figure 3.21b). However, owing to the Type D damages illustrated in Figure 3.21c, the building is categorized as heavily damaged.

a) b)

Figure 3.20 : a) The BNG-5-5-1 building (lightly damaged), b) Type A shear crack (METU).

a) b) c)

Figure 3.21 : a) The AFY-ÇO-05 building (heavily damaged), b) Type B flexural crack, c) Type D flexural and shear damages (METU)

At least two columns of the building shown in Figure 3.22a experienced Type C damage. In Figure 3.22b and 3.22c, two examples of spalling of concrete cover are given. The building also has elements with Type D damage. Thus, the damage state of the BNG-6-4-2 building is decided as heavy damage. Figure 3.23a shows another building that experienced Bingöl Earthquake (2003) and was subjected to heavy damage. Vertical reinforced concrete members of the building exhibited Type D shear crack, reinforcement buckling, crushing of concrete core and rupture of transverse reinforcement (Figure 3.23b, 3.23c).

a) b) c)

Figure 3.22 : a) The BNG-6-4-2 building (heavily damaged), b) Type C damage: Spalling of Concrete Cover, c) Type C damage: Spalling of Concrete Cover (METU).

The individual damage states determined for all evaluated buildings through the rapid damage assessment procedure explained above are given in Table B.1. The final damage distribution for each seismic event is given in Table 3.12. It should be noted that the only considered earthquake that had a significant aftershock among others is the Afyon earthquake. The mainshock was followed by a M_w=5.8 aftershock, the recorded PGA values of which were around 0.04~0.05g. Since the PGA values of the aftershock are not significant enough, it is assumed that damage states of buildings in Afyon occurred after the main shock.

a) b) c)

Figure 3.23 : a) The BNG-6-3-1 building (heavily damaged), b) Type D shear crack, reinforcement buckling, crushing of concrete core and rupture of transverse reinforcement, c) Type D flexural damage and crushing of concrete core (METU).

3.5.2 Results obtained by performance based rapid seismic safety assessment methodology

The SSR values of investigated 42 buildings are determined through the implementation of the PERA2019 procedure and are compared with the actual damage

states of the buildings that have been exposed to one of the Afyon (2002), Bingöl (2003), Aegean Sea (2020), or Kahramanmaras (2023) earthquakes to evaluate the reliability and safety margin of proposed performance based rapid seismic assessment method. As shown above, the amplitude of acceleration spectra computed for ground motion records of the Afyon (2002) and Aegean Sea (2020) earthquakes is slightly less than the design spectra of the seismic design codes. Additionally, spectral acceleration values of 2023 Kahramanmaras earthquake surpasses even maximum considered earthquake of TBEC-2018 in many stations, while the acceleration spectrum of Bingöl earthquake (2003) is closer to the design spectrum and even higher in the short-period range compared to other seismic events. Obviously, there should have been no seismic-induced collapse or heavy damage if the examined buildings have been constructed in accordance with the seismic design codes of their eras.

Table 3.12 : Damage distribution of the buildings for considered seismic events.

		DAMAGE TYPE				
		Collapse	Heavy	Moderate	Light	None
EVENT	Afyon	1	10	3	4	0
	Bingol	1	8	5	5	3
	Aegean Sea	0	0	0	0	2
	Kahramanmaras	0	5	0	1	1
TOTAL		2	23	8	10	6

Comprehensive information on the global damage levels, SSR values determined by the application of PERA2019, and structural properties such as the first period of vibration, base shear demand, axial stress on vertical elements, reinforcement details, material properties, and plan dimensions for each building are given in Table B.1. The trends between the observed damage levels and various structural parameters are illustrated in Figure 3.24. The findings of the study show that seismic-induced damages for buildings with the same number of stories can be at different levels. Hence, it would not be realistic to perform a building scale seismic evaluation based only on their number of stories. The compressive strength of the existing concrete is a critical parameter for the seismic performance of RC buildings. The relationship between observed damage levels and the compressive strength of the existing concrete does not exhibit a good trend. The building in which the highest compressive strength of the existing concrete is measured has collapsed, and the building with the lowest compressive strength of the existing concrete has not experienced any seismic damage. Also, the comparison of the average axial load on columns at the critical story resulting from gravity loads and the observed damage states of the buildings shows a large

scatter. Thus, estimating the seismic safety of individual buildings using simplified procedures without considering all crucial structural parameters may lead to grave misclassifications.

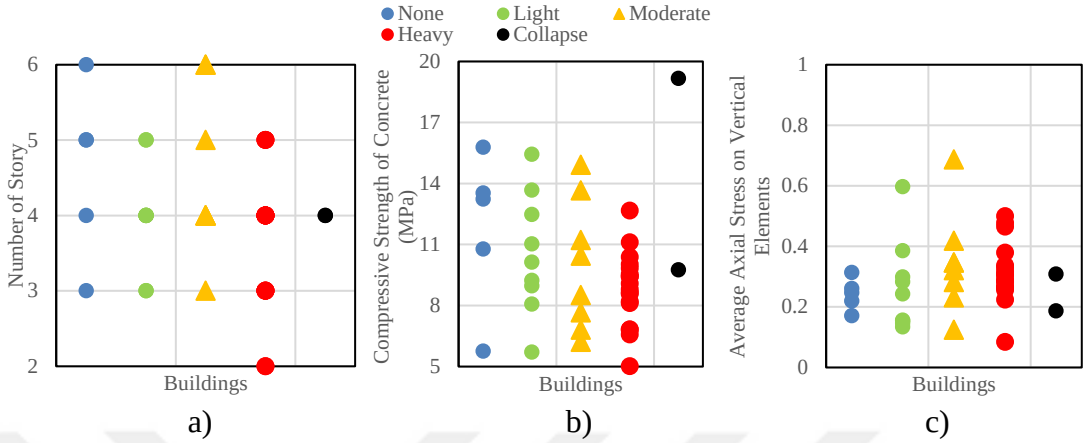

Figure 3.24 : The trends between the observed damage levels and various important structural parameters of the buildings: a) Number of stories, b) compressive strength of the existing concrete, c) average axial stress on vertical members. The horizontal axis illustrates different damage state groups.

Figure 3.25a demonstrates the harmony of the observed damage levels with SSR values and risk classes of the buildings computed through the implementation of the PERA2019 methodology. On contrary to the inadequate consistency of individual structural parameters investigated above compared to structural damages, the SSR values obtained for the examined buildings exhibit good conformity with observed damages and tend to decrease as the damage state increases. Figure 3.25b illustrates the risk class ratios of the buildings for each damage state group. Seismic risk classes of the buildings also show a promising consistency with the observed damages too.

The proposed methodology satisfactorily labels all collapsed buildings as E class, which corresponds to a very high seismic risk. The buildings severely damaged are also classified as either E or D class. Moreover, the SSR region above 40% does not contain any heavily damaged or collapsed buildings, which is a good safety indicator because a buffer zone of SSR values between 40 and 50% does not include any heavily damaged or collapsed buildings, while this range of SSR is still in D Class. Distinguishing the buildings with good seismic performance from the ones with poor seismic performance is another critical aspect of seismic assessment methods. The results of this study show that PERA2019 is able to determine almost 75% of the buildings without seismic damage or lightly damaged ones as C, B or A class, while none of them is categorized as E class or very high risk.

Table 3.12 yields the comparison of risk classes based on the SSR values and observed structural damage levels. The matrix given below illustrates the safe and unsafe classifications. According to numerical values given in Table 3.12, as expected, the average SSR values of the buildings in each observed damage group also decrease as the damage state increases. This study demonstrates that the present risk classification method is rational and contains a good safety margin. On the other hand, conducting site investigations after future earthquakes and adding more building data will increase the accuracy of this case study. The presented methodology is a rapid and approximate second-stage performance-based procedure, and exact results are not expected at this level of assessment. The target of this methodology is rapid and cost-effective prioritization of existing buildings with respect to their seismic risks to allocate limited sources/budget to further detailed analysis of those buildings which are prone to the highest risks. And such scaling down process of the huge problem is very important for cities like Istanbul with hundreds of thousands of substandard buildings. It should be further noted that the methodology has been validated through means of other methods, such as numerical analyses as aforementioned.

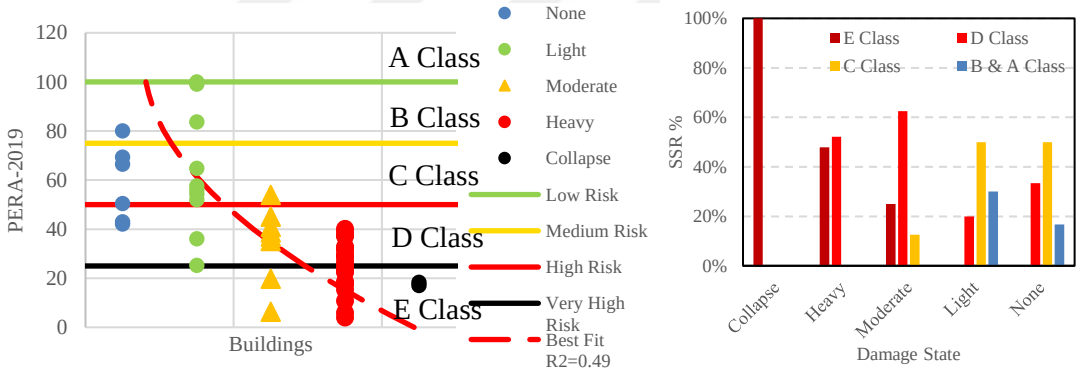

a) b)

Figure 3.25 : a) Distribution of SSR values of the investigated buildings computed through PERA2019 for each damage level groups, b) histogram of risk class distributions for each damage level groups.

Table 3.13 : Comparison of risk classes and SSR values with damage levels.

		Collapse	Heavy	Moderate	Light	None
PERA2019 RISK CLASS	E (Very High Risk)	2	11	2	0	0
	D (High Risk)	0	12	5	2	2
	C (Medium Risk)	0	0	1	5	3
	B-A (Low Risk)	0	0	0	3	1
SSR Range %		17-18	17-18	4-40	6-54	25-100
Mean SSR %		17.7	17.7	24.8	34.6	62.9
Std. Dev. SSR %		0.6	0.6	9.8	14.0	23.5

As mentioned before, uncertainties of ground motion may alter the results of this case study. Although the uncertainties of ground motion parameters were reduced scientifically as much as possible, heavily damaged and collapsed buildings were analyzed according to the median, median + standard deviation, and median - standard deviation acceleration spectra to monitor the error rate due to the seismic demand (Figure 3.26). Out of 25 buildings, near station records were used for the seismic demand of 3 buildings. Thus, the GMPE procedure wasn't used for those. Considering the median, estimated standard deviation, and +1 standard deviation results, all heavily damaged and collapsed buildings are determined under the High Risk limit. For the -1 standard deviation case, 8% and 36% of the buildings are estimated in low and moderate risk groups, respectively. The estimated acceleration spectra of 95% of buildings are higher than the predicted median spectrum. Despite the fact that the amplitudes of median -1 standard deviation values are quite low compared to the estimated spectra, most of the unsafely classified buildings are still in medium risk class.

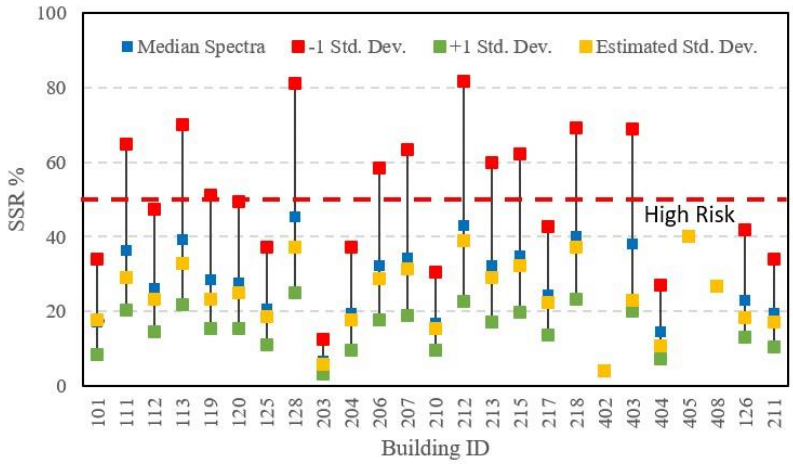

Figure 3.26 : SSR results of heavily damaged and collapsed buildings according to various levels of seismic loadings.

3.6 Outputs of the Validation Study Based on Actual Earthquake Damages

This study was conducted as the first step of the validation efforts of the proposed seismic risk classification/prioritization procedure. Within the scope of this study, SSR values of 49 buildings that experienced real seismic actions (2002 Afyon, 2003 Bingöl, 2020 Aegean Sea, and 2023 Kahramanmaras earthquakes) were evaluated through PERA2019 rapid seismic performance assessment methodology in a blind manner and

then the estimated SSRs of the buildings were compared to the observed seismic-induced damages to determine the reliability and safety margin of the proposed risk classification approach. It should be noted that the spectral accelerations calculated for the three strong ground motions presented in this study are quite close to the spectral design accelerations for Afyon, Bingöl, Izmir, and Kahramanmaras for a wide range of frequencies.

The results of this study demonstrated that the SSR values increase as the damages of the building decrease. The proposed risk classification approach succeeded to label all of the collapsed buildings in E Class (very high seismic risk). Moreover, all of the buildings subjected to heavy damage were classified as E or D Class, which correspond to very high and high seismic risk respectively. Risk classes of 97% of the moderately, heavily damaged or collapsed buildings that cannot be inhabited after the earthquake were determined as high or very high risk. Also, all of the severely damaged or collapsed buildings had an SSR value of less than 40%, which is a good safety indicator because a buffer zone of SSR values between 40 and 50% does not include any heavily damaged or collapsed buildings, while this range of SSR is still in D Class. This output demonstrates that the present risk classification method contains a good safety margin. As important as specifying the buildings with poor seismic performance, identifying the buildings with good seismic performance from the seismically deficient ones is another crucial task for risk mitigation efforts. Therefore, to evaluate the reliability of a seismic risk classification method, categorizing the buildings with adequate seismic performance in low risk class has grave importance, as well as determining the buildings with poor seismic performance as high risk. A method cannot be stated as successful as long as the method classifies the buildings with good seismic performance as high risk buildings. Based on the findings of this study, PERA2019 is able to classify almost 75% of the buildings without seismic damage or light damage as C, B or A class, while none of them is classified as very high risk (E class). The trends between the observed damage levels and structural parameters showed that individual structural parameters do not have sufficient conformity with the damage states of the buildings, even though structural parameters affect global seismic performance. Further site investigations are to be conducted after future earthquakes as well as additional numerical analyses to support current findings with further evidence in terms of the reliability of the presented approach.

4. STRUCTURAL CHARACTERISTICS OF THE EARTHQUAKE-PRONE BUILDING STOCK IN ISTANBUL AND PRIORITIZATION OF EXISTING BUILDINGS IN TERMS OF SEISMIC RISK-A PILOT STUDY CONDUCTED IN ISTANBUL[3]

4.1 Outlines of the Chapter

Earthquakes have caused catastrophic results in cities since the beginning of settled life, and the cumulative experience of these events has indicated that the lack of seismic resilience brings enormous economic losses and threatens human life. Consequently, the importance of seismic risk mitigation of earthquake-prone structures has arisen to reduce the primary and secondary losses resulting from seismic events in the last decades as developments in the earthquake engineering field occur. The first step for ensuring seismic resilience is the identification of risky buildings, which is a difficult challenge for metropolises like Istanbul since the building stock consists of over a million buildings. Applying code-based detailed assessments to so many buildings is not practical in terms of time and cost. Moreover, the current code-based detailed assessment methodologies such as Provisions for the Seismic Risk Evaluation of Existing Buildings under Urban Renewal Law (2019) and Turkish Building Earthquake Code (2018) provide discrete predictions for existing buildings as either risky or non-risky or satisfying life safety/controlled damage or not. However, a ranking system based on a reliable and realistic risk classification to prioritize the buildings is needed. Therefore, as a pilot project, nearly 23,000 reinforced concrete buildings in 37 different districts of Istanbul have been investigated by Istanbul Metropolitan Municipality (IMM) through PERA2019 performance-based rapid assessment methodology by considering the Design Level and Scenario-Based Earthquake cases. This is the most up-to-date and comprehensive site survey and

[3] This chapter is based on the following publication: Aydogdu, H. H., and A. Ilki. (2023). Structural Characteristics of the Earthquake-Prone Building Stock in Istanbul and Prioritization of Existing Buildings in Terms of Seismic Risk-A Pilot Study Conducted in Istanbul, Journal of Earthquake Engineering, DOI: 10.1080/13632469.2023.2247481

analysis conducted in Istanbul up to now. In this paper, the characteristics of the building stock in Istanbul based on the conducted site work and the outcomes of the rapid seismic safety assessment efforts are summarized. Then, a discussion on the seismic risk evaluation of the existing residential buildings based on the prioritization of the examined buildings is presented through the results obtained for the Design Level and Scenario-Based Earthquake cases.

4.2 Summary of the Literature

The Kocaeli and Düzce earthquakes (1999) that hit northwest Turkey and caused a large destruction and thousands of casualties have clearly demonstrated the urgency of seismic mitigation interventions to all relevant authorities (Bibbee et al, 2000; Holzer et al, 2000; Scawthorn and Johnson, 2000; Ozmen, 2000; Erdik, 2001; Bruneau, 2001). Starting with JICA (Japanese International Cooperation Agency) Report (2002), IMM has been working on the estimation of possible earthquake losses. Erdik et al. (2003) carried out an earthquake risk assessment for the metropolitan area of Istanbul. Karaman et al. (2008) performed a loss assessment study for Zeytinburnu District of Istanbul. In 2009, IMM prepared "Probable Earthquake Loss Estimates for Istanbul Province" study (IMM, 2009a). Ansal et al. (2009) conducted a loss estimation study for Istanbul based on deterministic earthquake scenarios. According to the latest study, "Project for Updating Probable Earthquake Loss Estimates for Istanbul Province, prepared by IMM and Boğaziçi University" (Cakti et al, 2019), the building inventory of Istanbul consists of 1,166,300 buildings, which include residential, industrial, commercial and public ones. Approximately 800,000 buildings in Istanbul were constructed before the year 2000 (Cakti et al, 2019), which is accepted as a milestone for seismic awareness in Turkey, due to the heavy losses of the 1999 Marmara region earthquakes (Ilki and Kumbasar, 2000; Ozdemir et al, 2002). A large number of those buildings did not receive a proper engineering service, and in most cases, they were not built in compliance with their original design projects and were constructed with poor workmanship, materials and details (Aydinoglu, 2007; Ilki and Celep, 2012). Moreover, these sub-standard buildings are experiencing time-dependent deteriorations; and one of the foremost and most common problems for building stock of Istanbul is the corrosion of reinforcing bars. The remarkably detrimental effects of corrosion of the reinforcement on the seismic behavior of reinforced concrete

buildings have been studied by Pantazopoulou et al. (2001), Inci et al. (2013), Meda et al. (2014), Zhou et al. (2014) and Goksu and Ilki (2014). The poor seismic performance of a similar building stock was observed after the 2020 Aegean Sea Earthquake (Yakut et al, 2021; Makra et al, 2021; Gurbuz et al, 2022). Having such deficiencies, this old building stock must be assessed to determine the priorities for interventions towards the reduction of losses urgently. In compliance with this need, the Report on Determining Measures to be Taken to Minimize Seismic Losses (2021) has been announced by the Grand National Assembly of Turkey recently. However, performing a code-based detailed assessment for such a high number of buildings is not efficient both in terms of time and cost. To cope with this problem, a simplified and economical, yet reliable and realistic rapid seismic assessment method need to be applied to hundreds of thousands of buildings to pave the way for planning interventions in a rational and prioritized way. Thus, this huge problem can be reduced to a manageable scale.

Earthquake engineering literature contains two different kinds of rapid seismic safety evaluation methods, rapid visual screening (RVS) and second-stage evaluation. RVS methods are sidewalk surveys developed to identify inventory characteristics on a visual basis and mechanical properties of the structural system are not considered in this phase of assessment. FEMA-154 (2015), the RVS method proposed by New Zealand Society for Earthquake Engineering (2006), and METU Method (Sucuoglu et al, 2007) are well-known examples of the RVS methods. Yakut et al. (2012) introduced the results of METU method applied to 6 districts of Istanbul. Achs and Adam (2012) conducted a pilot study aiming at the rapid assessment of masonry buildings in Vienna. Shah et al. (2016) prepared a case study for RVS application conducted in two districts of Jeddah, Saudi Arabia. Recently, a first-order loss assessment was performed in North Macedonia by Mircevska et al. (2019). Kohrangi et al. (2020) conducted a seismic risk and loss estimation study for Isfahan and summarized exposure data of the city comprehensively. Also, Silva et al. (2018) developed a global exposure model to reflect the spatial distribution of residential, commercial and industrial buildings. The second-stage assessment is a more detailed evaluation phase than RVS; these methods need a data gathering process from inside the buildings to perform mechanical computations of varying complexities. PERA Method (Ilki et al, 2014), the method proposed by New Zealand Society for Earthquake Engineering (2006), Japanese

Seismic Index Method (JBDPA, 1990), Hassan & Sozen Method (Hassan and Sozen, 1997), P25 Method (Bal et al, 2005), DURTES (Temur, 2006) and Yakut Method (Yakut, 2004) are some of the well-known methods among the second-stage evaluation procedures. Erberik (2008) generated fragility curves for typical sub-standard RC buildings considering 1999 Duzce Earthquake damage database. Ilki et al. (2019) developed a framework for rapid seismic assessment for sub-standard buildings in Turkey. For different type of RC buildings in Italy, Del Gaudio et al. (2019) prepared fragility and vulnerability curves based on damage data of the last 50 years. Yazgan et al. (2019) proposed a new strategy for vulnerability analysis of building stock with specific vulnerability models for the groups of substandard buildings. Ruggieri et al. (2022) proposed a mechanical approach to estimate the fragility of existing RC buildings considering all typologies and establishing idealized numerical models for buildings. Also, Del Gaudio et al. (2021) conducted a seismic loss prediction study for infilled reinforced concrete buildings via a simplified analytical method.

Current regulations on seismic assessment in Turkey such as Provisions for the Seismic Risk Evaluation of Existing Buildings under Urban Renewal Law (2019) (RBTE-2019) and Turkish Building Earthquake Code (2018) (TBEC-2018) classify the existing buildings either as risky or un-risky or satisfying a target performance level (such as life safety-controlled damage) or not. As aforementioned, a structural engineering investigation according to the code classification of the buildings of Istanbul will probably show the fact that almost every ordinary building constructed before the year 2000 is to be labeled as risky (or they will not satisfy the life safety/controlled damage performance target). Considering hundreds of thousands of such buildings, obviously, this is not a sustainable approach, and the vastness of the problem puts back the efforts to make Istanbul more resilient. A rapid, reliable, and realistic seismic performance ranking procedure for building stock is a key issue to prioritize buildings, which is missing in current official seismic design codes in most countries. A considerable way to fill this gap is sorting the building inventory by their approximately calculated seismic capacity to demand ratios so that the primary targets for mitigation works can be determined in an effective way. Actually, in some earthquake-prone countries, important steps have recently been taken toward such categorization. A risk-based framework for managing earthquake-prone buildings has been published in New Zealand (NZSEE, 2017), and the validation of the SLaMa

procedure available in this framework was made by Gentile et al. (2019). The procedure classifies buildings into six risk classes in terms of the New Building Standard% (NBS%). D and E Class buildings, with an NBS% less than 1/3, have to be intervened to reach at least 2/3 NBS level. The allowed time window to mitigate the seismic risk of the building changes with the seismicity of the region and the building's importance. In Italy, the Sismabonus framework which enables tax deductions after seismic strengthening interventions on buildings has been introduced (Di Ludovico et al, 2016; Polese et al, 2018; Cosenza et al, 2018). This mechanism defines the seismic risk class of a building as the minimum class defined by the building safety index at the ultimate limit state IS-V and the one related to expected annual loss EAL (Polese et al, 2018). The building safety index IS-V divides buildings into 7 different classes A+ to F.

In the latest risk mitigation studies of IMM, the PERA2019 methodology (initially introduced by Ilki et al, 2014 and then modified by Ilki et al, 2021) is applied to identify the individual building-based seismic performance of the existing buildings and provide risk ranking and prioritization. The PERA2019 methodology shares the common approach of defining the seismic safety index of the building as the ratio of the building's seismic capacity to demand (i.e. code-based demand for a new building or demand from a scenario earthquake) as also done for NBS% of NZSEE (2017) and IS-V of Sismabonus frameworks. The method is comprised of simplified data collection from the building, determination of seismic demand in means of peak ground acceleration (PGA), and a series of linear analyses for calculating the PGA capacity of the building corresponding to the critical story mechanism case. The PERA2019 approach steps forward among similar methods with its ease in application to low- and mid-rise reinforced concrete buildings not only for simplified data collection (an investigation team can inspect, assess and report three to five buildings per day) but also for easy-to-follow linear analysis algorithm already familiar to many engineers. The results of the latest campaign launched by IMM which are summarized in this paper, are expected to provide a good opportunity for the prioritization of buildings or areas with respect to their seismic vulnerability and the efficient use of the resources for mitigation of losses. While applying the rapid assessment method, priority was given to the buildings that were built before the year 2000, and nearly 23,000 reinforced concrete buildings from 37 different districts of Istanbul have

already been investigated by implementing the PERA2019 rapid assessment methodology (Ilki et al. 2021) by considering the Design Level and Scenario-Based Earthquake cases (these earthquake cases are explained in detail in section 4.3 below). In this paper, the structural characteristics of the building stock of Istanbul obtained through the site investigations conducted during this project are outlined. The detailed structural information is gathered, processed and presented from actual 23,000 pre-2000 buildings through an extensive site study campaign. These buildings are in Istanbul, which is one of the most critical cities in the world in terms of seismic risk. This is a very significant number for the application of a second-stage seismic assessment methodology. To the best knowledge of the authors, no such application in this scale exists in the summarized literature. Few previous screening studies are conducted through RVS (street survey) approaches and mostly on small scales as mentioned above. The main target of this study is to identify those with the highest risk of causing loss of life out of 800,000 pre-2000 buildings, which are known to have a certain level of risk, and to intervene them as quickly as possible. As aforementioned, randomly intervening this amount of buildings without implementing rapid yet reliable structural assessment procedures is not practical. Furthermore, a discussion is presented on the estimated seismic performances of the examined existing residential buildings based on the analyses conducted for the Design Level and Scenario-Based Earthquake cases through the presented algorithm. This study demonstrates that it would not be reasonable to prioritize this amount of buildings according to the design level earthquake, and this approach will require long years to complete the risk mitigation study in Istanbul, in which the probability of a catastrophic earthquake could hit is very high in the near future (Parsons et al, 2000).

4.3 Seismicity and the Soil Parameters

A scenario earthquake, which was described in the “Project for Updating Probable Earthquake Loss Estimates for Istanbul Province (Cakti et al, 2019)”, and a design level earthquake (DD-2 earthquake defined by TBEC-2018 and Turkish Seismic Hazard Map 2018) were used during the determination of Seismic Safety Ratios through the PERA2019 methodology. The first official Seismic Zones Map of Turkey was introduced in 1945; since then, the map has been updated (Ilki and Celep, 2012). Even though Istanbul has a well-known active seismic history, the megacity was not

considered in the highest seismicity region until 1996. In 2018, a coordinate-based raster map was introduced as Turkish Seismic Hazard Map (AFAD, 2018) with a new seismic design code (TBEC-2018) at the same time. The peak ground acceleration (PGA) distribution in Istanbul for DD-2 Earthquake according to this map is given in Figure 4.1a. The return period of the DD-2 earthquake, which is defined through a probabilistic seismic hazard analysis procedure by considering all known seismic sources, is 475 years (with an exceedance probability of 10% within 50 years). The spatial distribution of PGA values regarding the scenario earthquake is illustrated in Figure 4.1b.

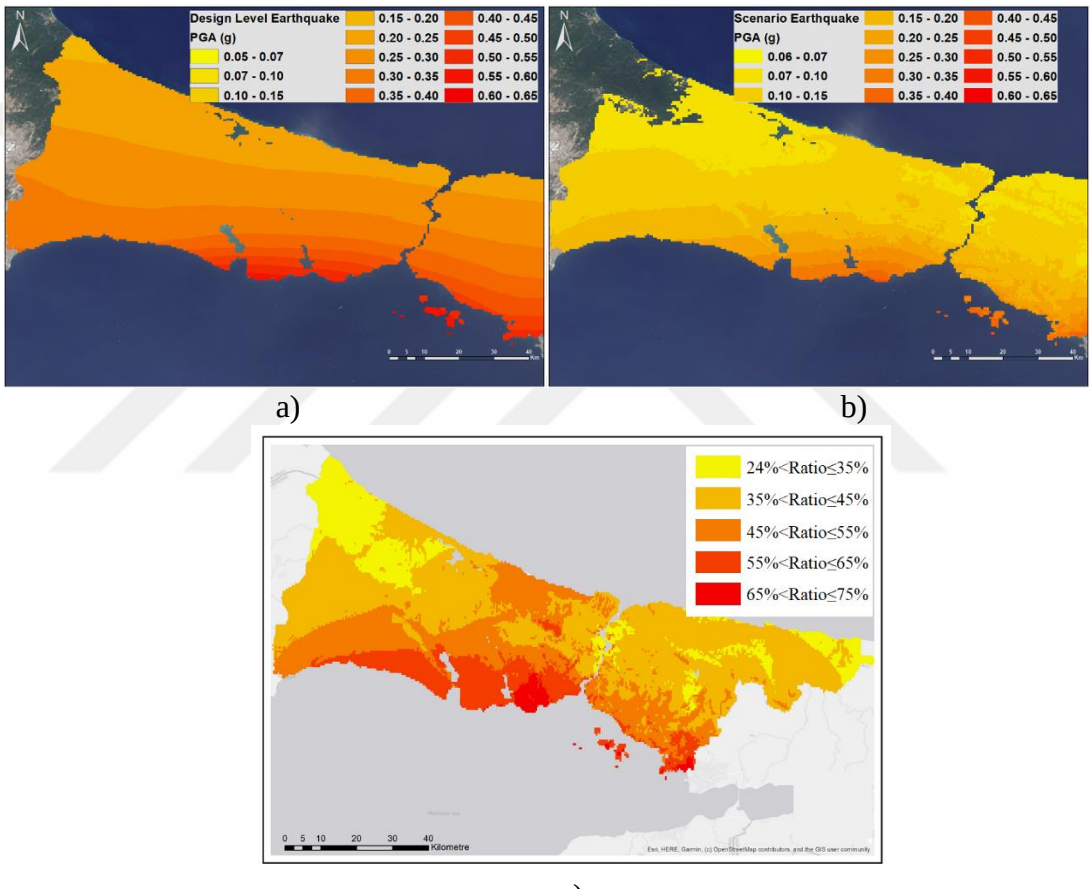

Figure 4.1 : PGA distribution in Istanbul according to a) Design Level Earthquake (DD-2), b) Scenario Earthquake, c) Spatial distribution of PGA ratio for considered earthquake cases (Scenario Earthquake/Design Level Earthquake) (plotted based on data provided by Cakti et al. 2019).

The scenario earthquake is based on a deterministic model, which takes into account a part of the North Anatolian Fault near Istanbul (Figure 4.2a). The length of the corresponding fault segment is nearly 120 km long, and the case considers that all the segments of the fault rupture at the same time, which can be perceived as the worst-

case scenario. The obtained median values were used to generate ground motion distributions. The assumed magnitude of the considered scenario is Mw=7.5, and its return period approximately corresponds to 250 to 300 years according to Cakti et al. (2019). The ratio of PGA values of scenario earthquake to design earthquake is given in Figure 4.1c. The use of scenario earthquake was implemented with the thought that it is worth examining buildings with a deterministic scenario to obtain more refined results and better differentiate the buildings for prioritization. Further details for the considered scenario earthquake can be found in Cakti et al. (2019).

In this study, local soil conditions were considered by using the V_{s30} maps developed through the previous microzonation studies of IMM. The spatial distribution of the average shear-wave velocity in the top 30 m layer of the soil (V_{s30}) is given in Figure 4.2b. Accordingly, V_{s30} values of the west of the Golden Horn and south of TEM Highway is less than 350 m/s in most cases, while the regions in Asia and the north of the Golden Horn in Europe have relatively stiff soil conditions.

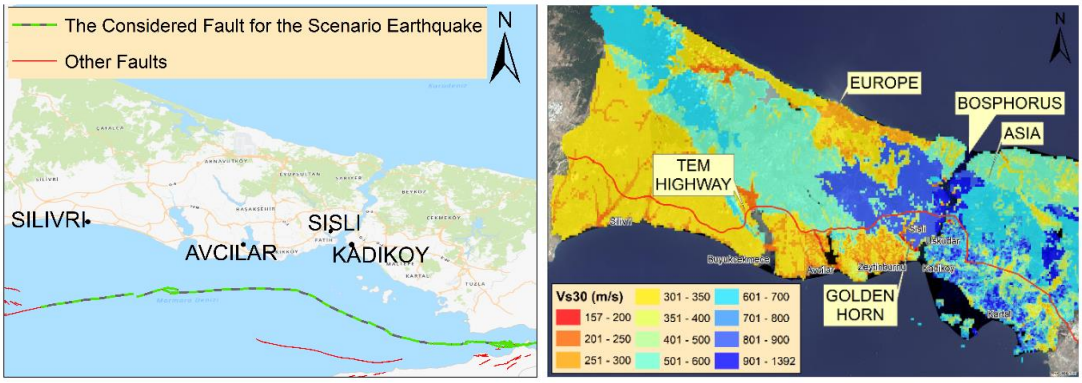

a) b)

Figure 4.2 : a) Considered fault rupture for the Mw=7.5 Scenario Earthquake (plotted based on data provided by Cakti et al, 2019), b) Vs30 map of Istanbul (Cakti et al, 2019), (plotted based on data provided by IMM, 2009b and c).

4.4 The General Characteristics of the Building Stock in Istanbul

In the scope of this thesis, almost 23,000 pre-2000 reinforced concrete buildings were examined through PERA2019 methodology in 37 districts of Istanbul. The general characteristics of those buildings are summarized below. In Figure 4.3a and 4.3b, frequencies of the number of stories of the buildings and the year of construction are given, respectively. Since the used methodology is limited to up to 10-story buildings, the number of stories varies between 1 and 10, and the most frequently encountered number of stories is 5. Most of the evaluated structures were built in the 1990s.

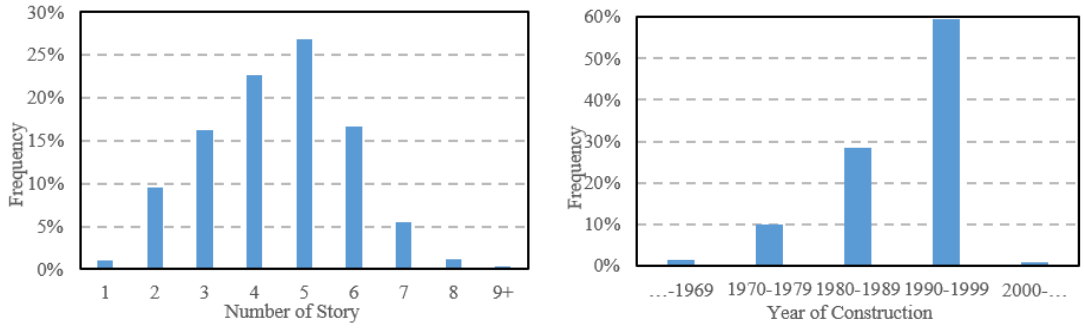

a) b)

Figure 4.3 : Distribution of the a) year of construction of the buildings, b) the number of story.

The distribution of the compressive strength of concrete values obtained from Concrete Hammer tests performed on the columns of the investigated buildings is given in Figure 4.4a. This figure illustrates the histogram of the results which is found to be compatible with the normal distribution curve (mean value=9.9 MPa, standard deviation=3.2 MPa) and previous reports (Bal et al, 2008; Maziliguney et al, 2008). Most of the buildings do not have a sufficient level of concrete strength compared to seismic design code requirements for their years of construction (i.e. 18 MPa in the Turkish Seismic Design Code (1975) (TSDC-1975) and 20 MPa in Turkish Seismic Design Code (1998) (TSDC-1998) for high seismicity zones). This finding stems from the fact that most of the evaluated buildings were constructed with hand-mixed concrete on-site without any supervision. Two examples of site-mixed concrete are represented in Figure 4.5b and 4.5c. The presence of seashells and un-sieved sand is very common for this kind of concrete in Istanbul. During the evaluation of the concrete strength, the age of the concrete (consequently, the influence of the carbonation) was taken into consideration. The reduction factor for the corresponding age of the concrete (Figure 3.8b) is adapted from AIJ (1983). The effect of the reduction factor on the reliability of concrete hammer results was also discussed in the preliminary stages of this study. A comparative study on 92 samples to evaluate the accuracy of concrete hammer results, which were reduced with the age factor to account for carbonation, compared to core sample results is given in (Figure 4.4c). Despite the fact that concrete hammer test results alone do not exhibit absolute outputs, the results demonstrate that the reduction factor considering the age of the sample provides an acceptable and partially conservative trend compared to core sample results. In terms of constraints on budget, acceptable level of destruction by the building owners and time, the concrete hammer method was found to be sufficient for

this stage of investigation after the consideration of verifications outlined above. The calibration of concrete hammers was continuously checked to prevent misidentification. Furthermore, the building owners tend to allow non-destructive tests rather than destructive ones. Thus, the concrete hammer method, which is a standardized method, was selected to measure the equivalent compressive strength of concrete.

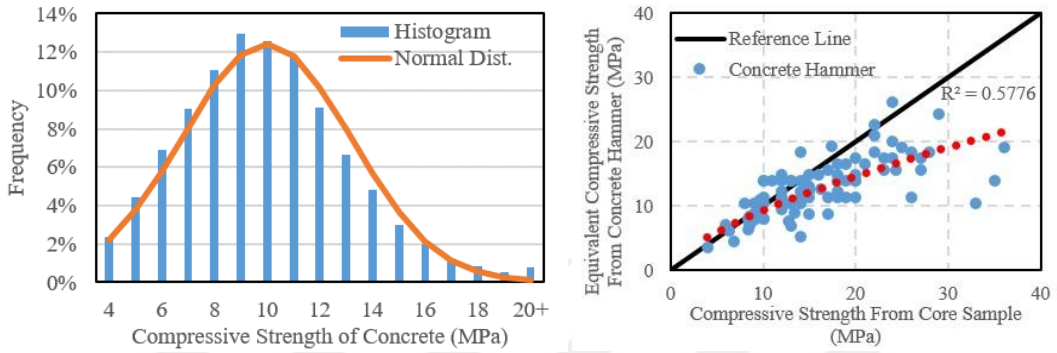

a) b)

Figure 4.4 : a) Distribution of the compressive strength of concrete on 112143 columns, b) comparative study for concrete hammer and core samples.

Corrosion of reinforcement in concrete is also a widespread problem for sub-standard buildings in Istanbul. Being constructed with low-strength concrete and insufficient thickness of concrete cover, numerous existing buildings in Istanbul have suffered corrosion damage. An increase in corrosion level results in the reduction of reinforcement area and damage in the concrete cover that may lead to remarkably poor seismic performance of such structural members due to reduced bond, strength and ductility. Figure 4.5a demonstrates the distribution of the cross-sectional area loss of longitudinal reinforcement from 23495 rebars of the inspected buildings. Around 30% of all the examined rebars have experienced at least 10% cross-sectional area loss due to corrosion. These losses are estimated by measurement of the diameter making use of calipers on-site. It should be noted that the reinforcing bar cross-section losses can be more than measured due to pitting-type corrosion which cannot be measured simply by site investigations. The calculated cross-sectional area loss due to the corrosion effects has been applied as a reduction to the longitudinal and transverse reinforcement areas. Further information on the effects of corrosion of reinforcing bars in extremely low-strength concrete has been studied by Inci et al. (2016).

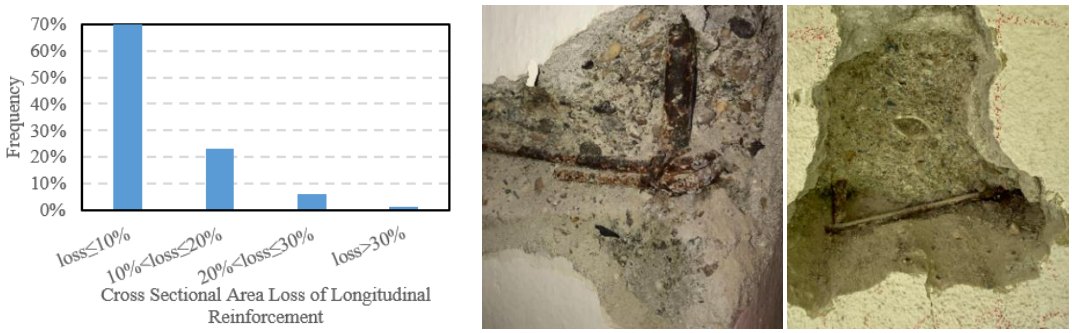

a) b) c)

Figure 4.5 : a) Distribution of reduction in longitudinal reinforcement area from 23495 rebar samples, b-c) site-mixed concrete textures and corroded rebars of existing buildings.

The reinforcement details for the examined buildings were obtained by removing the concrete cover and with the support of non-destructive measurements for all examined buildings. The overall frequencies of transverse reinforcement spacing at the column confinement zones are presented in Figure 4.6a. The collected data (i.e. Figure 4.6a) shows that almost none of the existing buildings constructed before the year 2000 is complying with the seismic design code in terms of stirrup spacing and volumetric ratio, except a small number of retrofitted ones. According to the previous versions of the Seismic Design Codes in Turkey (i.e. Specification for Structures to be Built in Disaster Areas 1975 and 1998, TSDC-1975 and TSDC-1998), the maximum spacing of transverse reinforcement is 100 mm for the confinement of zones of the columns. Although the transverse reinforcements are crucial elements for the shear force capacity and ductility of the reinforced concrete members, particularly during earthquakes, the average spacing of transverse reinforcement in 22868 samples is determined as 24.6 cm for confinement zones with a 4.4 cm standard deviation. The measured transverse reinforcement spacing (around 40 cm) for a column of a representative building is given in Figure 4.6b. It should be noted that this building in Istanbul has collapsed recently under gravity loads.

The distribution of longitudinal reinforcement ratios of columns of examined buildings is presented in Figure 4.7a. The presented data is based on an investigation of 23517 columns, where the reinforcement ratios were obtained by removing the concrete cover and using magnetic devices. Ilki et al. (2014) investigated 912 column cross-sections from 149 different buildings built before the year 2000 and found that the longitudinal reinforcement ratio for the columns is mostly around 1% (mean: 0.9% for buildings constructed before 1975, and 1.2% for buildings constructed after 1975, both with an

approximate standard deviation of 0.2%). Nevertheless, within this project, the longitudinal reinforcement ratio is decided to be checked for at least one column by removing the concrete cover and magnetic rebar locator. Reinforcement of another column was also examined by removal of concrete cover if the observed reinforcement ratio is not between 0.5% and 2.0%. The minimum longitudinal reinforcement ratio requirement for the columns in TSDC-1975 and TSDC-1998 is 1%. As seen, nearly 60% of the examined building columns do not satisfy the minimum longitudinal reinforcement ratio requirement provisions in the 1975 and 1998 Turkish Seismic Design Codes although almost 90% of them were constructed between the years 1980 and 1999 (Figure 4.3b). The longitudinal reinforcement ratio is a crucial parameter for the moment capacity of the columns. The combination of an insufficient amount of longitudinal reinforcement and a small cross-section of the column potentially leads to the strong beam/weak column problem, which can result in a story collapse mechanism during seismic actions, particularly when accompanied by insufficient transverse reinforcement. Furthermore, more than 90% of the examined buildings were built with plain reinforcing bars (Figure 4.7b). In addition to their lower tensile strength with respect to deformed bars, plain bars with inadequate lap splice length and poor anchorage details are known to have a remarkably poor seismic performance as also discussed by Goksu et al. (2014) based on the observations made during reversed cyclic lateral loading tests on such columns.

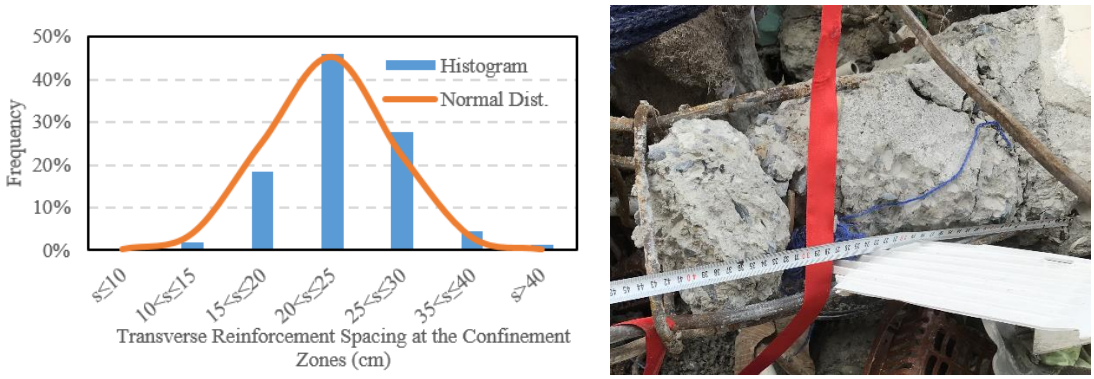

a) b)

Figure 4.6 : a) Distribution of the transverse spacing at column confinement zones, b) measured transverse reinforcement spacing of a column (around 40 cm) from a collapsed building in Istanbul.

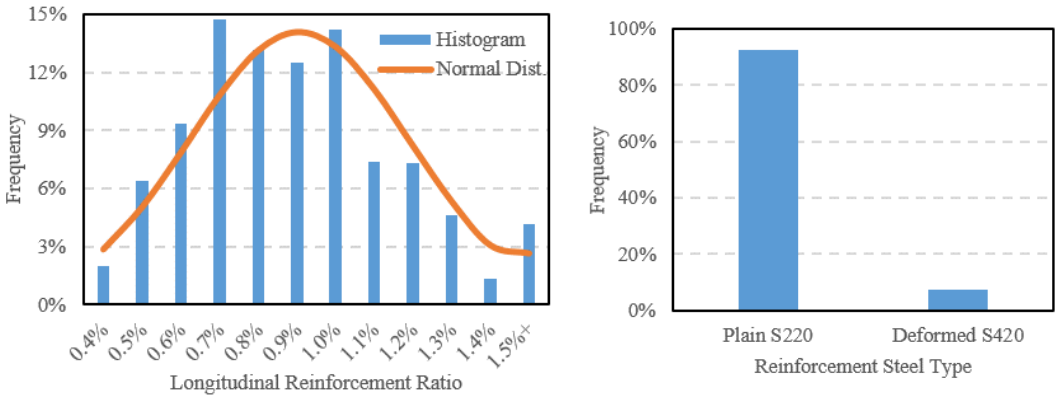

a) b)

Figure 4.7 : Distribution of the a) longitudinal reinforcement ratio of the columns, b) reinforcement steel types.

The axial load ratio on the columns (Eq. 2 above) is a critical factor effective on the ductility of reinforced concrete members/structures; the ductility of a member decreases as the axial load increases. Figure 4.8a demonstrates the average axial load ratios on the columns resulting from gravity loads at the critical stories of the buildings investigated in this project. Almost 20% of the buildings' columns are loaded over 50% of their axial load capacity on average.

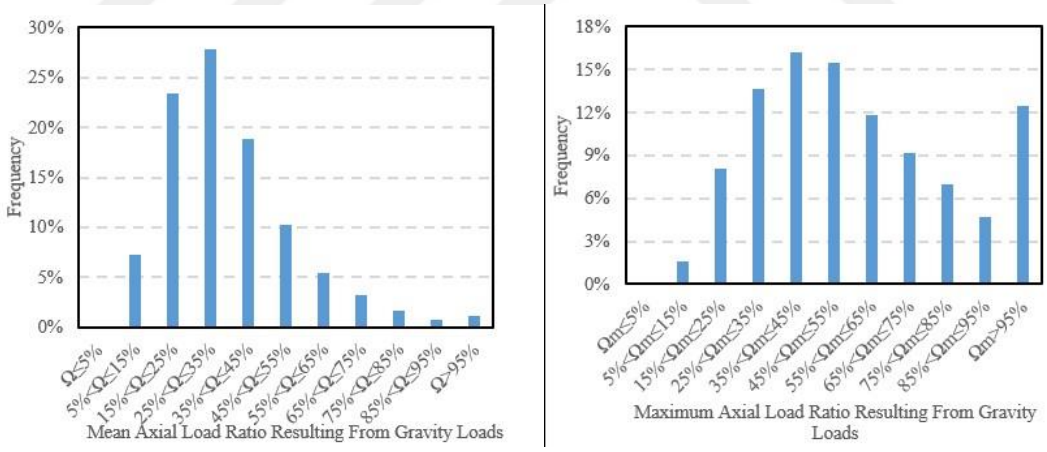

a) b)

Figure 4.8 : Distribution of the axial load ratios on columns resulting from gravity loads at the critical story a) average axial load (Ω), b) maximum axial load (Ωm) on the individual columns from 22,868 buildings.

The mean axial load ratio at the critical story is a decisive parameter of the shear force ratio limit, which is defined in Figure 3.2, and a building that exceeds that limit is to be considered critical. The column maximum axial load ratio distribution for the examined buildings is given in Figure 4.8b. Accordingly, over 10% of the investigated buildings have at least one member that is axially loaded beyond $f_{cm}A_c$, and it is

considered that the contribution of the longitudinal reinforcement prevents the collapse of these columns. Furthermore, in around 50% of the examined buildings, there are individual columns subjected to axial forces over $0.50f_{cm}A_c$, which was the allowed highest axial force on the columns according to TSDC-1975 and TSDC-1998.

4.5 Results and Discussion

In the scope of rapid assessment works, approximately 23,000 reinforced concrete buildings were analysed by employing the PERA2019 procedure, and the distribution of the SSR values determined. Design Level and Scenario Earthquakes are comparatively presented in Figure 4.9a. Accordingly, in parallel with the seismic demand distributions presented in Figure 4.1, the Design Level Earthquake yielded less SSR values compared to the Scenario Earthquake. Thus, in the case of the Design Level Earthquake, seismic risk classes of 82% of the investigated buildings are in D (high risk) or E (very high risk), which means that they had PGA capacities less than 50% of their respective PGA demands. However, the considered Scenario Earthquake yielded a more refined distribution where approximately 57% of the buildings are labeled as D or E Class. The mean SSR values computed through PERA2019 for Design Level and Scenario Earthquakes were 31% and 55%, respectively. Based on the fact that the seismic demands based on the scenario earthquake have been established considering the actual faulting mechanisms and local site conditions (Cakti et al, 2019) with the most recent data, these results indicate that for confinement and reduction of the huge problem in a rational and realistic approach, using the Scenario Earthquake at the initial stage of seismic risk mitigation would better serve the main purpose of the project, particularly due to lack of sufficient budget and time to deal with a much larger problem.

It should be noted that the inferences that are made here are based on the results of investigated buildings (Figure 4.10a), which are mostly located in high seismicity areas. However, since a large portion of the examined buildings are selected from the areas where the seismicity is relatively high, the given distribution of seismic risks could be estimated to be on the pessimistic/conservative side if extrapolated to the overall building stock of Istanbul. TBEC-2018 classifies the buildings into four Earthquake Design Classes (EDC) according to their short period design spectral acceleration coefficients (SDS): EDC-1 ($SDS \geq 0.75g$), EDC-2 ($0.75g > SDS \geq 0.5g$),

EDC-3 (0. 5g>SDS ≥ 0.25g) and EDC-4 (0.25g>SDS). Figure 4.10b compares EDC distribution of investigated/analyzed buildings and all of the 1 to 10 story reinforced concrete buildings that were built before the year 2000 in Istanbul. While a great portion of all buildings and investigated ones are in EDC-1, the share of buildings that are in EDC-2 in this study is 9%, while this percentage is 22% for the whole building stock of Istanbul. the distribution of the number of investigated buildings by districts is given in Table 4.1. The overall distributions in Istanbul scale may change as the distribution of the seismic risks of the examined buildings may not be correctly reflecting the distribution of all buildings in Istanbul. Moreover, the generalization of the results of this study to the whole building stock is not the purpose here.

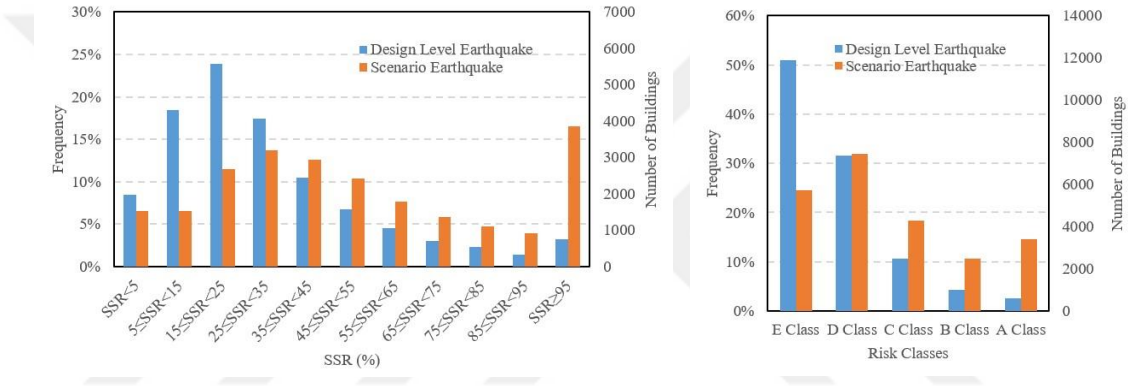

a) b)

Figure 4.9 : Comparison of a) SSR values, b) Risk classes obtained through PERA2019 method for Design Level and Scenario Earthquakes.

Experiences from past earthquakes show that increasing number of stories affect seismic performance of sub-standard buildings in Turkey negatively (Gurbuz et al, 2022). To evaluate the effect of this parameter on the seismic performance, change in SSRs for 1 to 10 story buildings is analyzed. As expected, the SSR values tend to decrease while number of stories increase as a result of the increase in the mean axial load, which leads to a significant reduction in ductility (and sometimes in the flexural capacity of the columns), at the story of investigation. SSR distributions obtained for the scenario earthquake for varying number of stories are presented in Figure 4.11a. The mean SSR values for 1-3, 4-6 and 7-10 story buildings are 77, 47 and 38%, respectively. In harmony with the mean SSRs, 81% of the 7-10 story buildings are classified as high or very high risky buildings, while this percentage is 43% and 74% for 1-3 and 4-6 story buildings, respectively. However, buildings with the same

number of stories may possess very different seismic performances. The information provided from the site work has shown that the seismic safety of buildings with the same number of stories built in the same period can be at different levels. Thus, it would not be realistic to classify buildings based only on their number of stories.

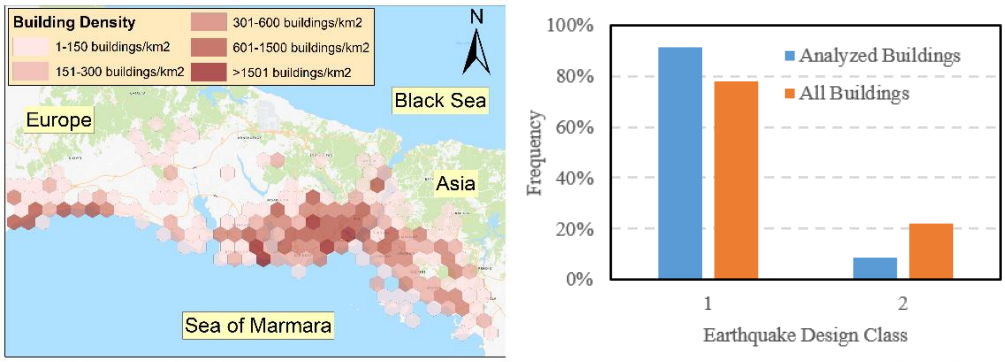

a) b)

Figure 4.10 : a) The density of the number of investigated buildings , b) EDC for Design Level Earthquake.

Table 4.1 : The distribution of the number of investigated buildings by districts.

District	# of Buildings	Ratio of Investigated Buildings	District	# of Buildings	Ratio of Investigated Buildings	District	# of Buildings	Ratio of Investigated Buildings
Adalar	12	1%	Catalca	144	2%	Pendik	603	2%
Arnavutkoy	532	4%	Cekmekoy	112	2%	Sancaktepe	353	3%
Atasehir	226	2%	Esenler	1010	6%	Sariyer	287	1%
Avcilar	4071	27%	Esenyurt	1109	5%	Silivri	1961	10%
Bagcilar	1652	5%	Eyupsultan	327	3%	Sultanbeyli	448	2%
Bahcelievler	583	3%	Fatiih	672	3%	Sultangazi	297	2%
Bakirkoy	443	5%	Gaziosmanpasa	254	2%	Sisli	177	1%
Basaksehir	205	2%	Gungoren	218	2%	Tuzla	281	3%
Bayrampasa	390	3%	Kadikoy	170	1%	Umraniye	383	2%
Besiktas	110	1%	Kagithane	159	1%	Uskudar	153	1%
Beylikduzu	73	1%	Kartal	454	2%	Zeytinburnu	2543	23%
Beyoglu	115	1%	Kucukcekmece	1401	6%			
Buyukcekmece	653	5%	Maltepe	285	2%			

Considering that the number of stories is a dominant parameter in Rapid Visual Screening (RVS) and fragility analysis methods, it is seen that these methods are prone to misclassification on a building scale. The reliability of RVS methods compared to code-based detailed assessment is studied comprehensively by Aydogdu et al. (2022). The average SSR values of buildings constructed over the time periods of various seismic design codes are given in Figure 4.11b (Aydogdu and Ilki, 2023b). As seen in this figure, although there is a tendency of a slight increase in SSR by time, despite the developments in material technology and seismic design codes, the increase in the average SSR values is limited until the year 2000. The site investigations have also demonstrated that most of the pre-2000 buildings in Istanbul have typically similar

sub-standard characteristics. Likewise, the standard deviations of SSR values are not significant for existing buildings constructed in different time ranges (Figure 4.11b). The number of investigated buildings are given in Table 4.2.

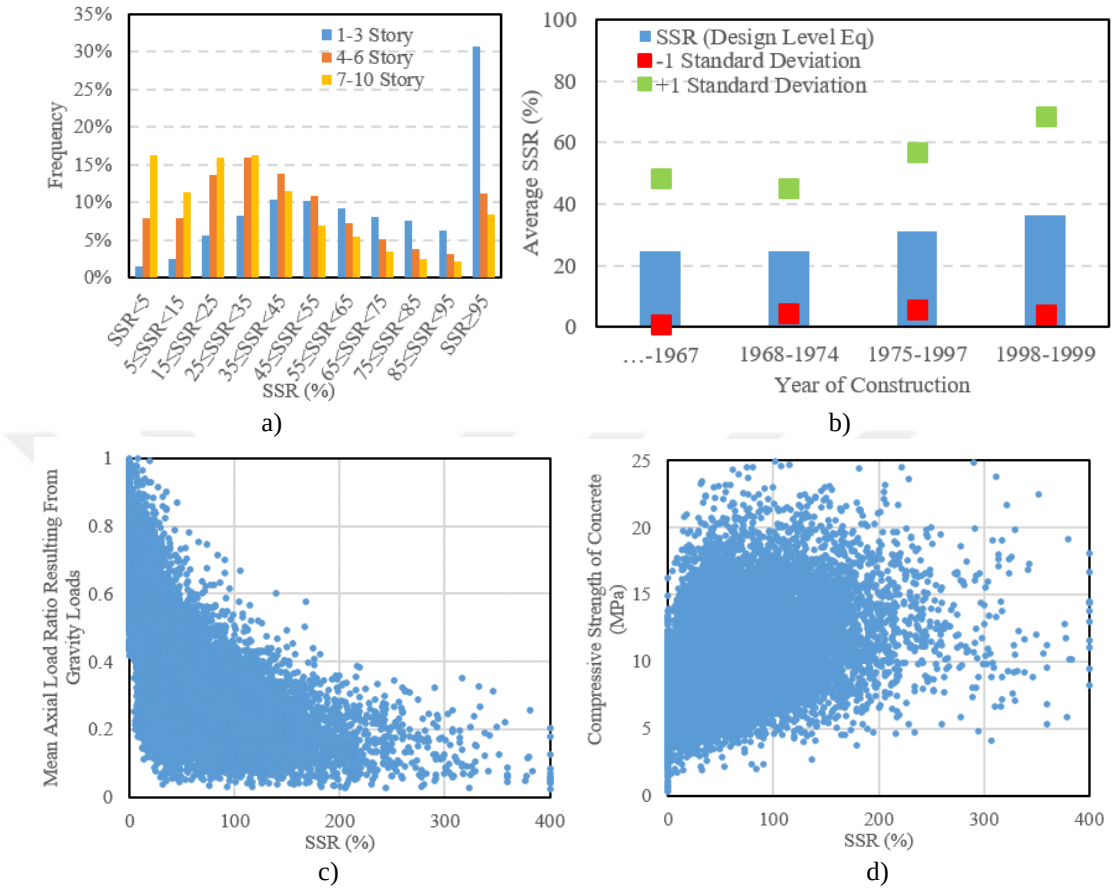

Figure 4.11 : a) SSRs obtained for 1-3, 4-6 and 7-10 story buildings for Scenario Earthquake case, b) The change in average SSR values over the considered time periods, c) relationship between mean axial load ratio resulting from gravity loads and SSR, d) relationship between compressive strength of concrete and SSR.

Figure 4.11c illustrates the relation of the mean axial load on columns at the critical story resulting from gravity loads and SSR values. As mentioned above, an increase in the axial load causes a reduction in the ductility of the members, and consequently in the SSRs. Figure 4.11d demonstrates the relationship between SSR values and the compressive strength of the concrete. Although there is an increasing trend of SSRs with increasing concrete compressive strength, both graphs (Figure 4.11c and 4.11d) reflect that these individual parameters are not sufficiently correlated with the SSR values. Thus, evaluating the seismic safety of building stock without considering all effective structural parameters may lead to serious misclassifications. It should be noted that the SSRs in Figure 4.11c and d generated considering the Scenario

Earthquake case, for which the spectral acceleration values are significantly less than that of the Design Level Earthquake as the location of a building gets further from the fault line. Thus, some SSR values greater than 200 are encountered among the investigated buildings, particularly for those further from the fault line.

GIS (Geographic Information System) tools are used to obtain the spatial distribution maps for each seismic risk class computed by PERA2019. Neighborhood-scale distributions of the densities of risk classes for Scenario and Design Level Earthquakes are given in Figure 4.12 to Figure 4.16. Such spatial distribution maps provide data visualization and help to identify high-priority regions. In parallel with the higher seismicity parameters of the Design Earthquake, as also indicated in Figure 4.1, the Design Level Earthquake was found to be remarkably more demanding posing higher risks to the building stock. As inferred from Figure 4.12 to Figure 4.16 , the density of the buildings in Risk Class E increases as the site gets closer to the main fault (Figure 4.2a) for both seismicity cases. The neighborhoods far from the fault segment represented in Figure 4.2a have a significantly lower share of buildings in Risk Class E and a higher density of buildings in Risk Class A in the case of scenario earthquake compared to design level earthquake loading. The findings of this study assert that the seismicity of the code-based design level earthquake is extremely high compared to scenario earthquake, particularly for the regions that are far from the main fault.

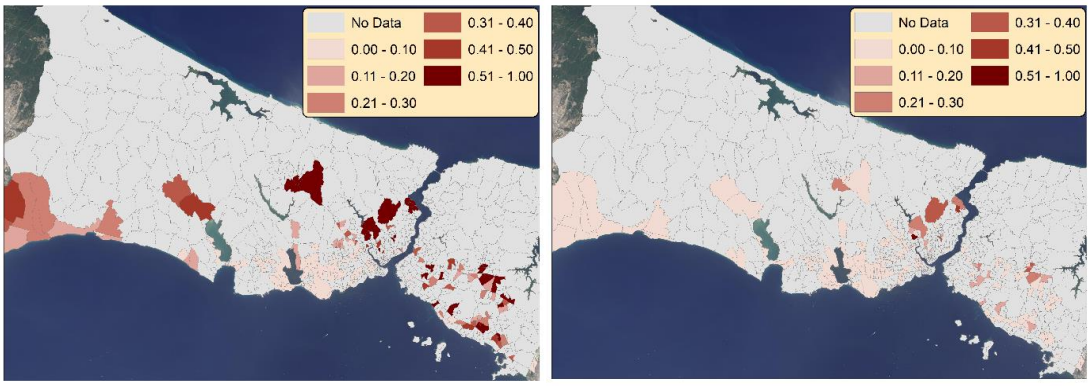

a) b)

Figure 4.12 : Distribution of the A class buildings on a neighborhood scale. The legend demonstrates the ratio of the corresponding risk class to the total number of assessed buildings in the neighborhood. a) Scenario Earthquake Case, b) Design Level Earthquake case.

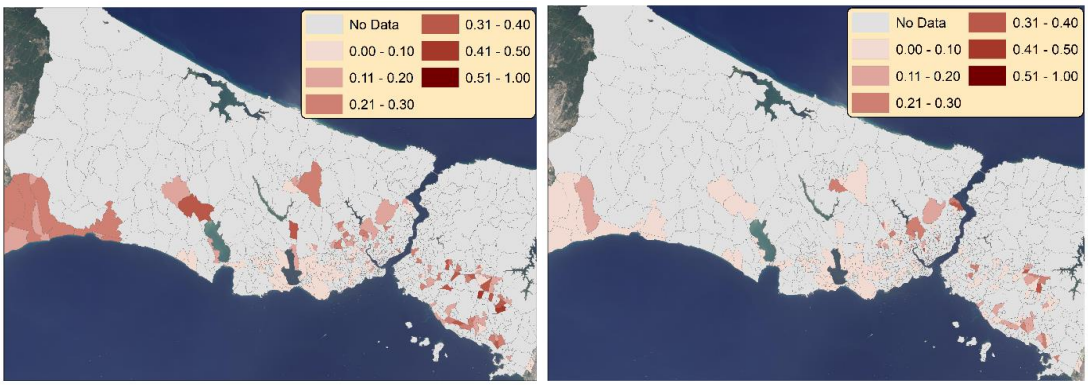

a) b)

Figure 4.13 : Distribution of the B class buildings on a neighborhood scale. The legend demonstrates the ratio of the corresponding risk class to the total number of assessed buildings in the neighborhood. a) Scenario Earthquake Case, b) Design Level Earthquake case.

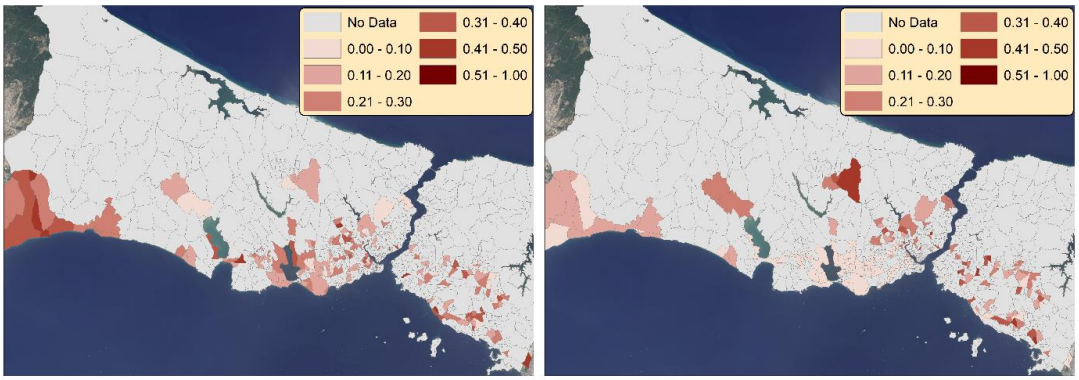

a) b)

Figure 4.14 : Distribution of the C class buildings on a neighborhood scale. The legend demonstrates the ratio of the corresponding risk class to the total number of assessed buildings in the neighborhood. a) Scenario Earthquake Case, b) Design Level Earthquake case.

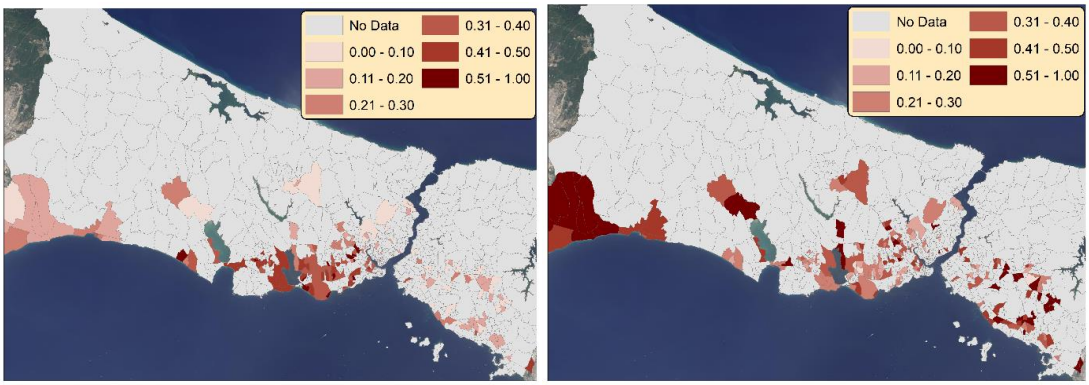

a) b)

Figure 4.15 : Distribution of the D class buildings on a neighborhood scale. The legend demonstrates the ratio of the corresponding risk class to the total number of assessed buildings in the neighborhood. a) Scenario Earthquake Case, b) Design Level Earthquake case.

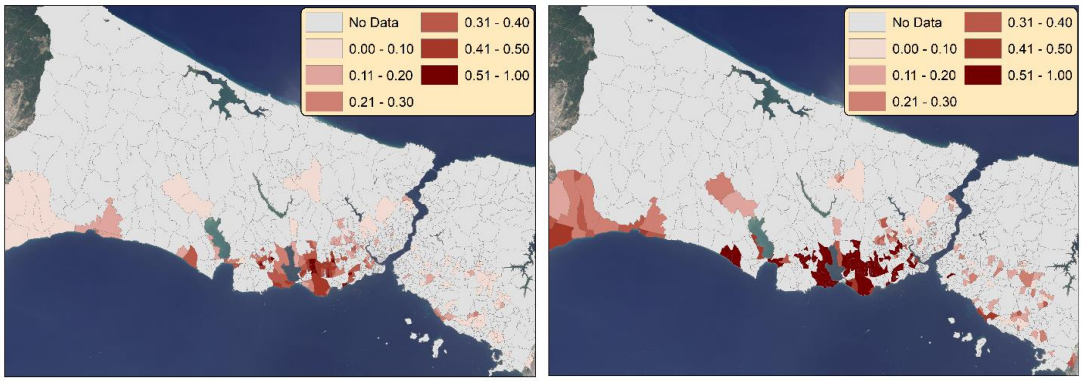

a) b)

Figure 4.16 : Distribution of the E class buildings on a neighborhood scale. The legend demonstrates the ratio of the corresponding risk class to the total number of assessed buildings in the neighborhood. a) Scenario Earthquake Case, b) Design Level Earthquake case.

Figure 4.16 presents the difference in seismicity of the scenario and design level earthquakes for near/far-field and loose/stiff soil cases: Silivri (far-field: 25 km, loose soil: average V_{s30}= 309 m/s), Sisli (far-field: 22 km, firm soil: average V_{s30}=808 m/s), Avcilar (near-field: 12 km, loose soil: average V_{s30}=279 m/s) and Kadikoy (near-field: 16 km, firm soil: average V_{s30}=707 m/s); the near or far-field cases were assigned based on the study conducted by Mavroeidis and Papageorgiou (2003), which states that investigated records including near-fault effects are located within 20 km from the causative fault. The locations of these districts are indicated in Figure 4.2a. For the design level earthquake, 15% of the buildings are in Risk Class A in Sisli, while only a negligible number of buildings were in Risk Class A in the other three districts. This clearly demonstrates remarkably lower seismic risk of existing buildings in Sisli as a consequence of slightly larger distance to fault and better ground conditions, in spite of similar characteristics of existing in all four districts. Quite interestingly, in Silivri, which is the district located furthest from the main fault segment in this group (25 km), scenario earthquake resulted in 13 times more buildings in Risk Class A compared to design level earthquake case. This clearly indicates the importance of consideration of a realistic earthquake scenario for assessing risks of huge stocks of existing buildings. The average SSRs of the buildings according to scenario earthquake were approximately two times greater than the design level earthquake, which shows the huge difference stemming from consideration of two different earthquake cases for these four districts. The histogram of Avcilar (Figure 4.17c) demonstrates that the severity of the scenario earthquake becomes closer to the design level earthquake as

the field gets closer to the fault segment. The number of low-risk structures is negligible in both earthquake cases in Avcilar. Kadikoy is the second nearest district to the main fault out of four towns, for which the outline of SSRs is presented in Figure 4.17. In Kadikoy, more than 70% of the buildings were labeled as Risk Class D or E under Design level earthquake loading, whereas being located on relatively firm soil, the buildings in Kadikoy had significantly higher SSR values for scenario earthquake despite its closeness to the fault. This information leads to the inference that the demand of design level earthquake is also significantly high for near-field regions on firm soil conditions. The ratio of buildings that are in Risk Class D or E is 26% in Sisli for scenario earthquake case, while this value is 44%, 49% and 92% in Silivri, Kadikoy and Avcilar respectively. On the other hand, the share of buildings that are in Risk Class D or E is 47%, 92%, 79% and 100% for design level earthquake in Sisli, Silivri, Kadikoy and Avcilar respectively.

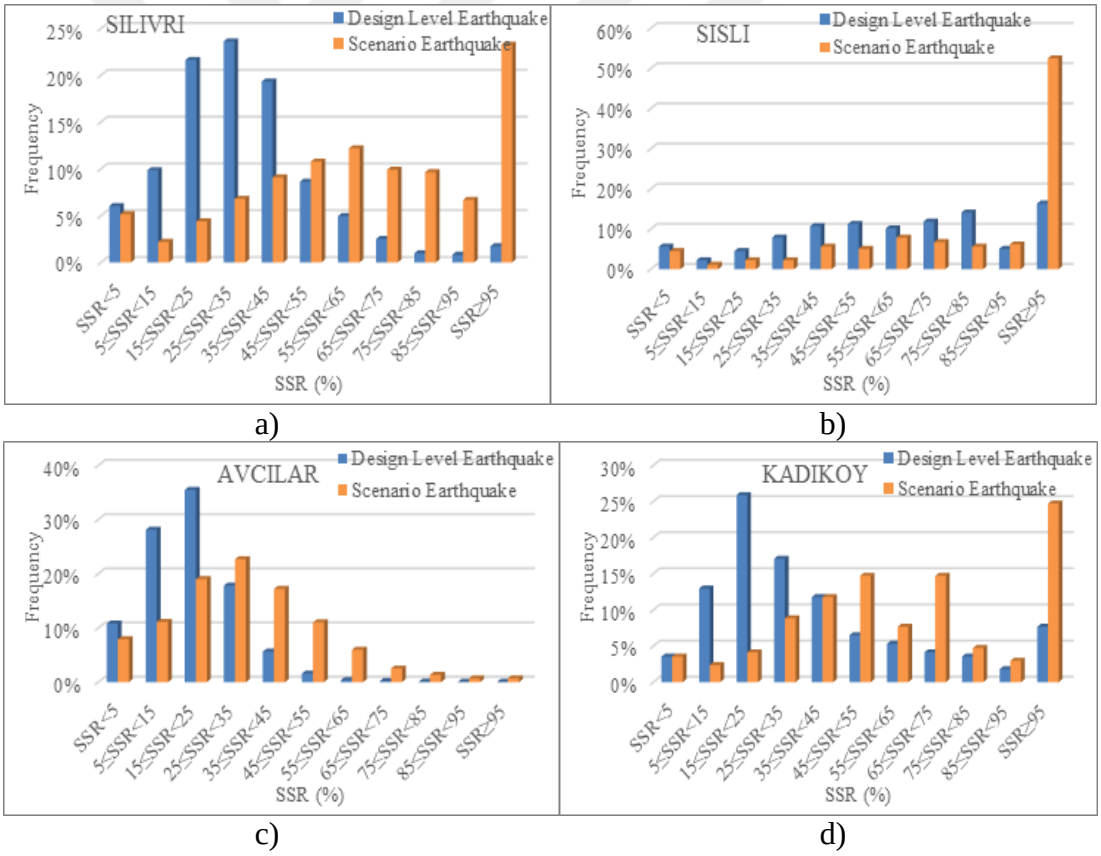

Figure 4.17 : a) Comparison of SSR distributions obtained through PERA2019 method for Design Level and Scenario Earthquakes a) Silivri, b) Sisli, c) Avcilar, d) Kadikoy districts.

The change in these ratios obtained for two seismic cases is significant, except for Avcilar, which represents near-fault and loose soil conditions. Design level earthquake

yields only 8% more buildings in Risk Class D or E in Avcilar compared to scenario earthquake case, while this ratio is 63%, 83% and 108% for Kadikoy, Sisli and Silivri districts. Hence, consideration of a realistic deterministic scenario earthquake instead of design earthquake (which are basically developed for design of new buildings) for cities like Istanbul, where sufficient amount studies has been conducted may remarkably reduce the problem to a more manageable scale and pave the way for a rational and feasible mitigation intervention. Recently, preliminary cost/benefit estimations for intervention strategies based on the data obtained from site investigations were conducted by Demir et al. (2022). The results demonstrated that the estimated economic loss after a potential earthquake could be significantly reduced by intervening to D and E class buildings of the building stock. Also, the results obtained using the data from the buildings within the scope of this study will be used to generate fragility curves for different building typologies as a further study. Then, the estimation of pre-earthquake intervention costs and post-earthquake losses to the whole building stock is also planned.

4.6 Developments in Seismic Safety of RC Building Stock of Istanbul According to the Years and Seismic Design Codes[4]

In Turkey, various seismic zoning maps were published in 1945, 1947, 1963, 1972, 1996, and 2018. Istanbul was in a second-degree seismic zone, according to the Turkish Ministry of Public Works and Settlement's 1972 Seismic Zoning Map (Figure 4.18a). Until publication of the 1996 Seismic Zoning Map (Figure 4.18b), which was prepared through a probabilistic seismic hazard assessment procedure for the first time, was published, Istanbul was in the second-degree seismic zone. Then, the southern part of Istanbul was designated to be in the first-degree seismic zone in 1996. In 2018, a new coordinate-based earthquake hazard map (Figure 4.18c) was published instead of the zonation map concept.

Change in the base shear coefficient for a representative 5-story building in Avcılar (with V_{s30}=300 m/s soil condition), Şişli (with V_{s30}=760 m/s soil condition), and

[4] This part is based on the following publication: Aydogdu, H.H., and A. Ilki. (2023). Developments in seismic safety of rc building stock of Istanbul according to the years and seismic design codes, *fib Symposium 2023 Building for the Future: Durable, Sustainable, Resilient*, 5-7 June, 2023, Istanbul, Turkey. DOI: 10.1007/978-3-031-32511-3_90

Kadıköy (with V_{s30}=760 m/s soil condition) districts of Istanbul according to various seismic design codes and zoning maps in Turkey is given in Figure 4.18d. The base shear is the maximum shear force demand predicted, which is correlated with the effective seismic weight of the building, seismicity, soil parameters, the importance of the building and ductility of the system. The graph demonstrates that base shear demand increased for the representative building in Avcılar district for every code update. There was no base shear force reduction calculated according to updated seismic design provisions in 1998 compared to TSDC-1975. According to the 2018 Turkish Building Earthquake Code (TBEC-2018) and 2018 Turkish Earthquake Hazard Map, the calculated base shear coefficient for the representative building in districts with relatively loose soil conditions (i.e. Avcılar) increased compared to previous codes, while the computed base shear coefficients for the locations with firm soil conditions (i.e. Kadıköy and Şişli) is significantly lower compared to preceding seismic provisions.

PERA2019 method was applied to more than 24,000 RC buildings. The target of the project was to assess the buildings that were built before 2000. However, a limited amount of buildings that were constructed after 2000 were also evaluated to examine the seismic safety of that building group in general. In this study, the buildings are grouped to reflect the significant milestones in seismic design codes in Turkey (Table 4.2).

Pre-1968 buildings are in a single group as almost no regulation on the design principles of the reinforced concrete buildings has been introduced by the previous seismic design codes according to Aydinoglu (2007), and the 1968 Turkish Seismic Design Code (TSDC-1968) is the first provision to introduce the dynamic properties of buildings, minimum cross-section details, confinement reinforcement, etc. (Aydinoglu, 2007). The buildings that were built in 1998 and 1999 are also grouped because these buildings are supposed to be built according to TSDC-1998. However, these buildings were constructed before the seismic awareness developed after the 1999 Earthquakes. The rest of the buildings are classified according to the seismic design codes that they had to be built in accordance with. Several minimum requirements in various versions of seismic design codes in Turkey are given in Table 3.5. Apparently, Turkish seismic design codes involve crucial provisions and requirements since 1975.

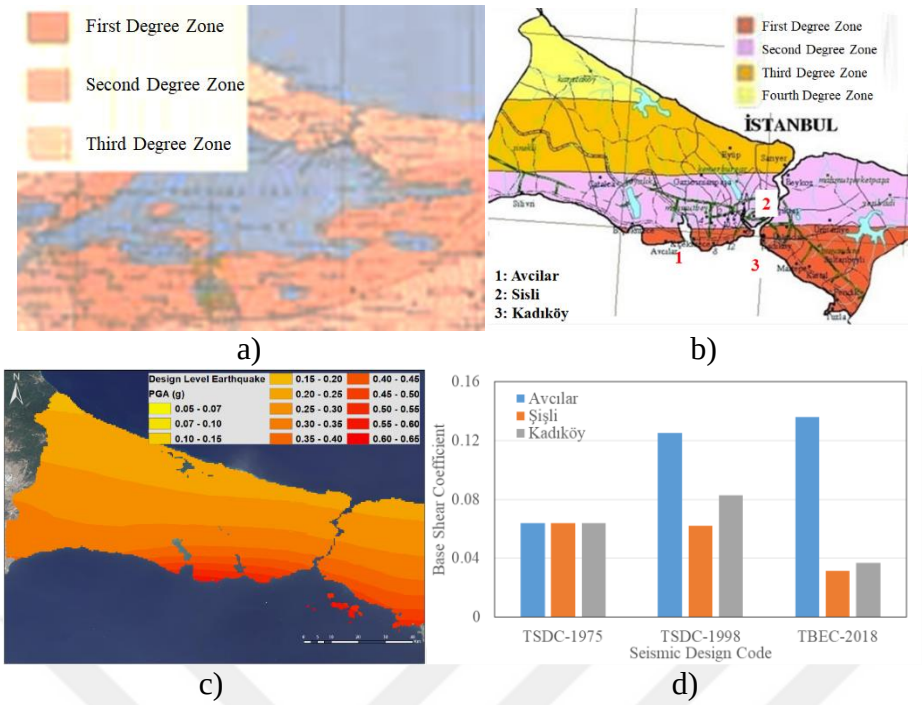

Figure 4.18 : a) 1972 Seismic Zoning Map of Turkey (adapted from Pampal and Ozmen, 2017), b) 1996 Seismic Zoning Map of Turkey, c) Earthquake Hazard Map of Turkey, d) Change in the base shear coefficient for a representative building in Avcilar, Sisli and Kadikoy districts according to various seismic design codes in Turkey.

Table 4.2 : Year of construction, number of buildings, and corresponding seismic design codes.

Year of Construction	Seismic Design Code	Number of Buildings
<1968	Various	274
1968-1974	TSDC-1968	897
1975-1997	TSDC-1975	19866
1998-1999	TSDC-1998	2930
2000-2006	TSDC-1998	112
2007-2017	TSDC-2007	86

The average compressive strength of the buildings over the years as measured on-site by non-destructive techniques is given in Figure 4.19a. The findings show that the average compressive strength of concrete has not changed significantly from mid 20th century until 2000. After that year, the newly established inspection mechanism and widespread availability of ready-mixed concrete provided a significant increase in the average compressive strength. Almost all buildings constructed before 1990 have been built with plain bars (S220 class), and only, in a negligible amount of pre-1990 buildings with deformed reinforcement bars (S420 class) were encountered. After the publication of TSDC-1998, the share of S420 class reinforcement started to increase. The ratio of plain reinforcement bars (S220 class) was not totally avoided until its use was banned by TSDC-2007 (Figure 4.19b). Confinement zones and reduced stirrup

spacing requirements are defined in TSDC-1975. However, this provision was only very rarely applied in construction practice until the year 2000 (Figure 4.19c). In parallel, the average minimum longitudinal reinforcement ratios of columns seem to satisfy the code requirements only after 2000 (Figure 4.19d).

The axial stress level on the columns is a critical factor for the ductility of a reinforced concrete section. An increase in axial load decreases the ductility and, if the section is loaded beyond the balanced loading level, the moment capacity of the section is also lower. Harmonious to material properties, Figure 4.19e states that the average axial stress of columns of the investigated buildings did not change from mid 20th century until 2000. After that year, the average axial load decreased drastically. The average spectral acceleration capacity ($S_{a,cap}$), which is calculated by the multiplication of SSR value and spectral acceleration demand ($S_{a,dem}$) corresponding to the period of the investigated buildings for the first mode of vibration (Equation 4.1) over the years is given in Figure 4.19f. Apparently, the average spectral acceleration capacity of the investigated buildings did not change significantly from the mid 20th century until the year 2000. The buildings that were constructed between the years 2000-2006 and 2007-2017 have approximately 2 and 3 times higher spectral acceleration capacity compared to the ones that were built before 2000.

The average SSR values of buildings for the considered period of time are given in Figure 4.20a. The average SSR distributions verify the information that generally the seismic safety of the buildings that were constructed after the 1999 Marmara Region Earthquakes have significantly higher seismic safety in Istanbul. In light of this information, prioritization of the buildings based on their year of construction can be a practical approach to reduce the size of the seismic risk mitigation works.

As aforementioned, seismic design codes in Turkey have always reflected their era's level of knowledge and requirements in the earthquake engineering field. However, construction practice in Turkey did not comply with these requirements for a long time. Figure 4.20b compares the average SSR distribution for the actual situation (as determined by on-site investigations) and for the state if the buildings had at least satisfied the minimum requirements of their era's seismic design code. It should be noted that the buildings that were constructed before 1975 are excluded from this comparison. The findings illustrate that if the minimum requirements of the codes were

met, the average SSR of the buildings that were constructed between 1975 and 2000 would be nearly twice as high.

$$S_{a,cap} = SSR\% \times S_{a,dem} \quad (4.1)$$

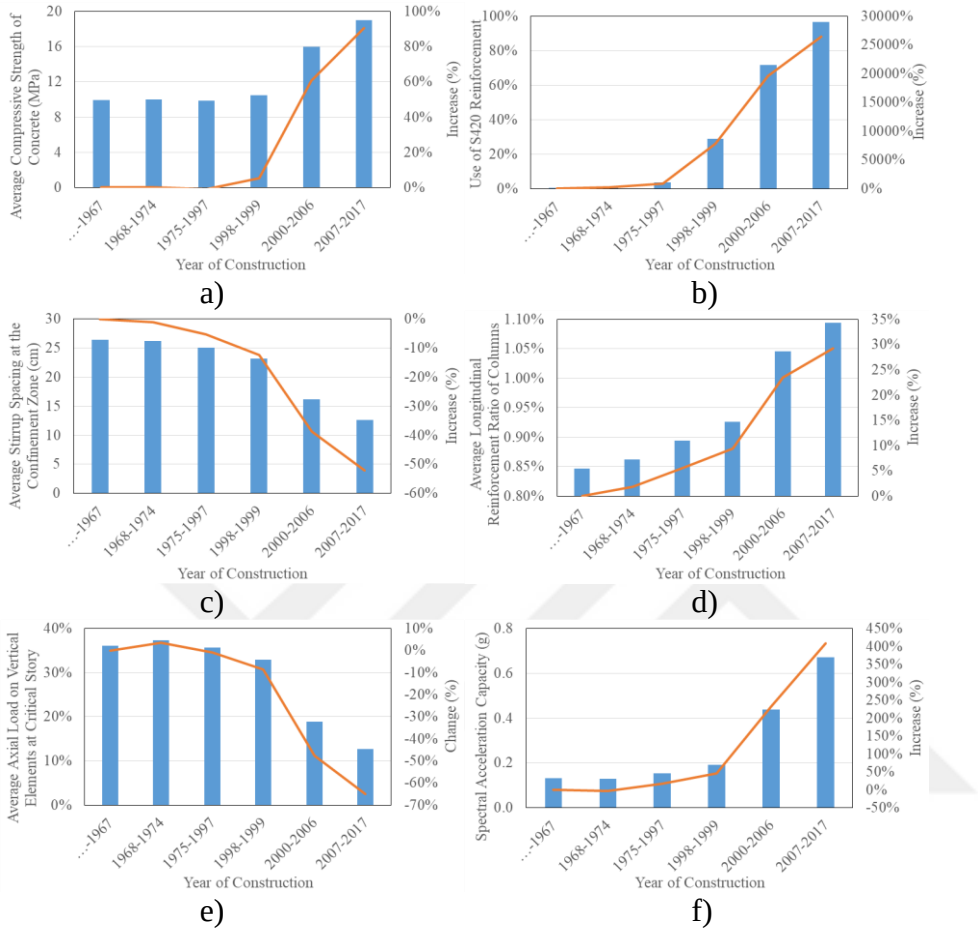

Figure 4.19 : The change in the average of various structural parameters and material properties of the investigated buildings (Table 4.2) over time periods: a) Average compressive strength, b) Use of deformed reinforcement bars, c) Average stirrup spacing, d) Average longitudinal rein-forcement ratio, e) Average axial load on vertical elements, f) spectral acceleration capacity.

4.7 Inferences on the Structural Characteristics of the Building Stock in Istanbul

After the catastrophic 1999 Kocaeli and Duzce earthquakes that hit Northwest Turkey, several projects have been carried out by Istanbul Metropolitan Municipality (IMM), Universities and other national and international institutions to prepare the city for the future earthquakes. In 2003, Istanbul Earthquake Master Plan (IEMP, 2003) was prepared in coordination with the universities. In Zeytinburnu, Fatih, Kucukcekmece, Bahcelievler, Gungoren, Bayrampasa and Bakirkoy districts, seismic performances of

the buildings were screened, mostly through street survey level investigations in between 2000 and 2009. In 2019, a new project has been initiated by IMM for a rapid and more accurate identification of highly vulnerable individual buildings built before the year 2000. The early results of this recent project obtained through application of PERA2019 methodology on nearly 23,000 buildings by considering two different earthquake cases (Design Level and Mw=7.5 Scenario Earthquakes), are summarized in this paper. Based on the findings of the project, the following conclusions are reached:

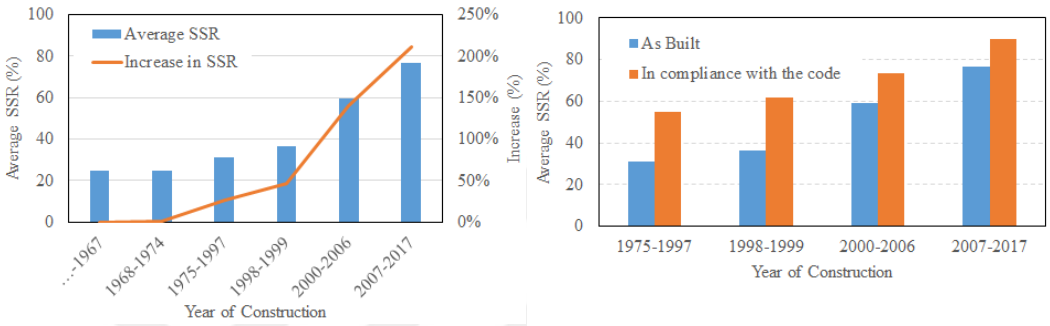

a) b)

Figure 4.20 : a) The change in average SSR values over the considered time periods, b) The comparison of average SSR values over the years for the actual situation and the state if the buildings had at least satisfied the minimum requirements of their era's seismic design code.

• The findings of the site work demonstrate that the mean compressive strength of the concrete is around 10 MPa for the examined building stock of Istanbul. This, together with small dimensions of the vertical structural members, lead to high axial forces on columns, which may cause a potential brittle seismic behavior against future earthquakes. Further, 60% of the examined buildings do not satisfy the minimum longitudinal reinforcement ratio requirements, and only a marginal portion of the examined buildings have proper column confinement reinforcement.

• Based on the analysis procedure used in this study and the structural properties of investigated buildings, more than 97% of the investigated buildings are not able to satisfy the requirements of current seismic regulations in Turkey. Thus, the buildings that are constructed before the year 2000 in Istanbul have significant structural deficiencies, and the seismic risk of these buildings is very high in common.

• To identify the risk on a building scale, determining the structural parameters have to be the primary focus. Since RVS methods and fragility analyses based on number of stories and other global data about the buildings, do not properly consider

the aforementioned deficiencies, using these methods to determine the seismic risk on a building scale for the building stock of Istanbul may cause serious misclassification of structures.

- The heatmaps of buildings in all risk classes represent that the seismic risk is clearly higher in the neighborhoods that are located at west of the Golden Horn and south of the TEM highway.

- Using deterministic scenario earthquake provides more refined results with respect to design level earthquake. Design level earthquake yields 46% more buildings in Risk Classes D and E with respect to scenario earthquake. This difference increases as the location gets further from the main fault or the soil gets firmer.

- The SSR distributions obtained through consideration of the design level or scenario earthquakes are closer to each other for near-fault districts. The seismic demand of scenario earthquake decreases remarkably with respect to design level earthquake as the site gets further from the fault.

- The density of the buildings in Risk Class A increases as the neighborhoods are getting further from the main Marmara fault. The better local soil parameters of the Asian part of the city have a positive impact on SSR values; the ratios of buildings in Risk Classes A and B on the coast of the Asian part are visibly more than the districts on the coast of the European part of Istanbul.

- The need and benefit of a triage system based on a rapid, robust, reliable and cost-effective methodology towards prioritization of hundreds of thousands of risky buildings is demonstrated within the framework of this study. Such individual building-based rapid and realistic seismic risk assessment and prioritization methods are needed to be included in the official legislations preferably by making use of deterministic scenario earthquakes rather than the design earthquake which considers a considerable level of safety margin.

- The seismic risk mitigation efforts and financial sources should be conveyed to the transformation or seismic retrofitting of buildings with high seismic risk, particularly to the buildings in seismic risk classes D and E as soon as possible to avoid/reduce potential casualties and huge economic losses. The probability of collapses and casualties is remarkably less for the examined buildings in seismic risk classes B and C although those building do not fully comply with the seismic design

codes either. Furthermore, the repair costs of these building are expected to be much less with respect to buildings in seismic risk classes D and E, if they are subjected to a future earthquake. Therefore, the investment on seismic retrofit and/or reconstruction of the buildings in risk classes B and C could be postponed to a stage after risk reduction activities are planned for the buildings in risk classes D and E.

In this chapter, the changes of several important structural characteristics, including compressive strength of concrete, steel class, stirrup spacing, longitudinal reinforcement ratio, axial stress on columns, and spectral acceleration capacity over a wide time range are evaluated considering the relevant seismic design provisions. The outputs of this study showed that the main structural characteristics listed above and the seismic safety of the existing structures had not significantly improved from mid 20th century until the year 2000. After the year 2000, the common use of deformed reinforcing bars, higher strength concrete, and better detailing of reinforcement led to remarkably higher quality constructions. The average SSR distributions verify quantitatively that the seismic safety of the buildings that were constructed after the 1999 Marmara Region Earthquakes have significantly higher seismic safety in Istanbul. In light of this information, prioritization of the buildings based on their year of construction can be a practical approach to reduce the size of the seismic risk mitigation efforts (i.e. the buildings constructed before the 2000s should definitely be examined with priority). Another important conclusion is that if the minimum requirements of the previous seismic design codes have been met, the seismic safety of existing buildings could have been remarkably higher (i.e. the average SSR of the buildings that were constructed between 1975 and 2000 could have been nearly twice as high).

On average, seismic performances of existing buildings have increased remarkably after the year 2000 with changes of attitudes of all relevant parties due to the consciousness that the 1999 Marmara earthquakes brought. Today in Turkey, the seismic demands required by the current seismic design code for ordinary residential buildings correspond to an earthquake with a probability of exceedance of 10% in 50 years. The buildings are typically designed for controlled damage performance level, for which severe damages to the building are possible if design spectral accelerations are exceeded, as was the case in Kahramanmaraş, Antakya and some other locations during the 2023 Kahramanmaraş earthquakes. Like was the case for Kahramanmaraş,

there are some areas (like Istanbul), where the probability of a destructive earthquake is quite high in coming years. Therefore, it is recommended that the new buildings in areas of such high seismic risks in coming years should be designed and constructed according to an advanced seismic performance level since their probability of experiencing a destructive earthquake higher than 10% in 50 years.

It should be noted that the inferences that are made here are based on the results of investigations and analyses of 22,868 buildings, which are mostly selected from high seismicity regions of the city, and the overall distributions of seismic risk may change as more buildings are assessed. Thus, generalization of the results of this study on the whole building stock of Istanbul will probably be a pessimistic/conservative approach compared to the actual case.

After the recent 2023 Kahramanmaras and Hatay Earthquakes in Turkey, the framework proposed herein is planned to be extended to thousands of additional buildings. Moreover, a risk mitigation campaign has been recently launched by IMM. In the scope of this campaign, more than 300 buildings prioritized in this study, with the risk of sudden axial collapse are being demolished and reconstructed. Additionally, seismic retrofit and urban renewal campaigns have also been recently launched for buildings that have been prioritized herein.

5. VALIDATION OF THE RAPID SEISMIC PERFORMANCE ASSESSMENT METHOD (PERA2019) THROUGH INCREMENTAL NONLINEAR DYNAMIC ANALYSES OF EXISTING RC BUILDINGS[5]

5.1 Outlines of the Study

One of the effective ways to examine the reliability of a rapid seismic evaluation method is to compare the results of the method with more sophisticated methods in the literature. IDA, which is basically the implementation of a series of nonlinear time history analyses incrementally to structural models, is chosen as a reference method to interpret the trustworthiness of PERA2019 and the risk classification approach because of its similarity to the incremental approach of evaluated rapid assessment procedure. Within the scope of this comparative study, SSR values and risk classes of 22 buildings, 10 of which are virtual buildings that are modeled according to their original blueprints, are computed by the implementation of each method to evaluate the reliability of the selected rapid performance-based assessment methodology. Then, the results of the reference analysis are compared with the assigned risk classes through the PERA2019 method.

IDA methodology emerged from the practice of increasing or down-scaling the severity of acceleration records by multiplying the records by a scaling factor: the incremental approach is made by increasing the scale coefficient at each step, starting from a low-intensity measure (IM). IDA may be applied based on either single ground motion record or multiple. However, the buildings exhibit very different behaviors under different seismic records. Figure 5.1a,b,c represents the IDA curves of a 5-story building with a first vibration period of 1.26s. According to Vamvatsikos and Cornell (2002), buildings may exhibit lower response at higher steps due to excessive hardening. Thus, the performance of a building under a single record cannot reflect the overall behavior of the building in future earthquakes, so in this chapter, IDA analyses are computed with multiple records; 11 ground motion records are appointed to each

[5] To be submitted as an article in 2024.

building as seismic demand. The records are scaled to match the design spectrum of TBEC-2018, which corresponds to seismicity with a return period of 475 years. Figure 5.1d represents a sample scaling procedure for a building with a first vibration period of 1.19s.

In the first step, 11 ground motion records are selected from the NGA-West2 database (PEER) to perform an IDA study. The attributes and acceleration-time histories of the selected records are given in Table 5.1 and Figure 5.2, respectively. The records are selected to reflect the expected earthquake near Istanbul: Shallow, strike-slip events with a moment magnitude between 6.60 and 7.51. The ground motions are scaled according to the rule that the amplitudes of the mean spectrum of all selected records will be larger than the amplitudes of the design spectrum in between 0.2Tp and 1.5Tp periods, as described in TBEC-2018.

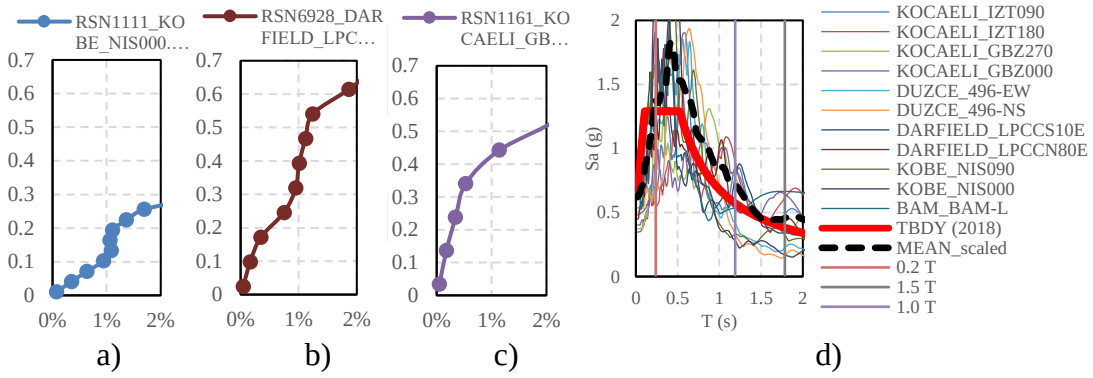

Figure 5.1 : a-b-c) IDA curves for a 5-story reinforced concrete building under various acceleration records (vertical axis: spectral acceleration, horizontal axis: maximum inter-story drift ratio), d) an example of scaling procedure of the ground motion records for a building with a first vibration period of 1.19s.

Table 5.1 : Selected ground motion records.

Earthquake Name	Year	Station	M_w	Depth (km)	Mechanism	V_{s30} (m/sec)	Horizontal-1	Horizontal-2
Kocaeli Turkey	1999	Izmit	7.51	16	Strike-slip	811	RSN1165_IZT180	RSN1165_IZT090
Kocaeli Turkey	1999	Gebze	7.51	16	Strike-slip	792	RSN1161_GBZ000	RSN1161_GBZ270
Duzce Turkey	1999	IRIGM 496	7.14	14	Strike-slip	760	RSN8165_496-NS	RSN8165_496-EW
Darfield New Zealand	2010	LPCC	7.00	11	Strike-slip	650	RSN6928_LPCCN80E	RSN6928_LPCCS10E
Kobe Japan	1995	Nishi-Akashi	6.90	18	Strike-slip	609	RSN1111_NIS000	RSN1111_NIS090
Bam Iran	2003	Bam	6.60	6	Strike-slip	487	RSN4040_BAM-L	

The flowchart of the IDA procedure is demonstrated briefly in Figure 5.3. Three-dimensional numerical models of the buildings are prepared in SeismoStruct software,

and the ground motion records are applied with 15% increments starting from 5% loading up to 140%. For each building, 11 ground motion records are applied in X and Y directions with 10 different scale factors at each step, which means that 220 nonlinear time-history analyses are conducted to perform the IDA procedure for every building. Then, the spectral acceleration values corresponding to first mode vibration period vs maximum inter-story drift ratio graphs are extracted at every incremental step of IDA for each acceleration record. The median IDA curve for the building is calculated consequently.

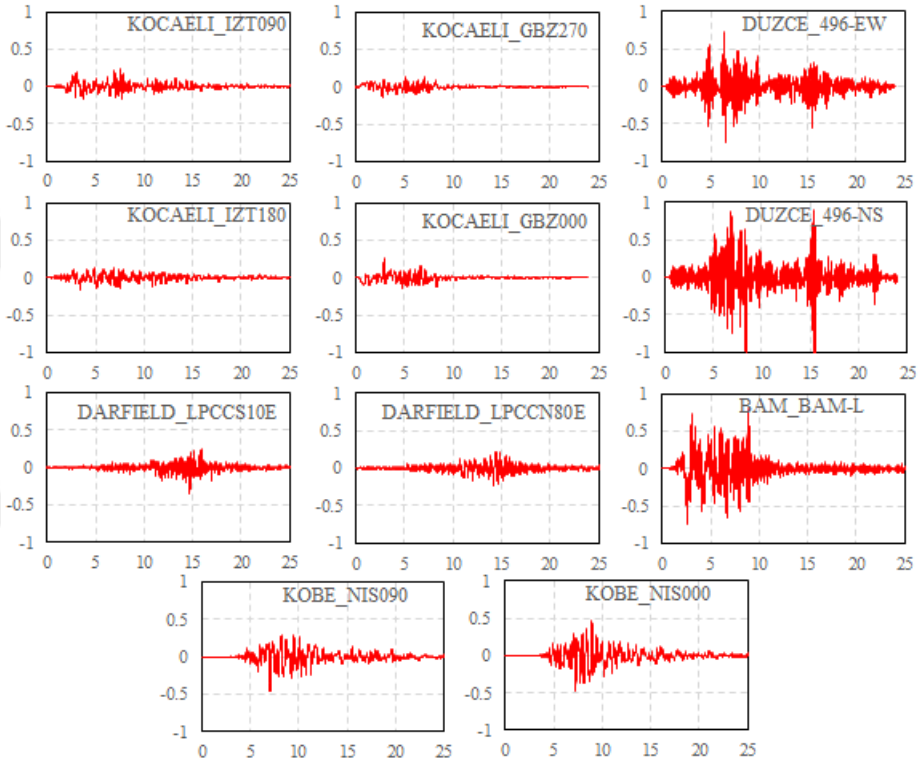

Figure 5.2 : Acceleration-time histories of the selected records. Vertical and horizontal axes are acceleration (g) and time (s) values respectively.

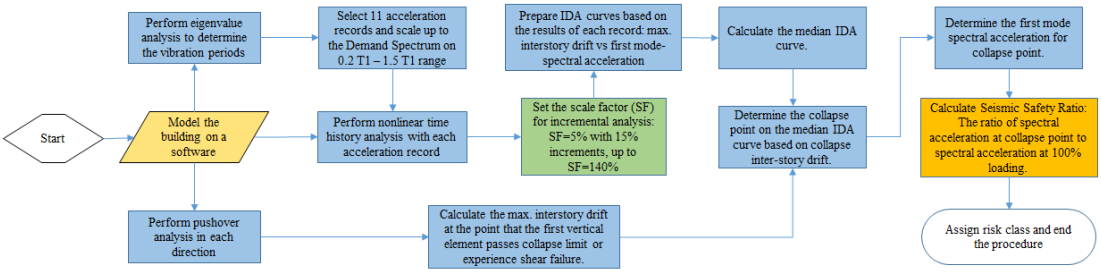

Figure 5.3 : Overall flowchart of IDA procedure.

A representative building for established 3D structural models is given in Figure 5.4. All sections are defined on Seismostruct software with reinforcement details.

Distributed inelasticity elements are used in the modelling phase. Beams are modelled as “Inelastic Force Based Plastic Hinge Elements”, while “Inelastic Displacement Based Plastic Hinge Element” type is defined to short beams to avoid convergence problems. Fiber models are established for columns and shear walls; they are modelled as “Inelastic Force Based Elements”. Mander and Menegotto-Pinto models are used to represent numeric models of the concrete and reinforcement, respectively. Rayleigh model is used for damping. The number of converged analyse results out of 11 records are given in Table 5.2 for all scale factors.

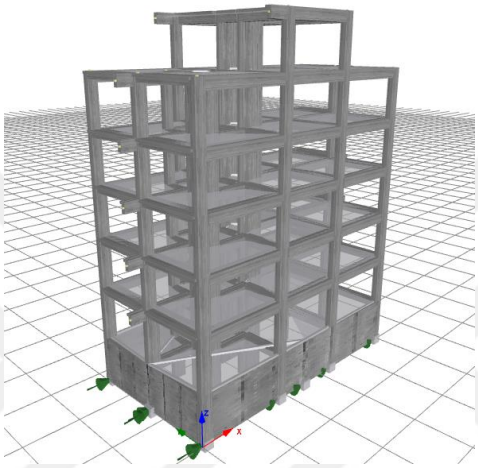

Figure 5.4 : Structural model of Building 301.

A static pushover analysis should be conducted to determine the maximum story drift of the building as the collapse point at the point that the first vertical element attains the collapse prevention chord rotation limit given in equation (5.1) or experiences shear failure. This approach is adopted in parallel with the rapid post-earthquake damage assessment procedure explained in Chapter 3 (Figure 3.19), which asserts that if at least one vertical RC element experiences D type damage, buildings is considered heavily damaged. In equation (5.1), $\emptyset_u$ is the ultimate curvature, $\emptyset_y$ is the yield curvature, L_p is the length of the plastic hinge, L_s is the shear span, db is the average longitudinal reinforcement diameter at the tension zone. The rotation value is measured from the angle between the tangent to the axis at the yielding end and the chord connecting that end with the end of the shear span.

$$\theta_p^{CP} = [(\emptyset_u - \emptyset_y)L_p\left(1 - 0.5\frac{L_p}{L_s}\right) + 4.5\emptyset_u d_b \qquad (5.1)$$

The ratio of the spectral acceleration of the first vibration period at the collapse point to the spectral acceleration of the 100% loading is the SSR value of the building, which is computed according to equation (5.2). It should be noted that ξ is the damping ratio in this equation.

$$SSR_{IDA} = \frac{S_{a,collapse}(T_1,\xi=5\%)}{S_{a,\%100}(T_1,\xi=5\%)} \tag{5.2}$$

Table 5.2 : Number of converged analyses.

		Scale Factor							
		0.35	0.50	0.65	0.80	0.95	1.10	1.25	1.40
Buildings	101	11	11	11	11	10	9	6	4
	201	11	11	11	11	11	11	8	7
	102	11	11	11	11	10	10	10	10
	202	11	11	11	11	11	11	11	11
	103	11	11	11	11	11	9	7	5
	203	11	11	11	11	11	11	10	8
	104	11	11	11	11	11	11	11	9
	204	11	11	11	11	11	11	11	11
	110	7	2	1	0	0	0	0	0
	210	11	10	10	9	9	9	9	9
	107	11	11	11	11	11	9	5	3
	207	11	11	11	11	11	11	11	11
	106	11	11	11	11	11	10	10	9
	206	11	11	11	11	11	11	11	10
	105	11	11	11	10	10	9	5	2
	205	10	10	10	10	10	10	10	10
	109	11	11	11	11	11	11	11	11
	209	11	11	11	11	11	11	11	11
	108	11	11	11	11	10	10	8	5
	208	11	11	11	11	11	11	11	11
	301	11	11	11	11	11	11	11	11
	302	11	11	11	11	11	11	11	11

5.2 Evaluated buildings

Within the scope of this comparative study, 12 existing buildings, which are located in Istanbul, reflecting a wide range of SSR values were selected and modeled in a computer software. Also, 10 of the studied buildings are modeled as in their original projects, which were designed in accordance with TSDC-1975. Two buildings are not modeled for the as-designed case; the projects of building 302 were not found in the archives, and it was observed that building 301 was built in compliance with its design project, so they are modeled for the as-built case. Comprehensive information on the structural properties such as the first period of free vibration, base shear demand, axial

stress on vertical elements, reinforcement details, material properties, and plan dimensions for each building are given in Table C.1. Most of the examined buildings consist of a reinforced concrete frame system, while 3 of the buildings have dual reinforced concrete frame+wall structural systems. The column layouts of 12 buildings are given in Figure 5.5. The number of stories above the buildings' critical story varied between four and six. All of the buildings investigated in this study, front views of five of which are given in Figure 5.6, have the ordinary residential type of use. The design projects of the buildings were provided by IMM during the site work was performed.

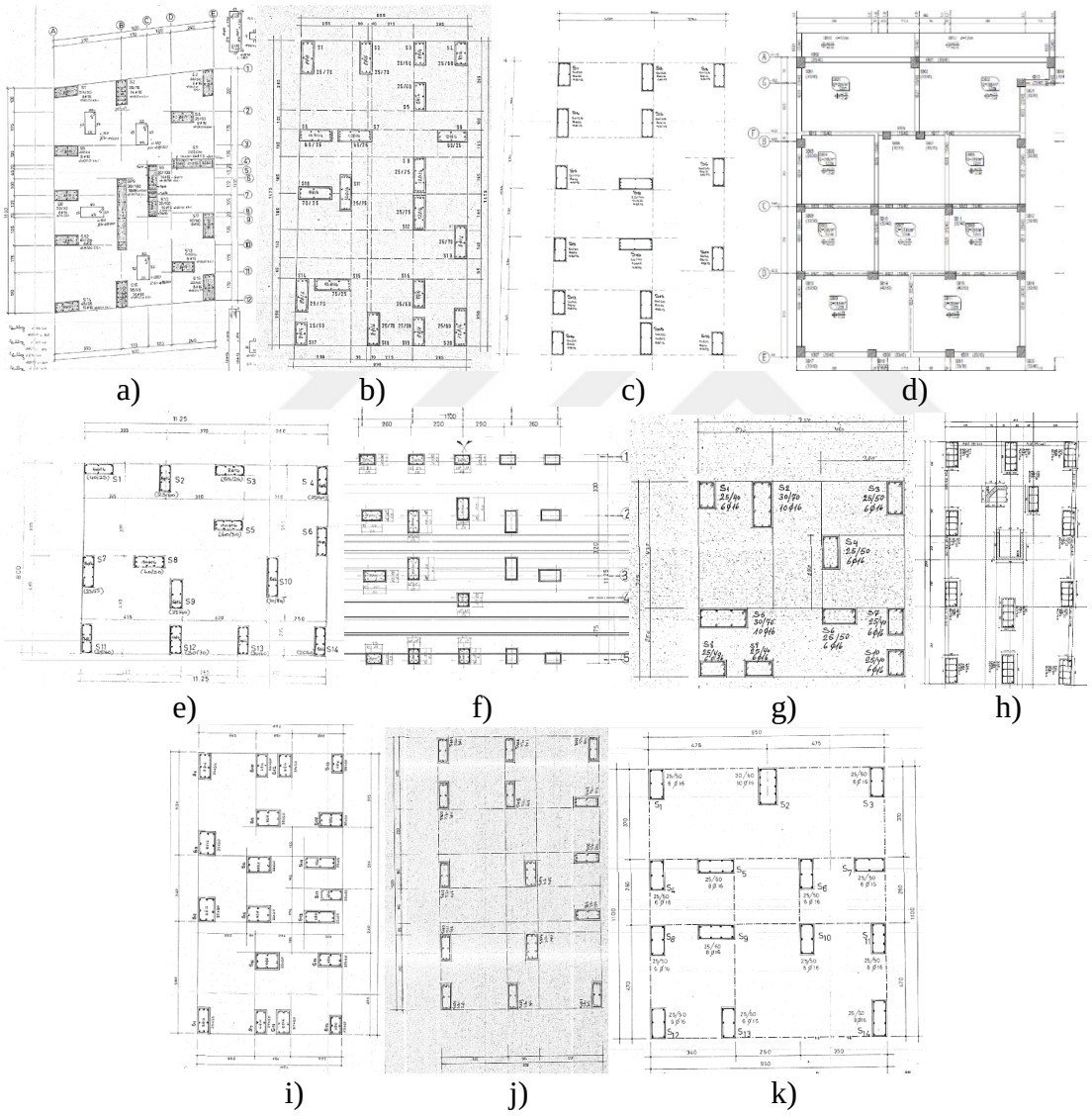

Figure 5.5 : The layouts of the buildings investigated in this study: a) 201, b) 204, c) 206, d) 302, e) 202, f) 203, g) 208, h) 301, i) 205, j)207, k) 209.

According to 1972 Seismic Zoning Map (Turkish Ministry of Public Works and Settlement), Istanbul was in second degree seismic zone. After publication of 1996 Seismic Zoning Map, southern parts of Istanbul became first degree seismic zone. In

2018, the zonation map concept was abandoned and a new location-based earthquake hazard was published (Turkish Ministry of Interior Affairs Disaster and Emergency Management Presidency 2018). The current earthquake hazard map of Turkey and Seismic zoning maps published in 1972 and 1996 are given in Figure 4.18.

The base shear demands have been changed subsequent to the developments in the seismic design codes and seismic zoning maps. Base shear demands computed based on the linear elastic approach for each building according to various seismic design codes are given in Figure 5.7. It can be seen from the figure, TSDC-1998 and TSDC-2007 yield 95% more base shear force than TSDC-1975 for Avcilar district, whilst the increase in base shear force computed according to TBEC-2018 varies between 53% and 115%. While the increase in the base shear force demand is at this level, inevitably, these buildings in Avcılar cannot satisfy the developed versions of seismic design codes.

a) b) c) d)

Figure 5.6 : The front views of representative buildings that are investigated in this study. IDs: a) 201, b) 204, c) 206, d) 202.

5.3 Results and discussion

The SSR values of 12 as-built and 10 as-designed case buildings are determined through the implementation of the PERA2019 and IDA procedures. Produced IDA curves for every building are given in Table C.2. Since the method applied involves an incremental procedure, the results of IDA are admitted as the reference values for the evaluation of the reliability of the iterative procedure and risk classification approach of PERA2019. The overall information on the structural properties, static pushover analysis results and SSR values computed by the application of PERA2019 and IDA for each building are given in Table C.1, while IDA curves plotted for each building are given in Table C.2.

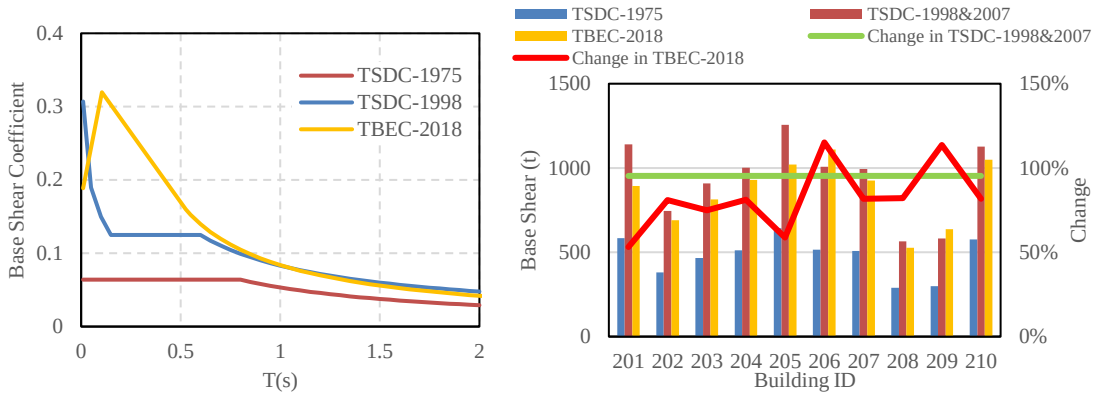

a) b)

Figure 5.7 : a) Design spectrum for ordinary residential building in Avcilar according to various seismic design codes, b) Base shear forces that the investigated buildings have to bear according to various seismic design codes.

SSR values that are found by both methods in the X and Y directions of the buildings are demonstrated in Figure 5.8a. When each direction is taken into consideration separately, the SSR values of 13 cases according to PERA2019 methodology are found on the unsafe side, while the SSR values of 31 cases are on the safe side. For the most unsafe case, the SSR value of the Y direction of building 204 according to PERA2019 is 64%, while the considered value is found 44% by IDA, which corresponds to an error of 20 units. However, the global SSR of a building is calculated based on the minimum value of both X and Y directions. The SSR values of the X direction of building 204 computed by PERA2019 and IDA are 38% and 43%, respectively. Hence, for this building, the minimum seismic safety is determined in the X direction, and the margin of error decreases to 5 units when both directions are considered on the global seismic performance. Figure 5.8b shows the distribution of the global SSR values of the buildings. The percentage of unsafe cases decreases from 30% to 23% when considering both X and Y directions of the buildings for the computation of the global performance. Moreover, the maximum gap between the SSR value of PERA2019 and IDA for the most unsafe condition is dropped to 8 units. For the analysis in one direction, the number of conservative results yielded by PERA2019 is 2.4 times more than the ones on the unsafe side. Thus, for PERA2019, the probability of yielding results in unsafe side both in X and Y directions at the same time is 9%. For that reason, if the PERA2019 procedure gives a result in the unsafe side in one direction, it often gives a more conservative result in the other direction, reducing the error margin of the probability of an unsafe evaluation. Figure 5.8 also demonstrates that the SSR values computed through PERA2019 and IDA methods have a good

harmony with the reference line. The best fit of the results considering one direction is parallel with the reference line, whilst the best fit for the global SSR values of the buildings tends to diverge from the reference line in favor of the conservative classification as the SSR value increases. The average global SSR values of the buildings evaluated in the scope of this study are 37.7 and 44.2 for PERA2019 and IDA methodologies, respectively.

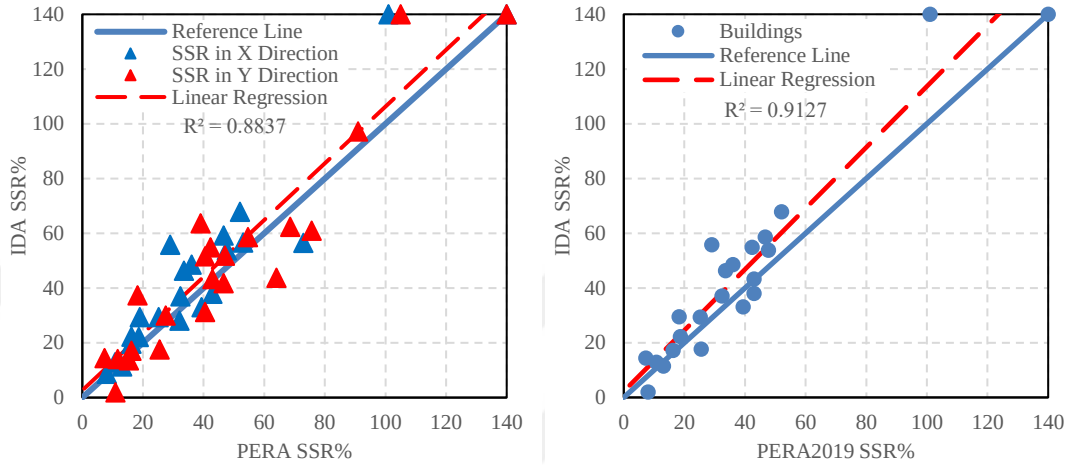

Figure 5.8 : SSR distributions computed through PERA2019 and IDA procedures, a) consideration of the single direction, b) consideration of both directions.

Figure 5.9a-b illustrate the SSR value histograms computed through both analysis methods for each building in the X and Y directions, respectively, while Figure 5.9c demonstrates the SSR distribution considering the minimum value of both directions. The results yielded by PERA 2019 exhibit a good agreement with the reference analysis method based on all of the histograms given below.

Seismic risk classes of the buildings based on the approach given in Chapter 3 (Table 3.4) are determined according to the SSR values computed by PERA2019 and IDA procedures. Figure 5.10 represents the risk classes of the buildings for each method, while the matrix prepared to compare the risk classifications of each method is given in Table 5.3. The red-colored cells of the matrix are unsafe classifications made by PERA2019. The findings demonstrate that PERA2019 yields only 1 result on the unsafe side, which corresponds to 5% of the building set. The only building evaluated in a less risky class is classified as very high risky by IDA procedure. It should be noted that this building is still evaluated as high risky by PERA2019. Meanwhile, PERA2019 yields more conservative results for 5 buildings and classifies 16 buildings, which correspond to 73% of the buildings, the same as IDA.

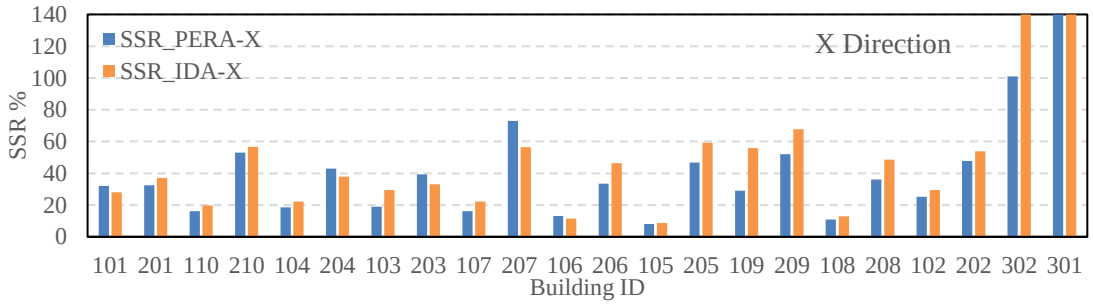

a)

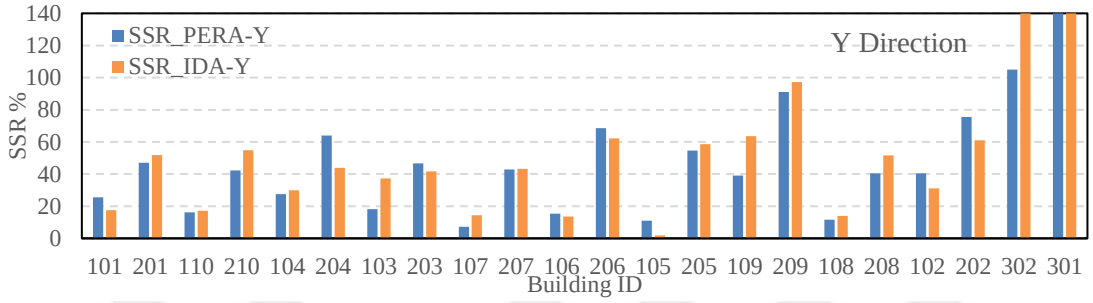

b)

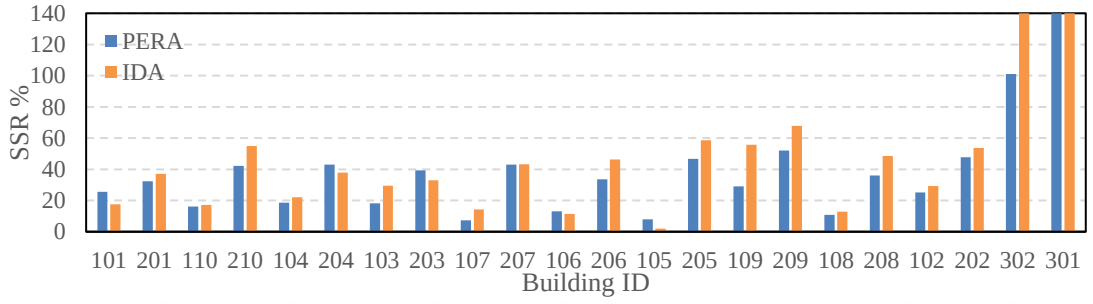

c)

Figure 5.9 : SSR histograms for each building computed through PERA2019 and IDA methods, a) X direction, b) Y direction, c) consideration of both directions.

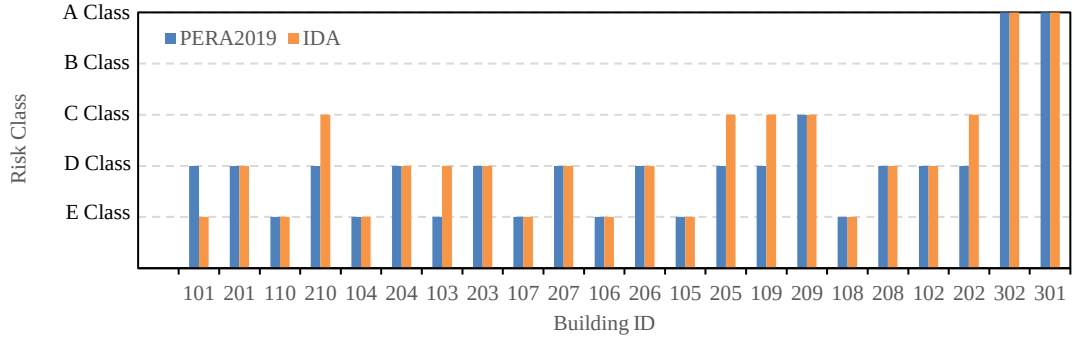

Figure 5.10 : Seismic risk class histograms for each building computed through PERA2019 and IDA methods.

As aforementioned, most of the buildings built before 2000 are not able to satisfy the requirements of the 2018 Turkish Building Earthquake Code due to improvements in seismic codes and seismic zoning maps. On the other hand, it has been observed in the past earthquakes the buildings - meeting the needs of the seismic regulations of the

period they were built - provide satisfactory earthquake safety. In this study, 10 buildings, which are designed according to TSDC-1975, are modeled as existing state and compliant with their original design projects to evaluate the seismic safety provided by TSDC-1975. Figure 5.11a-b compare the SSR results of as-designed and as-built cases computed through PERA2019 and IDA procedures, respectively. Based on the results of this study, the average SSR values of the buildings, which are modeled according to their design projects, are 41.6% and 48.1% for PERA2019 and IDA, respectively. Yet, these buildings were not built based on their projects; the average SSR values computed by PERA2019 and IDA are 17.2% and 21.2% for the existing state of the buildings, respectively. The results of this study demonstrate that if the buildings were built in accordance with their original projects prepared according to TSDC-1975, they would provide seismic safety more than 2 times compared to the current situation.

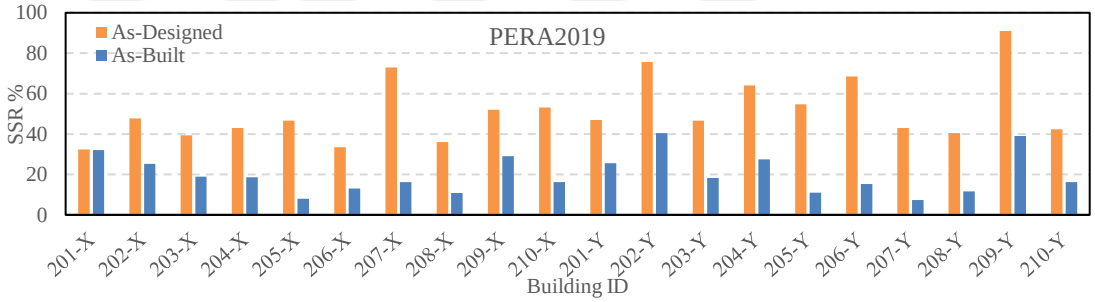

a)

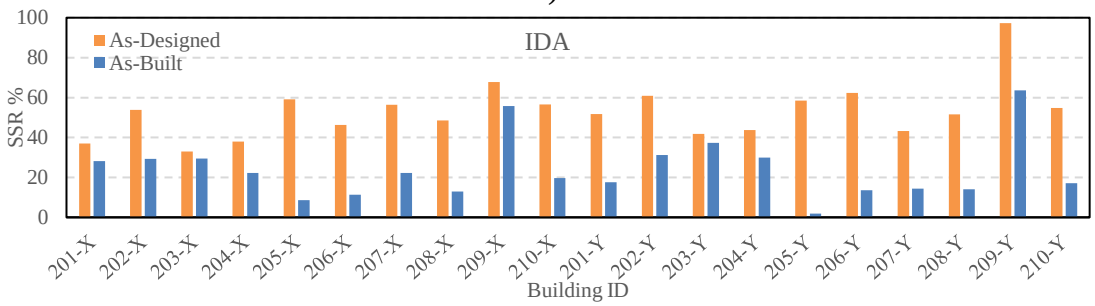

b)

Figure 5.11 : SSR values of the buildings computed by: a) PERA2019, b) IDA.

Even if they are built in accordance with the design projects prepared according to TSDC-1975, 90% of buildings that are investigated in this chapter are labeled as high or very high risk by PERA2019. As aforementioned, this stems from the fact that Istanbul had been in a second-degree seismic zone until 1996. Furthermore, the base shear coefficient was almost half of the TSDC-1998 for the first-degree seismic zones like Avcilar. The buildings investigated had to be designed to withstand, at least, the calculated base shear force according to TSDC-1975 ($V_{t,1975}$), and the current base

shear force demand ($V_{t,2018}$) of the building can be considered as the seismic demand. Thus, the increase in the base shear force can be calculated with equation (5.3).

Table 5.3 : Risk classification matrix of the building set. The red-colored cells in the matrix are unsafe cases for PERA2019, while the methodology yields conservative results in green-colored cells.

		IDA Risk Class				
		A	B	C	D	E
PERA Risk Class	A	2	0	0	0	0
	B	0	0	0	0	0
	C	0	0	1	0	0
	D	0	0	4	7	1
	E	0	0	0	1	6

$$Base\ Shear\ Change = \frac{V_{t,2018} - V_{t,1975}}{V_{t,2018}} \quad (5.3)$$

The comparison of SSR values computed by each method and change in the base shear force is given in Figure 5.12. The results showed that determining these buildings as high or very high risky is inevitable due to the change in the base shear force demand.

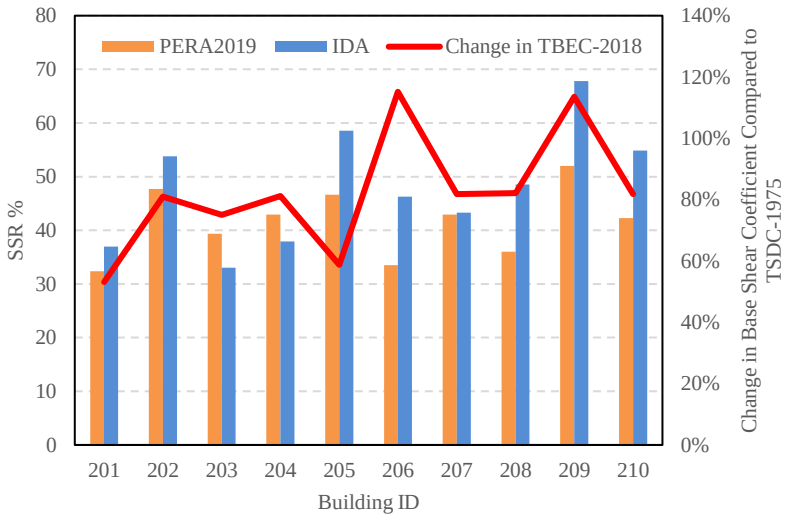

Figure 5.12 : Comparison of SSR values and the base shear ratio of TSDC-1975 to TBEC-2018 for each building.

5.4 Conclusions

This part of the thesis was conducted to evaluate the reliability of the proposed risk classification procedure of PERA2019 by comparing the results of a more complex procedure, for which IDA was chosen as the reference evaluation. Within the scope of

this study, the SSR values of – in total – 22 buildings are determined through the implementation of the PERA2019 and IDA procedures. Also, 10 buildings, which are designed according to TSDC-1975, are modeled as existing state and compliant with their original design projects to evaluate the seismic safety provided by TSDC-1975.

As stated by TBEC-2018, it should not be expected that performance evaluations to be made through linear and non-linear methods will give exactly the same results based on theoretical differences between the approaches. Thus, the deviations in the results are an expected phenomenon. Still, the results of the iterative procedure of PERA2019 and the regression line of the SSR scatter are found to be in a good agreement with the reference line; the R2 value of the regression line is approximately 90%, which is a good indicator of the reliability of the procedure. The risk classifications made through PERA2019 are also in harmony with the reference results. The classifications provided by PERA2019 remain on the unsafe side for merely one building, finding the risk of that building one class safer. By PERA2019 methodology, 73% of the buildings are determined in the same risk class as the reference procedure. Based on the outputs of this study, as a rapid performance-based assessment method, PERA2019 performed quite satisfactorily compared to a reference code-based detailed assessment procedure.

When each direction is considered separately, the results of PERA2019 for %70 of the cases are on the conservative side. Calculating the global SSR value of the building based on the minimum value of both directions decreases the probability of being on the unsafe side. The results of this study demonstrated that PERA2019 determines the global SSR value of 73% of the buildings lower than the SSR value computed by IDA.

The findings of this study show that if the buildings were designed according to TSDC-1975 and built compliant with their original design projects, they would have more than 2 times the seismic safety compared to their current state. The seismic demand of TSDC-1975 is half of described by TBEC-2018 for the high seismicity regions of Istanbul. However, these buildings can satisfy the seismic demand of TBEC-2018, if the building is located in low seismicity regions of the city. Thus, it is not an appropriate approach to label the buildings that comply with the previous seismic design codes as the same as the seismically deficient buildings and to classify both of them as risky. It is important to evaluate each building individually to assess the seismic safety provided by the structural system of the building.

6. RISK ESTIMATION STUDY ON THE BUILDING STOCK IN ISTANBUL AND COST-BENEFIT ASSESSMENT OF RISK MITIGATION STRATEGIES[6]

6.1 Extrapolation of the Outputs of Site Study to the Building Stock in Istanbul

Within the scope of risk mitigation studies, at least 5% of the buildings of each district are investigated through PERA2019 to provide unique structural information for the districts of Istanbul. Thus, the probability of exceedance of the spectral acceleration demands for actual buildings is determined for different typologies. Afterward, an estimation study is performed to predict the risk class distribution for all structures of the city on the district and neighborhood scale. This study highlights the high priority regions for performing widespread performance-based analysis work and foresight for further steps of the mitigation efforts, such as the approximate number of buildings to be intervened.

6.1.1 Methodology

The building inventory of Istanbul consists of 615,700 reinforced concrete buildings, of which the number of stories is between 1 and 10 and were constructed before 2000 (Table 6.1). In the first step of estimation study, the spectral acceleration demands must be assigned to all buildings in order to determine the risk class probabilities.

Experiences from past earthquakes show that the increasing number of stories generally affects the seismic performance of sub-standard buildings in Turkey negatively. To evaluate the effect of this parameter on the seismic performance, change in SSR for 1 to 10 story buildings is investigated based on the data gathered in the site works narrated in Chapter 4. As expected, spectral acceleration capacity values tend to decrease (Figure 6.1) while the number of stories increases as a result of the increase in the axial load, which leads to a reduction in ductility at the investigation story. For that reason, buildings are divided into 3 groups while generating probability of

[6] To be submitted as an article in 2024.

exceedance curves to capture similar average seismic performance: 1-3 story, 4-6 story and 7-10 story buildings. The overall SSR distribution of these groups is demonstrated in Figure 4.11. It should be noted that the given relationship between spectral acceleration values and number of stories contain a wide scatter. However, this relationship was used for just the categorization of the buildings, not for estimation of the building capacity.

Table 6.1 : Reinforced concrete building stock of Istanbul (Cakti et al. 2019).

Year of Construction	# of Stories	# of Buildings
Before 1980	1-3	47,760
	4-6	107,923
	7-10	8,722
	11+	1,369
1980-2000	1-3	201,650
	4-6	239,516
	7-10	20,125
	11+	4,438
After 2000	1-3	168,306
	4-6	145,925
	7-10	21,339
	11+	8,960
Total		976,033

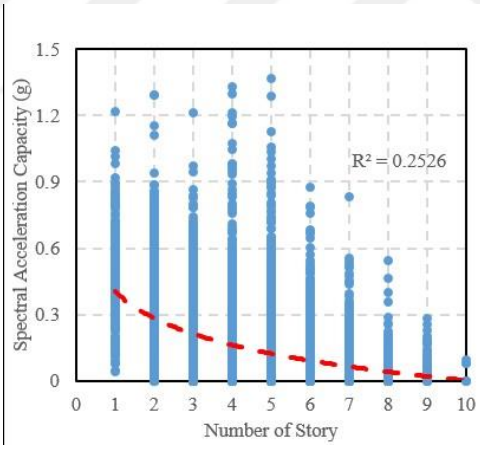

Figure 6.1 : The relationship between spectral acceleration capacity and the number of story.

The seismicity parameters are appointed to all buildings in the GIS environment. To assign spectral acceleration demand to the buildings, first mode fibration period must be predicted first. Seismic design codes suggest empirical equations for periods of the buildings. However, additional to the number of stories, footprint areas of the buildings from base maps are known. Since the correlation of these parameters with the period determined through PERA2019 is prepared from nearly 23000 buildings (Figure 6.2), obtaining more accurate period relationship using plan area and number of stories is

possible for our case. It should be noted that this generalization will lead certain uncertainties. The effects of all uncertainties on the estimation study is evaluated in the following validation study part of this chapter. The summation of the area and the number of stories roughly represents the mass of the structure, while the number of stories is also connected with the height of the structure. Story heights are assumed to be the same on each story. The period of each structure is calculated through equation (6.1) which is the regression curve provided by the data from Figure 6.2b. It should be noted that T, n and A are period in seconds, the number of stories and the projection area in m^2.In the final step, probabilities for each risk class are determined according to frequencies of corresponding spectral acceleration demand.

$$T = 0.1778(n^5(n+1)A)^{0.114} \tag{6.1}$$

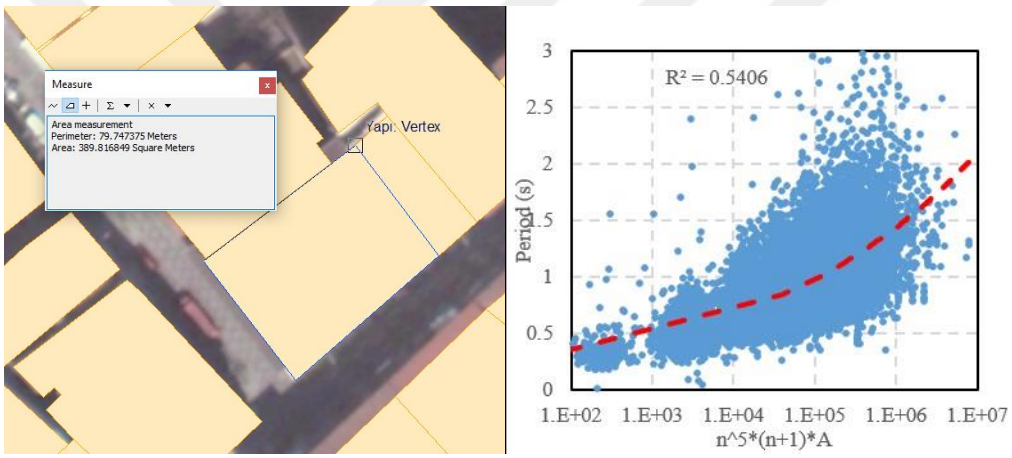

a) b)

Figure 6.2 : a) Building inventory from GIS network, b) The relationship of the first mode period with number of stories (n) and footprint area of the building (A).

Then, estimated spectral acceleration demands for all buildings in the inventory of Istanbul are computed. An example of the calculation of spectral acceleration demand corresponding to the first vibration period of 0.8s is given in Figure 6.3.

Reinforced concrete buildings in Istanbul are divided into categories considering the year of construction, the number of stories and located districts. For each category, probabilities of exceedance of considered spectral acceleration demands are determined based on the capacity values of all buildings in considered categories, which are provided from site works and results of the PERA2019 procedure. Probability of exceedance curves are generated by taking into account the spectral acceleration capacity values of buildings. The capacities of all buildings give the

probability of exceedance of the spectral acceleration values in that group (Figure 6.4). It should be noted that SSR values of some of the buildings are determined 0, so those buildings do not have any seismic load bearing capacity, and some probability of exceedance curves do not start from 0. Equation (6.2) is used to calculate the spectral acceleration capacity of the building. $S_a(g)$ is spectral acceleration demand herein. Spectral acceleration value of the first vibration period is used herein, but as explained in Chapter 3, SSR is computed through scaling PGA value. Since the theoretical PGA value of the demand spectrum is 0.4 times short range spectral value of the spectrum according to TBEC-2018, scaling considering PGA or spectral acceleration of the first vibration period will not cause any difference in the computation phase.

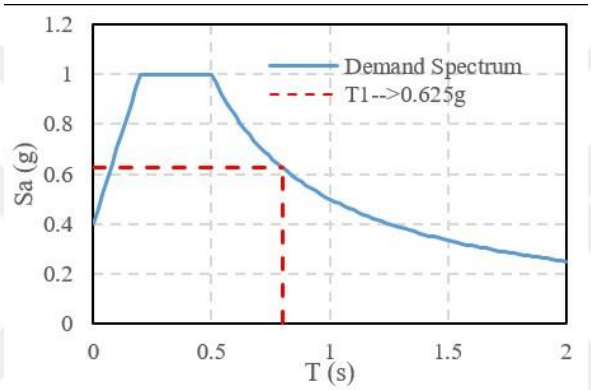

Figure 6.3 : An example calculation of the spectral acceleration demand corresponding to first vibration period.

$$\text{Capacity (g)} = S_a(g) \times \frac{\text{SSR}}{100} \tag{6.2}$$

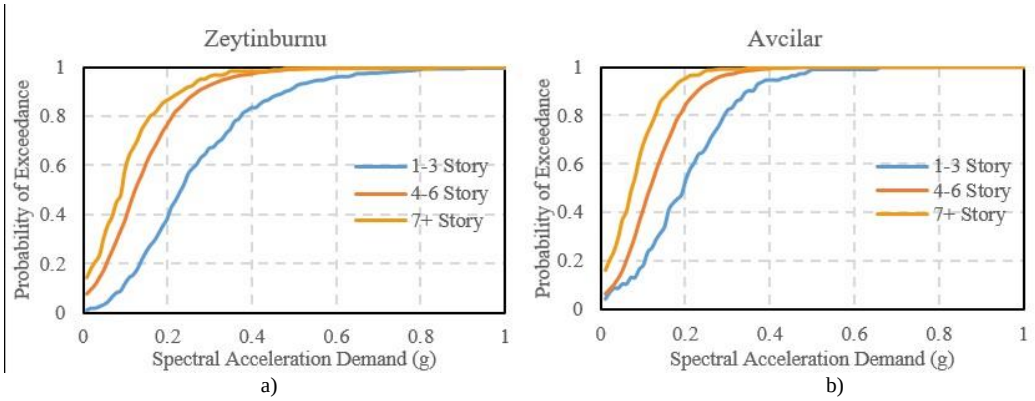

Figure 6.4 : Probability of exceedance curves for Zeytinburnu and Avcilar districts obtained from site work.

Consequently, the exceedance probability of the assigned spectral acceleration demand is calculated to compute the building's probability of being in each risk class. An example calculation for a 1 to 3 story building in Avcılar with 0.4g spectral

acceleration demand is given in Table 6.2. The difference between the probability of each load fraction represents the probability of the related risk class. Also, a schematic demonstration of the computation phases is given in Figure 6.5. General flowchart of the estimation study is given in Figure 6.6. The computation of probabilities are made through equation (6.3) to equation (6.7), where P is probability, $S_a(g)$ is spectral acceleration demand, Sa_{cap} is spectral acceleration capacity, n is number of buildings in that category that satisfies the condition, N is total number of building in that typology.

Table 6.2 : An example calculation for 1 to 3 story building in Avcilar with 0.4g spectral acceleration demand.

	Load Coefficient				
	25%	50%	75%	100%	
Spectral Acceleration Demand (g)	0.1	0.2	0.3	0.4	
Probability of Exceedence	19.6%	52.3%	84.1%	94.4%	
Risk Class	E Class	D Class	C Class	B Class	A Class
Probability of Each Class	19.6%	32.7%	31.8%	10.3%	5.6%

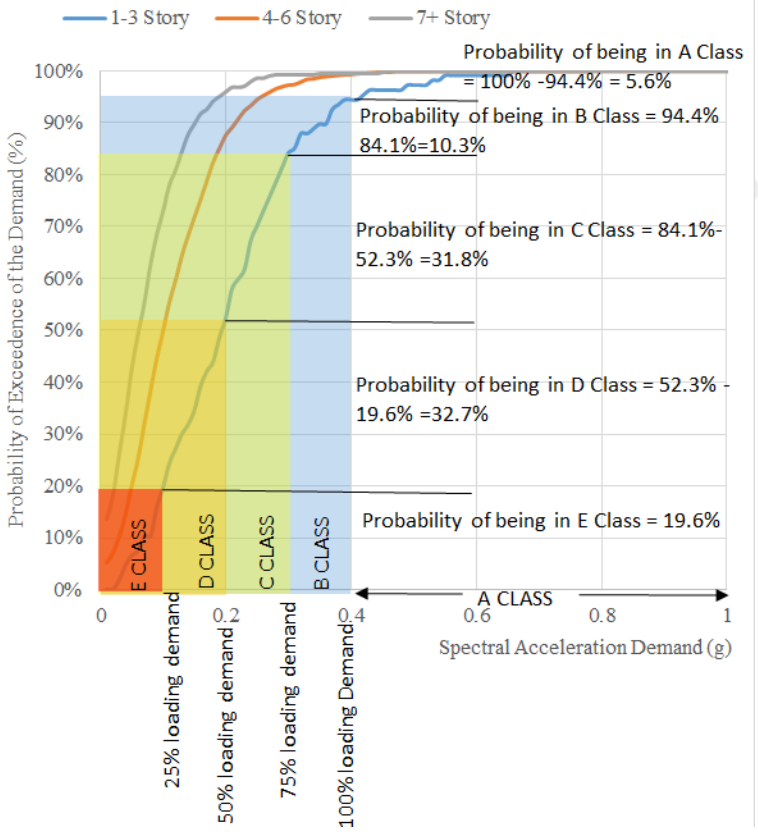

Figure 6.5 : An example calculation for 1 to 3 story building in Avcilar with 0.4g spectral acceleration demand.

$$P(A\ Class) = \frac{n(Sa_{cap} \geq S_a(g))}{N} \tag{6.3}$$

$$P(B\ Class) = \frac{n(Sa_{cap} \geq S_a(g)*0.75) - n(Sa_{cap} > S_a(g))}{N} \quad (6.4)$$

$$P(C\ Class) = \frac{n(Sa_{cap} \geq S_a(g)*0.50) - n(Sa_{cap} > S_a(g)*0.75)}{N} \quad (6.5)$$

$$P(D\ Class) = \frac{n(Sa_{cap} \geq S_a(g)*0.25) - n(Sa_{cap} > S_a(g)*0.5)}{N} \quad (6.6)$$

$$P(E\ Class) = \frac{n(Sa_{cap} < S_a(g)*0.25)}{N} \quad (6.7)$$

Note that, since the summation of all probabilities equals to 1, the cumulative summation of all risk classes' probabilities for all buildings gives the total number of buildings. Therefore, the summation of all buildings' probability of being in each class will give the number of buildings in the corresponding risk class.

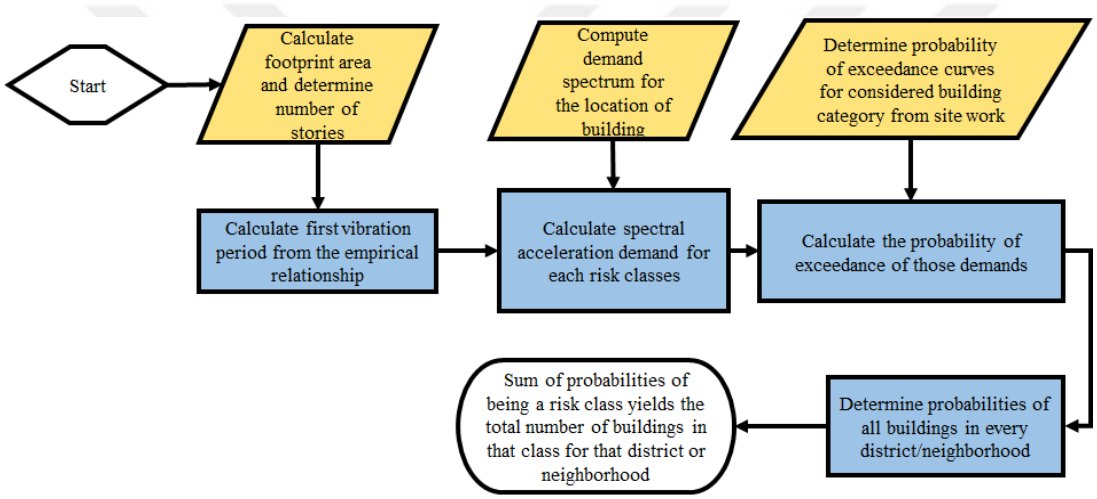

Figure 6.6 : The flowchart of risk estimation study.

6.1.2 Validation study

A validation study is performed to check the reliability of the estimation methodology. The three most densely evaluated districts, which are Silivri, Avcilar and Zeytinburnu, are selected among the others. As proposed, 5% of the evaluated buildings are assigned as a sample group to predict the risk class frequencies for actual cases. The predictions are mostly consistent with the actual risk distributions (Figure 6.7). The biggest calculated error rates are 6.3 % for D class buildings and 5.8% for C class buildings in Zeytinburnu; the computed error rates are less than 5% for the other cases.

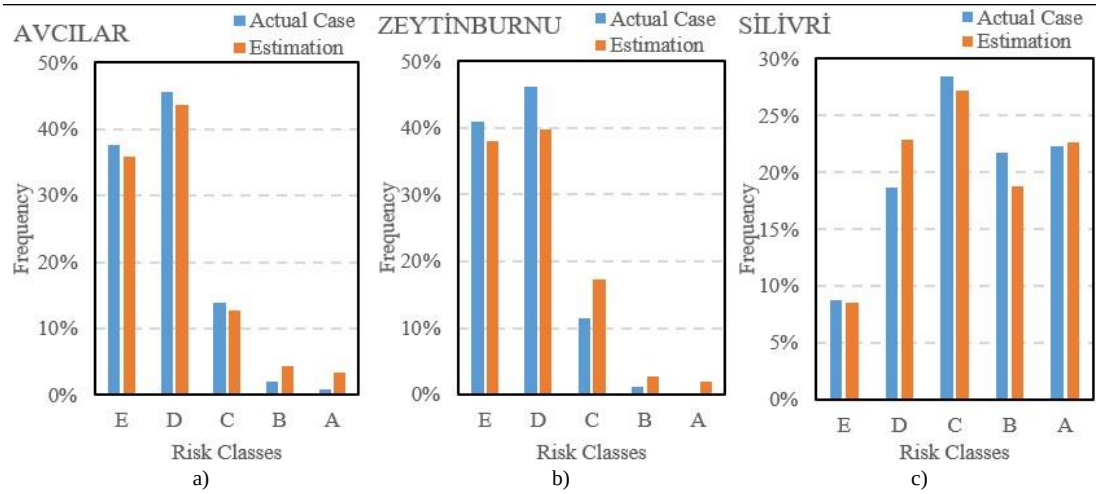

Figure 6.7 : Results of the validation study, a) Avcılar, b) Zeytinburnu, c) Silivri districts.

The comparison of the actual probability of exceedance curve obtained from 3179 buildings in Avcılar and the curves determined from 161 sample buildings is given in Figure 6.8a. The figure shows that the fit of the estimated and actual curve will get closer as the number of samples increases. It should be noted that the assessed buildings are assumed the whole building stock of a district. The average number of buildings, which are up to 10 stories and built before the year 2000, in the districts of Istanbul is over 15000, so sampling with 5% will grant better prediction ability over the building stock. To test the representativeness of the 5% sampling procedure on a district level, all investigated 4-6 story buildings are assumed to form a single typology as a complete group regardless of their locations, and bootstrap analyses are conducted 1000 times selecting 810 buildings (5% of the stock) from this group completely randomly as the sampling group (Figure 6.8b). The estimated median, 16%, and 84% percentile curves are given in Figure 6.8c. The median curve is almost in perfect agreement with the determined probability curve. Standard deviation values are low compared to median values; the maximum standard deviation value is measured around 0.19g demand with a 2.4% probability.

6.1.3 Outputs of the extrapolation study

The probabilities for each risk class are assigned to 579944 reinforced concrete buildings in 37 districts, while probabilities could not be assigned to 35756 reinforced concrete buildings due to lack of data. The probability of exceedance curves generated from the data provided by site works are given in Figure D.1. The heatmaps of all risk

classes determined through estimation methodology according to the Scenario and Design Level Earthquake cases are represented in Figure 6.9 to 6.13.

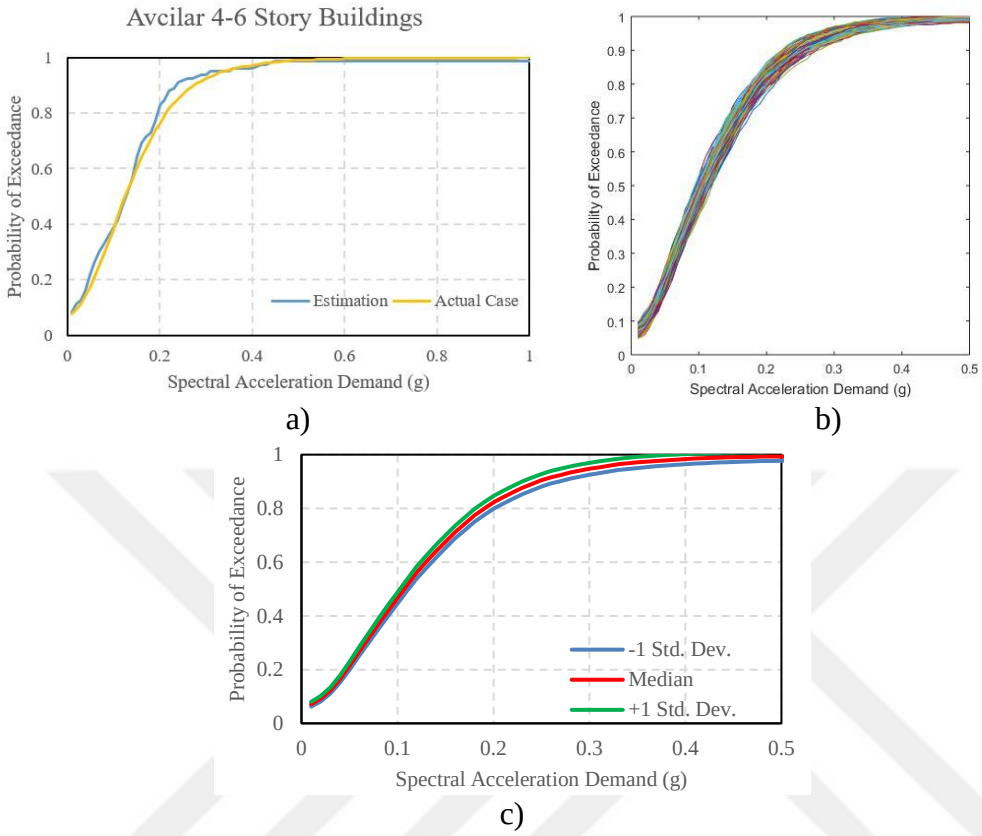

Figure 6.8 : a) Comparison of an estimated and actual probability of exceedance curve for Avcilar district, b) probability curves generated from bootstrap analyses, c) median, 16%, and 84% percentile curves.

The prediction study complies with the site works. For the Scenario Earthquake case, the density of the A-class buildings increases as the neighborhoods are getting farther from the main Marmara fault. The stiff soil characteristics of the Anatolian side of the city have a positive impact on the estimated seismic safety of the buildings; the estimated ratios of A and B class buildings for the coast of the Anatolian side are visibly more than the districts on the coast of the European side of Istanbul. The high priority areas clearly come forward as the volume of the buildings in D and E classes can be distinguished.

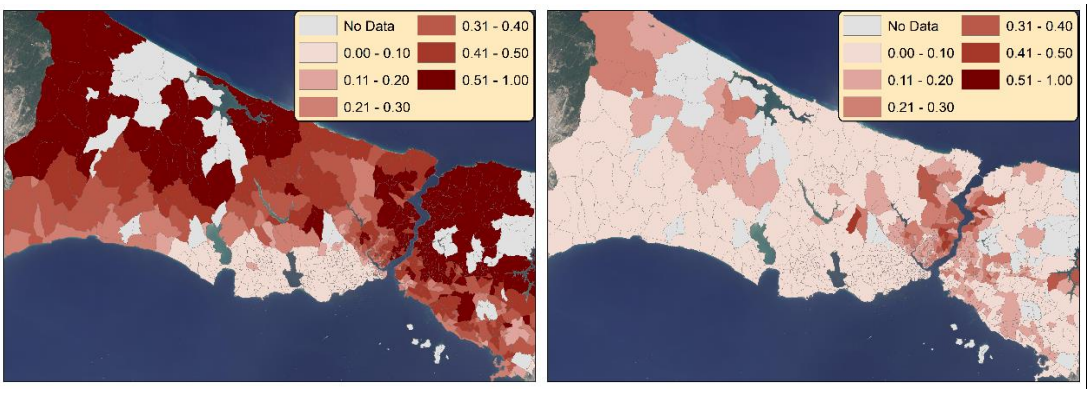

a) b)

Figure 6.9 : Distribution of the A class buildings on a neighborhood scale according to estimation study. The legend demonstrates the ratio of the corresponding risk class to the total number of assessed buildings in the neighborhood. a) Scenario Earthquake Case, b) Design Level Earthquake case.

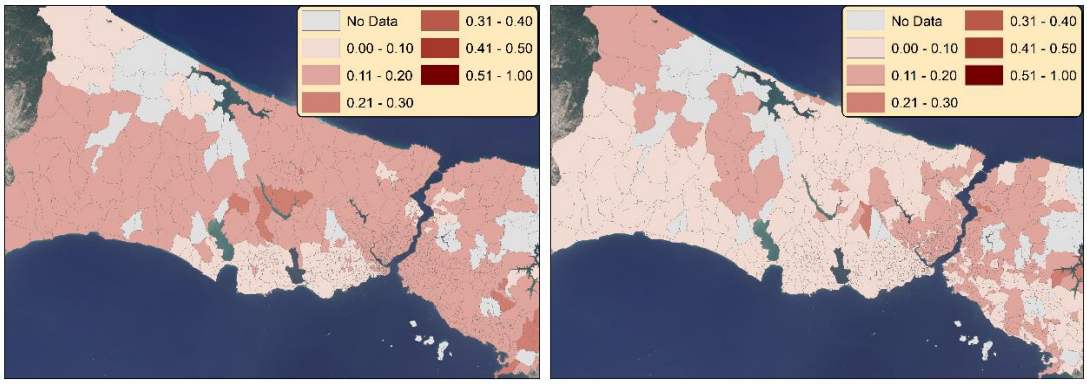

a) b)

Figure 6.10 : Distribution of the B class buildings on a neighborhood scale according to estimation study. The legend demonstrates the ratio of the corresponding risk class to the total number of assessed buildings in the neighborhood. a) Scenario Earthquake Case, b) Design Level Earthquake case.

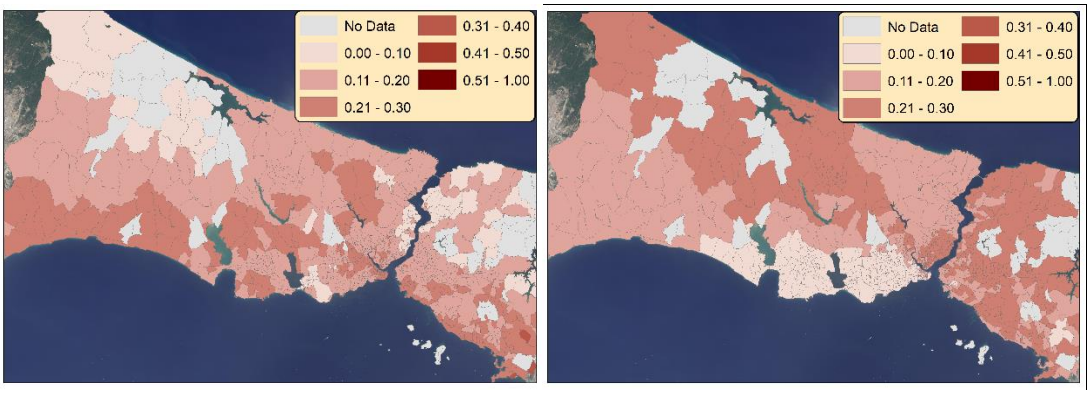

a) b)

Figure 6.11 : Distribution of the C class buildings on a neighborhood scale according to estimation study. The legend demonstrates the ratio of the corresponding risk class to the total number of assessed buildings in the neighborhood. a) Scenario Earthquake Case, b) Design Level Earthquake case.

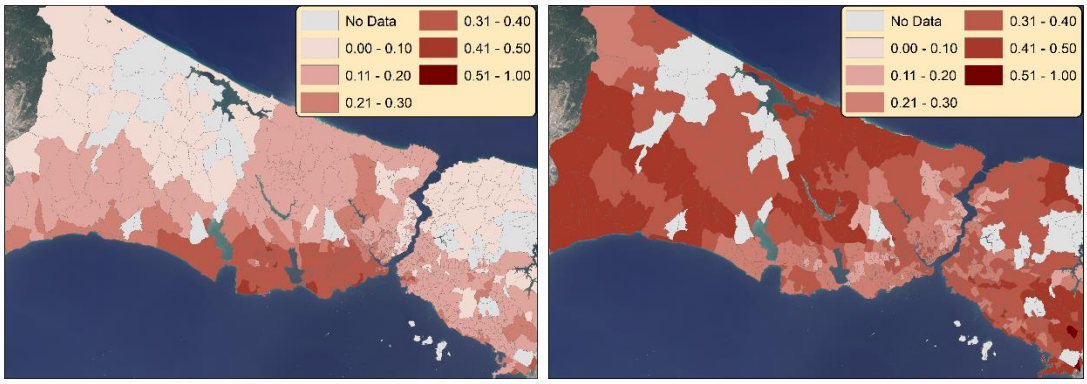

a) b)

Figure 6.12 : Distribution of the D class buildings on a neighborhood scale according to estimation study. The legend demonstrates the ratio of the corresponding risk class to the total number of assessed buildings in the neighborhood. a) Scenario Earthquake Case, b) Design Level Earthquake case.

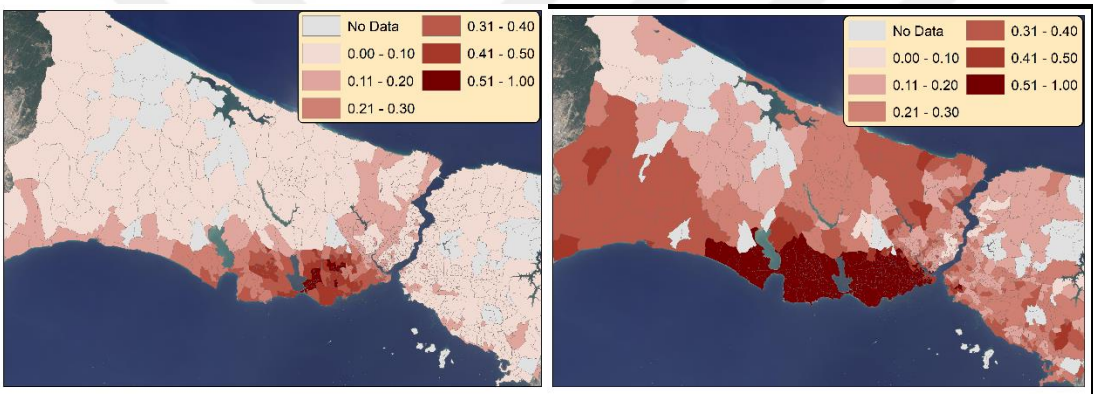

a) b)

Figure 6.13 : Distribution of the E class buildings on a neighborhood scale according to estimation study. The legend demonstrates the ratio of the corresponding risk class to the total number of assessed buildings in the neighborhood. a) Scenario Earthquake Case, b) Design Level Earthquake case.

For the Design Level Earthquake case, as processed with the results of the site-work, more than 50% of the buildings are found to be in E class for the west side of the Golden Horn. Apparently, almost all buildings of the districts located on the coast of the Marmara Sea need seismic intervention to reach certain seismic safety. The results of the prediction study on a district scale are listed in Table 6.3 and Table 6.4. Kucukcekmece, Zeytinburnu, Bagcilar, Bahcelievler, Bakirkoy and Esenyurt districts are the most vulnerable districts according to this study. 41.3% of the buildings need an intervention according to the Scenario Earthquake loading. For the Design Level Earthquake case, this ratio rises to 70.4%. Thus, the Scenario Earthquake case comes forward as the more manageable case. The Design Level Earthquake is clearly more demanding in terms of seismic load.

The total number of buildings in each risk class according to Design Level and Scenario Earthquake cases are given in Table 6.5. The Design Level Earthquake yields 2.1 and 1.4 times more buildings in E and D risk classes compared to Scenario Earthquake, respectively. Also, the number of A class buildings for the Scenario Earthquake case is 3.6 greater than Design Level Earthquake loading. It is clear that Scenario Earthquake responds to the need of determining low priority buildings and taking them out of the scope of immediate risk mitigation studies. However, according to Design Level Earthquake, 92.1% of the existing reinforced concrete buildings fail to withstand the defined PGA demand.

Table 6.3 : Ratio of estimated risk classes for each district (Design Level Earthquake case).

	Ratio of Corresponding Risk Classes to Total Number of Buildings in the District				
District	E Class	D Class	C Class	B Class	A Class
ARNAVUTKÖY	25%	40%	23%	7%	4%
ATAŞEHİR	26%	37%	19%	10%	8%
AVCILAR	64%	29%	6%	1%	0%
BAĞCILAR	70%	22%	5%	2%	1%
BAHÇELİEVLER	74%	23%	3%	0%	0%
BAKIRKÖY	69%	24%	5%	1%	1%
BAŞAKŞEHİR	28%	43%	17%	6%	6%
BAYRAMPAŞA	57%	34%	7%	2%	1%
BEŞİKTAŞ	11%	21%	23%	16%	30%
BEYKOZ	13%	28%	22%	15%	22%
BEYLİKDÜZÜ	64%	33%	3%	0%	0%
BEYOĞLU	24%	28%	20%	13%	15%
BÜYÜKÇEKMECE	65%	28%	5%	1%	1%
ÇATALCA	18%	37%	22%	11%	13%
ÇEKMEKÖY	19%	32%	24%	12%	14%
ESENLER	65%	25%	6%	2%	1%
ESENYURT	73%	22%	3%	1%	0%
EYÜPSULTAN	27%	31%	17%	10%	15%
FATİH	61%	30%	6%	1%	1%
GAZİOSMANPAŞA	24%	31%	19%	13%	14%
GÜNGÖREN	55%	37%	6%	2%	1%
KADIKÖY	32%	35%	16%	9%	8%
KAĞITHANE	25%	28%	20%	12%	15%
KARTAL	23%	33%	22%	11%	11%
KÜÇÜKÇEKMECE	76%	20%	3%	1%	0%
MALTEPE	26%	35%	22%	9%	8%
PENDİK	25%	36%	20%	10%	8%
SANCAKTEPE	26%	36%	20%	10%	8%
SARIYER	24%	26%	18%	11%	21%
SİLİVRİ	37%	40%	16%	4%	3%
SULTANBEYLİ	23%	44%	23%	7%	4%
SULTANGAZİ	28%	33%	19%	10%	10%
ŞİŞLİ	17%	28%	23%	14%	18%
TUZLA	25%	44%	18%	7%	5%
ÜMRANİYE	20%	32%	23%	11%	15%
ÜSKÜDAR	25%	31%	20%	11%	13%
ZEYTİNBURNU	74%	24%	2%	0%	0%

Table 6.4 : Ratio of estimated risk classes for each district (Scenario Earthquake case).

	Ratio of Corresponding Risk Classes to Total Number of Buildings in the District				
District	E Class	D Class	C Class	B Class	A Class
ARNAVUTKÖY	7%	14%	17%	18%	45%
ATAŞEHİR	8%	15%	20%	18%	39%
AVCILAR	33%	37%	17%	7%	6%
BAĞCILAR	44%	31%	14%	6%	5%
BAHÇELİEVLER	46%	35%	14%	4%	2%
BAKIRKÖY	42%	39%	12%	4%	4%
BAŞAKŞEHİR	9%	19%	25%	19%	29%
BAYRAMPAŞA	28%	36%	22%	8%	6%
BEŞİKTAŞ	5%	9%	13%	15%	58%
BEYKOZ	1%	7%	10%	11%	70%
BEYLİKDÜZÜ	30%	40%	22%	7%	2%
BEYOĞLU	11%	20%	18%	15%	35%
BÜYÜKÇEKMECE	26%	38%	19%	9%	8%
ÇATALCA	4%	8%	13%	14%	62%
ÇEKMEKÖY	3%	11%	11%	14%	60%
ESENLER	38%	32%	17%	7%	6%
ESENYURT	39%	36%	16%	5%	4%
EYÜPSULTAN	10%	20%	18%	15%	37%
FATİH	31%	33%	20%	10%	7%
GAZİOSMANPAŞA	11%	22%	19%	14%	33%
GÜNGÖREN	27%	32%	25%	10%	6%
KADIKÖY	9%	22%	22%	16%	31%
KAĞITHANE	15%	17%	18%	14%	36%
KARTAL	7%	16%	21%	19%	37%
KÜÇÜKÇEKMECE	50%	32%	12%	4%	3%
MALTEPE	10%	15%	18%	17%	40%
PENDİK	8%	17%	21%	19%	36%
SANCAKTEPE	5%	16%	18%	16%	44%
SARIYER	10%	11%	12%	12%	54%
SİLİVRİ	11%	20%	21%	17%	31%
SULTANBEYLİ	5%	15%	21%	21%	38%
SULTANGAZİ	14%	24%	20%	15%	27%
ŞİŞLİ	9%	15%	19%	17%	40%
TUZLA	7%	23%	27%	19%	24%
ÜMRANİYE	4%	13%	14%	15%	53%
ÜSKÜDAR	8%	14%	17%	14%	47%
ZEYTİNBURNU	41%	38%	16%	4%	2%

The estimated risk distribution herein significantly differs compared to the damage prediction of Cakti et al. (2019). This disharmony is inevitable considering the nature of the different approaches of the methodologies. In this thesis, risk distribution was predicted instead of damage distribution; there will be slightly or moderately damaged buildings among the estimated 240,000 D and E class buildings after the scenario earthquake according to Chapter 3. The other main reason is that the methodology of determining the probability of exceedance of the seismic demand is not similar to the fragility analysis used by Cakti et al. (2019). As aforementioned, the probability of exceedance curves are generated based on the theoretical capacities of all evaluated existing buildings. Considering the fact that approximately 5% of evaluated buildings

do not have any lateral load-bearing capacity, these curves do not start from 0%. The probability curves are determined using real structural data of at least 5% of the building stock in most districts. However, fragility curves are mostly prepared from representative buildings for different typologies of buildings for each damage state.

Table 6.5 : Number of buildings for each risk classes estimated in this thesis. The total number of building is 579,944, which are 1-10 story pre-2000 RC buildings from 37 districts in Istanbul.

	Risk Classes				
	E Class	D Class	C Class	B Class	A Class
Scenario Earthquake	109,623	130,030	101,506	72,526	166,259
Design Level Earthquake	230,054	178,121	84,913	41,301	45,555

6.2 Cost-Benefit Assessment of Risk Mitigation Strategies for the Building Stock in Istanbul

The seismic preparedness studies to be made before earthquakes prevent the enormous economical losses that will occur after the earthquake. In this section, the outputs of the studies carried out within the scope of this thesis and the efficiency of seismic risk mitigation strategies in terms of risk and cost reduction are determined based on the example of the building stock in Istanbul. In the final step, a comment is made on the most efficient intervention strategies.

6.2.1 Proposed Intervention Strategies

Four intervention approaches and their economic impacts are evaluated in this section.

- Reconstruction of the buildings: This is the most common risk mitigation approach in Turkey. In this case, it is assumed that the existing buildings will be rebuilt with the same total area and number of stories.
- Seismic retrofitting of buildings: rough cost estimations are made based on the information of previously retrofitted buildings. The retrofitting costs are calculated in proportion to the cost of rebuilding.
- Strategy-1: If the retrofitting cost exceeds 50% of the cost of reconstruction, the building should be demolished and rebuilt; otherwise, it should be strengthened.

- Strategy-2: If the retrofitting cost exceeds 40% of the cost of reconstruction, the building should be demolished and rebuilt; otherwise, it should be strengthened.

It should be noted that Strategy-1 and Strategy-2 will be modified in the following sections based on the outputs of this chapter.

6.2.2 Costs

In the cost analysis, two basic phases are taken into consideration: pre-earthquake and post-earthquake costs. Structural interventions before a destructive earthquake bring an economic burden to the budget. However, the effect of post-earthquake costs is usually higher than the pre-earthquake costs.

Pre-earthquake interventions are divided into two main strategies: retrofitting and reconstruction. After the earthquake, the repairs to be made in the buildings are accepted as primary costs. There are also secondary costs like fiscal costs, infrastructure, etc.

6.2.2.1 Pre-Earthquake costs

The reconstruction case is assumed as the buildings will be rebuilt with the same total area and number of stories. Retrofitting costs, which includes structural and non-structural costs both, are estimated based on the information on previously retrofitted buildings provided by Demir et al. (2022). The empirical relationship for retrofitting cost is provided in Figure 6.14.

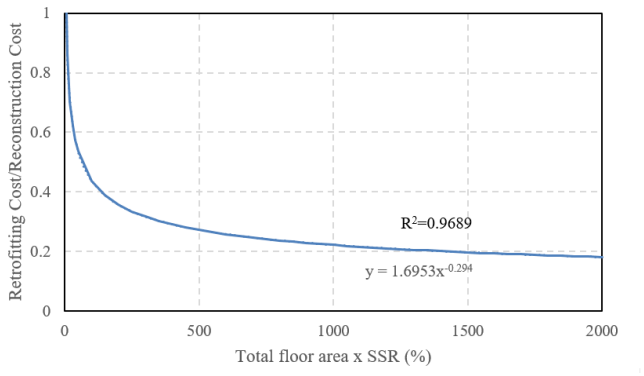

Figure 6.14 : Empirical relationship of retrofitting cost and SSR of the building (Demir et al. 2022).

The relationship is established between the cost and the product of the SSR value of the building and total floor area. Retrofitting expenses decreases as the total floor area

and SSR value increase. Note that, all costs are determined based on the ratio of retrofitting cost to the reconstruction cost per m2 for each building, so it is unitless.

6.2.2.2 Post-Earthquake costs

Similar to pre-earthquake interventions, the cost of repair and secondary losses are calculated based on the ratio to the reconstruction cost per m2 for each building. In the case of no intervention, there will be a need for repair and reconstruction efforts for damaged buildings after a destructive earthquake. To compute the repair costs, the empirical relationship defined by Di Ludovico et al. (2021) is used. The relationship is defined based on the damage state and the ratio of repair cost to reconstruction cost. Since the output of our pre-earthquake assessments is SSR value, the damage states are converted to SSR values roughly considering the validation study performed in Chapter 3. Figure 3.25a demonstrates the relationship between real seismic-induced damages and SSR values. Based on the results given in Figure 3.25a, the assumption given in Table 6.6 is made for repair costs. Inherently, repair cost increases as the SSR value decreases. An exponential best fit curve is generated for the intermediate values between SSR% 75 and 10, and a linear fit is defined between 75 and 100 (Figure 6.15).

In connection with repair costs, secondary losses (i.e. infrastructure damages, fiscal losses, value-added losses, etc.) linked with seismic damages will occur. Repair costs of moderately and lightly damaged buildings are calculated in accordance with TCIP data gathered after Kahramanmaras Earthquakes. An assumption is made to compute the secondary losses that will arise after the earthquake based on the OECD report after the 1999 Kocaeli Earthquake (Bibbee et al. 2000). Post-Kocaeli Earthquake direct and indirect costs are given in Table 6.7. Housing costs are adopted as repair and demolishing/reconstruction costs. The information provided by Bibbee et al. (2000) states that the secondary costs are 3.2 times more than the repair costs.

Table 6.6 : Post-earthquake repair cost of the buildings (Di Ludovico et al. 2021).

	Damage State	Corresponding SSR (%)	Repair Cost/Reconstruction Cost (%)
None	DS0	100	1
Light	DS1	60	2
Moderate-Heavy	DS2	40	10
	DS3	25	100
Very Heavy-Collapse	DS4	10	100
	DS5	5	100

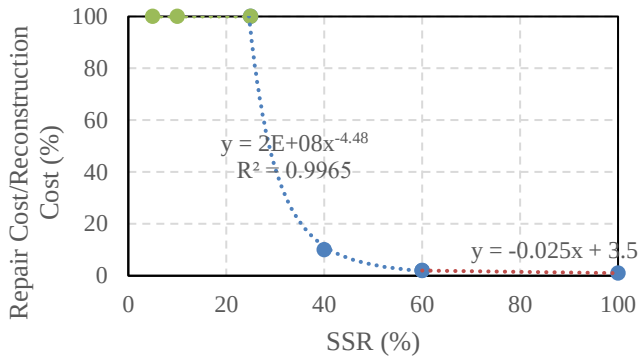

Figure 6.15 : Post-earthquake repair cost of the buildings.

Table 6.7 : Post-Earthquake direct and indirect costs (Bibbee et al. 2000).

		Billion USD	Ratio to Repair Cost
Direct cots	Housing	4	1
	Enterprises	4.5	1.125
	Infrastructure	1.5	0.375
Indirect Costs	Value-added loss	2	0.5
	Emergency relief expenditures	0.8	0.2
Secondary effects	Current account losses	2	0.5
	Fiscal Costs	2	0.5

Finally, the cost of human life is applied as 775190 USD per fatality, the information of which was given by Daniell et al. (2015). The buildings that may cause life loss is assumed in the SSR<6% range According to Aydogdu et al. (2024). The number of collapsed buildings in the investigated group overlaps with the number of buildings with an SSR of less than 6%. In Kahramanmaraş, 12622 people lost their lives after the earthquakes (Url-7). This corresponds to 3.36 life losses per collapsed building. In this thesis, approximately 2.6 million USD cost of human life per building under 6% SSR value is assumed (Aydogdu et al. 2024).

6.2.3 Pre and post-earthquake intervention cost/benefit analysis

For the buildings, of which risk estimation was made in Chapter 5, pre and post-earthquake costs, which are illustrated in Figure 6.16 separately, are also estimated in this chapter. In Figure 6.16, the ratios of the total costs for 579,944 buildings are given for each intervention strategy and the total repair and secondary costs.

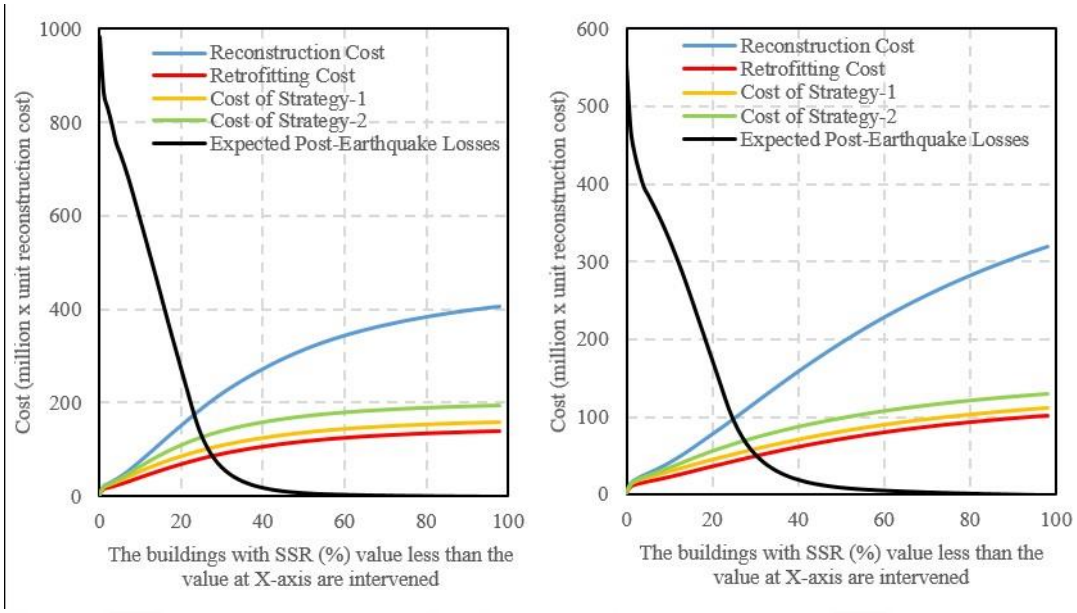

a) b)

Figure 6.16 : Pre-earthquake cost of the intervention strategies. a) Design Level Earthquake case, b) Scenario Earthquake case. The cost is given in construction cost per m^2 unit.

The x-axis of the graph indicates that each SSR value on the axis is the scenario that all buildings with SSR values less than that value will be intervened. Normally, the increasing value of SSR corresponds to the increasing number of intervened buildings. Thus, pre-earthquake intervention costs increase as the number of retrofitted or reconstructed buildings increases. In the initial state, making no intervention results highest seismic-induced economic losses, and the total cost is maximum in that case. However, the repair and secondary costs after the earthquake decreases drastically as the number of intervened buildings increases.

Figure 6.17 and Figure 6.18 illustrate the spatial distribution of the reconstruction and retrofitting costs of all the buildings with SSR less than 100% according to the Design Level Earthquake and Scenario Earthquake cases. It can be inferred from the maps that reconstruction of the buildings is far more demanding in terms of cost compared to retrofit alternative. Also, the intervention cost considering the Scenario Earthquake loading is clearly less than the cost of the Design Level Earthquake.

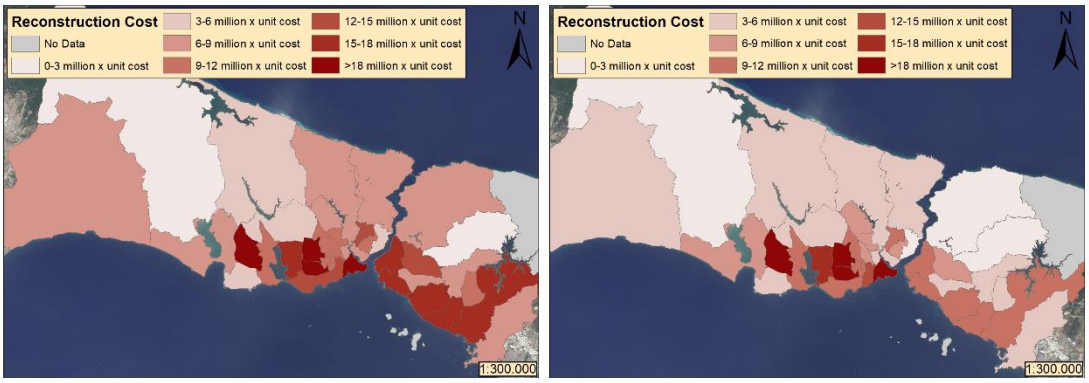

a) b)

Figure 6.17 : Reconstruction of all of the buildings with SSR<100. a) Design Level Earthquake case, b) Scenario Earthquake case. The cost is given in construction cost per m^2 unit.

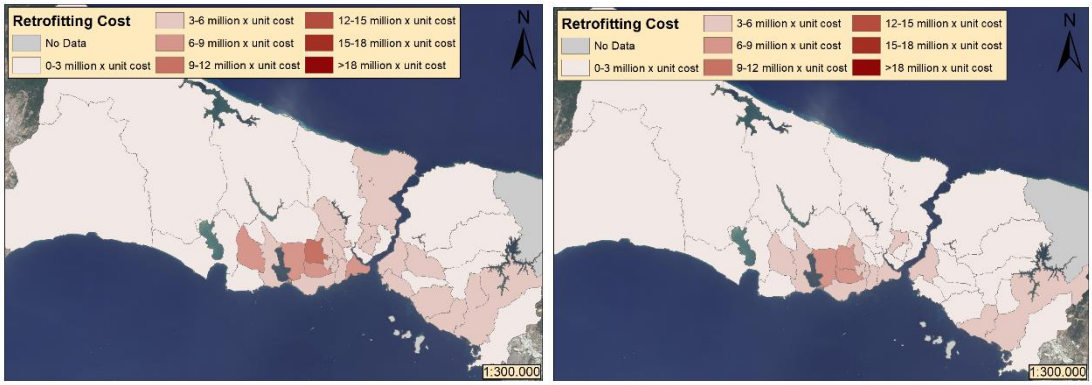

a) b)

Figure 6.18 : Retrofitting all of the buildings with SSR<100. a) Design Level Earthquake case, b) Scenario Earthquake case. The cost is given in construction cost per m^2 unit.

In the absence of any intervention, the highest post-earthquake costs are observed according to Figure 6.16. The spatial distribution of the post-earthquake repair costs and secondary losses for the current state of the building stock in Istanbul are given in Figure 6.19. It can be inferred from the maps that, making no intervention is the most costly scenario for risk mitigation efforts in Istanbul.

The total costs of each strategy are calculated by adding the post-earthquake costs and the pre-earthquake intervention costs (Figure 6.20). The decrease in total pre and post-earthquake costs provided by each intervention strategy with respect to SSR values is illustrated in Figure 6.21. Both of the graphs show that the maximal calculated cost reduction is provided when all buildings with SSR% values less than:

- 33 will be intervened for reconstruction case (72% and 70% cost reduction for the Design Level and Scenario Earthquake cases respectively),

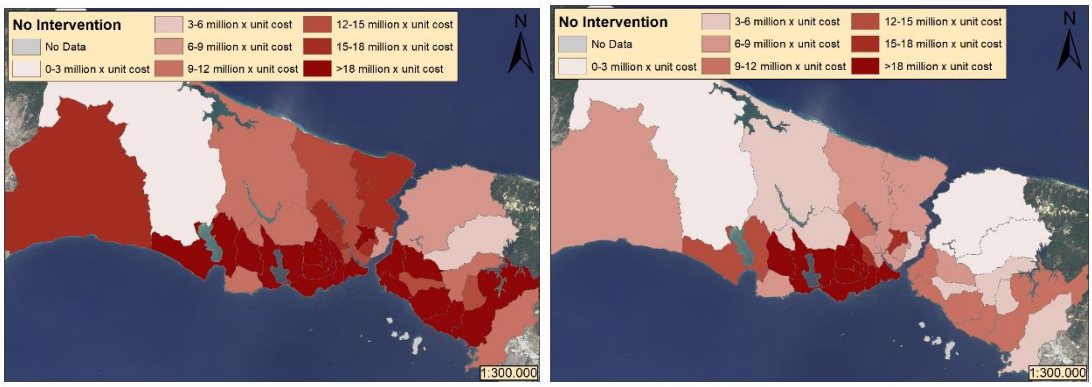

a) b)

Figure 6.19 : Total post-earthquake cost for current state of the building stock (No intervention case). a) Design Level Earthquake case, b) Scenario Earthquake case. The cost is given in construction cost per m^2 unit.

- 44 will be intervened for retrofitting case (87% and 86% cost reduction for the Design Level and Scenario Earthquake cases respectively),
- 44 will be intervened for Strategy-1 case (86% and 84% cost reduction for the Design Level and Scenario Earthquake cases respectively),
- 43 will be intervened for Strategy-2 case (82% and 81% cost reduction for the Design Level and Scenario Earthquake cases respectively).

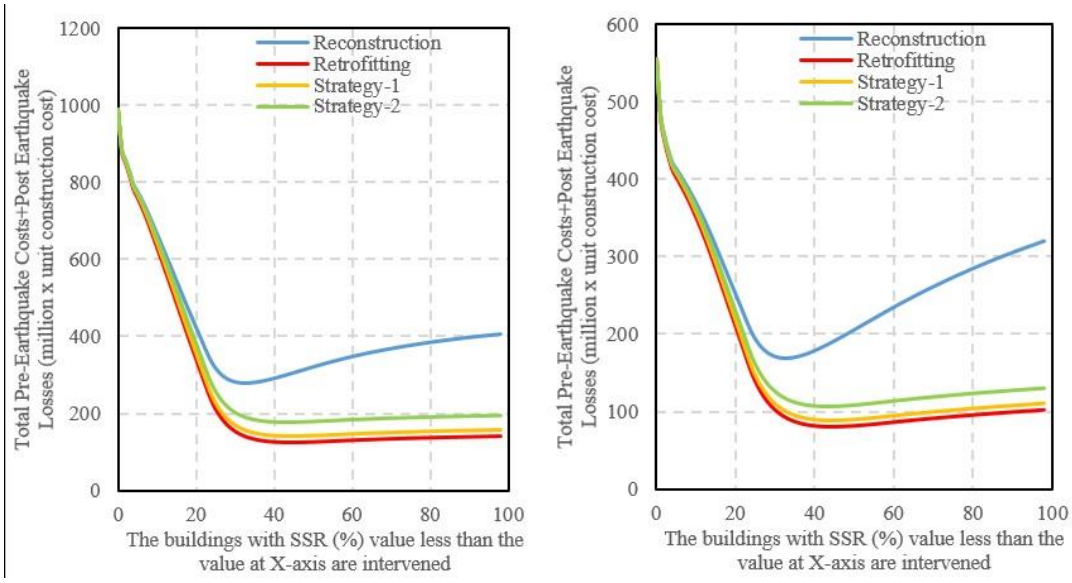

a) b)

Figure 6.20 : Total pre+post-earthquake cost of the intervention strategies. a) Design Level Earthquake case, b) Scenario Earthquake case. The cost is given in construction cost per m^2 unit.

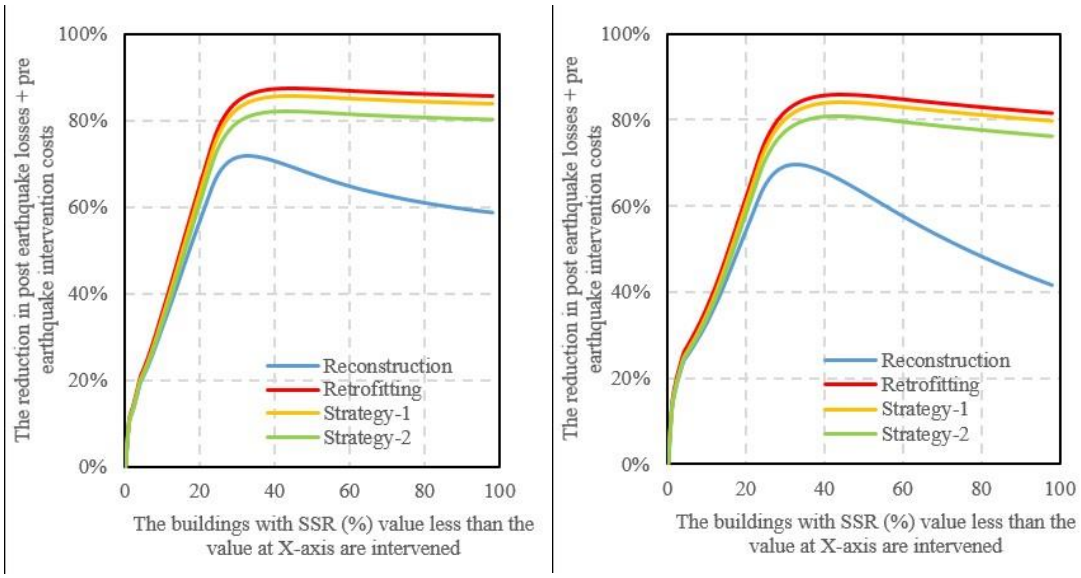

a) b)

Figure 6.21 : Decrease in total pre+post-earthquake cost of the intervention strategies with respect to SSR values. a) Design Level Earthquake case, b) Scenario Earthquake case.

Although the maximum cost reduction occurs around 44% SSR region for retrofitting case, retrofitting all buildings with SSR less than 30 provides almost the same cost reduction; in this case, the cost reduction regresses from 87% to 85% for the Design Level Earthquake loading. To reach the maximum cost reduction, more than 95,000 buildings, which is the number of buildings estimated between SSR% 30 and 44, must be intervened, which is not an efficient approach in terms of practicality.

Figure 6.22 exhibits the total cost reduction with respect to the number of intervened buildings. For the reconstruction strategy, 314,498 and 163,822 buildings must be reconstructed to reach the maximum cost reduction, which can be named as the optimum point according to the Design Level and Scenario Earthquake cases respectively. Due to its high cost, reconstructing more buildings than the optimum point increases the total costs. According to the Scenario Earthquake case, retrofitting the worst 150,000 buildings provides a 82% decrease in cost. However, retrofitting 150,000 extra buildings increases the cost reduction by around 3%, which is literally a marginal gain compared to the size of the efforts.

The total cost reductions granted by strategies in terms of pre and post-earthquake stages per intervened building according to SSR values are given in Figure 6.23. When the graphs are examined, it can be clearly seen that the maximum cost reduction provided for both cases reached SSR<10% region, which is an indicator of the

information that intervening the buildings with the worst seismic performance grants the maximum cost reduction. The decrease provided in cost gradually diminishes as the seismic performance of the buildings increases.

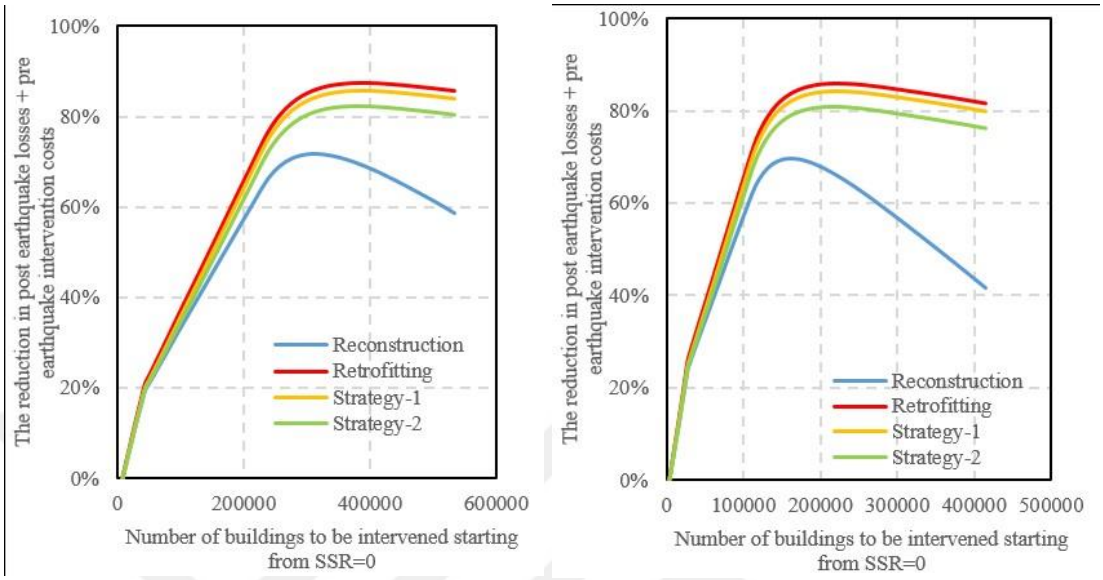

a) b)

Figure 6.22 : Decrease in total pre+post-earthquake cost of the intervention strategies compared to number of intervened buildings. a) Design Level Earthquake case, b) Scenario Earthquake case.

After getting the results of this study, intervention strategies are modified. Two different alternatives come forward:

- Strategy-1: Economically effective option is intervening the buildings with SSR value less than 40%. Still, if the retrofitting cost exceeds 50% of the cost of reconstruction, the building should be demolished and rebuilt; otherwise, it should be strengthened.
- Strategy-2: The safer option for life safety is reducing the seismic risk of the buildings under the SSR=50% limit as the designated high risk threshold is 50%. Still, if the retrofitting cost exceeds 40% of the cost of reconstruction, the building should be demolished and rebuilt; otherwise, it should be strengthened.

The spatial distribution of the total pre and post-earthquake costs of Scenario-1 and Scenario-2 are given in Figure 6.24 and Figure 6.25 respectively. The maps frankly show that hybrid scenarios with intervening optimum amount of buildings decrease

the seismic-induced losses drastically. Also, considering reconstruction as the main intervention strategy leads to small amounts of cost reduction. With its rapid application compared to rebuilding and cost-effectiveness, seismic retrofit should be the main intervention method for most buildings.

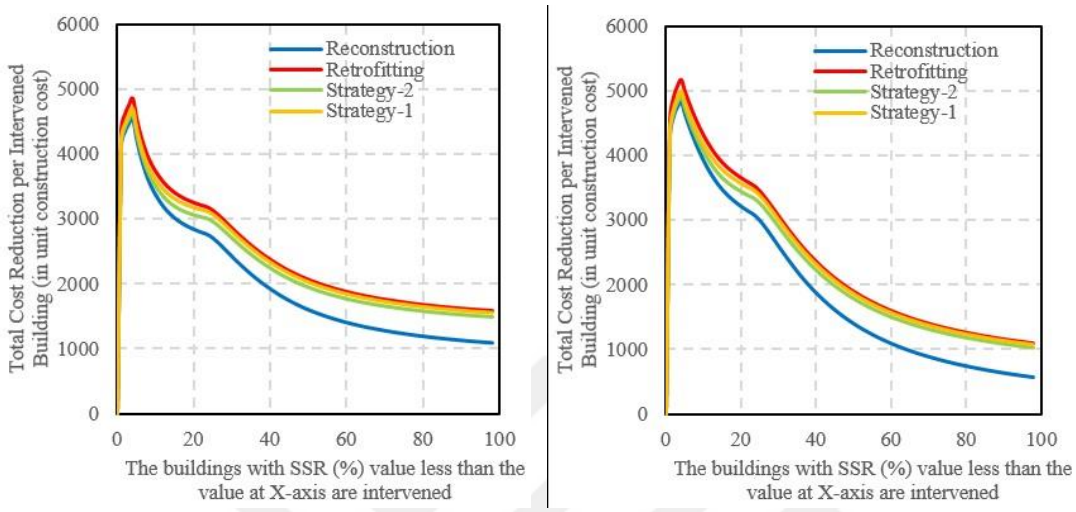

a) b)

Figure 6.23 : Total pre+post-earthquake cost reduction per intervened building compared to SSR values. a) Design Level Earthquake case, b) Scenario Earthquake case. The cost is given in construction cost per m^2 unit.

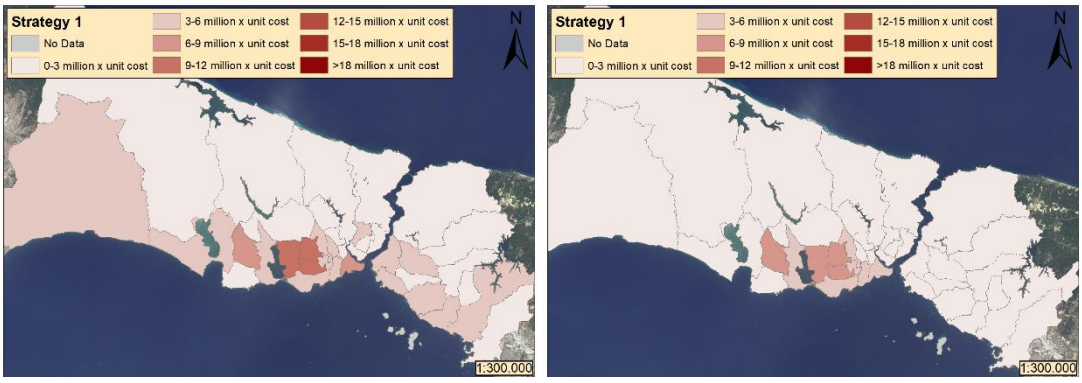

a) b)

Figure 6.24 : Total pre+post-earthquake cost for Intervention Strategy-1. a) Design Level Earthquake case, b) Scenario Earthquake case. The cost is given in construction cost per m^2 unit.

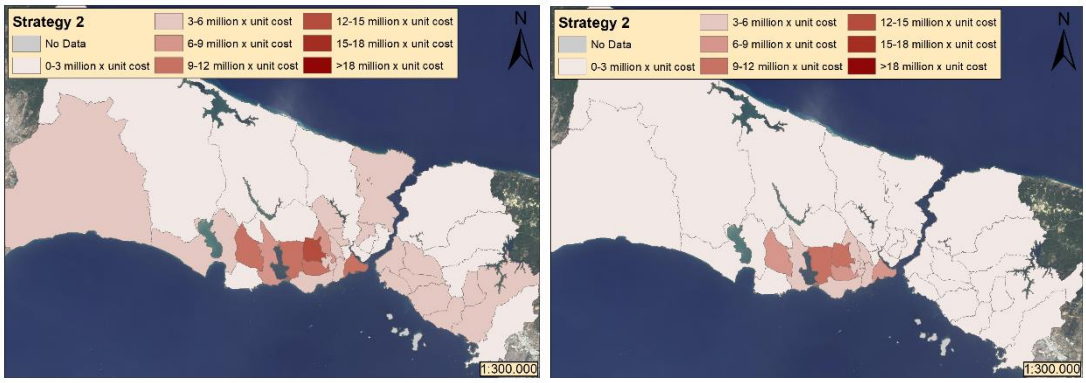

a) b)

Figure 6.25 : Total pre+post-earthquake cost for Intervention Strategy-2. a) Design Level Earthquake case, b) Scenario Earthquake case. The cost is given in construction cost per m^2 unit.

The total cost of each intervention scenario in billion USD is given in Table 6.8. While computing the real costs, 1000 USD/m^2 unit cost of construction is assumed. When the scale of the problem is considered, designing the risk mitigation efforts using the Scenario Earthquake case will be more practical in terms of cost and time. Retrofitting all buildings with SSR<100% costs less than both intervention strategies defined in this thesis. However, it is expected to retrofit or rebuild almost 200000 fewer buildings for Strategy-1 in the case of Scenario Earthquake, which is a more effective approach in terms of time, when the urgency of the risk mitigation studies is considered. The decrease in total cost provided by Strategy-1 and Strategy 2 is 84% and 81% for the Scenario Earthquake case, while these values are 85% and 82% for the Design Level Earthquake case.

Table 6.8 : Results of the cost estimation study (in billion).

		Design Level Earthquake		Scenario Level Earthquake	
		USD	TRY	USD	TRY
Pre-Earthquake Costs	Retrofitting All Buildings with SSR<100	140	4340	101	3131
	Reconstructing All Buildings with SSR<100	405	12555	318	9858
Post-Earthquake Costs	Repair Costs in Case of no Intervention	233	7223	116	3596
	Secondary Costs in Case of no Intervention	746	23126	435	13485
	Total Cost in Case of no Intervention	979	30349	551	17081
Pre+Post-Earthquake Costs	Total Cost of Strategy1	142	4402	88	2728
	Reduction in Cost Compared to no Intervention Case (Strategy1)	85%		84%	
	Total Cost of Strategy2	176	5456	106	3286
	Reduction in Cost Compared to no Intervention Case (Strategy2)	82%		81%	

Costs are in billion USD. 1000 USD/m^2 unit cost of construction is assumed.
A conversion rate of 1 USD = 31 TRY is assumed.

6.3 Conclusions

In this part of the thesis, based on the outputs of the site work conducted on nearly 23,000 buildings in Istanbul, the structural parameters of investigated buildings are extrapolated to 579,944 pre-2000 buildings in 37 districts of Istanbul. The extrapolation study highlighted the high priority regions for risk mitigation efforts. The outputs of this study demonstrated that 70% of the building stock will need an intervention to reach seismic safety according to the Design Level Earthquake case, while this ratio is estimated 41% for the Scenario Earthquake case. Also, using Scenario Earthquake yields 3.6 times more buildings in A Class group compared to the Design Level Earthquake case.

In the absence of any intervention, the highest post-earthquake costs are observed according to the findings of this thesis. The maximum reduction in the cost is not reached in the case of intervening all buildings. The optimum amount of building must be intervened to reach the maximum cost reduction varies with respect to considered intervention strategy. For the Design Level Earthquake case, retrofitting the buildings with SSR less than 40% and 50% changes the cost reduction by 1%, while the number of buildings in the SSR 40-50% region is estimated to be more than 50000. Retrofitting more than 50000 buildings grants only 0.04% reduction in total cost. According to the Scenario Earthquake case, retrofitting the worst 150000 buildings provides 82% decrease in cost. However, retrofitting 150000 extra buildings increases the cost reduction around 3%, which is literally a mariginal gain compared to the size of the efforts.

Maximum cost reduction per building is reached by intervening the most critical buildings with the worst seismic performance decreases. Performing risk reduction studies for buildings with SSR greater than 50% does not contribute to the effectiveness of the seismic risk mitigation efforts.

7. CONCLUSIONS AND RECOMMENDATIONS

The first part of this thesis was conducted as a preliminary stage of a widespread structural safety assessment campaign to be carried out in Istanbul by IMM. The predictions of the selected RVS and the second stage evaluation methods are compared with the code-based detailed seismic assessment results for 72 service buildings of IMM in the scope of this study. Thereafter, the most accurate and efficient rapid seismic safety assessment method in terms of time and cost has been applied to approximately 23,000 reinforced concrete buildings that were built before the year 2000 as the continuation of this study. Consequently, the objective of this study was to decide on a quick, yet reliable rapid safety seismic safety assessment procedure to determine the buildings with poor seismic performance in huge building stocks and rank them with respect to their seismic risks.

RVS procedures demonstrated a fair anticipation of the general vulnerability of the buildings investigated in the scope of this article. However, the individual building-based risk determination capability of these methods is found insufficient. The main reason for this is the large differences in seismic performances of existing buildings which look similar from the outside. This is due to non-standard construction practices of buildings that have been constructed before 2000s without a proper inspection. This study clearly demonstrated that it may lead to remarkable mistakes if seismic risks of such substandard individual buildings are estimated based on RVS procedures without collecting and processing further and more detailed information from the buildings. In light of these facts, the use of RVS procedures on substandard and non-code-complying building stocks like the ones in Istanbul should be limited to the assessment of risks in a regional scale.

As expected, it is observed that the second stage assessment methods generally showed a better agreement with code-based detailed seismic performance assessment results when compared to RVS methods. Based on the extensive comparisons outlined above, the PERA2019 method is determined as the most convenient procedure due to its consistency with the code-based detailed assessment procedure, and its efficiency in

terms of time and cost for application in a huge city like Istanbul, where hundreds of thousands of existing substandard buildings are to be examined. The buildings determined to be in D and E risk classes according to PERA2019 method (two highest risk classes among five in this method) cover 96% of the buildings determined to be in "collapse" state according to the code-based detailed seismic performance assessment results for the buildings that are examined in the scope of this research. Likewise, most of the buildings determined to be satisfying the performance limits of "controlled damage" or "collapse prevention" according to the code-based detailed seismic performance assessment results were in the risk classes of C, B and A, which correspond to moderate and low risk in PERA2019 method.

The examination of the costs and the time needed to conduct a structural investigation on hundreds of thousands of buildings demonstrated that conducting the second stage assessment methods to the whole building stock of Istanbul constructed before the year 2000 costs 1.7~4.0% of that of the detailed seismic performance assessment through TBEC-2018. As a final comparison, the application of PERA2019 procedure to 615,700 existing reinforced concrete buildings in Istanbul that were built before the year 2000 by an estimated workforce of 100 technical teams composed of an engineer and a technician will take approximately 4-5 years, whereas the detailed assessment of seismic performances of these buildings according to the TBEC-2018 would take 150 years with same source of workforce. Consequently, it is clear that only a widespread application of the second stage assessment procedures may realistically address the need for classifying all buildings in terms of seismic risk in big cities like Istanbul due to limited financial resources available to be allocated for this purpose and time constraints.

Two-stage validation study to determine the reliability of PERA2019 and proposed risk classification approach was conducted in the second part of this thesis

A validation study to determine the reliability of PERA2019 and proposed risk classification approach was conducted in Chapter 2 of this thesis. Within the scope of this study, SSR values of 49 buildings that experienced real seismic actions (2002 Afyon, 2003 Bingöl, 2020 Aegean Sea, and 2023 Kahramanmaras earthquakes) were evaluated through PERA2019 rapid seismic performance assessment methodology in a blind manner and then the estimated SSRs of the buildings were compared to the observed seismic-induced damages to determine the reliability and safety margin of

the proposed risk classification approach. It should be noted that the spectral accelerations calculated for the three strong ground motions presented in this thesis are quite close to the spectral design accelerations for Afyon, Bingöl, Izmir, and Kahramanmaras for a wide range of frequencies.

The results of this study demonstrated that the SSR values increase as the damages of the building decrease. The proposed risk classification approach succeeded to label all of the collapsed buildings in E Class (very high seismic risk). Moreover, all of the buildings subjected to heavy damage were classified as E or D Class, which correspond to very high and high seismic risk respectively. Risk classes of 97% of the moderately, heavily damaged or collapsed buildings that cannot be inhabited after the earthquake were determined as high or very high risk. Also, all of the severely damaged or collapsed buildings had an SSR value of less than 40%, which is a good safety indicator because a buffer zone of SSR values between 40 and 50% does not include any heavily damaged or collapsed buildings, while this range of SSR is still in D Class. This output demonstrates that the present risk classification method contains a good safety margin. As important as specifying the buildings with poor seismic performance, identifying the buildings with good seismic performance from the seismically deficient ones is another crucial task for risk mitigation efforts. Therefore, to evaluate the reliability of a seismic risk classification method, categorizing the buildings with adequate seismic performance in low risk class has grave importance, as well as determining the buildings with poor seismic performance as high risk. A method cannot be stated as successful as long as the method classifies the buildings with good seismic performance as high risk buildings. Based on the findings of this study, PERA2019 is able to classify almost 75% of the buildings without seismic damage or light damage as C, B or A class, while none of them is classified as very high risk (E class). The trends between the observed damage levels and structural parameters showed that individual structural parameters (for example number of stories, compressive strength of concrete and average axial stress on vertical elements) do not have sufficient conformity with the damage states of the buildings, even though structural parameters affect global seismic performance. Further site investigations are to be conducted after future earthquakes as well as additional numerical analyses to support current findings with further evidence in terms of the reliability of the presented approach.

- Second validation study was conducted to evaluate the reliability of the proposed risk classification approach and iterative procedure of PERA2019 by comparing the results of a more complex method, for which IDA was chosen as the reference evaluation. Within the scope of this study, the SSR values of – in total – 22 buildings are determined through the implementation of the PERA2019 and IDA procedures. Also, 10 buildings, which are designed according to TSDC-1975, are modeled as existing state and compliant with their original design projects to evaluate the seismic safety provided by TSDC-1975.

- As stated by TBEC-2018, it should not be expected that performance evaluations to be made through linear and non-linear methods will give exactly the same results based on theoretical differences between the approaches. Thus, the deviations in the results are an expected phenomenon. Still, the results of the iterative procedure of PERA2019 and the regression line oenaf the SSR scatter are found to be in a good agreement with the reference line; the R2 value of the regression line is approximately 90%, which is a good indicator of the reliability of the procedure. The risk classifications made through PERA2019 are also in harmony with the reference results. The classifications provided by PERA2019 remain on the unsafe side for merely one building, finding the risk of that building one class safer. By PERA2019 methodology, 73% of the buildings are determined in the same risk class as the reference procedure. Based on the outputs of this study, as a rapid performance-based assessment method, PERA2019 performed quite satisfactorily compared to a reference code-based detailed assessment procedure.

- When each direction is considered separately, the results of PERA2019 for %70 of the cases are on the conservative side. Calculating the global SSR value of the building based on the minimum value of both directions decreases the probability of being on the unsafe side. The results of this study demonstrated that PERA2019 determines the global SSR value of 73% of the buildings lower than the SSR value computed by IDA.

- The findings of this study show that if the buildings were designed according to TSDC-1975 and built compliant with their original design projects, they would have more than 2 times the seismic safety compared to their current state. The seismic demand of TSDC-1975 is half of described by TBEC-2018 for the high seismicity regions of Istanbul.

In 2019, a new project has been initiated by IMM for a rapid and accurate evaluation of sub-standard buildings after the validation studies. The early results of this recent study obtained through application of PERA2019 methodology on nearly 23,000 buildings by considering two different earthquake cases (Design Level and Mw=7.5 Scenario Earthquakes), are summarized in this thesis. Based on the findings of this thesis, the following conclusions are reached:

- The findings of the site work demonstrate that the mean compressive strength of the concrete is around 10 MPa (with a standard deviation of 3.2 MPa) for the examined building stock of Istanbul. This, together with small dimensions of the vertical structural members, lead to high axial forces on columns, which may cause a potential brittle seismic behavior against future earthquakes. Further, 60% of the examined buildings do not satisfy the minimum longitudinal reinforcement ratio requirements, and only a marginal portion of the examined buildings have proper column confinement reinforcement.

- Based on the analysis procedure used in this thesis and the structural properties of investigated buildings, more than 97% of the investigated buildings are not able to satisfy the requirements of current seismic regulations in Turkey. Thus, the buildings that are constructed before the year 2000 in Istanbul have significant structural deficiencies, and the seismic risk of these buildings is very high in common.

- The heatmaps of buildings in all risk classes represent that the seismic risk is clearly higher in the neighborhoods that are located at west of the Golden Horn and south of the TEM highway.

- Using deterministic scenario earthquake provides more refined results with respect to design level earthquake. Design level earthquake yields 46% more buildings in Risk Classes D and E with respect to scenario earthquake. This difference increases as the location gets further from the main fault or the soil gets firmer. Thus, using a deterministic scenario earthquake rather than a design level earthquake may be a practical approach for risk mitigation efforts. Similarly, targeting “collapse prevention” performance rather than “life safety” may allow focusing the buildings with the worst seismic performances.

- The SSR distributions obtained through consideration of the design level or scenario earthquakes are closer to each other for near-fault districts. The seismic

demand of scenario earthquake decreases remarkably with respect to design level earthquake as the site gets further from the fault.

- The density of the buildings in Risk Class A increases as the neighborhoods are getting further from the main Marmara fault. The better local soil parameters of the Asian part of the city have a positive impact on SSR values; the ratios of buildings in Risk Classes A and B on the coast of the Asian part are visibly more than the districts on the coast of the European part of Istanbul.

- The need and benefit of a triage system based on a rapid, robust, reliable and cost-effective methodology towards prioritization of hundreds of thousands of risky buildings is demonstrated within the framework of this study. Such individual building-based rapid and realistic seismic risk assessment and prioritization methods are needed to be included in the official legislations preferably by making use of deterministic scenario earthquakes rather than the design earthquake which considers a considerable level of safety margin.

- The seismic risk mitigation efforts and financial sources should be conveyed to the transformation or seismic retrofitting of buildings with high seismic risk, particularly to the buildings in seismic risk classes D and E as soon as possible to avoid/reduce potential casualties and huge economic losses. The probability of collapses and casualties is remarkably less for the examined buildings in seismic risk classes B and C although these building do not fully comply with the seismic design codes either. Furthermore, the repair costs of these building are expected to be much less with respect to buildings in seismic risk classes D and E, if they are subjected to a future earthquake. Therefore, the investment on seismic retrofit and/or reconstruction of the buildings in risk classes B and C could be postponed to a stage after risk reduction activities are planned for the buildings in risk classes D and E.

It should be noted that the inferences that are made here are based on the results of investigations and analyses of 22,868 buildings, which are mostly selected from high seismicity regions of the city, and the overall distributions of seismic risk may change as more buildings are assessed. Thus, generalization of the results of this study on the whole building stock of Istanbul will probably be a pessimistic/conservative approach compared to the actual case.

After the recent 2023 Kahramanmaras and Hatay Earthquakes in Turkey, the framework proposed herein is planned to be extended to thousands of additional buildings. Moreover, a risk mitigation campaign has been recently launched by IMM. In the scope of this campaign, more than 300 buildings prioritized based on the findings of this study, with the risk of sudden axial collapse are being demolished and reconstructed (Url-8). Additionally, seismic retrofit and urban renewal campaigns have also been recently launched for buildings that have been prioritized herein (Url-9).

It should be noted that performed rapid performance based assessment procedure, PERA2019, is a second-stage assessment and contains its own approximations. Studies done within the scope of this thesis are made based on some assumptions and include inherent uncertainties. Thus, obtaining more accurate SSR values of the buildings and providing absolute seismic safety for a building is only possible by evaluating and retrofitting it based on the approaches introduced by current seismic design codes, which still include uncertainties as well.

In the last part of this thesis, an estimation study was performed to predict the risk class distribution for all buildings of the city on the district and neighborhood scale. The probabilities for each risk class are assigned to 579,944 reinforced concrete buildings in 37 districts. Consequently, cost/benefit analysis was performed to evaluate the efficiencies of intervention strategies based on the estimated seismic safety of the building stock. This study highlights the high priority regions for performing widespread performance-based analysis work and foresight for further steps of the mitigation efforts, such as the approximate number of buildings to be intervened. Findings demonstrated that:

- For Design Level Earthquake case, as processed with the results of the site-work, more than 50% of the buildings are found to be in E class for the west side of the Golden Horn. Apparently, almost all buildings of the districts located on the coast of the Marmara Sea need seismic intervention to reach certain seismic safety.
- 41.3% of the buildings need an intervention according to the Scenario Earthquake loading. For the Design Level Earthquake case, this ratio rises to 70.4%. Thus, the scenario earthquake case comes forward as the more

manageable case. The design level earthquake is clearly more demanding in terms of seismic load.

- Design Level Earthquake yields 2.1 and 1.4 times more buildings in E and D risk classes compared to Scenario Earthquake, respectively. Also, the number of A class buildings for Scenario Earthquake case is 3.6 greater than Design Level Earthquake loading. It is clear that Scenario Earthquake responds to the need of determining low priority buildings and taking them out of the scope of immediate risk mitigation studies. However, according to Design Level Earthquake, 92.1% of the existing reinforced concrete buildings fail to withstand the defined PGA demand.

In the absence of any intervention, the highest post-earthquake costs are observed according to the findings of this thesis. The maximum reduction in the cost is not reached in the case of intervening all buildings. The optimum amount of building must be intervened to reach the maximum cost reduction varies with respect to considered intervention strategy. For the Design Level Earthquake case, retrofitting the buildings with SSR less than 40% and 50% changes the cost reduction by 1%, while the number of buildings in the SSR 40-50% region is estimated to be more than 50000. Retrofitting more than 50000 buildings grants only 0.04% reduction in total cost.

According to the Scenario Earthquake case, retrofitting the worst 150000 buildings provides 82% decrease in cost. However, retrofitting 150000 extra buildings increases the cost reduction around 3%, which is literally a marginal gain compared to the size of the efforts.

When the scale of the problem considered, planning the risk mitigation efforts using the Scenario Earthquake case will be more practical in terms of cost and time. Retrofitting all buildings with SSR<100% costs less than both intervention strategies defined in this thesis. However, it is expected to retrofit or rebuild almost 200000 less buildings for Strategy-1 in the case of Scenario Earthquake, which is a more effective approach in terms of time, when the urgency of the risk mitigation studies is considered.

Maximum cost reduction per building is reached by intervening the most critical buildings with the worst seismic performance decreases. Performing risk reduction

studies for buildings with SSR greater than 50% does not contribute to the effectiveness of the seismic risk mitigation efforts.

The vertical component of the earthquake, the detrimental effect of which was observed during the 2023 Kahramanmaras Earthquake widely, was not considered in the scope of this thesis. For buildings with long-span frames or high average axial stress on the vertical elements, this may increase the current risk of the building. High axial stress is considered by PERA2019 methodology and increasing axial stress generally decreases SSR value. To avoid unsafe classifications for buildings with long-span frames, the suggested intervention threshold may be changed for that kind of buildings; C-class buildings may also be retrofitted. Taking vertical seismic loading into consideration is explained in TBEC-2018 thoroughly. During the retrofitting and reconstruction phase, the vertical component of the earthquake must be considered accordingly with TBEC-2018.

It should be noted that performed rapid performance based assessment procedure, PERA2019, is a second-stage assessment and contains its own approximations. Studies done within the scope of this thesis are made based on some assumptions and include inherent uncertainties. Thus, obtaining exact SSR values of the buildings and providing absolute seismic safety for a building is only possible by evaluating and retrofitting it based on the approaches introduced by current seismic design codes.

REFERENCES

Achs, G., and Adam, C. (2012). A rapid-visual-screening methodology for the seismic vulnerability assessment of historic brick-masonry buildings in Vienna, *15th World Conference on Earthquake Engineering*, 2012 Lisbon, Portugal.

AFAD (2020). Disaster and Emergency Management Presidency, TADAS Ground Motion Database. Ankara, Turkey.

AIJ (1983). Manual of non-destructive test methods for the evaluation of concrete strength. Architectural Institute of Japan (in Japanese).

Akkar, S., Ilki, A., Goksu, C., and Erdik, M. (2021) Advances in Assessment and Modeling of Earthquake Loss. 10.1007/978-3-030-68813-4.

Alyamaç, K. E. and Erdoğan, E. S. (2005), Geçmişten Günümüze Afet Yönetmelikleri ve Uygulamada Karşılaşılan Tasarım Hataları. 23-25 March 2005 *Deprem Sempozyumu Kocaeli 2005*, s: 707-715

American Society of Civil Engineers (2017) Seismic Rehabilitation of Existing Buildings, ASCE 41-17, United States.

Ansal, A., Akinci, A., Cultrera, G., Erdik, M., Pessina, V., Tönük, G. and Ameri, Gabriele. (2009). Loss estimation in Istanbul based on deterministic earthquake scenarios of the Marmara Sea region (Turkey). *Soil Dynamics and Earthquake Engineering*. 29. 699-709. 10.1016/j.soildyn.2008.07.006.

Assessment and Improvement of the Structural Performance of Buildings in Earthquakes (2006). New Zealand Society for Earthquake Engineering Study Group on Earthquake Risk Buildings, New Zealand.

ATC-40 (1996). *Seismic Evaluation and Retrofit of Concrete Buildings*, 555. Twin Dolphin Drive, Redwood City, California, United States.

Aydinoglu, M.N. (2007). From seismic coefficient to performance based design: 40 years of earthquake engineering from an engineer's viewpoint, *Sixth National Conference on Earthquake Engineering*, October 16-20, ,15–41, Istanbul, Turkey (in Turkish).

Aydogdu, H. H., Demir, C., Kahraman, T., and Ilki, A. (2023a) Evaluation of Rapid Seismic Safety Assessment Methods on a Substandard Reinforced Concrete Building Stock in Istanbul. *Structures*. Volume 56, October 2023, 104962, https://doi.org/10.1016/j.istruc.2023.104962.

Aydogdu, H. H., Demir, C., Comert, M., Kahraman, T. and Ilki, A. (2023b). Structural characteristics of the earthquake-prone building stock in Istanbul and prioritization of existing buildings in terms of seismic risk-A pilot study conducted in Istanbul, Journal of Earthquake Engineering. *Journal of Earthquake Engineering.* Doi: 10.1080/13632469.2023.2247481.

Aydogdu, H. H., and A. Ilki. (2023a). Case study for a performance based rapid seismic assessment methodology (PERA2019) based on actual earthquake damages, Bulletin of Earthquake Engineering, submitted on 17 January 2023, accepted on 05/12/2023, Preprint (Version 1) available at Research Square. https://doi.org/10.21203/rs.3.rs-2467979/v1

Aydogdu, H.H., and A. Ilki. (2023b). Developments in seismic safety of rc building stock of Istanbul according to the years and seismic design codes, *fib Symposium 2023*, 5-7 June, 2023, Istanbul, Turkey. http://dx.doi.org/10.1007/978-3-031-32511-3_90

Bal, I.E., Tezcan, S.S. and Gulay, G. (2007). P25 scoring method for defining rapidly the collapse vulnerability of rc structures. *Sixth National Conference on Earthquake Engineering*, October 16-20, 661-674, Istanbul, Turkey.

Bal, I.E., Crowley, H., Pinho, R. and Gulay, F. (2008). Detailed assessment of structural characteristics of Turkish RC building stock for loss assessment model, *Soil Dynamics and Earthquake Engineering*, 28. 914-932. 10.1016/j.soildyn.2007.10.005.

Bal, I. E. and Smyrou, E. (2016) Simulation of the earthquake-induced collapse of a school building in Turkey in 2011 Van Earthquake. *Bulletin of Earthquake Engineering*. 14. 10.1007/s10518-016-0001-x.

Beyen, K. (2018) Hanging wall and footwall effects in the largest reverse-slip earthquake of Turkey, October 23, 2011, MW 7.2 Van Earthquake. *Arabian Journal for Science and Engineering*. 44. https://doi.org/10.1007/s13369-018-3547-x.

Bhalkikar, A. and Ramancharla, P. R. (2021). A comparative study of different rapid visual survey methods used for seismic assessment of existing buildings. *Structures*, 2021, 29: 1847-1860. http://dx.doi.org/10.1016/j.istruc.2020.12.026 **.**

Bibbee, A., Gönenç, R., Jacobs, S., Konvitz, J. and Price, R. (2000). Economic Effects of the 1999 Turkish Earthquakes: An Interim Report. OECD, Economics Department, OECD Economics Department Working Papers.

Binici, B., Yakut, A., Ozcebe, G. and Erenler, A. (2013). Provisions for the seismic risk evaluation of existing rc buildings in Turkey under Urban Renewal Law, *Earthquake Spectra*, 31. 141208072728004. 10.1193/040513EQS093M.

Bommer, J. J. and Martínez-Pereira, A. (1999). The effective duration of earthquake strong motion. *Journal of Earthquake Engineering*, 3:2, 127-172, DOI: 10.1080/13632469909350343.

Brando, G., Cianchino, G., Rapone, D., Spacone, E. and Biondi, S. (2021). A CARTIS-based method for the rapid seismic vulnerability assessment of minor Italian historical centres, *International Journal of Disaster Risk Reduction*, 63 (2021), 102478. https://doi.org/10.1016/j.ijdrr.2021.102478 .

Bruneau, M. (2001). Building damage from the Marmara, Turkey earthquake of August 17, 1999, *Journal of Seismology*, 6, 357–377.

Calvi G., Pinho R, Magenes G., Bommer J., Restrepo-Vélez L. and Crowley H., (2006). Development of seismic vulnerability assessment methodologies over the past 30 years. *ISET Journal of Earthquake Technology*. 43.

Cakti, E., Safak, E., Hancilar, U. and Sesetyan, K. (2019). Updating probable earthquake loss estimates for Istanbul province, Technical Report prepared for Istanbul Metropolitan Municipality.

Celep, Z., Erken, A., Taskin, B. and Ilki, A. (2011). Failures of masonry and concrete buildings during the March 8, 2010 Kovancılar and Palu (Elazığ) Earthquakes in Turkey. *Engineering Failure Analysis*. 18. 868-889. 10.1016/j.engfailanal.2010.11.001.

CEN (2004). *Eurocode 8: Design of structures for earthquake resistance*. Part 1: General rules, seismic actions and rules for buildings. EN-1998-1. European Committee for Standardization, Brussell, Belgium.

Cimellaro, G. P., Giovine, T. and Lopez-Garcia, D. (2014). Bidirectional pushover analysis of irregular structures. *Journal of Structural Engineering*, 140(9), 04014059. doi:10.1061/(asce)st.1943-541x.00.

Comert, M., Demir C, Aydogdu H.H. and Ilki A. (2022). Deprem kayıplarının azaltılmasına yönelik yapısal müdahalelerin fayda-maliyet açısından değerlendirilmesine yönelik bir ön çalışma. *TMMOB Afet Sempozyumu*, April 2022 in Ankara, Türkiye (in Turkish).

Cosenza, E., Del Vecchio, C., Di Ludovico, M., Dolce, M., Moroni, C., Prota, A. and Renzi, E. (2018). The Italian guidelines for seismic risk classification of constructions: technical principles and validation. *Bulletin of Earthquake Engineering* 16, 5905–5935 (2018). https://doi.org/10.1007/s10518-018-0431-8

Del Gaudio C., Di Ludovico M., Polese M., Manfredi G., Prota A., Ricci P. and Verderame G.M. (2021). Seismic fragility for Italian RC buildings based on damage data of the last 50 years. *Bulletin of Earthquake Engineering*, 18, pages 2023–2059 (2020) doi:10.1007/s10518-019-00762-6

Del Gaudio, C., De Risi, M., T. and Verderame, G. (2021). seismic loss prediction for infilled rc buildings via simplified analytical method. *Journal of Earthquake Engineering*. 10.1080/13632469.2021.1875940.

Demir, C., Comert, M., Aydogdu, H. H., and, Ilki, A. (2022). Seismic risk assessment and preliminary intervention cost-benefit analysis for the building stock of Istanbul. *3ECEES The Third European Conference on Earthquake Engineering and Seismology*, September 2022 in Bucharest, Romania.

Di Ludovico, M., Prota, A., Moroni, C., Manfredi, G. and Dolce, M. (2017). Reconstruction process of damaged residential buildings outside historical centres after the L'Aquila earthquake: part II—"heavy damage" reconstruction. *Bulletin of Earthquake Engineering*, 15(2), 693-729.

Di Ludovico, M., De Martino, G., Prota, A., Manfredi, G., Dolce, M. (2021). Damage assessment in Italy, and experiences after recent earthquakes on reparability and repair costs, Advances in Assessment and Modeling of Earthquake Loss, Springer, Cham.

Dogan, T.P., Kizilkula, T., Mohammadi, M. and Erkan, I.H. (2021). A comparative study on the rapid seismic evaluation methods of reinforced concrete buildings, *International Journal of Disaster Risk Reduction*, 56(6):102143. https://doi.org/10.1016/j.ijdrr.2021.102143

Dolce, M., Prota, A., Barbara, B., Porto, F., Lagomarsino, S., Magenes, G., Maroni, C., Penna, A., Polese, M., Speranza, A., Verderame, G.M. and Zuccaro, G. (2020). Seismic risk assessment of residential buildings in Italy, *Bulletin of Earthquake Engineering*, 19, 2999–3032 (2021). https://doi.org/10.1016/j.ijdrr.2021.102478

Dolce, M. (2012). The Italian National Seismic Prevention Program, *15th World Conference on Earthquake Engineering*, 2012 Lisbon, Portugal.

Erberik, M. A. (2008). Fragility-based assessment of typical mid-rise and low-rise RC buildings in Turkey. *Engineering Structures*. 30. 1360-1374. 10.1016/j.engstruct.2007.07.016.

Erdik, M. (2001). Report on 1999 Kocaeli and Düzce (Turkey) earthquakes, Structural Control for Civil and Infrastructure Engineering, 149-186, 2001.

Erdik, M., Aydinoglu, M.N., Fahjan, Y., Sesetyan, K., Demircioglu, M., Siyahi, B., Cakti, E., Ozbey, C., Biro, Y., Akman, H. and Yuzugullu, O. (2003). Earthquake risk assessment for the Istanbul metropolitan area final report. Earthquake Engineering and Engineering Vibration, 2. 1-23. 10.1007/BF02857534.

FEMA (2015). *Rapid Visual Screening of Buildings for Potential Seismic Hazards: A Handbook*, Third Edition, FEMA 154, prepared by the Applied Technology Council for the Federal Emergency Management Agency, Washington, D.C.

General Directorate of Mineral Exploration and Research (2003). 1 May 2003 Bingöl Earthquake Evaluation Report. Department of Geology Studies, Ankara, Turkey.

Gentile, R., Del Vecchio, C., Pampanin, S., Raffaele, D. and Uva, G. (2019). Refinement and validation of the simple lateral mechanism analysis (SLaMA) procedure for rc frames. *Journal of Earthquake Engineering*. 25. 10.1080/13632469.2018.1560377.

Goksu, C. and Ilki, A. (2016). Seismic behavior of reinforced concrete columns with corroded deformed reinforcing bars, *ACI Structural Journal*, 113. 1053-1064. 10.14359/51689030.

Goksu, C., Yilmaz, H., Chowdhury, S. R., Orakcal, K. and Ilki, A. (2014). The effect of lap splice length on the cyclic lateral load behavior of rc members with low-strength concrete and plain bars. *Advances in Structural Engineering*, 17(5), 639–658. https://doi.org/10.1260/1369-4332.17.5.639

Greek Seismic Design Code (2000). Greek Ministry for Environmental Planning and Public Works, Athens, Greece (in Greek).

Gurbuz, T., Cengiz, A., Kolemenoglu, S., Demir, C. and Ilki, A. (2022). "Damages and failures of structures in Izmir (Turkey) during the October 30, 2020 Aegean Sea earthquake", *Journal of Earthquake Engineering*, accepted, April, 2022

Harirchian, E. and Lahmer, T. (2020a). Improved rapid visual earthquake hazard safety evaluation of existing buildings using a type-2 fuzzy logic model. *Applied Sciences*, 2020, 10, 2375. https://doi.org/10.3390/app10072375

Harirchian, E. and Lahmer, T. (2020b). Developing a hierarchical type-2 fuzzy logic model to improve rapid evaluation of earthquake hazard safety of existing buildings. *Structures*, 2020, 28, 1384-1399. https://doi.org/10.1016/j.istruc.2020.09.048

Hassan, A.F. and Sozen M.A. (1997). Seismic vulnerability assessment of low-rise buildings in regions with infrequent earthquakes, *ACI Structural Journal*, 94(1): 31 - 39.

Holzer, T. L., Barka, A. A., Carver, D., Celebi, M., Cranswick, E., Dawson, T., Dieterich, J. H., Ellsworth, W. L., Fumal, T., Gross, J. L., Langridge, R., Lettis, W. R., Meremonte, M., Mueller, C., Olsen, R. S., Ozel, O., Parsons, T., Phan, L. T., Rockwell, T., Toprak, S. (2000). Implications for earthquake risk reduction in the United States from the Kocaeli, Turkey, earthquake of August 17, 1999. *US Geological Survey Circular*, (1193), 1-64.

Housner, G. W. (1975). Measures of severity of ground shaking, *US National Conference on Earthquake Engineering*, Ann Arbor, Michigan, pp. 25-33

Ilki, A. and Kumbasar, N. (2000). Marmara and Duzce earthquakes in Turkey-structural damage. *ASCE 14th Engineering Mechanics Conference*, on CD, Austin, Texas, USA.

Ilki, A., Comert, M., Demir, C., Orakcal, K., Ulugtekin, D., Tapan, M. and Kumbasar, N. (2014). Performance based rapid seismic assessment method (PERA) for reinforced concrete frame buildings, *Advances in Structural Engineering*, 17, 3, 439-459, 2014. https://doi.org/10.1260%2F1369-4332.17.3.439

Ilki, A. and Celep, Z. (2012). Earthquakes, existing buildings and seismic design codes in Turkey, *Arabian Journal for Science and Engineering*, 37 (2): 365-380.

Ilki, A., Halici, O. F., Comert, M. and Demir, C. (2020). The Modified Post-earthquake Damage Assessment Methodology for TCIP (TCIP-DAM-2020). *in Advances in Assessment and Modeling of Earthquake Loss*, eds.

Ilki, A., Kahraman, T., Ozkan, S., Aydogdu, H.H., Demir, C. and Comert, M. (2021a). Seismic risk assessment of building stock in Istanbul. *ACE2020 14th International Congress on Advances in Civil Engineering*, Sep 6-8, Istanbul, Turkey.

Ilki, A., Halici, O. F., Kupcu, E., Comert, M. and Demir, C. (2021b). Modifications on seismic damage assessment system of TCIP based on reparability. 17WCEE, *The 17th World Conference on Earthquake Engineering*, Sendai, 2020-2021.

Ilki, A., Yazgan, U., Demir, C., Ates, A., Demir U., Küpçü, E., Unal, G., Altınok, M. A., Karakaya, B. and Narlıtepe, F. (2019). Development of a framework for rapid earthquake risk assessment for substandard buildings in Turkey. *2nd International Workshop on Advanced Materials and Innovative Systems in Structural Engineering*, September 20, Istanbul, Turkey.

Inci, P., Goksu, C., Ilki, A. and Kumbasar, N. (2013). Effects of reinforcement corrosion on the performance of rc frame buildings subjected to seismic actions, *Journal of Performance of Constructed Facilities*, 27. 683-696. 10.1061/(ASCE)CF.1943-5509.0000378.

IMM (2009a) *Probable Earthquake Loss Estimates for Istanbul Province*, Department of Earthquake Risk Management and Urban Improvement, 2009.

IMM (2009b) *Production of Microzonation Maps and Reports (European Side)*, Istanbul Metropolitan Municipality, Department of Earthquake Risk Management and Urban Improvement, October 2009.

IMM (2009c) *Production of Microzonation Maps and Reports (Anatolian Side)*, Istanbul Metropolitan Municipality, Department of Earthquake Risk Management and Urban Improvement, November 2009.

Istanbul Earthquake Master Plan (2003). Istanbul Metropolitan Municipality, Istanbul, Turkey.

Kaplan, O., Guney, Y., Topcu, A., and Ozcelikors, Y. (2018). A rapid seismic safety assessment method for mid-rise reinforced concrete buildings. *Bulletin of Earthquake Engineering*. 16. 10.1007/s10518-017-0229-0.

Karaman, H., Sahin, M., Elnashai, A. and Pineda, O. (2008). loss assessment study for the Zeytinburnu district of Istanbul using Maeviz-Istanbul (HAZTURK). *Journal of Earthquake Engineering* - J EARTHQU ENG. 12. 187-198. 10.1080/13632460802014030.

Kassem, M.M., Beddu, S., Ooi, J.H., Tan, C.G, El-Maissi, A.M. and Nazri, F.M. (2021). Assessment of seismic building vulnerability using rapid visual screening method through web-based application for Malaysia. *Buildings*, 2021, 11(10), 485. https://doi.org/10.3390

Kohrangi, M., Bazzurro, P. and Vamvatsikos D. (2021). Seismic risk and loss estimation for the building stock in Isfahan. Part I: exposure and vulnerability. *Bulletin of Earthquake Engineering*, 19(4), 1709–1737. doi:10.1007/s10518-020-01036-2

JBDPA (2001). *Standard for Seismic Evaluation of Existing Reinforced Concrete Buildings*, Japan Building Disaster Prevention Association, 2001.

Macleod, I. A. (1972). Simplified analysis for shear wall-frame interaction. *Building Science*, Volume 7, Issue 2, 1972, 121-125, https://doi.org/10.1016/0007-3628(72)90048-5.

Mai, P. M., Spudich, P. and Boatwright, J. (2005). Hypocenter locations in finite-source rupture models. *Bulletin of the Seismological Society of America* 95: 965–980. https://doi.org/10.1785/0120040111

Makra, K., Rovithis, E., Riga, E., Raptakis, D. and Pitilakis, K. (2021). Amplification features and observed damages in İzmir (Turkey) due to 2020 Samos (Aegean Sea) earthquake: identifying basin effects and design requirements, *Bulletin of Earthquake Engineering*, 19, pages 4773–4804 (2021) https://doi.org/10.1007/s10518-021-01148-3.

Marasco, S., Zamani Noori, A., Domaneschi, M. and Cimellaro, G. P. (2021). A computational framework for large-scale seismic simulations of residential building stock. Engineering Structures, 244, 112690. https://doi.org/10.1016/j.engstruct.2021.112690.

Mavroeidis, G. and Papageorgiou, A. S. (2003). A mathematical representation of near-fault ground motions. *Bulletin of The Seismological Society of America - BULL SEISMOL SOC AMER*. 93. https://doi.org/10.1785/0120020100.

Maziligüney, L., Yaman, I. and Azılı, F. (2008). In-situ concrete compressive strength of residential, public and military structures, *8th International Congress on Advances in Civil Engineering*, Eastern Mediterranean University, Famagusta, North Cyprus.

Meda, A., Serena, M., Rinaldi, Z. and Riva, P. (2014). Experimental evaluation of the corrosion influence on the cyclic behaviour of RC columns, *Engineering Structures*. 76. 112–123. 10.1016/j.engstruct.2014.06.043.

METU (2003). SERU Database Middle East Technical University, Ankara, Turkey. https://seru.metu.edu.tr/

Mircevska, V., Abo El Ezz, A., Gjorgjeska, I., Smirnoff, A. and Nastev, M. (2019). First-order seismic loss assessment at urban scale: a case study of Skopje, North Macedonia. *Journal of Earthquake Engineering*. 1-19. 10.1080/13632469.2019.1662342.

New Zealand Society for Earthquake Engineering (NZSEE). (2017). *The seismic assessment of existing buildings – technical guidelines for engineering assessments*. Wellington, New Zealand.

NRCC (1993). *Manual for screening of buildings for seismic investigation*. Ottawa: National Research Council of Canada; 1993.

Ozdemir, P., Taskin, B., Vatansever, C., Sezen, A., Ilki, A. and. Boduroglu, H. (2002). November 12, 1999 Duzce earthquake: reconnaissance report for the town of Kaynasli. *12th European Conference on Earthquake Engineering*, on CD, London, UK.

Ozmen, B. (2000). The Damage State of the Izmit Bay on 17 August 1999. TDV/DR 010-53, Turkish Earthquake Foundation, 132 pg.

Pantazopoulou, S., Bonacci, J., Sheikh, S., Thomas, M. and Hearn, N. (2001). Repair of corrosion-damaged columns with FRP wraps, *Journal of Composites for Construction - J COMPOS CONSTR*, 5. 10.1061/(ASCE)1090-0268(2001)5:1(3).

Parsons, T., Toda, S., Stein, R. S., Barka, A. and Dieterich, J. H. (2000). Heightened odds of large earthquakes near Istanbul: An interaction-based probability calculation. *Science*, 288, pp. 661-665, 2000.

PEER (2013). NGA-West2 Database, https://ngawest2.berkeley.edu/ (accessed 25th february 2022).

Perrone D., Aiello M., Pecce M. and Rossi F. (2015). Rapid visual screening for seismic evaluation of RC hospital buildings. *Structures*. 18. 10.1016/j.istruc.2015.03.002.

Polese, M., Gaetani d'Aragona, M., Di Ludovico, M. and Prota, A. (2018). Sustainable selective mitigation interventions towards effective earthquake risk reduction at the community scale. *Sustainability*, 10(8), 2894.

PROCEQ (2002). User manual for Schmidt Hammer type N-L-NR-LR. Zurich, Switzerland.

Provisions for the Seismic Risk Evaluation of Existing RC Buildings under Urban Renewal Law (2013). Ministry of Environment and Urbanization, Ankara, Turkey.

Provisions for the Seismic Risk Evaluation of Existing RC Buildings under Urban Renewal Law (2019). Ministry of Environment and Urbanization, Ankara, Turkey.

Ruggieri S., Perrone D., Leone M., Uva G. and Aiello M.A. (2020). A prioritization RVS methodology for the seismic risk assessment of RC school buildings. *International Journal of Disaster Risk Reduction*, 101807. doi:10.1016/j.ijdrr.2020.101807

Ruggieri S., Chatzidaki A., Vamvatsikos D. and Uva G. (2022a). Reduced-order models for the seismic assessment of plan-irregular low-rise frame buildings. *Earthquake Engineering & Structural Dynamics*. 51. 10.1002/eqe.3725.

Ruggieri S., Calò M., Cardellicchio A. and Uva G. (2022b). Analytical-mechanical based framework for seismic overall fragility analysis of existing RC buildings in town compartments. *Bulletin of Earthquake Engineering*. 20. 10.1007/s10518-022-01516-7.

Scawthorn, C. and Johnson, G.S. (2000). Preliminary report: Kocaeli (Izmit) earthquake of 17 August 1999. *Engineering Structures*. 22. 727–745. 10.1016/S0141-0296(99)00106-6.

Sextos, A. G., Kappos, A. J. and Stylianidis K. C. (2007). Computer-aided pre- and post-earthquake assessment of buildings involving database compilation, GIS visualization, and mobile data transmission. *Computer-Aided Civil and Infrastructure Engineering*, 23(1), 59–73. doi:10.1111/j.1467-8667.2007.00513

Selman, E. (2019). Alternative procedures of damage evaluation integrated rapid assessment techniques for reinforced concrete buildings. *International Journal of Engineering Science and Application*, Vol.3, No.2, 2019.

Shah, F., Ahmed, A., Kegyes-B, K., Al-Ghamadi, A. and Ray, R.P. (2016). A case study using rapid visual screening method to determine the vulnerability of buildings in two districts of Jeddah, Saudi Arabia. *12th New Technologies for Urban Safety of Mega Cities in Asia*, November 2016, Tacloban, Philippines.

Specification for Structures to be Built in Disaster Areas, TSDC-1975 (1975). Turkish Ministry of Public Works and Settlement, Ankara, Turkey.

Specification for Structures to be Built in Disaster Areas, TSDC-1998 (1998). Turkish Ministry of Public Works and Settlement, Ankara, Turkey.

Specification for Structures to be Built in Disaster Areas, TSDC-2007 (2007). Turkish Ministry of Public Works and Settlement, Ankara, Turkey.

Sucuoglu, H., Yazgan, U. and Yakut, A. (2007). A screening procedure for seismic risk assessment in urban building stocks. Earthquake Spectra - EARTHQ SPECTRA. 23. 10.1193/1.2720931.

Tapan, M., Cömert, M., Demir, C., Sayan, Y., Orakcal, K. and Ilki, A. (2013). Failures of structures during the October 23, 2011 Tabanli (Van) and November 9, 2011 Edremit (Van) earthquakes in Turkey. *Engineering Failure Analysis*. 34. 10.1016/j.engfailanal.2013.02.013.

Temur, R. (2006). *Hızlı durum tespit (DURTES) yöntemi ve bilgisayar programının geliştirilmesi*. Master Thesis, Istanbul University, İstanbul, Turkey.

Tezcan S.S, Gürsoy M., Kaya E. and Bal I.E. (2003). Depremde Can Kaybını Önleme Projesi, *Kocaeli'99 Acil Durum Konferansı*, İstanbul Teknik Üniversitesi, 16-17 Ocak 2003, İstanbul, Turkey (in Turkish).

The Report on Determining Measures to be Taken to Minimize Seismic Losses (2021), Grand National Assembly of Turkey, Ankara, Turkey.

Turkish Building Earthquake Code (2018). Disaster and Emergency Management Presidency, Ankara, Turkey.

Turkish Seismic Hazard Map (2018). https://tdth.afad.gov.tr/. Disaster and Emergency Management Presidency, Ankara, Turkey.

Vamvatsikos, D., Cornell, C., (2002). Incremental Dynamic Analysis. *Earthquake Engineering & Structural Dynamics*. 31. 491 - 514. 10.1002/eqe.141.

Yakut, A. (2004). Preliminary seismic performance assessment procedure for existing RC buildings, *Engineering Structures*, 26-10, August 2004, 1447-1461. https://doi.org/10.1016/j.engstruct.2004.05.011

Yakut A, Sucuoğlu H, Binici B, Canbay E, Donmez C, İlki A, Caner A, Celik O.C. and Ay B.Ö. (2021). Performance of structures in İzmir after the Samos Island Earthquake. *Bull Earthq Eng*. https://doi.org/10.1007/s10518-021-01226-6

Ilki, A., Yazgan, U., Demir, C., Ates, A., Demir U., Küpçü, E., Unal, G., Altınok, M. A., Karakaya, B. and Narlıtepe, F.

Yazgan, U., Ilki, A., Demir, C., Demir, U., Ates, A., Küpçü, E., Ünal, G., Altınok, M. A., Karakaya, B. and Narlıtepe, F. (2019). Challenges in developing seismic vulnerability models for substandard building stocks in Turkey. *2nd International Workshop on Advanced Materials and Innovative Systems in Structural Engineering*, September 20, Istanbul, Turkey.

Zhou, Y., Gencturk, B., Willam, K. and Attar, Ar. (2014). Carbonation-Induced and chloride-induced corrosion in reinforced concrete structures. *Journal of Materials in Civil Engineering*. 27. 10.1061/(ASCE)MT.1943-5533.0001209.

Url-1<*https://www.izmir.bel.tr/tr/Haberler/izmir-de-yapi-durum-tespiti-icin-basvurular-basladi/48022/156*>, date retrieved 26.12.2023.

Url-2<*https://www.bursa.bel.tr/haber/bursanin-rontgeni-cekiliyor--32644*>, date retrieved 26.12.2023.

Url-3<*https://mudanya.bel.tr/haberler/depreme-dayanikli-mudanya-icin-hizli-tarama-ile-bina-testi-basladi*>, date retrieved 26.12.2023.

Url-4 < *https://deprem.afad.gov.tr/tarihteBuAy?id=74*>, date retrieved 21.03.2020.

Url-5 < *https://usgs.maps.arcgis.com/apps/webappviewer/index.html?id=8ac1 9bc334f747e486550f32837578e1*>, date retrieved 15.01.2022.

Url-6 < *http://www.koeri.boun.edu.tr/sismo/depremler/onemliler/01mayis2003 _bingoldepremi.pdf*>, date retrieved 20.03.2020.

Url-7 <*https://www.haber46.com.tr/kahramanmarasta-depremlerde-12-bin-622-kisi-hayatini-kaybetti*>, date retrieved 15.05.2023.

Url-8 < *https://www.cnnturk.com/video/turkiye/ibb-agir-riskli-318-apartmandan-20sini-yikti*>, date retrieved 20.08.2023.

Url-9 < *https://istanbulgucleniyor.ibb.istanbul/*>, date retrieved 10.11.2023.

APPENDICES

APPENDIX A: Information of the buildings that are evaluated in Chapter 2.
APPENDIX B: Information of the buildings that are evaluated for the reliability assessment, which are given in Chapter 3.
APPENDIX C: Information of the buildings that are evaluated for the validation study through incremental nonliear dynamic analyses, which are given in Chapter 5.
APPENDIX D: Probability of exceedance curves obtained from site data.

APPENDIX A: INFORMATION OF THE BUILDINGS THAT ARE EVALUATED IN CHAPTER 2.

Table A.1 : Properties of the buildings investigated in Chapter 2.

Building ID	Detailed Assessment Result	fc (MPa)	fs (MPa)	Transverse Reinforcement Spacing at Confinement Zone (cm)	# of Columns	# of Stories	Area of First Floor Ceiling (m2)	Total Floor Area (m2)	Beam Height (cm)	Beam Width (cm)	Year of Construction	Apparent Quality	Torsion	Vertical Element Discontinuity	Soft/Weak story	Pounding Effect	Slab Discontinuity	Irregularity on Plan	Overhangs	Order of the Plan	Short Column	Seismic Code	Sds	Sd1	Ta	Tb
1	C	9	220	20	10	2	78	156	40	20	1980	Fair	0	1	0	0	0	0	0	Separate	0	2007	1.000	0.522	0.15	0.6
2	C	19	220	20	10	1	112	112	85	35	1980	Good	0	0	0	0	0	0	0	Separate	0	2007	1.000	0.522	0.15	0.6
3	C	14	220	20	40	1	1025	1025	70	40	1972	Poor	0	0	0	0	0	0	0	Separate	0	2007	1.000	0.664	0.15	0.6
4	C	10	420	20	18	7	183	1282	50	15	1977	Fair	1	0	0	0	0	0	0	Separate	0	2007	1.000	0.664	0.15	0.6
5	C	7	220	25	40	3	450	1349	60	30	1976	Poor	1	1	1	0	0	0	0	Separate	0	2007	0.750	0.664	0.1	0.3
6	C	15	220	20	20	4	187	972	35	100	1980	Good	1	0	1	1	0	0	1	Adjacent Middle	0	2007	1.000	0.664	0.15	0.6
7	C	10	220	20	10	4	134	537	35	100	1980	Fair	1	0	1	1	0	0	1	Adjacent Middle	0	2007	1.000	0.664	0.15	0.6
8	C	10	220	20	29	2	278	580	45	20	1970	Fair	1	0	0	0	0	0	0	Separate	0	2007	1.000	0.664	0.15	0.4
9	C	18	420	25	21	3	379	1136	45	20	1970	Good	1	0	0	0	0	0	0	Separate	0	2007	1.000	0.664	0.15	0.4
10	C	13	420	25	22	1	223	223	45	20	1985	Fair	0	0	0	0	0	0	0	Separate	0	2007	1.000	0.664	0.15	0.4
12	CP	20	220	20	28	6	626	3756	65	40	1990	Fair	1	0	0	0	0	1	0	Separate	0	2007	0.750	0.664	0.15	0.4
13	C	9	420	25	16	4	155	621	60	25	1994	Good	1	0	1	0	0	0	1	Adjacent Corner	0	2019	1.070	0.372	N/A	N/A
14	CD	20	420	10	22	2	348	737	50	35	2008	Good	1	0	0	0	1	0	1	Separate	1	2007	1.000	0.664	0.15	0.4
15	C	8	220	20	20	2	196	391	65	30	2008	Fair	1	0	0	0	0	0	0	Separate	0	2007	1.000	0.664	0.1	0.3
16	C	16	220	20	24	4	512	1314	60	30	1978	Poor	0	1	0	0	1	0	0	Adjacent Corner	0	2018	1.908	0.668	N/A	N/A
19	C	11	220	20	24	3	512	1023	35	60	1978	Poor	0	0	0	0	0	0	0	Adjacent Middle	0	2018	1.908	0.668	N/A	N/A
22	C	15	220	20	24	3	512	1022	35	60	1978	Poor	0	0	0	0	0	0	0	Adjacent Middle	0	2018	1.908	0.668	N/A	N/A
25	C	13	220	20	24	3	512	1022	35	60	1978	Poor	0	0	1	0	0	0	0	Adjacent Middle	0	2018	1.908	0.668	N/A	N/A
28	C	15	220	20	56	4	1050	2700	60	30	1978	Poor	0	1	0	0	1	0	0	Adjacent Corner	0	2018	1.908	0.668	N/A	N/A
31	C	12	220	20	40	3	1050	2100	60	20	1978	Poor	0	0	1	0	0	0	0	Adjacent Middle	0	2018	1.908	0.668	N/A	N/A
34	C	16	220	20	40	3	1050	2100	60	20	1978	Poor	0	1	1	0	1	0	0	Adjacent Middle	0	2018	1.908	0.668	N/A	N/A
37	C	22	220	20	40	3	1050	2100	80	50	1978	Poor	0	1	1	0	1	0	0	Adjacent Corner	0	2018	1.908	0.668	N/A	N/A
40	C	10	220	20	14	2	135	270	40	40	1978	Poor	0	0	1	0	0	0	0	Separate	0	2018	1.908	0.668	N/A	N/A
43	C	12	220	20	38	3	250	1650	60	30	1978	Poor	0	0	1	0	0	0	0	Separate	0	2018	1.908	0.668	N/A	N/A
49	C	23	420	22	18	4	217	868	60	25	1999	Good	1	0	0	0	1	0	0	Separate	0	2018	1.709	0.598	N/A	N/A
50	C	8	220	20	12	8	112	896	30	40	1985	Poor	1	1	1	1	1	1	0	Adjacent Corner	0	2018	1.013	0.519	N/A	N/A
51	C	8	220	25	12	2	164	329	40	100	1990	Poor	0	1	0	0	0	0	0	Separate	0	2007	1.000	0.664	0.15	0.4
52	C	5	220	20	15	4	104	417	25	100	1990	Poor	0	1	0	0	0	0	0	Separate	0	2007	1.000	0.664	0.15	0.6
53	C	9	220	20	15	4	94	375	40	100	1990	Poor	0	1	0	0	0	0	0	Separate	0	2007	1.000	0.664	0.15	0.6

Table A.1 (continued) : Properties of the buildings investigated in Chapter 2.

Building ID	Detailed Assessment Result	fc (MPa)	fs (MPa)	Transverse Reinforcement Spacing at Confinement Zone (cm)	# of Columns	# of Stories	Area of First Floor Ceiling (m2)	Total Floor Area (m2)	Beam Height (cm)	Beam Width (cm)	Year of Construction	Apparent Quality	Torsion	Vertical Element Discontinuity	Soft/Weak story	Pounding Effect	Slab Discontinuity	Irregularity on Plan	Overhangs	Order of the Plan	Short Column	Seismic Code	Sds	Sd1	Ta	Tb
54	C	11	220	25	23	4	200	800	50	100	1990	Fair	0	0	0	0	0	0	0	Separate	0	2007	1.000	0.664	0.15	0.4
55	C	7	220	20	13	2	92	184	50	20	1985	Poor	0	1	0	0	0	0	0	Separate	0	2007	1.000	0.664	0.15	0.4
56	C	13	220	20	18	2	200	400	50	25	1966	Fair	0	0	0	0	0	0	0	Separate	0	2018	1.709	0.598	N/A	N/A
57	CD	23	420	8	17	3	239	717	50	30	2009	Good	0	0	0	0	0	1	0	Separate	0	2007	1.000	0.664	0.15	0.6
61	CD	21	420	20	18	3	349	1046	30	100	1999	Good	0	0	0	0	0	0	0	Separate	0	2018	0.967	0.345	N/A	N/A
62	CD	30	420	10	29	4	473	1894	30	100	2005	Good	0	0	0	0	0	1	0	Separate	0	2007	1.000	0.664	0.15	0.6
63	C	15	420	20	27	4	343	1374	30	55	2004	Fair	0	0	0	0	0	0	0	Separate	0	2018	1.709	0.598	N/A	N/A
64	C	18	420	10	26	3	898	2695	35	60	2001	Fair	0	0	0	0	0	1	0	Separate	0	2018	1.709	0.598	N/A	N/A
68	CD	25	420	20	18	3	349	1046	30	100	1999	Good	0	0	0	0	0	0	0	Separate	0	2018	0.967	0.345	N/A	N/A
69	C	17	220	20	15	5	155	774	50	25	1979	Good	1	0	0	0	0	0	0	Separate	0	2018	1.000	0.664	0.15	0.4
70	C	10	220	20	10	5	142	709	50	25	1979	Poor	1	0	0	0	0	0	0	Separate	0	2018	1.000	0.664	0.15	0.4
71	C	12	220	20	19	5	319	1596	50	25	1979	Fair	1	0	0	0	0	0	0	Separate	0	2018	1.000	0.664	0.15	0.4
72	CD	27	420	10	30	4	679	2715	45	25	2005	Good	1	0	0	0	0	0	0	Separate	0	2007	1.000	0.664	0.15	0.6
73	C	8	220	20	27	4	277	1110	50	25	1994	Poor	1	0	0	0	0	0	0	Separate	0	2007	1.000	0.664	0.15	0.6
74	CD	35	420	10	25	3	347	1040	60	25	2012	Good	1	0	0	0	0	0	0	Separate	0	2007	1.000	0.664	0.15	0.6
75	C	29	420	20	18	2	349	697	30	100	1999	Good	0	0	0	0	1	0	0	Separate	0	2018	0.967	0.345	N/A	N/A
77	CD	30	420	20	18	2	349	697	30	100	1999	Good	0	0	0	0	0	0	0	Separate	0	2018	0.967	0.345	N/A	N/A
78	C	24	420	10	35	4	529	2116	50	30	2002	Good	0	0	1	0	0	1	0	Separate	0	2007	1.000	0.664	0.15	0.6
81	CP	18	420	10	35	4	357	1428	50	30	2000	Good	0	0	1	0	0	1	0	Separate	0	2007	1.000	0.664	0.15	0.6
84	C	13	220	10	34	2	564	1127	30	55	1998	Fair	1	0	1	0	0	0	0	Separate	0	2007	1.000	0.664	0.15	0.6
87	CD	19	420	10	30	3	456	1369	35	100	1995	Good	0	0	0	0	0	0	0	Separate	0	2007	1.000	0.664	0.15	0.6
90	C	5	220	20	32	2	344	712	55	20	1985	Poor	0	0	0	0	0	1	1	Separate	0	2007	1.000	0.664	0.15	0.6
91	C	12	220	20	32	4	560	2239	45	30	1997	Fair	0	0	1	0	0	0	0	Separate	0	2007	1.000	0.664	0.15	0.6
92	CP	12	420	20	32	2	560	1120	50	30	1996	Fair	0	0	1	0	0	0	0	Separate	0	2007	1.000	0.664	0.15	0.6
95	CP	23	420	10	32	4	620	2480	60	30	2002	Good	1	0	0	0	0	0	0	Separate	0	2007	1.000	0.664	0.15	0.6
98	CD	22	420	10	20	3	315	944	60	30	2005	Good	0	0	1	0	0	0	0	Adjacent Corner	0	2007	1.000	0.664	0.15	0.6
101	CD	17	420	10	25	3	315	944	60	30	2005	Good	0	0	1	0	0	0	0	Adjacent Middle	0	2007	1.000	0.664	0.15	0.6
104	CD	17	420	10	20	3	315	944	60	30	2005	Good	0	0	1	0	0	0	0	Adjacent Corner	0	2007	1.000	0.664	0.15	0.6
107	C	12	420	20	44	6	625	4270	50	35	1998	Fair	0	0	0	0	0	0	1	Separate	0	2007	1.000	0.664	0.15	0.6
108	CP	18	420	10	27	3	578	2008	50	35	1995	Good	0	0	1	0	0	0	0	Separate	0	2007	0.750	0.664	0.15	0.6

Table A.1 (continued) : Properties of the buildings investigated in Chapter 2.

Building ID	Detailed Assessment Result	fc (MPa)	fs (MPa)	Transverse Reinforcement Spacing at Confinement Zone (cm)	# of Columns	# of Stories	Area of First Floor Ceiling (m2)	Total Floor Area (m2)	Beam Height (cm)	Beam Width (cm)	Year of Construction	Apparent Quality	Torsion	Vertical Element Discontinuity	Soft/Weak story	Pounding Effect	Slab Discontinuity	Irregularity on Plan	Overhangs	Order of the Plan	Short Column	Seismic Code	Sds	Sd1	Ta	Tb
109	CD	18	420	10	32	4	498	1992	60	30	2000	Good	1	0	1	0	0	1	0	Separate	0	2007	1.000	0.664	0.15	0.6
110	C	9	220	25	13	6	101	629	50	20	1990	Poor	1	0	0	0	0	0	1	Adjacent Corner	0	2019	1.299	0.683	N/A	N/A
111	C	6	220	30	22	6	239	1432	50	20	1990	Fair	1	0	1	0	0	0	1	Separate	1	2019	1.274	0.671	N/A	N/A
112	C	13	220	25	14	5	113	565	50	20	1990	Poor	0	0	0	0	0	0	1	Adjacent Corner	0	2019	1.560	0.525	N/A	N/A
113	C	8	220	30	14	5	147	734	50	20	1990	Fair	0	0	1	1	0	0	1	Adjacent Corner	0	2019	1.287	0.678	N/A	N/A
114	C	15	220	28	25	6	207	1421	50	20	1990	Fair	0	0	1	1	0	0	1	Adjacent Corner	0	2019	1.257	0.665	N/A	N/A
115	C	13	220	28	21	6	148	1011	50	20	1990	Fair	0	0	1	1	0	0	1	Adjacent Corner	0	2019	1.261	0.666	N/A	N/A
116	C	8	220	28	13	4	91	474	50	20	1990	Poor	0	0	0	0	0	0	1	Separate	0	2019	1.294	0.679	N/A	N/A
117	C	6	220	31	16	4	153	612	50	20	1990	Good	0	0	0	0	0	0	1	Adjacent Corner	0	2019	1.498	0.506	N/A	N/A
118	C	10	220	28	14	6	122	901	50	20	1990	Fair	0	0	1	1	0	0	1	Adjacent Corner	0	2019	1.198	0.624	N/A	N/A
119	C	5	220	25	14	5	132	845	50	20	1990	Fair	0	0	1	1	0	0	1	Adjacent Corner	1	2019	1.418	0.480	N/A	N/A
120	C	7	220	26	60	5	663	3339	50	20	1990	Good	0	0	0	0	0	0	1	Separate	0	2019	1.314	0.689	N/A	N/A
121	C	14	220	26	12	5	161	807	50	20	1990	Fair	1	0	0	0	0	0	1	Separate	0	2019	1.304	0.684	N/A	N/A

C: Collapse, CP: Collapse Prevention, CD: Controlled Damage, fc: Compressive Strength of Concrete, fs: Tensile Strength of Steel,
Seismic code, 2007: TSDC-2007, 2018: TBEC-2018, 2019: RBTE-2019.
0: Parameter does not exist, 1: Parameter exists.

APPENDIX B: INFORMATION OF THE BUILDINGS THAT ARE EVALUATED FOR THE RELIABILITY ASSESSMENT

Table B.1 : The structural information and analysis results of the buildings used for further validation of PERA2019 based on actual earthquake damages.

Building Code	SSR-Y	SSR-X	Global SSR	Observed Earthquake Damage	Max. Axial Stress	Average Axial Stress	Period in Y Direction (s)	Period in X Direction (s)	Base Shear in Y Direction (kN)	Base Shear in X Direction (kN)	f_c (MPa)	f_y (MPa)	Stirrup Spacing (cm)	Number of Columns	Number of Risky Columns	Spectral Acceleration Demand_x (g)	Spectral Acceleration Demand_y (g)	Number of Stories	Total Floor Area (m2)	Year of Construction	Total Area of Vertical Elements (cm2)	Longitudinal Reinforcement Ratio (%)	Type of Use
BNG-10-4-9	69.3	94.0	69.3	None	53%	25%	0.46	0.45	21298	14478	13.5	420	20	33	3	0.58	0.86	5	2476	2002	123700	1.0%	Residential
BNG-3-4-4	42.0	72.0	42.0	None	38%	22%	0.48	0.58	14296	9656	10.8	220	25	53	15	0.51	0.75	4	1900	1980	91700	1.0%	Residential
BNG-6-3-11	50.4	50.4	50.4	None	38%	31%	0.53	0.53	4625	4599	5.8	220	25	26	26	0.65	0.66	3	705	1980	39000	1.0%	Residential
Karşıyaka01	129.0	80.0	80.0	None	34%	26%	0.95	1.10	2602	2290	13.2	220	10	16	3	0.23	0.26	6	1014	1998	30450	1.1%	Residential
Izmir01	70.5	66.4	66.4	None	28%	17%	0.78	0.75	1265	1297	15.8	220	20	13	4	0.28	0.27	5	462	1985	17250	0.5%	Residential
BNG-10-4-7	48.6	39.7	39.7	Light	59%	24%	0.55	0.75	25578	13411	9.3	220	25	69	65	0.41	0.77	4	3311	1988	164225	1.0%	Residential
BNG-10-5-11	114.3	57.6	57.6	Light	32%	13%	0.49	0.61	3132	2994	13.7	220	25	13	13	0.65	0.68	5	460	1988	26525	1.0%	Residential
BNG-3-4-1	79.0	36.0	36.0	Light	40%	28%	0.52	0.51	10122	14817	8.1	220	25	50	50	0.77	0.52	4	1930	1998	85000	1.0%	Residential
BNG-5-5-1	25.2	56.7	25.2	Light	61%	38%	1.02	0.85	8725	6850	9.0	220	25	32	32	0.35	0.44	5	1974	1985	57875	1.0%	Residential
BNG-6-3-4	56.0	116.0	56.0	Light	20%	15%	0.49	0.40	2396	2724	12.5	220	20	12	6	0.83	0.73	3	329	2003	18000	1.0%	Residential
AFY-B-02	170.0	99.0	99.0	Light	47%	16%	0.47	0.58	5763	4761	15.4	220	25	26	10	0.35	0.43	3	1042	1976	61650	1.0%	Public
AFY-Ç-11	111.6	83.7	83.7	Light	20%	15%	1.14	1.22	3278	2981	11.0	220	20	31	31	0.22	0.24	4	1341	2002	78463	1.0%	Residential
AFY-ÇO-04	84.6	64.8	64.8	Light	51%	30%	0.71	0.77	3400	3188	5.7	220	25	22	12	0.35	0.38	4	903	1994	52800	1.0%	Residential
AFY-M-02	66.0	52.0	52.0	Light	80%	60%	0.96	1.21	4775	3507	10.1	220	25	40	32	0.11	0.14	4	2551	1970	57600	1.0%	Public
BNG-10-3-3	54.0	38.7	38.7	Moderate	37%	23%	0.60	0.63	7786	7779	7.7	220	30	24	24	0.65	0.65	3	918	1975	67200	0.7%	Public
BNG-10-4-4	32.8	19.7	19.7	Moderate	59%	42%	0.76	0.92	23704	13659	8.5	220	25	57	57	0.33	0.57	6	4159	1998	117850	1.0%	Residential
BNG-10-4-6	48.1	34.3	34.3	Moderate	47%	16%	0.64	0.49	14315	26154	14.9	220	25	61	29	0.84	0.46	4	2408	1976	137822	1.0%	Residential
BNG-10-5-1	38.7	27.0	27.0	Moderate	109%	45%	1.05	1.64	16130	10045	10.5	220	30	41	41	0.24	0.39	6	3210	1990	108925	1.0%	Residential
BNG-10-5-2	23.4	6.3	6.3	Moderate	109%	69%	1.46	1.95	6826	6903	6.2	220	25	32	32	0.23	0.22	5	3059	1990	75300	1.0%	Residential
AFY-B-01	53.9	83.1	53.9	Moderate	95%	32%	0.99	0.91	4884	5296	11.2	220	40	37	24	0.22	0.20	4	1853	1974	78900	0.7%	Public
AFY-Ç-05	64.0	45.0	45.0	Moderate	43%	28%	0.65	0.79	2704	2230	13.7	220	25	16	16	0.36	0.44	4	615	1985	16000	0.7%	Residential
AFY-Ç-12	66.6	36.9	36.9	Moderate	54%	35%	0.68	1.19	2705	1503	6.8	220	25	20	20	0.23	0.42	4	649	1985	27500	1.0%	Residential
BNG-10-3-10	17.7	18.4	17.7	Heavy	49%	38%	0.53	0.81	18655	7459	6.8	220	30	59	59	0.29	0.71	4	2611	1980	101300	0.4%	Residential
BNG-11-4-1	29.2	45.9	29.2	Heavy	45%	34%	0.68	0.65	5983	6547	9.1	220	35	21	21	0.61	0.56	4	1078	1998	39600	0.8%	Residential
BNG-11-4-2	23.3	27.0	23.3	Heavy	40%	29%	0.71	0.82	3527	2135	9.4	220	35	17	17	0.37	0.62	4	571	1989	21325	0.7%	Residential

Table B.1 (Continued) : The structural information and analysis results of the buildings used for further validation of PERA2019 based on actual earthquake damages.

Building Code	SSR-Y	SSR-X	Global SSR	Observed Earthquake Damage	Max. Axial Stress	Average Axial Stress	Period in Y Direction (s)	Period in X Direction (s)	Base Shear in Y Direction (kN)	Base Shear in X Direction (kN)	f_c (MPa)	f_y (MPa)	Stirrup Spacing (cm)	Number of Columns	Number of Risky Columns	Spectral Acceleration Demand_x (g)	Spectral Acceleration Demand_y (g)	Number of Stories	Total Floor Area (m2)	Year of Construction	Total Area of Vertical Elements (cm2)	Longitudinal Reinforcement Ratio (%)	Type of Use
BNG-11-4-4	40.1	32.8	32.8	Heavy	49%	26%	0.60	0.60	3145	2903	8.8	220	35	14	14	0.60	0.65	4	486	2000	21000	1.1%	Residential
BNG-6-2-8	63.4	23.3	23.3	Heavy	55%	33%	0.42	0.73	1717	1220	5.0	220	25	10	10	0.52	0.74	2	233	1992	14000	1.7%	Residential
BNG-6-3-1	34.0	25.1	25.1	Heavy	26%	26%	0.54	0.54	5544	4842	8.6	220	40	20	20	0.59	0.67	3	821	1991	37800	0.5%	Residential
BNG-6-4-2	26.0	18.6	18.6	Heavy	43%	31%	0.68	0.82	11671	8700	10.4	220	25	42	42	0.43	0.58	4	2021	2001	63000	1.0%	Residential
BNG-6-4-7	40.5	37.3	37.3	Heavy	45%	32%	0.57	0.67	7007	6468	8.6	220	30	27	27	0.56	0.61	4	1154	1996	46500	0.5%	Residential
AFY-Ç-02	5.9	36.1	5.9	Heavy	38%	28%	0.71	0.62	1638	1820	9.5	220	35	15	15	0.45	0.41	3	403	2000	15000	0.9%	Residential
AFY-Ç-03	32.4	17.8	17.8	Heavy	75%	48%	0.66	1.37	1552	695	6.8	220	30	11	11	0.19	0.43	3	358	1991	11000	1.2%	Residential
AFY-Ç-06	61.7	28.9	28.9	Heavy	37%	22%	0.45	0.71	2115	1442	10.0	220	25	16	16	0.40	0.59	3	359	1990	16000	0.9%	Residential
AFY-Ç-07	41.6	31.3	31.3	Heavy	40%	27%	0.71	0.81	2659	2340	11.1	220	25	12	12	0.35	0.40	5	662	1975	22200	0.3%	Residential
AFY-Ç-13	15.3	23.3	15.3	Heavy	45%	27%	0.60	0.99	2000	1221	12.7	220	35	12	12	0.29	0.47	4	424	1976	12450	0.6%	Residential
AFY-ÇO-02	43.7	38.9	38.9	Heavy	70%	46%	1.25	1.27	2627	2549	8.1	220	25	27	27	0.20	0.20	5	1300	1990	35400	1.0%	Residential
AFY-ÇO-03	29.2	34.8	29.2	Heavy	56%	50%	0.92	0.80	6946	8028	6.6	220	30	44	44	0.33	0.29	5	2397	1997	76200	0.7%	Residential
AFY-ÇO-05	35.4	32.8	32.8	Heavy	90%	30%	0.56	0.58	1668	1641	8.2	220	30	17	16	0.46	0.47	3	353	2002	15800	0.7%	Residential
AFY-S-01	22.3	28.9	22.3	Heavy	122%	29%	0.51	0.41	3425	3962	9.4	220	30	19	19	0.64	0.55	4	623	1985	26350	1.0%	Residential
AFY-Y-01	36.5	40.8	36.5	Heavy	20%	13%	0.53	0.46	4227	4811	9.8	220	45	32	32	0.60	0.52	3	806	1970	64000	0.5%	Residential
BNG-6-4-3	25.4	19.5	19.5	Collapse	21%	19%	0.49	0.67	4996	4028	19.2	420	30	16	16	0.59	0.73	4	686	2003	19200	0.6%	Residential
AFY-ÇO-01	17.0	25.1	17.0	Collapse	41%	31%	0.52	0.49	4929	5194	9.8	220	30	22	19	0.52	0.50	4	994	2002	33000	0.8%	Residential
nurdagi2	7.0	4.0	4.0	Heavy	70%	39%	0.67	0.67	3931	6127	6.4	220	20	18	18	1.51	0.97	2	312	1980	16200	0.5%	Residential
nurdagi3	101.0	23.0	23.0	Heavy	52%	34%	1.09	1.42	17600	23086	11.6	420	15	36	23	0.50	0.38	7	4597	2022	137035	0.6%	Residential
nurdagi4	25.2	10.8	10.8	Heavy	115%	58%	1.67	2.39	9328	8001	8.9	420	20	21	18	0.23	0.27	7	3458	2010	77275	1.0%	Residential
iskenderun1	83.1	40.1	40.1	Heavy	33%	25%	1.62	1.29	7245	13387	12.8	420	15	26	21	0.44	0.24	7	3075	2008	104160	1.0%	Residential
maras1	30.8	26.7	26.7	Heavy	42%	23%	0.52	0.93	29811	9364	10.1	220	27	25	25	0.48	1.53	5	1501	1990	108250	1.3%	Public
nurdagi1	43.0	79.0	43.0	None	45%	21%	0.24	0.14	13937	8780	12.7	220	20	17	4	1.02	1.62	2	660	1988	80400	0.5%	Residential
iskenderun2	186.3	204.9	100.0	Light	24%	14%	0.73	0.74	4263	6027	14.0	420	10	13	0	0.74	0.52	5	814	2023	45375	1.0%	Residential

SSR: Seismic Safety Ratio, f_c: Compressive strength of concrete, f_y: The characteristic yield strength of reinforcement steel.

Stirrup Spacing is observed for reinforced concrete columns at the critical story.

The Longitudinal Reinforcement Ratio parameter is observed or assumed for columns from a representative column.

The Maximum and Average Axial Stress parameters are determined at the critical story.

Spectral Acceleration Demand is determined for considered earthquake event.

BNG: Buildings from Bingol Earthquake, AFY: Buildings from Afyon Earthquake

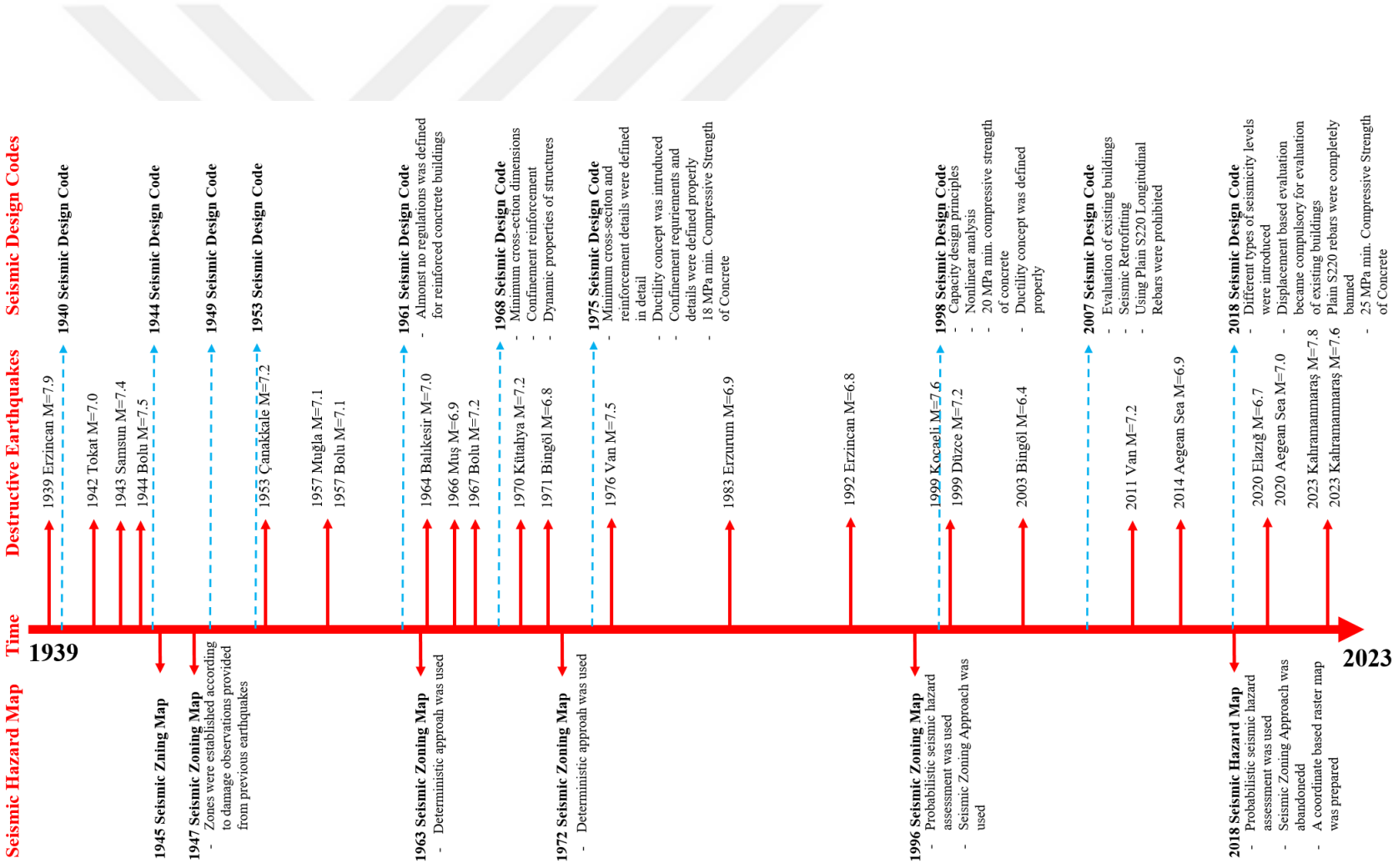

Figure B.1: The evolution of the seismic design codes and seismic hazard maps in Turkey and the devastating earthquakes in Turkey.

APPENDIX C: INFORMATION OF THE BUILDINGS THAT ARE EVALUATED FOR THE VALIDATION STUDY THROUGH IDA

Table C.1: The structural information and analysis results of the buildings in the work of validation of PERA2019 based on IDA results.

Building ID	Model Type	Sds (g)	Sd1 (g)	Base Shear X (kN)	Base Shear Y (kN)	Period X (s)	Period Y (s)	SSR_PERA-X %	SSR_PERA-Y %	SSR_IDA-X %	SSR_IDA-Y %	Fcm (MPa)	fs (MPa)	Stirrup Spacing (cm)	Number of Columns	Number of Stories	Total Story Area (m2)	Drift at Collapse State - X	Drift at Collapse State - Y	Year of Construction	Cross-sectional area of columns (cm2)	Longitudinal Reinforcement Ratio %	Torsion Irregularity	Vertical Discontinuity	Soft/Weak story	Pounding Effect	Slab Discontinuity	Irregularity on Plan
101	As-Built	1.278	0.671	4714	4616	1.28	1.34	32.1	25.5	28.1	17.6	9	220	20	16	6	930	0.4%	0.2%	1992	31875	1.1%	1	1	1	0	0	0
102	As-Built	1.278	0.671	5512	4817	1.67	1.09	25.2	40.5	29.3	31.2	12	220	25	14	5	608	0.4%	0.7%	1990	21150	0.8%	1	0	0	0	0	0
103	As-Built	1.281	0.673	4034	3930	1.71	1.75	19.0	18.2	29.4	37.3	12	220	25	20	5	741	0.3%	0.3%	1980	17500	1.0%	1	0	1	1	0	0
104	As-Built	1.280	0.672	6696	5848	1.26	1.05	18.6	27.5	22.2	29.9	10	220	25	20	5	817	1.2%	1.3%	1991	23250	1.0%	1	0	0	1	0	0
105	As-Built	1.284	0.674	5830	5739	1.81	1.75	8.0	10.9	8.6	1.9	6	220	30	19	6	1024	0.4%	0.4%	1979	28125	1.1%	1	0	1	1	0	0
106	As-Built	1.285	0.674	6708	5764	1.33	0.88	13.1	15.3	11.4	13.5	8	220	25	16	4	821	0.8%	0.7%	1990	22750	1.3%	1	0	1	1	0	0
107	As-Built	1.283	0.674	4896	5733	1.20	1.99	16.2	7.3	22.2	14.4	6	220	25	15	5	810	0.9%	0.9%	1995	23100	1.1%	1	0	0	1	0	0
108	As-Built	1.286	0.675	3315	3213	1.54	1.87	10.8	11.7	12.9	14.1	6	220	25	10	5	461	1.0%	0.9%	1990	12950	1.0%	0	0	1	0	0	0
109	As-Built	1.276	0.669	5703	4968	1.69	1.19	29.0	39.0	55.7	63.7	14	220	25	14	4	475	0.4%	0.4%	1984	20000	1.1%	0	0	0	0	0	0
110	As-Built	1.277	0.670	6308	6421	1.40	1.49	16.2	16.2	19.7	17.1	7	220	25	17	5	919	1.1%	1.2%	1991	25050	1.0%	0	0	1	0	0	0
201	As-Designed	1.278	0.671	5439	5325	1.09	1.12	32.4	47.0	37.0	51.8	16	220	20	16	6	930	0.2%	0.2%	1992	31875	1.1%	1	0	1	0	0	0
202	As-Designed	1.278	0.671	5889	5147	1.47	0.94	47.7	75.6	53.8	60.9	16	220	10	14	5	608	0.8%	0.9%	1990	21150	1.0%	1	0	0	0	0	0
203	As-Designed	1.281	0.673	4476	4360	2.14	2.08	39.4	46.7	33.0	41.8	18	220	10	20	5	741	0.1%	0.1%	1980	17500	1.0%	1	0	1	1	0	0
204	As-Designed	1.280	0.672	7592	6631	0.91	0.75	42.9	64.0	37.9	43.8	16	220	10	20	5	817	1.1%	1.1%	1991	23250	1.0%	1	0	0	1	0	0
205	As-Designed	1.284	0.674	7603	7484	2.51	2.44	46.7	54.7	59.2	58.5	18	220	10	19	6	1024	1.4%	1.1%	1979	28125	1.1%	1	0	1	1	0	0
206	As-Designed	1.285	0.674	8324	7153	1.82	1.22	33.5	68.5	46.3	62.3	18	220	10	16	4	821	1.7%	1.8%	1990	22750	1.3%	1	0	1	1	0	0
207	As-Designed	1.283	0.674	6360	7447	1.79	2.99	72.9	42.9	56.4	43.3	18	220	10	15	5	810	0.4%	0.4%	1995	23100	1.1%	1	0	0	1	0	0
208	As-Designed	1.286	0.675	4384	4250	1.78	2.13	36.0	40.5	48.5	51.6	18	220	10	10	5	461	1.6%	1.5%	1990	12950	1.0%	0	0	1	0	0	0
209	As-Designed	1.276	0.669	6061	5295	1.89	1.35	52.0	91.0	67.8	97.2	18	220	8	14	4	475	0.9%	0.4%	1984	20000	1.1%	0	0	0	0	0	0
210	As-Designed	1.277	0.670	8095	8240	2.13	2.24	53.1	42.3	56.6	54.9	18	220	10	17	5	919	1.0%	0.9%	1991	25050	1.0%	0	0	1	0	0	0
301	As-Built	0.729	0.183	2169	2925	1.15	1.74	140.0	140.0	140.0	140.0	31	420	10	17	6	843	1.2%	1.0%	2006	46975	1.1%	0	0	0	0	0	0
302	As-Built	0.802	0.200	1198	1157	2.46	2.33	101.0	105.0	140.0	140.0	14	220	25	20	6	627	1.0%	0.8%	1975	20700	0.7%	0	0	0	0	0	0

SSR: Seismic Safety Ratio, , f_c: Compressive strength of concrete, f_s: The type of reinforcement steel.

Table C.2: IDA curves of the buildings. The horizontal axis is the maximum inter-story drift ratio (%) and the vertical axis is the spectral acceleration (g) of corresponding first mode vibration period.

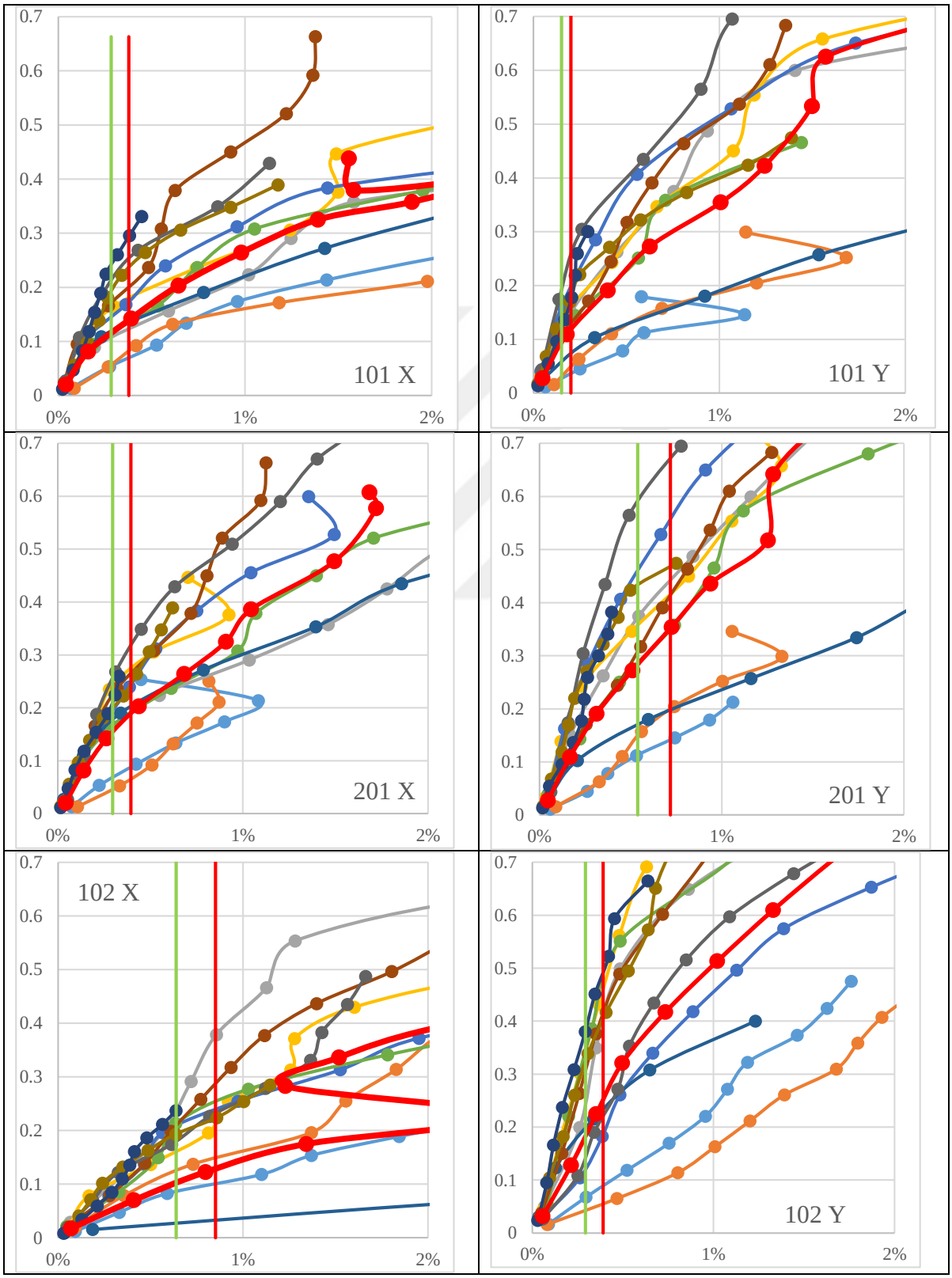

Table C.2 (Continued) : IDA curves of the buildings. The horizontal axis is the maximum inter-story drift ratio (%) and the vertical axis is the spectral acceleration (g) of corresponding first mode vibration period.

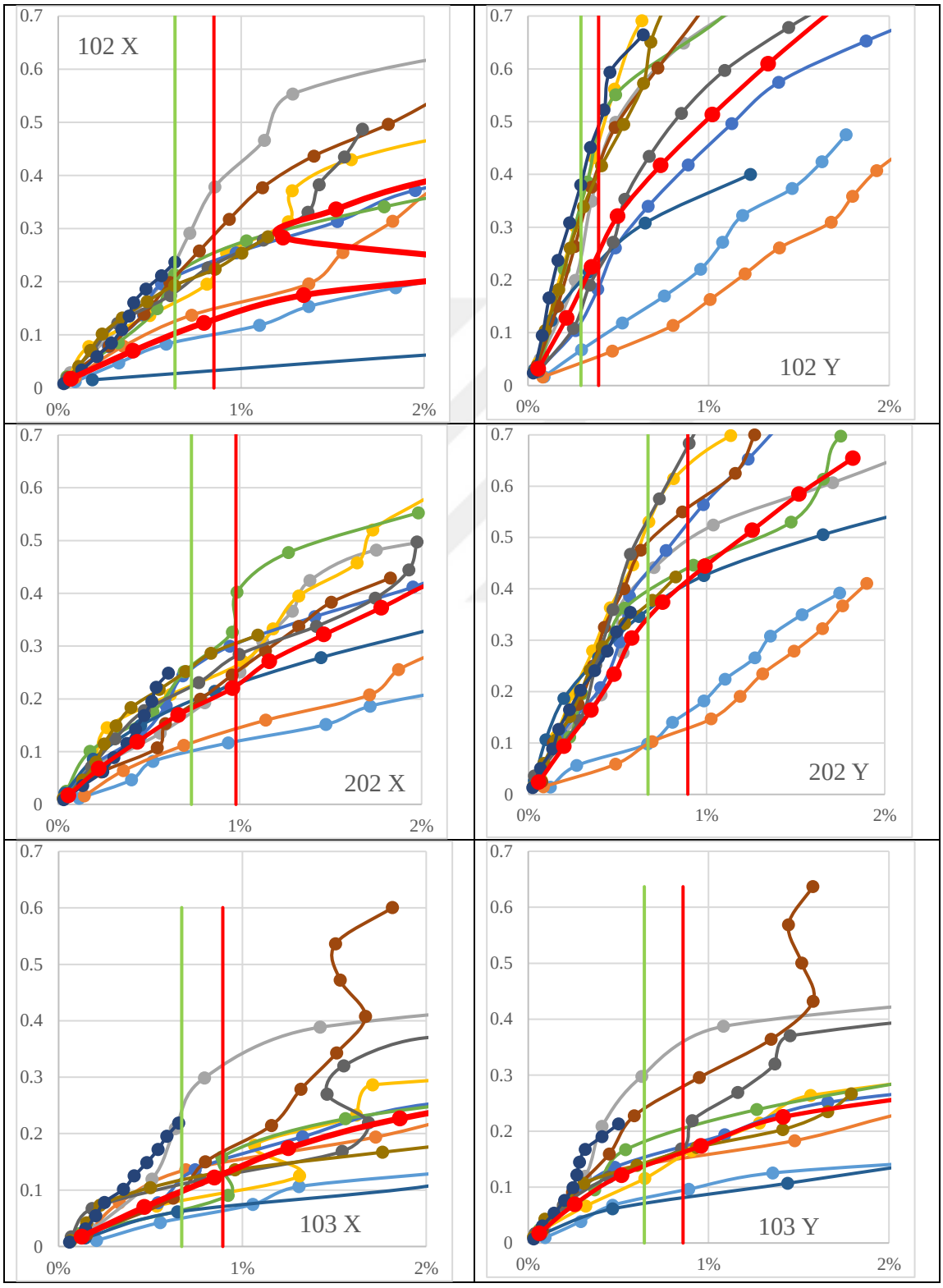

Table C.2 (Continued) : IDA curves of the buildings. The horizontal axis is the maximum inter-story drift ratio (%) and the vertical axis is the spectral acceleration (g) of corresponding first mode vibration period.

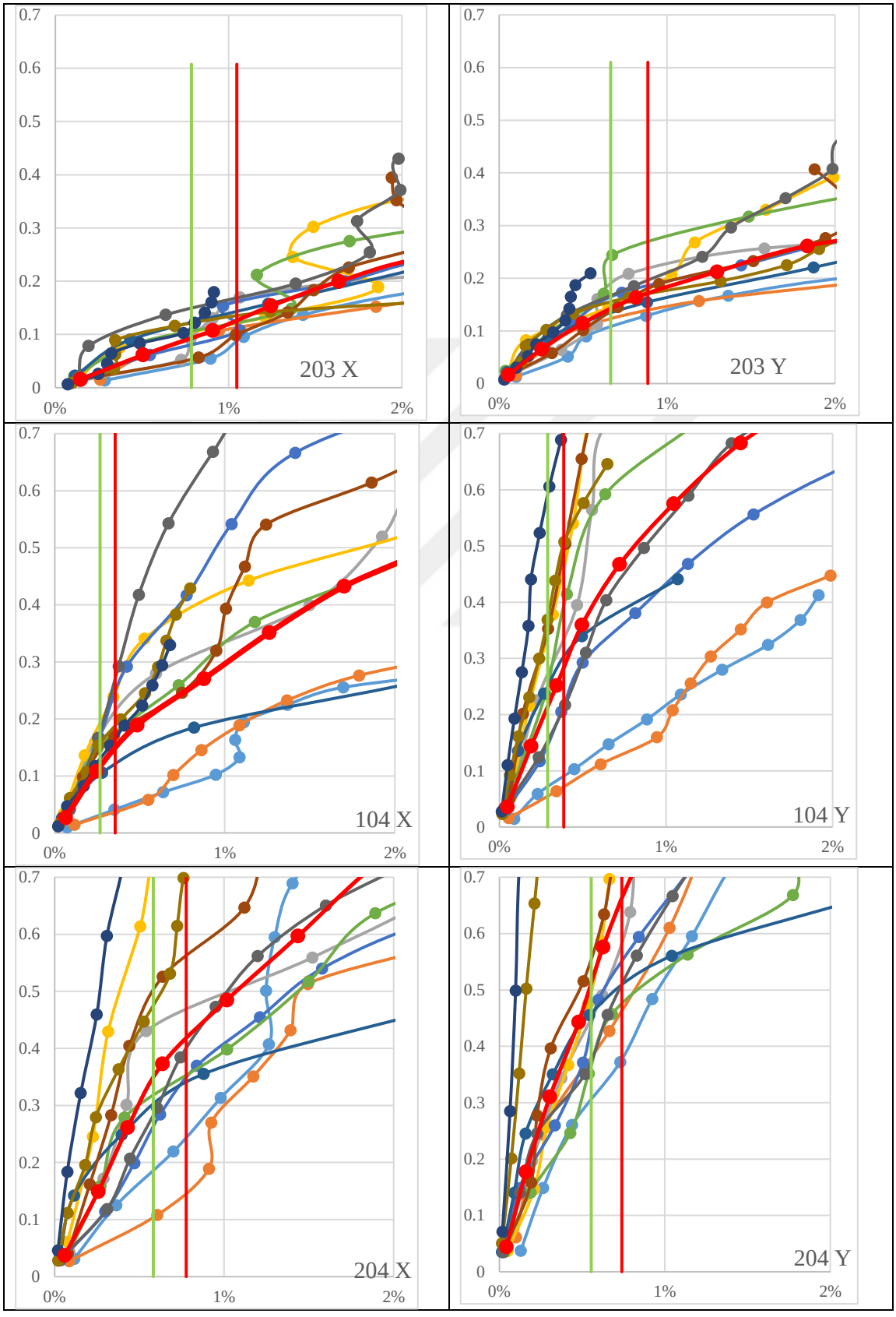

Table C.2 (continued): IDA curves of the buildings. The horizontal axis is the maximum inter-story drift ratio (%) and the vertical axis is the spectral acceleration (g) of corresponding first mode vibration period.

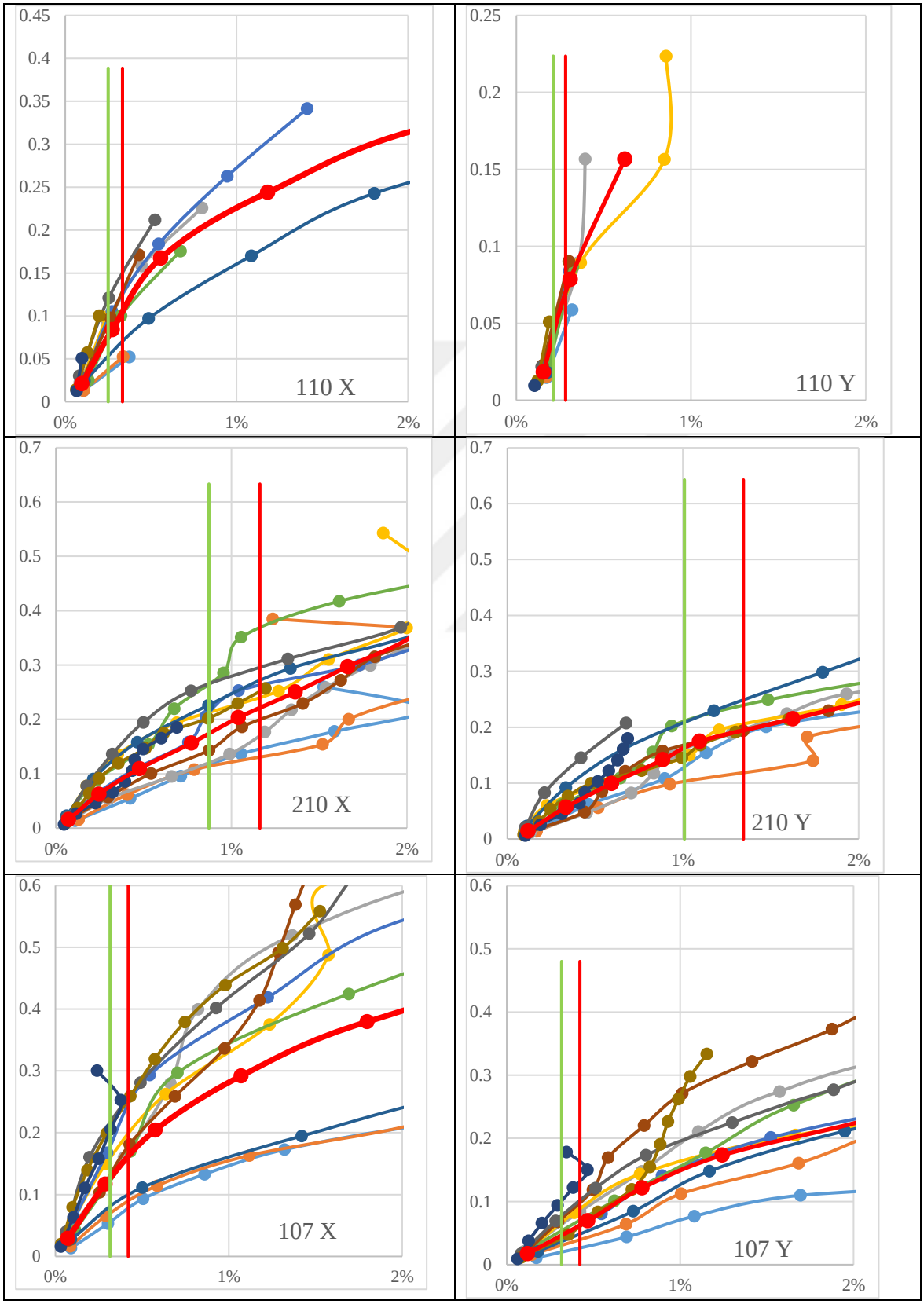

Table C.2 (continued): IDA curves of the buildings. The horizontal axis is the maximum inter-story drift ratio (%) and the vertical axis is the spectral acceleration (g) of corresponding first mode vibration period.

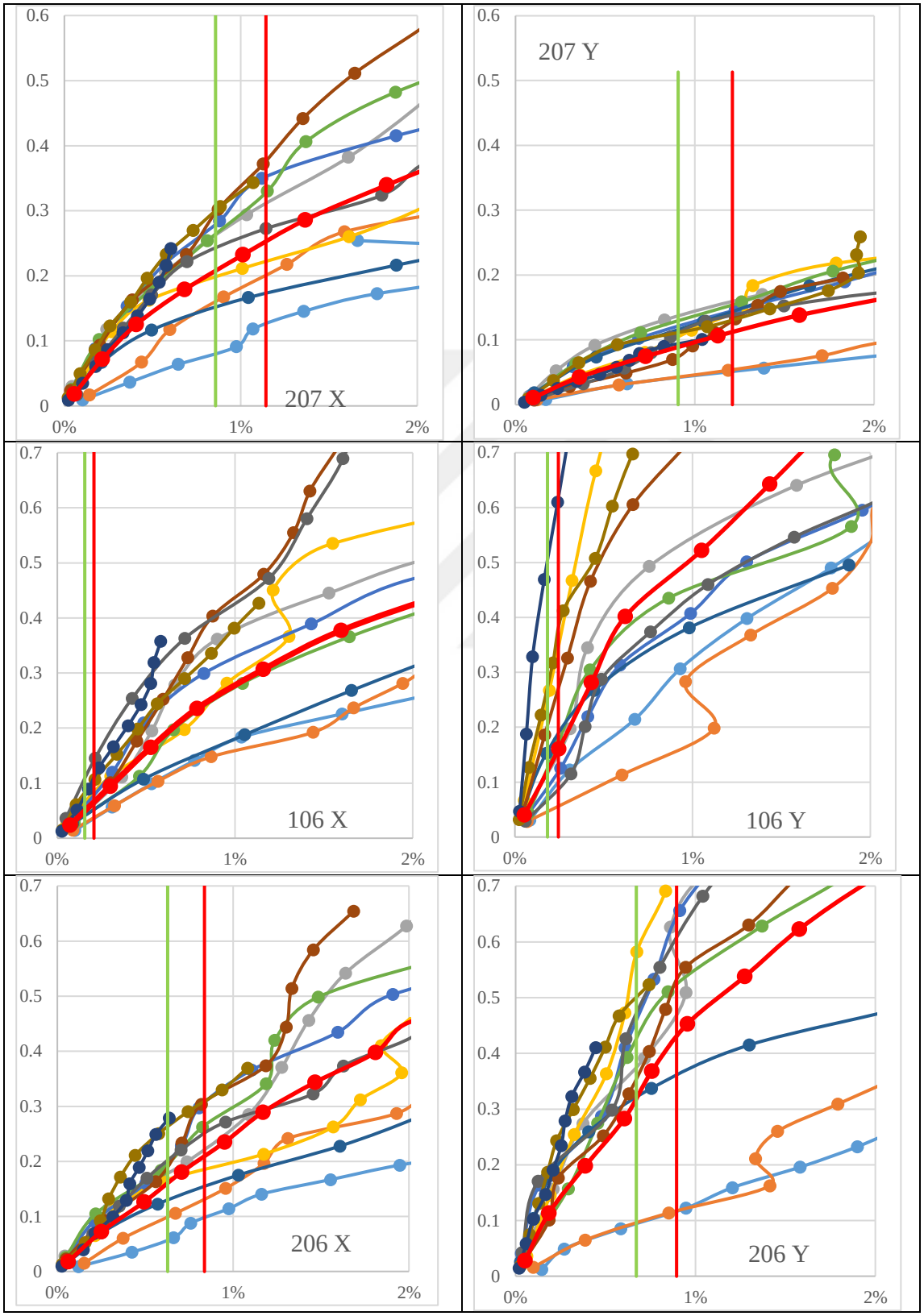

Table C.2 (continued): IDA curves of the buildings. The horizontal axis is the maximum inter-story drift ratio (%) and the vertical axis is the spectral acceleration (g) of corresponding first mode vibration period.

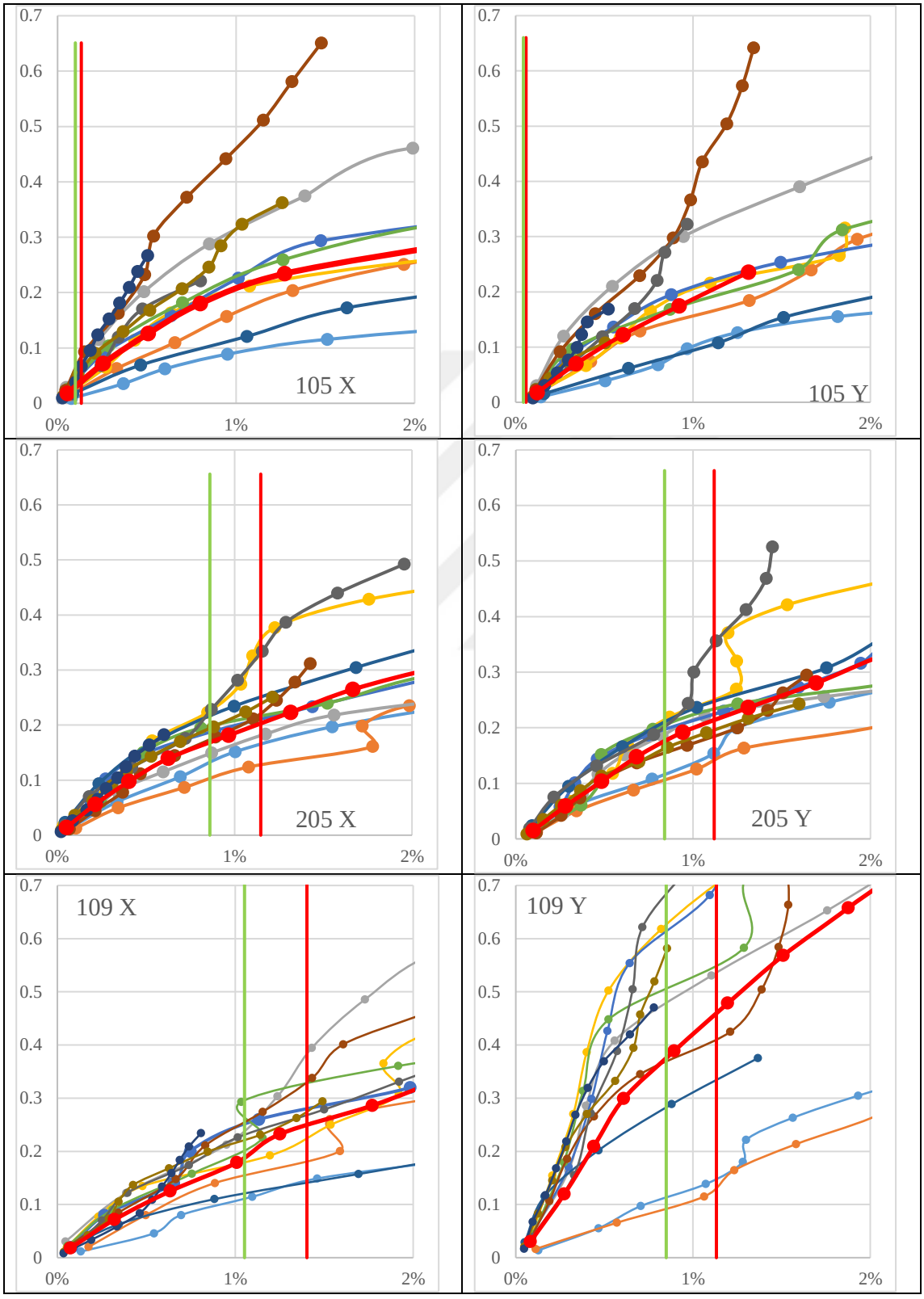

Table C.2 (continued): IDA curves of the buildings. The horizontal axis is the maximum inter-story drift ratio (%) and the vertical axis is the spectral acceleration (g) of corresponding first mode vibration period.

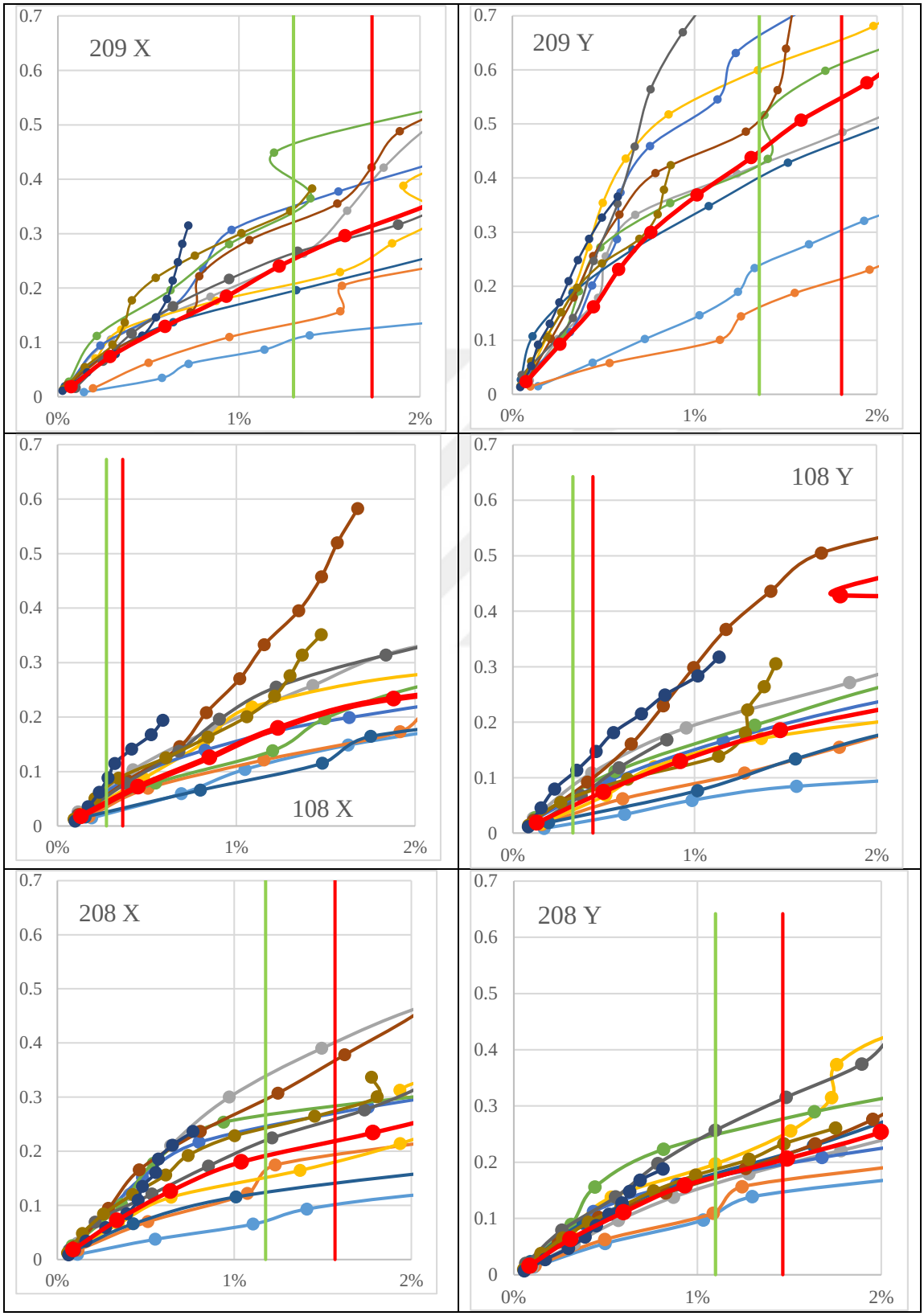

Table C.2 (continued): IDA curves of the buildings. The horizontal axis is the maximum inter-story drift ratio (%) and the vertical axis is the spectral acceleration (g) of corresponding first mode vibration period.

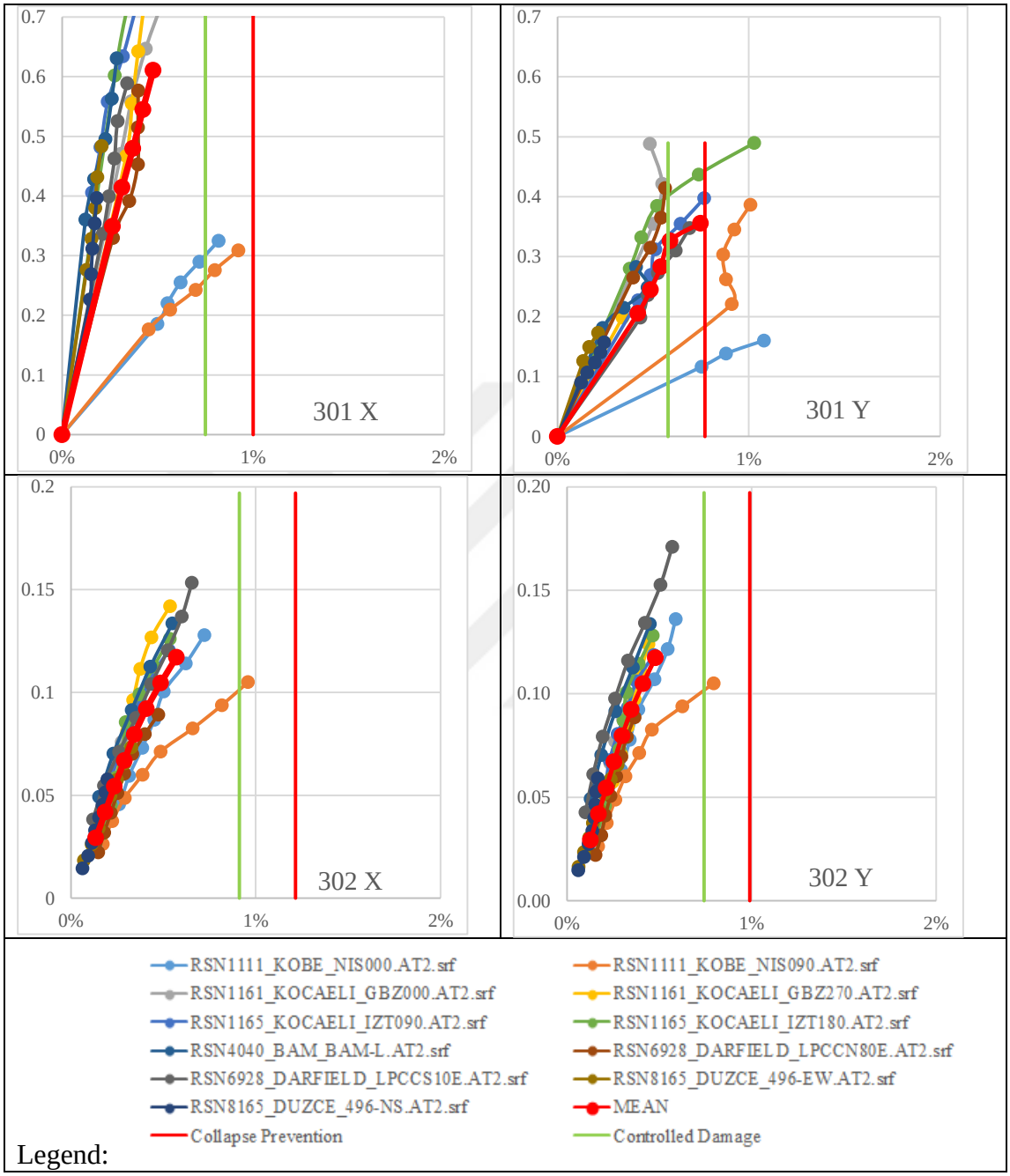

APPENDIX D: PROBABILITY OF EXCEEDANCE CURVES

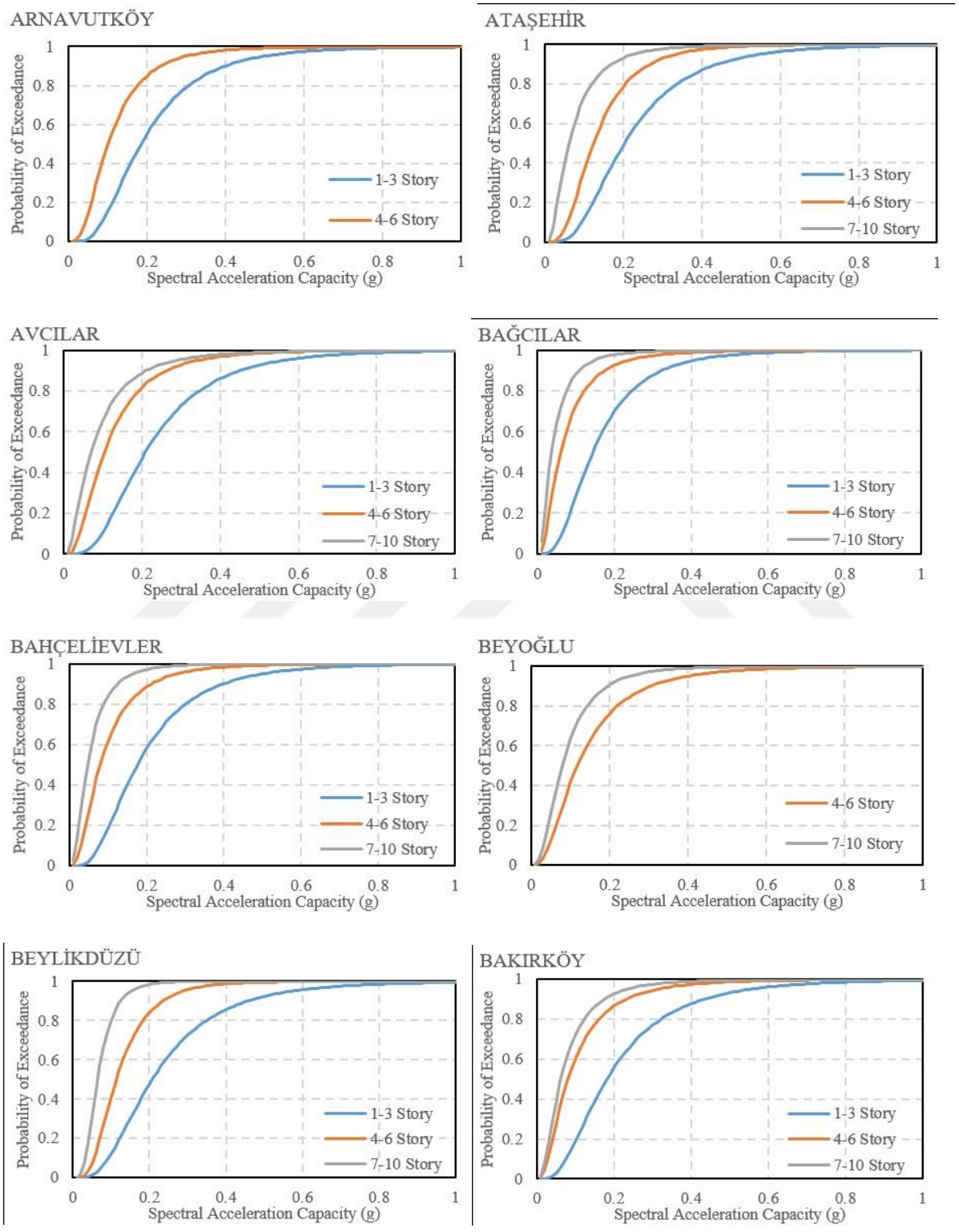

Figure D.1: Probability of exceedance curves computed from the data obtained from each district.

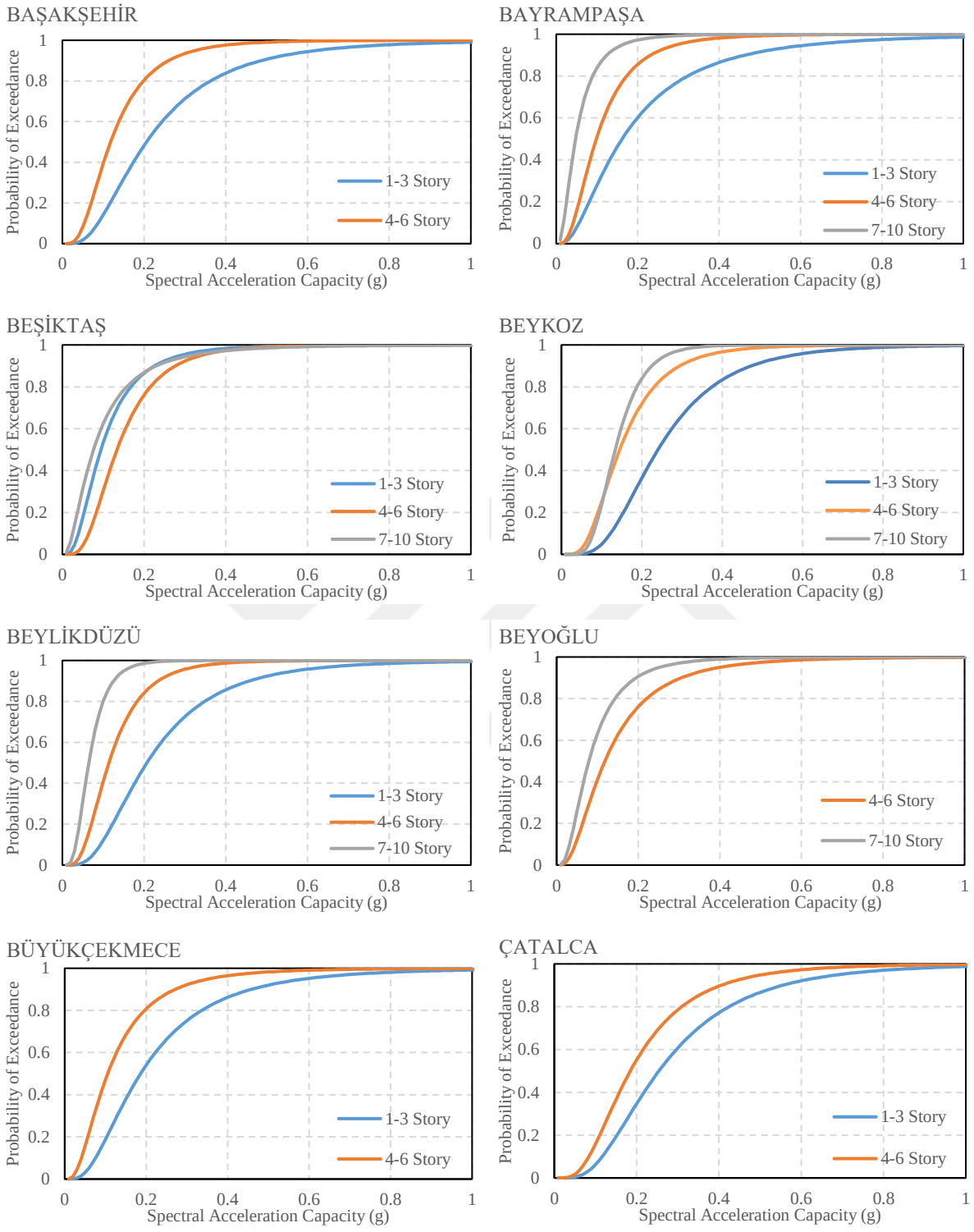

Figure D.1 (continued) : Probability of exceedance curves computed from the data obtained from each district.

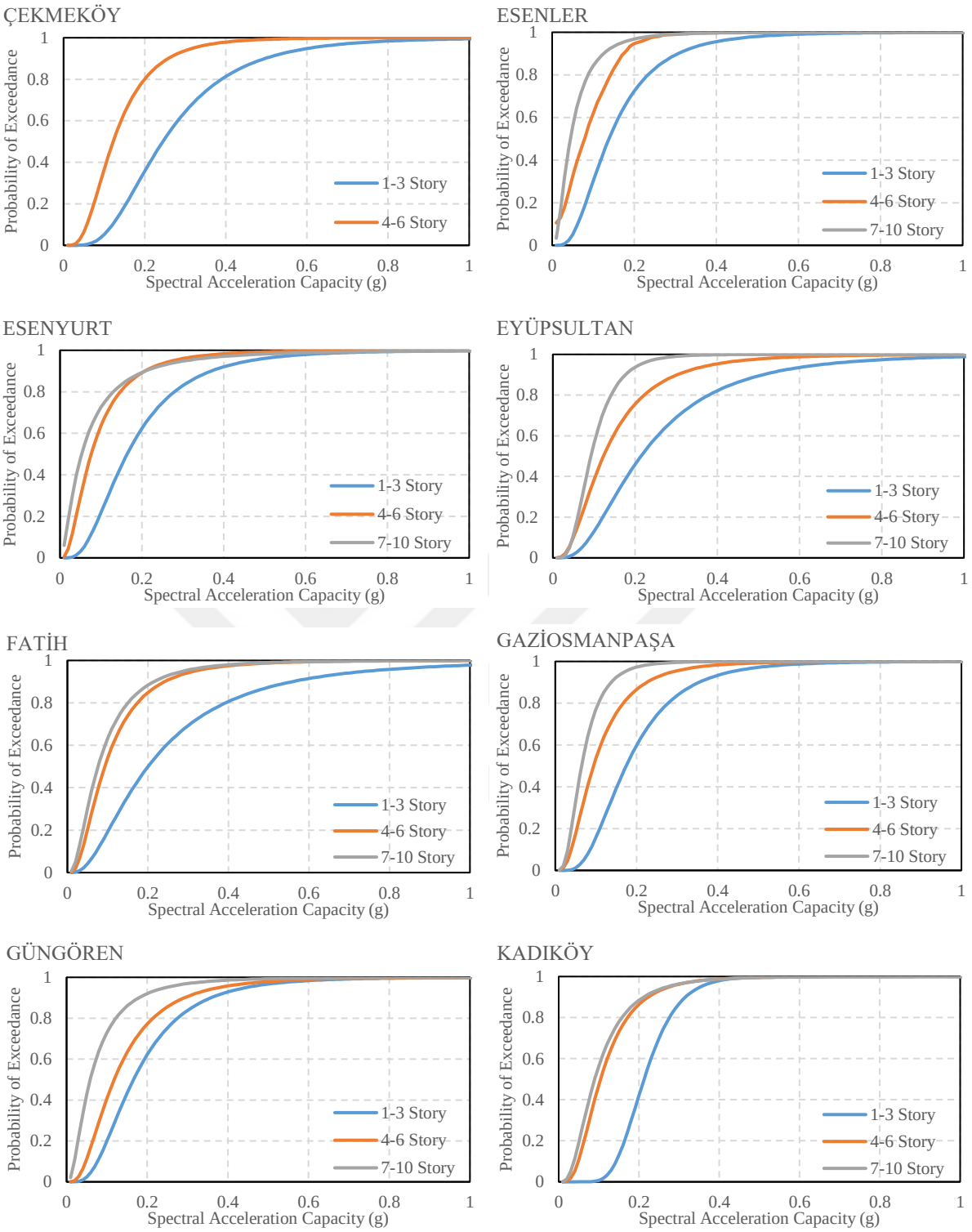

Figure D.1 (continued) : Probability of exceedance curves computed from the data obtained from each district.

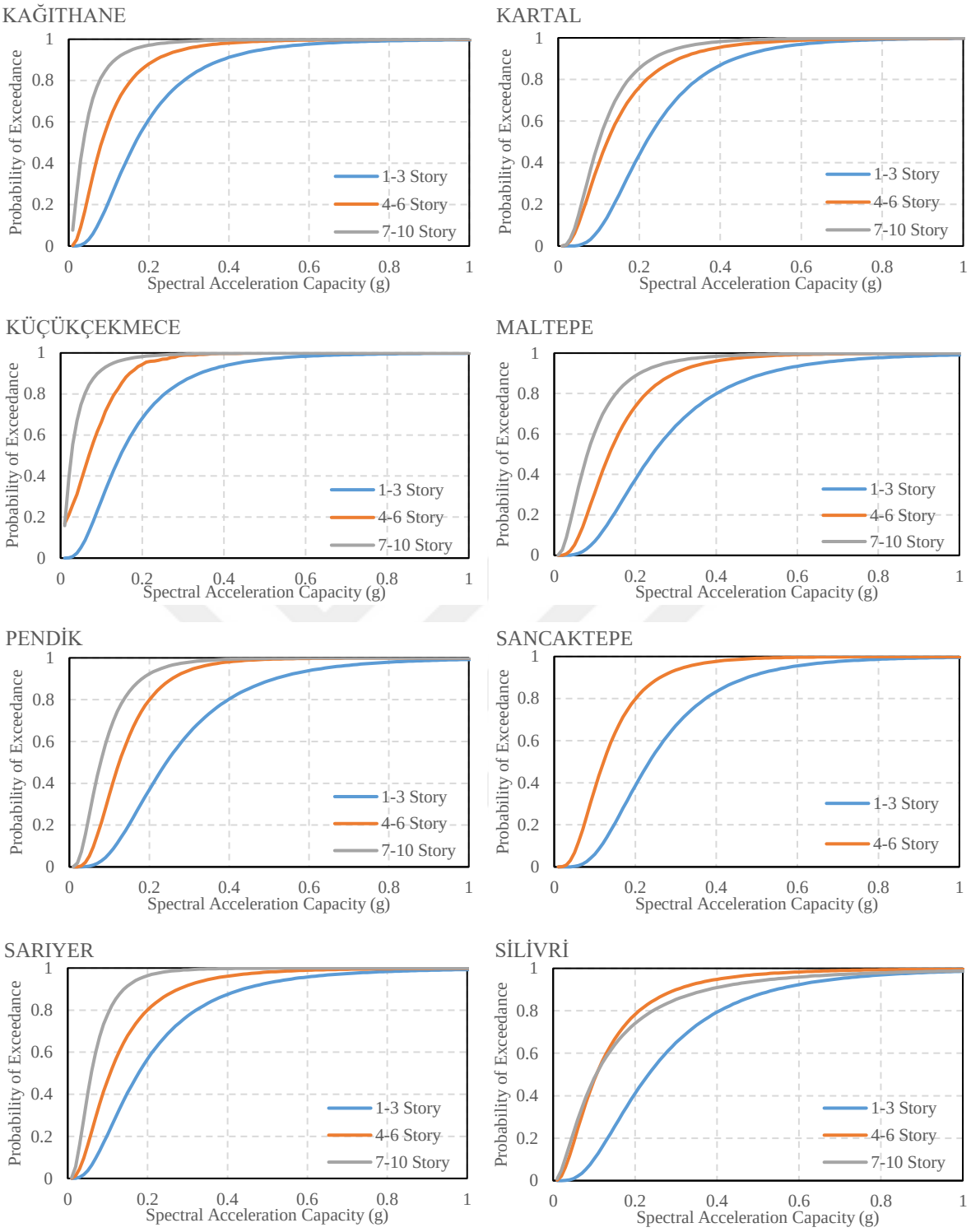

Figure D.1 (continued) : Probability of exceedance curves computed from the data obtained from each district.

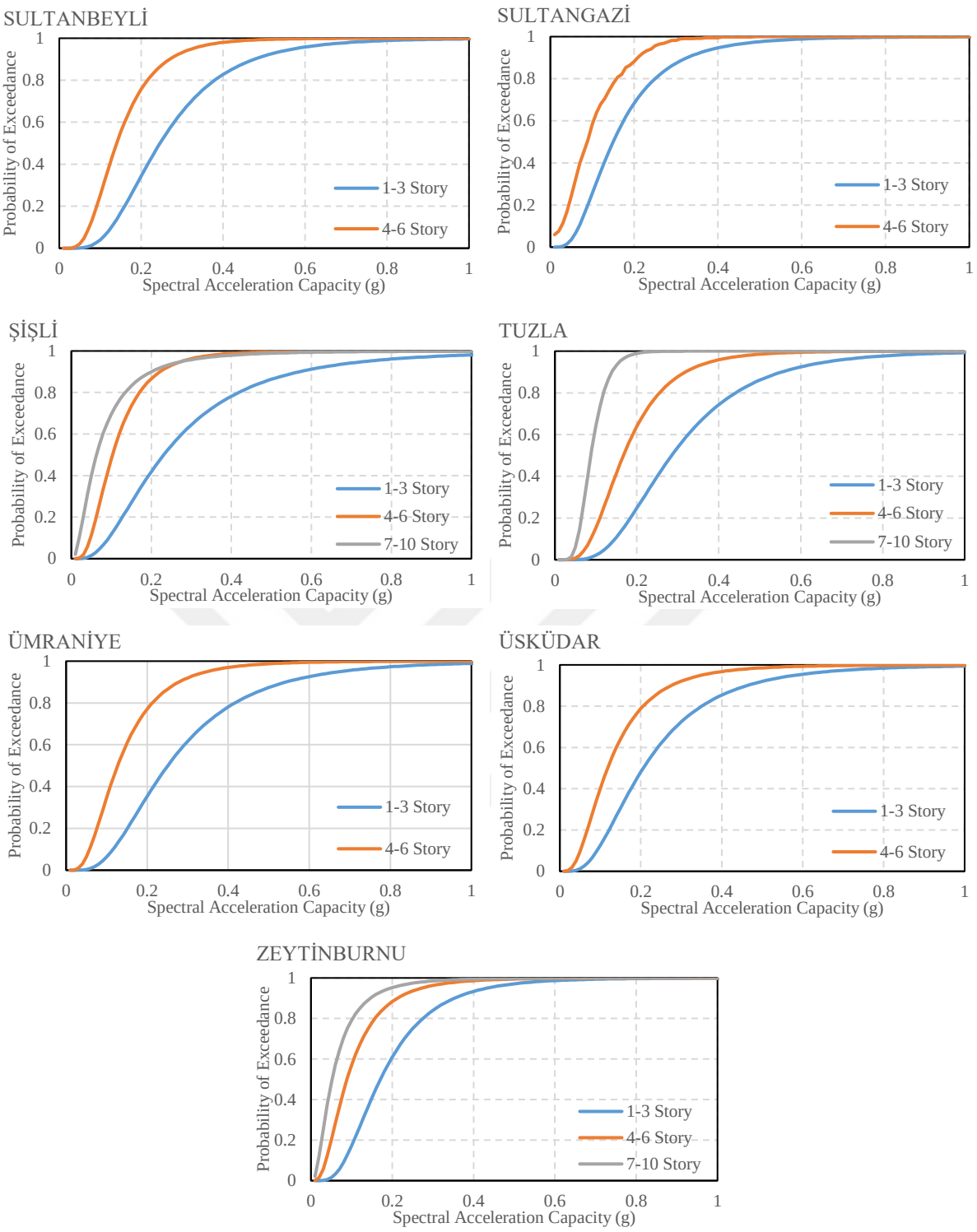

Figure D.1 (continued) : Probability of exceedance curves computed from the data obtained from each district.

CURRICULUM VITAE

Name Surname **: Hasan Hüseyin AYDOĞDU**

EDUCATION **:**

- **B.Sc.** **:** 2008-2012, Anadolu University, The Engineering and Architecture Faculty , Department of Civil Engineering
- **M.Sc.** **:** 2014-2016, Istanbul Technical University, Institute of Earthquake Engineering and Disaster Management, Department of Earthquake Engineering

PROFESSIONAL EXPERIENCE AND REWARDS:

- 2013-… Istanbul Metropolitan Municipality
- 2023- Rapid Seismic Evaluation of Existing Buildings through PERA2019 Methodology Project. Raci Bademli Good Practices Encouragement Award – Turkish Chamber of City Planners
- 2024-2026 JSPS Postdoctoral Fellowships for Research in Japan, Tohoku University

PUBLICATIONS, PRESENTATIONS AND PATENTS ON THE THESIS:

- **Ilki, A., Kahraman, T., Ozkan, S., Aydogdu, H. H., Demir, C., and Comert, M.,** (2021). Seismic Risk Assessment of Building Stock in Istanbul. 14th International Congress on Advances in Civil Engineering, September 2021 in Istanbul, Turkey.
- **Comert, M., Demir, C, Aydogdu, H. H., and, Ilki, A.** (2022). Deprem zararlarının azaltılmasına yönelik yapısal müdahalelerin fayda-maliyet açısından değerlendirilmesine yönelik bir ön çalışma. TMMOB Afet Sempozyumu, 20-22 April 2022, Ankara, Turkey.

- **Aydogdu, H. H., Tut, O., and, Ilki, A.** (2022). Mevcut binaların deprem riski tespitinde İstanbul Büyükşehir Belediyesinin yaklaşımı. 1. Deprem Risk Yönetiminde Yazılım ve Deprem Mühendisliği Çalıştayı, 26 May 2022
- **Demir, C, Comert, M., Aydogdu, H. H., and, Ilki, A.** (2022). Seismic Risk Assessment and Preliminary Intervention Cost-Benefit Analysis for the Building Stock of Istanbul. The Third European Conference on Earthquake Engineering and Seismology, September 2022 in Bucharest, Romania.
- **Aydogdu, H. H., Demir, C, Comert, M., Kahraman, T., and, Ilki, A.** (2023). Structural characteristics of the earthquake-prone building stock in Istanbul and prioritization of existing buildings in terms of seismic risk-A pilot project conducted in Istanbul. Journal of Earthquake Engineering, https://doi.org/10.1080/13632469.2023.2247481.
- **Aydogdu, H. H., Demir, C, Kahraman, T., and, Ilki, A.** (2023). Evaluation of Rapid Seismic Safety Assessment Methods on a Substandard Reinforced Concrete Building Stock in Istanbul. Structures. Volume 56, October 2023, 104962, https://doi.org/10.1016/j.istruc.2023.104962.
- **Aydogdu, H. H., Ilki, A.** (2023). Case Study for a Performance Based Rapid Seismic Assessment Methodology (PERA2019) based on Actual Earthquake Damages. Bulletin of Earthquake Engineering 22, 1965–1999 (2024). https://doi.org/10.1007/s10518-023-01841-5.
- **Aydogdu, H. H., Ilki, A.** (2023). Developments in Seismic Safety of RC Building Stock of Istanbul According to the Years and Seismic Design Codes. fib Symposium 2023, Building for the future: Durable, Sustainable, Resilient 5-7 June, 2023, Istanbul, Turkey
- **Aydogdu, H. H., Ilki, A.** (2024). Calibration of the proposed evaluation and risk classification methodology with incremental dynamic analysis and seismic safety provided by the previous seismic design codes. (To be submitted).
- **Aydogdu, H. H., Ilki, A.** (2024). Seismic loss estimation of Istanbul and cost-benefit analysis of the seismic risk mitigation strategies. (To be submitted).

OTHER PUBLICATIONS, PRESENTATIONS AND PATENTS:

- **Atasever, K., Aydogdu, H. H., Erkus, B.** (2017). Comparison of Ground Motion Scaling Methods for Seismic Isolated Structures. 4th International Earthquake Engineering Conference, Eskisehir.
- **Aydogdu, H. H., Ilki, A.** (2019). An overview of research on SMAs with a focus on seismic risk mitigation. *5th International Conference on Smart Monitoring, Assessment and Rehabilitation of Civil Structures*, August 2019 in Potsdam, Germany (SMAR 2019).
- **Cömert, M., Demir, C., Aydogdu, H. H., Ilki, A.** (2022). Deprem zararlarının azaltılmasına yönelik yapısal müdahalelerin fayda-maliyet açısından değerlendirilmesine yönelik bir ön çalışma. *TMMOB Afet Sempozyumu*, 20-22 April 2022, Ankara, Turkey (in Turkish).
- **Ilki, A., Goksu, C., Sari, B., Aydogdu, H. H., Demir, C.** (2023). 2023 Kahramanmaraş Earthquakes and Lessons Learnt Towards Building Resilient

Cities with a Focus on Istanbul, 20 th International Symposium of MASE, Skopje, North Macedonia.

- **Ilki, A., Goksu, C., Sari, B., Demir, C., Aydogdu, H. H.** (2023). 2023 Kahramanmaraş and Hatay earthquakes: Structural seismic performance, lessons learnt, measures for resilient cities. *2nd International Conference on Advances and Innovations in Engineering, 2ICAIE*, Elazığ, Turkey.
- **Aydogdu, H. H., , Goksu, C., Sari, B., Demir, C., Ilki, A.** (2023). İstanbul'da yapı stokunun durumu ve değerlendirmesi. *TMMOB 5. İstanbul Kent Sempozyumu.* 2-3 December 2023, Istanbul, Turkey.
- **Ilki, A., Goksu, C., Demir, C., Sari, B., Aydogdu, H. H.** (2023). February 2023 Turkey Earthquake Sequence and Rapid Seismic Safety Assessment of Existing Buildings in Mega City Istanbul. *The Tenth Kwang-Hua Forum Innovations and Implementations in Earthquake Engineering Research.* 8-11 December 2023, Shanghai, China.
- **Tajiri, S., Yazgan, U., Maeda, M., Liu, H., Shegay, A., Monical, J., … Aydogdu, H. H., …** (2024). Japanese and Turkish Joint Detailed Survey of RC Buildings Damaged by the 2023 Turkey Earthquake, 18th World Conference on Earthquake Engineering, Milano, Italy.
- **Ilki, A., Unal, G., Aydogdu, H. H., Comert, M., Demir, C.** (2024). Cost-Benefit Evaluation for the RC Building Stock of Istanbul Using PERA2019 Methodology, 18th World Conference on Earthquake Engineering, Milano, Italy.
- **Aydogdu, H. H., Atasever, K, and, Ilki, A.** (2024). The Evaluation of a Risk Prioritization Approach and Cost/Benefit Analysis of its Efficiency on Loss Reduction Studies: A Case Study Based on the Damages that Occurred in the 2023 Kahramanmaras Earthquake. Journal of Earthquake Engineering (To be submitted).